In Vitro and In Vivo Investigation into the Role of Lysine Specific Demethylases in the Molecular Circadian Oscillator

Hazel Louise Shepherd (BA Oxon. MSc Oxon.)

St Johns College Oxford

Hilary 2015

The Nuffield Department of Clinical Neurosciences, Division of Medical Sciences, University of Oxford

Mammalian Genetics Unit, Medical Research Council, Harwell

Supervisors: DR PATRICK NOLAN

PROF RUSSELL FOSTER

ABSTRACT

Lysine Specific Demethylases (LSD1 and LSD2 also known as KDM1A and KDM1B) are histone modifiers known to specifically demethylate dimethyl and monomethyl H3K4. They play roles in development and cancer mechanisms through regulation of the cell cycle and progenitor differentiation pathways but have not yet been characterised in the circadian system.

LSD1 and LSD2 were shown to play a role in circadian oscillation *in vitro* in unpublished preliminary work. Knockdown of either gene caused dampened circadian oscillations of gene and protein expression. However, circadian rhythms could not be assessed *in vivo* as the *Kdm1a*$^{-/-}$ animal was embryonic lethal and the *Kdm1b*$^{-/-}$ animal displayed reproductive deficits.

In order to generate a viable animal model of LSD disruption for assessment of adult circadian phenotypes *in vivo* the Harwell ENU mutant archive was screened for ENU-induced point mutations in non-catalytic domains of the two genes. The mutations found in the screen were investigated *in vitro* and *in silico*, and subsequently four mutations chosen for re-derivation by IVF (*Kdm1a*^{E440G}, *Kdm1a*^{L491H}, *Kdm1b*^{T357M} and *Kdm1b*^{P281L}).

LSD1 and LSD2 were found to interact with circadian clock proteins *in vitro*. The LSD1 mutations were found to decrease the ability of LSD1 to bind to its primary cofactor CoREST and to CLOCK, BMAL1 and PER1 and PER2. Furthermore, chromatin immunoprecipitation studies were used to investigate LSD1 mutant binding of circadian promoters and demethylation of histone H3. Non-significant impairment of demethylase activity and binding suggest that the resulting phenotype is more subtle than in knockout cells.

In vivo, adult LSD1 and LSD2 mutant animals were shown to display background strain-dependent circadian phenotypes. *Kdm1a*$^{E440G/E440G}$ animals displayed a deficit in circadian masking but a normal phase response to nocturnal light pulses and normal pupillary constriction. This suggests that LSD1 plays a role in phase resetting. *Kdm1b*$^{T357M/T357M}$ animals displayed an increased phase shift in response to 15-minute light pulses at CT22 indicating a phase resetting phenotype. Gene expression

in mutant animal livers was assessed and only subtle changes in circadian gene expression were observed.

In neurobehavioural phenotyping, *Kdm1a*$^{E440G/E440G}$ mutants were hyperresponsive to handling, showed impaired learning and memory, and displayed subtle discrepancies in anxiety and social dominance parameters. *Kdm1b*$^{T357M/T357M}$ animals displayed less neurobehavioural abnormalities, including an increase in time freezing in response to foot shock in fear conditioning.

Histological examination revealed a hypogonadal phenotype in *Kdm1a*$^{E440G/E440G}$ animals which may be accounted for by disruption of the previously established developmental roles of LSD1.

Finally a screen of epigenetic modifier compounds revealed that small molecule demethylase inhibitors alter circadian period in fibroblasts and in the SCN itself.

This investigation lends an insight into the roles of LSD1 and LSD2 in the circadian system and neurobehaviour and identifies future avenues of investigation that could clarify these roles further.

ACKNOWLEDGEMENTS

I must express my gratitude to many people for their support and help throughout my DPhil studies.

Firstly and most prominently, I thank Dr Patrick Nolan for the chance to undertake this investigation. Thank you for your support and advice throughout the project. I have developed professionally and also personally, and have learnt a great deal from you and the lab over the last 4 years.

I would also like to thank those who I have had the chance to work alongside, especially in the neurobehavioural lab. Specifically, thanks to Dr Jessica Edwards, Dr Sneha Anand, and Dr Christine Damrau with whom I studied and showed a great deal of support through lab work over the past 4 years. Dr Gareth Banks and Dr Mike Parsons for help and advice throughout and Dr Ines Heise who advised on all manner of experiments and was always there and willing to help. I hope to continue our friendships going forward and wish you all the best in current and future projects.

I thank Louise Bird and Heather Rada for advice and training (OPPF, Rutherford Appleton Laboratories), the Foster lab in Oxford University Ophthalmology Department for ongoing advice and collaboration, the Reinke lab in Düsseldorf for collaboration, and the core services at MRC Harwell.

I thank the Medical Research Council, and Oxford University for supporting and funding my studies.

With thanks to St Johns College Oxford which as well as supporting my academic endeavours for the last 8 years, will forever be home to me. I consider the staff and students at St Johns my friends for life and hope to stay in touch in future.

I would also like to thank my friends. In particular I thank the SJCBC Sirens for their support and my County team in particular Kerry and Louise. Jack and Ellie, you have been bon since undertaking my studies at St Johns and I couldn't do any of it without you.

Most importantly I thank my family and siblings, Kerrie Nikki and Neil. We have been through difficult times and you have helped me through this project with the utmost love and belief. I am so proud of you all and I look forward to the future. Lastly thank you Mum and Dad for everything.

CONTENTS

LIST OF FIGURES

LIST OF TABLES

ABBREVIATIONS

5HT	Serotonin (5-Hydroxytryptamine)
AANAT	Arakylamine N-acetyltransferase
ACTH	Adrenocorticotrophin Releasing Hormone
AD	Alzheimer's Disease
Afh	Afterhours
AMPK	AMP-Activated Protein Kinase
ASPA	Animals (Scientific Procedures) Act
AVP	Arginine Vasopressin
Bdr	Blind Drunk
BHC80	BRAF35/histone deacetylase complex 80
BMAL1	Brain and muscle ARNT-like 1
cAMP	cyclic Adenosine Monophosphate
CCG	Clock Controlled Gene
cDNA	circular DNA
ChIP	Chromatin Immunoprecipitation
CK1	Casein Kinase 1
CLOCK	Circadian Locomotor Output Cycles Kaput
CNS	Central Nervous System

CoIP	Co Immunoprecipitation
CoREST	Corepressor of RE-1 Silencing Transcription Factor
CRISPR	Clustered Regularly Interspaced Short Palindromic Repeat
CRY	Cryptochrome
CT	Circadian Time
DAPI	4',6-Diamidino-2-Phenylindole
DD	Constant Darkness
DISC1	Disrupted in Schizophrenia 1
DLIC	Dynein Light Intermediate Chain
DMH	Dorsomedial Hypothalamus
DNA	Deoxyribonucleic Acid
DNMT1	DNA Methyltransferase 1
DPC	Days Post Coitum
DSPS	Delayed Sleep Phase Syndrome
E##	Embryonic day
EBM	Eagles Balanced Medium
EBSS	Earle's Balanced Salt Solution
ECL	Electro-chemical Luminescence
EMT	Epithelial to Mesenchymal Transition
ENU	N-ethyl-N-nitrosourea

EZH2	Enhancer of Zeste homolog 2
FAD	Flavine Adenine Dinucleotide
FASPS	Familial Advanced Sleep Phase Syndrome
FBS	Foetal Bovine Serum
FBXL3	F-box and Leucine-rich Repeat Protein 3
FESA	Froxen Embryo and Sperm Archive
FRET	Forster Resonance Energy Transfer
FST	Forced Swim Test
G1	1st Generation
GBSS	G Balanced Salt Solution
GSK3β	Glycogen Synthase Kinase 3
GST	Glutathione-S-Transferase
GWAS	Genome Wide Association Studies
H and E	Haemotoxylin and Eosin
H_2O_2	Hydrogen Peroxide
H3K4	Histone 3 Lysine 4
HA	Haemaglutinnin
HDAC	Histone Deacetylase
HEK	Human Embryonic Kidney
HIHS	Heat Inactivated Horse Serum

HLA	Human Leukocyte Antigen
IEG	Immediate Early Gene
ipRGC	intrinsically photosensitive Retinal Ganglion Cell
IVF	In Vitro Fertilisation
JARID1A	Jumonji AT-rich Interactive Domain 1 A
KCL	Potassium Chloride
KDM1A	Lysine Specific Demethylase 1A
KDM1B	Lysine Specific Demethylase 1B
KI	Inhibitory constant
LB	Lysogeny Broth
LD	12:12 Light-Dark cycle
LHX1	Lim Homeobox 1
LL	Constant Light
LUC	Luciferase
MAO	Monoamine Oxidase
MAOI	Monoamine Oxidase Inhibitor
Me	Methyl Group
MEF	Mouse Embryonic Fibroblast
MeOH	Methanol
$MgCl_2$	Magnesium Chloride

MLL1	Myeloid/Lymphoid or mixed-lineage leukaemia 1
MLL4	Myeloid/Lymphoid or mixed-lineage leukaemia 4
MRC	Medical Research Council
mRNA	messenger RNA
NaCl	Sodium Chloride
NAD	Nicotinamide-Adenine Dinucleotide
NAHCO3	Sodium Bicarbonate
NFkB	Nuclear Factor k B
NP40	Nonylphenoxypolyethoxyethanol
NPAS2	Neuronal PAS Domain 2
OPN4	Melanopsin
P##	Postnatal day
PBS	Phosphate Buffered Saline
PBST	Phosphate Buffered Saline with Tween 20
PCR	Polymerase Chain Reaction
Pdb	Protein database
PER	Period
PFA	Paraformaldehyde
PHD	PH Domain
PHF11	PHD Finger Protein 11

PPI	Pre-Pulse Inhibition
PVDF	Polyvinylidene difluoride
qPCR	quantitative PCR
REM	Rapid Eye Movement
RIKEN	Institute of Physical and Chemical Research
RISC	RNA-Induced Silencing Complex
RNA	Ribonucleic Acid
RNAi	RNA interference
ROR	RAR-related Orphan Receptor
SAD	Seasonal Affective Disorder
SAHA	Suberoylanilidehydroxamic Acid
SANT	Swi3, Ada2, N-Cor, TF111B
SCF	SKP-Cullin F-box
SCN	Suprachiasmatic Nucleus
SDS	Sodium Doedecyl Sulphate
SHIRPA	Smithkline Beecham, Harwell, Imperial College, Royal London hospital Phenotype Assessment
shRNA	short hairpin RNA
siRNA	small interfering RNA
SIRT1	Sirtuin 1

SNAP25	Soluble NSF Attachment Protein
SNP	Single Nucleotide Polymorphism
SPZ	Subparaventricular Zone
TALEN	Transcription activator-like effector nuclease
TBST	Tris-buffered Saline with Tween 20
TGCE	Temperature Gradient Capillary Electrophoresis
TGFα	Transforming Growth Factor α
TMN	Tuberomamillary Nucleus
TSA	Trichostatin A
TSD	Total Sleep Deprivation
TST	Tail Suspension Test
TTFL	Transcription Translation Feedback Loop
U2OS	human Osteosarcoma
VIP	Vasoactive Intestinal Polypeptide
VLPO	Ventrolateral Preoptic Nucleus
VPAC	Vasoactive Intestinal Polypeptide Receptor
WDR5	WD Repeat 5
ZT	Zeitgeber Time

Chapter 1

INTRODUCTION

CHAPTER 1: Introduction

1.1: Circadian Rhythms

1.1.1: What is a Circadian Rhythm?

Circadian rhythms are repetitive self-sustained oscillations of a biologically measurable parameter which occur over a period of approximately 24 hours (from the Latin roots *Circa* meaning approximately and *Diem* meaning day). Circadian rhythms have been demonstrated in the simplest of organisms (Johnson et al. 2008; Haydon et al. 2013), and can perpetuate in cell free systems (Nakajima et al. 2005) as well as being present in nearly every individual cell in the human body (Alvarez et al. 2003). Circadian rhythms have developed independently across different phyla and as such can be assumed to bear a high degree of importance in the evolution of successful and competitive organisms (Dunlap 1999; Johnson et al. 1999).

1.1.2: Why are Circadian Rhythms important?

Circadian rhythms affect many processes impacting on the success of an organism in any given environmental condition (Dunlap 1999; Johnson et al. 1999). As well as the most easily observed outputs of the mammalian clock, which include sleep-activity profiles, alertness, feeding patterns and social behaviour, internal events such as the expression of key metabolic enzymes, immune system activity and body temperature also rise and fall over a 24 hour cycle (Bell-Pedersen et al. 2005). It is sensible that a mechanism by which an organism can adapt to its environment best over the course of a day would benefit survival rates (Dunlap 1999; Johnson et al. 1999). For example, waking in the absence of predators or being active at times optimal for hunting will directly affect survival chances in a group of animals (Dunlap 1999). Even in the case of single-cell organisms, being most metabolically active at a time of day where temperature is optimal for enzyme activity maximises efficiency and leads to outcompeting of less optimally suited individuals (Johnson et al.

2008). But why are they important in complex organisms like *Homo sapiens* living and working in the modern 24-hour culture? Even in the present day, the ability to process nutrients efficiently at meal times through appropriate timing of key enzyme expression, to maintain a good nights' sleep or to modulate timing of stress hormone expression can impact on health and on predisposition to disease in daily life (Dunlap 1999). As such it is important to understand the mechanisms by which circadian rhythms perpetuate and the implications of their disruption.

1.1.3: What happens in circadian disruption?

When circadian synchrony with the external environment is misaligned, consequences can be far reaching and pervasive for a range of organisms (Escobar et al. 2011). In primitive organisms, circadian misalignment renders colonies much less able to compete for resources compromising their ability to thrive (Johnson et al. 2008). With regards man the situation is evidently more complex. In lab-controlled constant conditions, arrhythmic individuals can fare as well as rhythmic ones (Johnson et al. 2008). Similarly, there is no selective pressure for maintaining robust circadian output for cells in a dish under constant conditions. However if cellular rhythms do not oscillate in synchrony with rhythmic changes in the environment; if cells within a given tissue are not synchronised; if tissues are misaligned with each other; or if the organism is totally unable to entrain to the 24 hour schedule then peripheral disruptions can arise, especially in complex organisms (Escobar et al. 2011).

The consequence of peripheral clock misalignment can be demonstrated by ablating the clock in a tissue specific manner, for instance using conditional knockouts in murine models of desynchrony. A pancreatic loss of *Bmal1* expression and subsequent loss of circadian rhythmicity induces a diabetic state (Lee et al. 2011), whereas a liver specific disruption affects the expression of gluconeogenic and metabolic genes, causing a metabolic syndrome in the whole animal (Buijs et al. 2013a).

Forced desynchrony of human peripheral clocks using 28 hour light dark cycles has been shown to trigger psychological changes such as altered reward behaviour rhythms and task performance rhythms (Murray et al. 2009; Zhou et al. 2011), and in man chronic desynchrony can be observed *in situ* in shift work disorder (Escobar et al. 2011). More acutely, jet lag can be accompanied by a syndrome encompassing a drop in mood and cognitive ability, indigestion and gastrointestinal complaints (Roenneberg et al. 2012).

Although many of the peripheral effects of clock disruption appear to have negative impacts on physiology, manipulation of daily rhythms has been shown to have a positive effect on some clock-regulated outputs. Total sleep deprivation (TSD) and follow up phase shifts in sleep schedule have been shown to act as a fast acting antidepressant treatment in bipolar, suicidal and even drug-refractory depressed patients (Echizenya et al. 2013; Sahlem & Kalivas 2014). The disruption of the circadian mechanism has consequences for humans and research into manipulation of rhythms has the potential for far reaching applications impinging on many related behaviours.

1.2: The Molecular Clock

1.2.1: Core Clock

The circadian oscillator (clock) in mammals depends on the transcriptional and translational oscillation of a selection of "core clock" genes (Dunlap 1999; Reppert & Weaver 2002). Daily rhythms are present in almost every cell in the body, most are evident as cyclic gene transcription and translation (Ko & Takahashi 2006). Genes comprising the "core clock" are expressed in most tissues (Yoo et al. 2004). Interestingly these genes are expressed but do not oscillate in the testis (Alvarez et al. 2003). Each cell organises its outputs according to the molecular oscillator, detectable primarily as a transcriptional-translational feedback loop (Ko & Takahashi 2006) as depicted in Figure 1.1. Briefly, the transcriptional activators CLOCK and BMAL1 heterodimerise and bind to E-box elements to increase transcription of the target genes (Ko & Takahashi 2006). Among these targets are the output genes (Clock controlled genes, CCGs) as well as the negative clock regulators, the period and cryptochrome genes (Ko & Takahashi 2006). *Per* and *Cry* are subsequently transcribed and accumulate. As the concentration of these negative regulators increases, they interact with each other and translocate to the nucleus to bind to the CLOCK:BMAL1 complex thereby repressing their own transcription (Ko & Takahashi 2006). The accumulated PER and CRY are phosphorylated by CK1 (Casein kinase 1) and AMPK respectively and targeted for degradation, and so the levels fall once again (Landgraf et al. 2012; Vanselow et al. 2006; Lamia et al. 2009). This cycle takes 24 hours in each cell and adjustments to maintain synchronisation are made through posttranslational modification to the core clock components (Ko & Takahashi 2006). These modifications are heavily regulated by secondary transcription-translation feedback loops such as the REV-ERBα and ROR pathways (Gallego & Virshup 2007; Ripperger & Merrow 2011).

Interestingly, the transcription-translation feedback loop (TTFL) may not account for all circadian activity, as rhythms have been observed in red blood cells (with no nucleus so no transcription)

(O'Neill & Reddy 2011), in cells where transcription is inhibited and in cells where translation is inhibited (O'Neill et al. 2011) as well as in cell-free systems (Nakajima et al. 2005). However, in the case of the current investigation, the extensively characterised mammalian TTFL will remain the point of molecular focus.

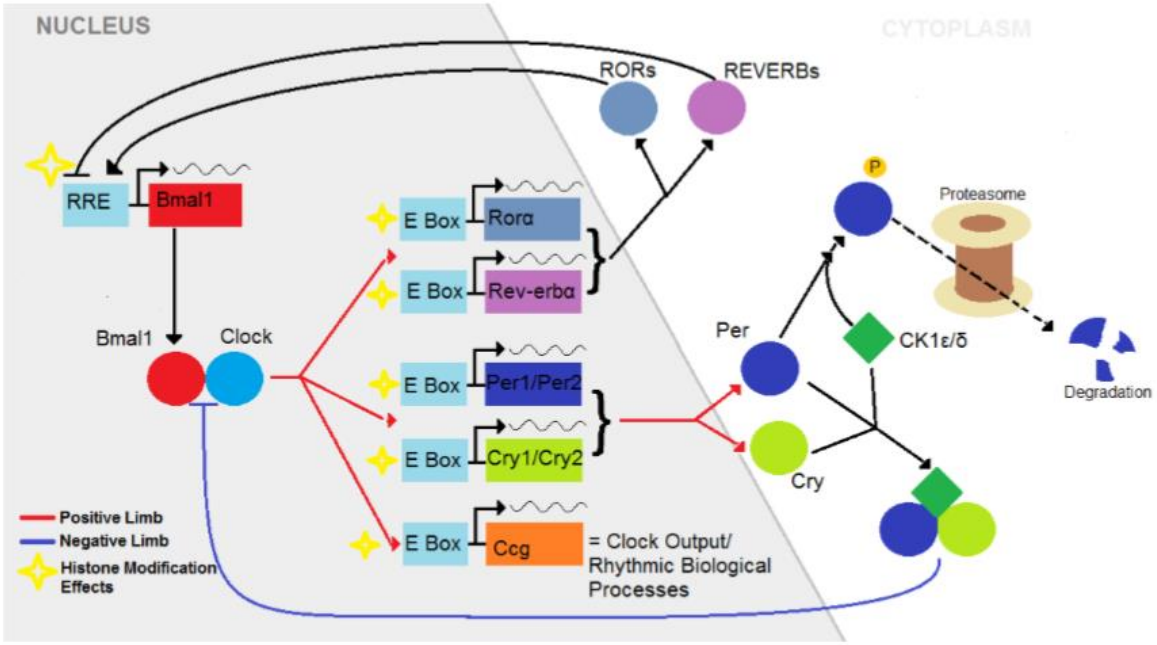

Figure 1.1: Outline of the molecular clock.

Positive limb components CLOCK and BMAL1 heterodimerise and bind to E-box elements in promoters of clock controlled genes. Negative limb components (*Cry* and *Per* genes) contain E-box elements in their promoters as well, and the positive limb upregulates their transcription. The negative limb clock components accumulate in the cytoplasm, dimerise and translocate into the nucleus and act to inhibit CLOCK:BMAL1 so inhibiting their own transcription allowing the levels to fall again. Negative limb components are also modified by phosphorylation and ubiquitination, targeted for degradation in the cytoplasm so modifications affecting degradation can also affect the speed of the clock. (Ko & Takahashi 2006)

1.2.2: Posttranslational modifications

1.2.2.1: Phosphorylation states

It has been conclusively shown that the phosphorylation of clock components can affect the period of the clock. Phosphorylation of CRY and PER clock components is known to direct their degradation by the proteasome (Eide et al., 2005; Lowrey et al., 2000; Meng et al., 2008; Ralph and Menaker, 1988) as well as influencing their localisation (Virshup et al. 2007) and stability (Camacho et al. 2001; Virshup et al. 2007; Meng et al. 2008). When considering one particular model, the *Tau* mutant, it has been shown that the mutant displays a free-running period of 20 hours (Lowrey et al. 2000). The mutation causes a gain of function in *CK1ε*, which is responsible for PER protein phosphorylation (Meng et al. 2008). The increased rate of phosphorylation increases protein clearance, and is most effective at early circadian night when PER levels are accumulating. As such increased clearance of PER causes a short free running period, as expected of a reduction of PER protein level at this circadian time (Section 1.4.2.1). The *Tau* mutant was contrasted to the *CK1ε* knockout which displays a lengthened period to confirm its role in this degradation process (Meng et al. 2008). Conversely to the *CK1ε* knockout, interference in AMPK-mediated phosphorylation shortens circadian period through stabilising CRY1 (Lamia et al. 2009). Here, enhancement of AMPK signalling was shown to shorten circadian period and decrease amplitude mimicking the changes seen upon glucose depletion, and modifying the response to glucose administration (Lamia et al. 2009). This links the AMPK phosphorylation of CRY1 to metabolic events in the cell (Lamia et al. 2009). This effect was time of day dependent which supports the hypothesis that the negative limb of the oscillator can be manipulated to phase shift the clock in different ways at different times of day (Lamia et al. 2009). In summary, phosphorylation of clock components can affect circadian outputs, so must be accounted for in the characterisation of molecular circadian mechanisms.

1.2.2.2: Proteasome function and ubiquitination

Modifiers of proteasome function can affect the degradation of clock components and as such can regulate the period length and amplitude of the clock. For example, the phosphorylation of CRY1 proteins by AMPK discussed earlier (which causes period shortening through stabilising CRY1) was shown to act by increasing FBXL3 binding and as such increase ubiquitination (Yoo et al. 2013; Hirano et al. 2013). The *Fbxl3* mutant afterhours (*Afh*) has a free-running period of approximately 26.5 hours (Anand et al. 2013). CRY1 degradation by the Skp1/Cul1/F-box (SCF) E3 ubiquitin ligase is slower in *Afh* mutants due to a lack of FBXL3-mediated ubiquitination of CRY1 which targets the protein for degradation. The period of the clock is subsequently lengthened (Siepka et al. 2007; Godinho et al. 2007) . *Cry1* and *Cry2* knockout models have discrepant period lengths (*Cry1* knockouts displaying a free-running period of 22.5 hours, and *Cry2* 24.6 hours) (van der Horst et al. 1999), and *Afh-Cry* knockouts although both lengthened in comparison to the *Cry* knockouts alone, display different periods to one another (Anand et al. 2013). Period length in the *Afh* mutant is closer to the *Cry2* knockout-*Afh* cross than *Cry1* knockout-*Afh* cross demonstrating that CRY1 function is more essential to maintaining the clocks natural period than CRY2 (Anand et al. 2013). This demonstrates that there exist subtle complexities of clock regulation by posttransl ational modification which can alter circadian properties in multiple ways.

In vitro, proteasome inhibitors such as epoxomicin have also been shown to change circadian parameters and small doses lengthen period by 9-10 hours in Ostreococcus tauri (Van Ooijen et al. 2011). Proteasomal functioning must be taken into account when characterising unknown gene functions as the rate of degradation of circadian proteins affects circadian period.

1.3: The Circadian Mechanism

1.3.1: Synchronisation to the environment

Peripheral clocks are intrinsic to individual tissues and can be observed in culture. In *ex vivo* tissue preparations, an approximately 24-hour rhythm can be detected, and this gradually fades as the cell oscillations become out of phase with one another. *In vivo*, all rhythms are maintained by a pacemaker which oscillates in a self-sustained manner observable in constant conditions. Alignment of peripheral tissues is directed by the outputs from the central circadian oscillator (or pacemaker); the suprachiasmatic nucleus (SCN) in the hypothalamus (Figure 1.2). This group of approximately 20000 neurons (in rodents (Welsh et al. 2010)) signals via neural, hormonal (mainly glucocorticoid) and humoral outputs to the periphery to synchronise all tissues (Schwartz & Roth 2008; Buijs & Kalsbeek 2001; Bartness et al. 2001). Peripheral cells and tissues can be entrained by SCN efferents but also to secondary inputs (for example, the liver entrains well to feeding regimes which deliver nutrients rhythmically to the tissue (Stokkan et al. 2001), and many peripheral clocks entrain to temperature cues (Buhr et al. 2010; Brown et al. 2002)). This is not the case for the SCN which entrains to few external cues or 'zeitgebers' (Aschoff 1960). Most importantly and strongest of all zeitgebers is light from the external environment, and although other cues can entrain SCN neurons, light is the overriding input (Aschoff 1960). The SCN does not express glucocorticoid receptors, thus avoiding entrainment by its own main hormonal output and is also temperature compensated again avoiding self-entrainment (Oster et al. 2006; Rosenfeld et al. 1988). This is important for maintaining a sustained rhythm, unperturbed by irrelevant and noisy environmental cues. Light oscillates with a reliable 24-hour period, due to the rotation of the Earth about its axis. As light entrains the pacemaker so effectively, *in vivo* SCN investigations such as the work presented here involve manipulation of light.

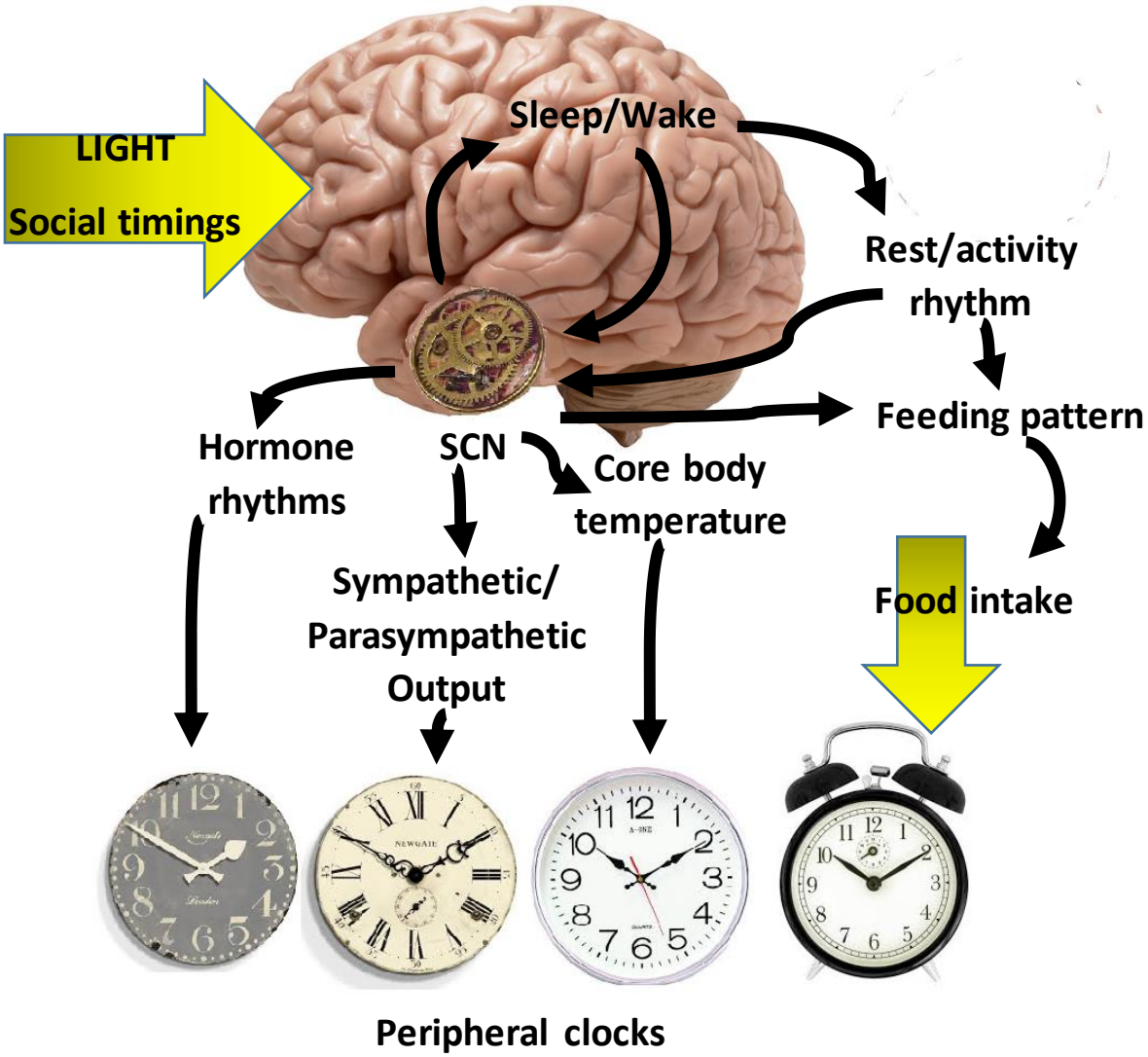

Figure 1.2: The SCN is the master pacemaker

Peripheral tissues such as liver, heart and muscle all behave in a circadian manner, oscillating with a peripheral clock. The peripheral clocks are entrained to the environment by feeding times, but also by signals from the SCN. The SCN is entrained primarily by light. It controls the rhythms of peripheral oscillators through controlling the timing of hormonal output, body temperature, feeding patterns and neural output via sympathetic and parasympathetic pathways.

1.3.2: Circadian neural pathways

The pathway by which external light cues are processed and synchronise circadian rhythms (subsequently regulating many output functions including activity and sleep cycles) consists of a detection event, followed by a direct input to the SCN, gating of signals within the SCN and several output pathways (Welsh et al. 2010; Hattar et al. 2003; Siepka et al. 2007). Manipulation of the clock at any of these points could result in a sleep-wake or activity level phenotype. Therefore when a phenotype is observed, it is important to discern which part of the clock is truly affected by the genetic perturbation; the input, gating or output from the SCN.

1.3.2.1: Circadian Pathways: Input

SCN entrainment to light

The pathway by which the SCN regulates so many outputs begins with a detection event. The SCN receives direct input from the retinohypothalamic tract which projects directly from the ipRGCs of the retina via the optic nerve to the hypothalamus (Schmidt et al. 2011). Rods and cones synapse with ipRGCs in the retina, but ipRGCs also express melanopsin (*Opn4*) so are intrinsically photosensitive. The SCN of *OPN4* knockout animals entrains to the weak input from rods and cones, but rodless, coneless *OPN4* knockouts free-run as they are unable to entrain to light at all (Lucas et al. 2003; Panda, Sato, et al. 2002; Ruby et al. 2002). iPRGC projections signal via glutamate to cells in the dorsomedial core of the SCN, by induction of immediate early genes (IEGs) including *fos* and *CREB* which lead to upregulation of *Period 1* (*Per1*) (Dunlap et al. 1997; Lupi et al. 2006). As *Per1* expression increases, the negative limb of the oscillator is reset and the master clock entrained directly to light input (Balsalobre et al. 2000; Kuhlman et al. 2003). This induction of *Per1* expression can alter the onset of circadian activity cycles in either direction (Phase advancing or phase delaying the clock) depending on where in the circadian cycle the SCN is when IEG upregulation of *Per1* occurs (Balsalobre et al. 2000; Kuhlman et al. 2003). This could be explained as follows; if PER1 is

accumulating and light upregulates it further, the clock is sped up and the clock phase advances in response, whereas if light induces *Per1* as PER1 is decreasing in the SCN, the clock period is lengthened as it takes longer to clear the PER1 and the phase is delayed. Therefore administering a light pulse during the dark phase at CT14-18 (early in subjective night) causes a phase delay and if light is administered at CT19-23 (late in subjective night), the phase is advanced (Figure 2.1). The phase resetting ability of light administered at different circadian time-points can be used to tease apart pacemaker function *in vivo*.

Consequences of input disruption

Disruption of input pathways to the central clock can cause changes in circadian behavioural outputs. If the retinal input to the SCN is experimentally ablated, animals free-run (do not entrain to light displaying sleep-wake timings centrally generated by the SCN with no adjustment to external time cues) (Johnson et al. 1988). So if input pathways are affected in a circadian model this may be seen in measurements where the animal is required to entrain to light-dark schedules or respond in any way to light input (such as the response to light pulses (Shuboni & Yan 2010)). If the disruption to the input pathway were not complete ablation but rather a more subtle impairment, more sensitive entrainment assays would be required to tease it apart, for example using very low lux level light intensities for entrainment (Edwards 2012). Measures can therefore be taken to discern whether a circadian phenotype is due to the disruption of input pathways to the SCN.

1.3.2.2: Circadian Pathways: Pacemaker mechanism

Disrupting the SCN causes phenotypes involving all output pathways, but in order to pinpoint the location of the perturbation, some functions unique to the SCN can be teased out by measuring parameters such as the elasticity of the pacemaker using jet lag paradigms (Hatori et al. 2014), or internal synchrony of the cells constituting the pacemaker (Hastings et al. 2014).

Recently LIM homeobox 1 (*Lhx1)* has been examined using a jet lag paradigm. Firstly microarray screening was undertaken to identify genes expressed in the SCN which were rhythmically-expressed and light-regulated (Hatori et al. 2014). *Lhx1* expression was supressed in response to light in the expected manner in response to pulses at circadian times (CTs) in afternoon, early evening and late evening. The ablation of *Lhx1* impairs suppression of *Vip* expression in response to light and attenuates coupling of neurons in the SCN. SCNs from *Lhx1* conditional knockout animals are faster to synchronise to new Light:Dark (LD) regimes in jet lag paradigms and show a dampened circadian rhythm in constant darkness (DD), characteristic of desynchrony in the SCN. Impairment of such paracrine signalling causes the coupling of the cells to become looser and the oscillator becomes more responsive to weaker zeitgebers, shifts more readily after nocturnal light pulses and takes less time to entrain to new circadian schedules (Hastings et al. 2014). This makes cellular coupling of interest clinically in the treatment of shift work disorder and jetlag where a shift in light dark schedules results in desynchrony between tissues and desynchrony between the SCN and external time (Herzog 2007; Yamaguchi et al. 2013).

In the current investigation, the ability of the pacemaker to entrain to light schedules is recorded to explore the impact of any disruption to cell-cell coupling.

1.3.2.3: Circadian Pathways: Output

If output from the SCN is lost or disrupted, various peripheral consequences can arise due to the loss of synchronisation of peripheral tissues by the SCN (Bartness et al. 2001).

The SCN projects directly to the Dorsomedial Hypothalamus (DMH) (which projects to areas regulating rhythms in feeding behaviour and temperature regulation) and Sub Paraventricular Zone (SPZ) (which projects to the areas associated with control of sleep) as well as to several less densely innervated structures including the vetrolateral preoptic nucleus (VLPO), orexinergic hypothalamic neurons and the cortex (Schwartz & Roth 2008). SCN outputs utilise glutamate and firing tends to increase during the day, and fade during the night (Wagner et al. 1997). The SCN has much further-reaching autonomic outputs and signals via the vagus nerve controlling cardiac tone and heart rate as well as insulin response, respiratory rate and adrenal activity (Bartness et al. 2001; Buijs & Kalsbeek 2001). The hypothalamic output of the SCN has a knock on effect on circulating hormone levels as it increases the release of hormones including adrenocorticotrophin releasing hormone (ACTH) (so increasing circulating cortisol and adrenaline), growth hormone, leutinising hormone, follicle-stimulating hormone, thyrotrophin-releasing hormone, melatonin (although melatonin is absent in some organisms such as the C57BL/6 mouse strain (Ebihara et al. 1986)) and orexin. It can also signal to surrounding areas with no neural efferents via diffusible factors (putatively Transforming Growth Factor (TGFα) or Prokineticin 2 (Silver et al. 1996)) and synchronises cells within its own structure using paracrine factors including arginine vasopressin (AVP) and vasoactive intestinal polypeptide (VIP) acting on VPAC and VIP receptors respectively (Hastings et al. 2014; Harmar et al. 2002; Maywood et al. 2011; Aton et al. 2005). Each peripheral tissue expresses its own slave oscillator (peripheral clock), which maintains synchrony in the cells of that tissue and can oscillate for a limited time independent of the SCN (Reppert & Weaver 2002). Peripheral clocks involve different molecular components to the central pacemaker. For example; NPAS2 is specific to the central SCN tissue and liver cells (DeBruyne et al. 2006); PER3 is essential for pituitary and lung

rhythms but not SCN (Pendergast et al. 2010); and expression of most CCGs are different between tissues (only 5% overlap (Reppert & Weaver 2002)). Peripheral clocks are under the control of hormonal, neural and body temperature rhythm outputs of the SCN as well as environmental factors; for example the liver can be entrained by feeding rhythms (Stokkan et al. 2001). Peripheral clocks control the output of the peripheral tissue resulting in circadian oscillation in many physiological parameters such as rate of liver lipid metabolism (Feng et al. 2011), pancreatic insulin secretion (Peschke & Peschke 1998), pineal melatonin secretion (Isobe et al. 2001) and multiple other cardiovascular and metabolic phenotypes (Bass & Takahashi 2010).

Consequences of output disruption

Peripheral investigations can lend a lot of insight into the role of a gene in the clock. Peripheral clocks have easily measurable outputs, are more elastic than the pacemaker and can entrain to various zeitgebers of various strengths, whereas it takes extensive manipulation to record output from the SCN *in vivo* or to alter the oscillation of the pacemaker (Yoo et al. 2004). In an environment with distinct circadian outputs circadian measures can be clearly assessed.

Peripheral clocks can undergo manipulation whereby the clock mechanism can be tested (Yoo et al. 2004). The size of the outcome of a perturbation on the clock in any given tissue depends on several factors. Firstly, when the molecular event occurs in the circadian cycle affects the outcome. This is because genes are being expressed at high levels at different times in the cycle, so the effect of the manipulation in question could depend on what target it acts on and how highly it is expressed.

Secondly, each tissue clock has a different threshold over which zeitgebers are effective, for example the liver clock can be entrained by feeding but is more strongly entrained by cues from the central pacemaker (Buijs et al. 2013b).

And lastly, effects of molecular manipulation of the clock can be masked by redundancy mechanisms at play in the affected tissue. For example, *CLOCK* knockout animals remain rhythmic due to the

redundancy in the SCN whereby *NPAS2* expression fulfils the role of *CLOCK* in the pacemaker by binding to BMAL1 (DeBruyne et al. 2007). When NPAS2 is also abolished, the animal is arrhythmic. The knockout of *CLOCK* affects peripheral clocks differently and renders them arrhythmic where *NPAS2* is not expressed, therefore no compensation occurs (DeBruyne et al. 2007).

Another example of redundancy in clock mechanisms is that upon knockout of *Cry1*, *Cry2* allows the pacemaker to oscillate, and the reverse is true. CRY ablation only causes arrhythmicity when both proteins are absent from the pacemaker (Anand et al. 2013). In this instance, there is functional redundancy at work although each gene allows the clock to run at different free-running periods due to differences in the kinetics and function of each CRY (Anand et al. 2013).

Surprisingly, the SCN still fires rhythmically in the behaviourally arrhythmic double knockout (Anand et al. 2013). This is similar in the case of *Bmal1* knockout animals which are also behaviourally arrhythmic but maintain rhythmic firing in the SCN and express *Per2* rhythmically as determined using luciferase assays (Takahashi et al. 2010).

1.4: Circadian Behaviour

In order to investigate the clock, circadian behaviour must be investigated with precision and care in interpretation. In the following section I will explore the fundamental elements of behaviour which are intrinsic to circadian function and, in the subsequent section, the methods which can be used to examine them.

1.4.1: Sleep-wake cycles

Circadian rhythms regulate multiple outputs synchronising them to the 24-hour oscillation of zeitgeber cues. The clock is integral to the sleep wake cycle which is an experimentally measurable output.

Sleep timing is synchronised to the external light-dark cycle by the central pacemaker (Ko & Takahashi 2006). Light is processed starting with detection by specialised intrinsically photosensitive retinal ganglion cells (ipRGCs) in the retina. The signals are transmitted directly through the optic nerve to the dorsomedial core of the SCN. The SCN gates sleep signals through direct neural outputs signalling to the VLPO, DMH and lateral hypothalamus (orexin neurons which maintain the awake state) as well as contributing to sleep timing through regulation of the sleep-promoting hormone melatonin (Isobe et al. 2001).

The circadian mechanism regulates sleep timing alongside the homeostatic mechanism (Borbély 1982). The homeostatic mechanism is responsible for the build-up of sleep pressure over the waking day, and promotes the onset of sleep according to the number of hours of waking. Networks involved in the homeostatic process also feed back on and influence the central clock (Borb & Achermann 1999). One example of this interplay is evident in states of sleep deprivation where firing in the SCN is shown to be decreased (Deboer et al. 2007).

Disruption of the pacemaker itself can cause various degrees of change to sleep and activity rhythms. If the pacemaker is abolished in rats, there is little effect on recovery of sleep or total sleep

time suggesting that the homeostatic process maintains sleep-wake regulation (Mistlberger et al. 1983). This also suggests that the role of the SCN in sleep regulation is independent of the homeostatic process (Mistlberger et al. 1983). If the SCN played a role in the homeostatic process, its ablation would be expected to cause insomnia, much like ablation of the VLPO (Mistlberger 2005). In lesioned diurnal squirrel monkeys, however, ablation of the SCN increases total sleep time suggesting that the role of the SCN is not supporting the homeostatic process. Rather this result might suggest an opposing role for the SCN, or a basic role merely to increase arousal (Edgar et al. 1993). As only one study of many on SCN ablation studies concluded this, perhaps this is an exceptional organism. Overall is it widely believed that the SCN plays a role in homeostatic sleep control as well, but the precise pathways at play are still not fully elucidated (Schwartz & Roth 2008).

1.4.2: The link between the clock and neurobehaviour

Sleep and circadian disruption are causally linked to additional behavioural disturbances due to the multiple outputs of the pacemaker (Section 1.3.2.3). Sleep disorders are highly prevalent in all manner of psychiatric illness including Alzheimer's Disease (AD), Huntington's Disease (HD), Anxiety, Schizophrenia and unipolar, bipolar and seasonally variable Depression (Benca 2000; Brunello et al. 2000; McCurry & Ancoli-Israel 2003; Morton et al. 2005; Cohrs 2008). Circadian misalignment in man has been causally linked to mood disorders (Hasler 2010; Emens et al. 2009).

Experimentally, depression and stress have been known to be able to cause disruption to circadian parameters (Savali et al. 2014; Cheeta et al. 1997) and models of circadian disruption often display secondary neuropsychiatric disturbances ranging from the blind-drunk model which displays schizophrenic traits (Oliver et al. 2012) to *Clock* mutants which are hyperactive resembling a manic state similar to bipolar depression as well as displaying hyperhedonia and increased preference for cocaine (Roybal et al. 2007). Multiple elements of behaviour should be investigated when considering novel mutant investigations, as the interplay between the behavioural disruptions and circadian disruptions is extensive.

1.4.3: Models of circadian disruption and neurobehavioural disruption

Mutant models of core clock disruption have been shown to display multiple behavioural abnormalities upon perturbation of the clock.

Period genes are part of the negative limb of the core clock and are necessary for circadian oscillation in mammalian cells including human and mouse. Disruption of one or a combination of *Per* genes have various behavioural consequences demonstrating the importance of both genes as well as the different roles of both. Ablating *Per2* expression causes increased alcohol consumption (Gamsby et al. 2013) and affects anxiety-related behaviour in various ways. Anxiety behaviour is increased in *Per2* knockout animals in the elevated plus maze (spending less time in the open arm, demonstrative of anxiety) and the open field (where some changes in certain measures suggesting anxiety). However, a double knockdown affecting both *Per* genes results in consistent anxiety-like phenotypes across elevated plus maze, light dark box and open field tests (Spencer et al. 2013). Consistent with behavioural investigations in mouse, knockdown of the two genes in the nucleus accumbens (which is thought to regulate stress responses in the mouse and in humans) with RNA interference (RNAi) also caused an anxiety phenotype. Furthermore, in models of social defeat stress which leads to anxiety in animal models, *Per* genes are downregulated in the nucleus accumbens. Treatment of the mood disorder with fluoxetine normalises *Per* gene expression in these animals (Spencer et al. 2013). The conclusions that can be drawn from mutant models such as the *Per1* and *Per2* mutants therefore have far reaching behavioural implications, but initial clarification of the differences between function of the two genes in animal models must be used to direct clinical applications.

Fbxl3 encodes a ubiquitin ligase that degrades cryptochromes, therefore its activity impacts on circadian mechanisms. Homozygous FBXL3 (*Afh*) mutants display a lengthened circadian free-running period of approximately 27 hours (Godinho et al. 2007). The animals also display reduced anxiety-like and depression behaviour as determined using the open field, holeboard, elevated plus maze,

light dark box and forced swim paradigms (Keers et al. 2012). This syndrome is reminiscent of the manic phase of bipolar depression. The mania phenotype observed in this model bears similarity to other models of circadian disruption including GSK3β transgenic mice (which experience circadian shifts in DD and suffer from sleep fragmentation (Ahnaou & Drinkenburg 2011)), *Clock* mutants (homozygotes free running with an approximate period of 28 hours, lengthened similar to *Fbxl3* mutants) and *Prokineticin 2* knockouts (where circadian rhythms are dampened in amplitude although period unaffected), and treatment with Lithium has been shown to ameliorate symptoms in animal models similarly to human bipolar disorder (Kennaway 2010; Prickaerts et al. 2006; Easton et al. 2003; J. Li et al. 2012). This evidence suggests that circadian models can be used in investigation of other behaviours which affect human populations, and that the interplay of the clock and behaviour can be investigated using such models.

1.4.4: Human Genetic disorders

Lessons about genes involved in the clock can be learned through investigating human circadian disorders. Many neurobehavioural disturbances in man are attributed to a plethora of complex combinations of subtle genetic discrepancies and the interaction of individuals with their environment. However, there are some well-characterised familial disorders mapped to a single genetic locus, much like mutations which can be simulated in an ENU model.

The most straightforward example of a genetic circadian disorder in man is Familial ASPS (FASPS) where sleep timing is deregulated (Xu et al. 2005; Toh et al. 2001). FASPS can be attributed to a single loss of function mutation affecting *Per1*, *CK1ɖ* or *CK1ε*. Symptoms include sleep-timing irregularities, poor sleep quality and social and professional disruption, demonstrating clearly the impact of the internal clock being misaligned to environment. This disruption can be seen to cause wider problems than regulation of sleep-wake cycles, for example depression as well as other physical and psychological problems are often comorbid with FASPS cases (Leloup & Goldbeter 2008). *CK1ɖ* and *CK1ε* are responsible for the phosphorylation and degradation of PER proteins, and

their disruption prevents normal degradation of PER proteins and subsequently shortens the period of the clock (Vanselow et al. 2006).

Mouse models of the mutations found in familial FASPS have a short free running period similar to the FASPS patient population (Xu et al. 2005). Such models therefore provide a tool for understanding disease mechanisms in the human patient population. Comparison of one specific targeted mis-sense mutation in mouse and *D. Melanogaster* demonstrates that disrupting even one specific (and conserved) residue across different model systems can cause dramatically different phenotypic outcomes. Whilst in mouse, the $CK1\varepsilon^{T44A}$ mutation causes a short period emulating FASPS in humans, in *D. Melanogaster* the $CK1\varepsilon^{T44A}$ mutation conversely yields a model with a long free-running period (Xu et al. 2005). Understanding the reason why this happens is key to helping patients with specific mutations in such genes. This example supports using a multidisciplinary approach to extensive characterisation of mutations of genes in circadian investigations, using multiple models to ensure accurate representation of the gene function in the clock.

Some human psychiatric disorders with circadian or sleep-wake comorbidities like bipolar disorder have been linked to single nucleotide polymorphisms (SNPs) in circadian genes using association studies based on the results of linkage or GWAS searches (for example, clock genes *Per3*, *Arntl*, *Dec1* and *RorB* (Nievergelt et al. 2006; McCarthy & Welsh 2012; Ersland et al. 2012)). Genome-Wide Association (GWAS) and linkage studies do suffer from the major limitation that detection of SNPs affecting any given parameter is dependent on the size of the effect and frequency of mutation in the population (Manolio et al. 2009). This is an important consideration in searching for circadian regulators in human populations as the contribution of such genes to a circadian perturbation often culminates in a modest change in behaviour. Few studies examine circadian behaviour, most utilising high throughput techniques to screen for changes in gene expression in select tissues or using brief questionnaires to ascertain chronotype. Also, GWAS fails to detect rare SNPs unless the effect on the output is extremely large and easy to separate from the properties of a control sample. Very few

studies encompass enough samples to cover different populations across the globe, most being selective to one continent or country alone. Therefore the investigation of genetic aberrations in human populations is limited, and genetic models must be approached in alternative ways to examine clock mechanisms (Li 2013).

1.5: Changing circadian properties; modelling the clock

1.5.1: Genetic considerations

In dissecting the elements of the molecular clockwork, identification of the gene products involved in the central, peripheral and regulatory clock mechanisms has been of great importance in understanding the role of circadian biology in health and disease. Genetic approaches to investigating an unknown pathway have been accelerated by the sequencing of the human genome (Lander et al. 2001; Schmutz et al. 2004; Venter et al. 2001). Having the sequence available for research has allowed genetic abnormalities to be spotted in affected population studies, and gives information which can be used to manipulate (mutagenize, inhibit with RNAi, knockout or knockin for example) gene and non-coding sequences *in vitro* and more recently *in vivo*. Although the genome has been sequenced and much genetic investigation followed, not all genes have been identified and only a fraction of the functions of genes and non-coding regions have been elucidated. Murine genomes have also been sequenced, and as these mammalian sequences are 99% similar to that of *Homo sapiens* work on such organisms can give great insight into the human genome. The use of mouse in genetic studies pertaining to human disease has been extensively reviewed (Wartha et al. 2014; Schofield et al. 2012; Vijg & Campisi 2008; Rees & Alcolado 2005; Neumann et al. 2011), and a summary of the major advantages of using the mouse as a model organism are listed in Table 1.1. Many strains are available and inbred lines can be maintained simply and manipulated in various ways to examine one gene of interest at a time. *N*-ethyl-*N*-nitrosourea (ENU) mutagenesis is of particular merit in examining gene roles (Justice et al. 1999) as detailed in Table 1.2 and further explored in (Section 1.5.3).

Parameter	Advantage	Disadvantage
Cost	Can be maintained in large numbers	Not as cost effective as invertebrates or plants eg) *C. elegans/ D. melanogaster/ A. Thaliana*
Timescale	Time between generations 63 days, gestation 21 days	Ageing effects different to longer timescale in humans
Genetic considerations	Murine genome sequenced, well characterised and furnished with many tools for manipulation	Still some differences between man and mouse genome
Brain complexity	Networks organised in similar way to other mammals (including human)	Not as complex as human brain processing, especially higher function and emotional processing. Social hierarchy also vastly different to human interactions
Circadian behaviour	Wheel running robust and easy to measure	Wheel running is circadian output, so indirect measure of SCN function
Numbers	Can breed many mice, bigger sample size than human studies	Cannot breed cohorts as vast as eg) Drosophila due to cost/space considerations

Table 1.1: Advantages of mouse models in circadian investigations

Parameter	Advantage	Disadvantage
Bias	ENU mutations are randomly generated, can screen entirely unbiased (forward genetics) or target exon only (reverse genetics)	Gene targeting not available unlike knockouts/TALENs etc. Can target domains through selective screening, but not residues
Variety of phenotypes	Can lead to knockout, knockdown, splicing changes, knock in	Cannot guarantee phenotype for any given SNP. Many human disorders complex and polygenic, only a subset are caused by a single SNP
Translation into human	Human disorders involve genetic changes which can be compared to SNPs induced by ENU	Lack of targeting means exact base pair change not often emulated

Table 1.2: Advantages of ENU mutagenesis in identifying novel mutants

1.5.2: Genetic mutants

The phenotypes of knockout model animals are subject to redundancy and compensation, which may mask deletion of the knockout gene. As such mutant models where the gene is still expressed and compensatory changes do not mask the phenotype can give a different perspective when investigating novel genes (Justice 1999).

Despite its prominent role in the "core clock", *Clock* knockout animals are rhythmic (DeBruyne et al. 2007) because NPAS2 compensates for CLOCK function in the SCN. Only when both proteins are ablated is the animal arrhythmic. In fact, some of the most profound circadian abnormalities are seen in mutants affecting second messenger systems as feedback and all external circadian inputs converge to produce one cellular response in SCN neurons. This response results in changes in SCN firing patterns which involve calcium signalling, cAMP and G-protein signalling molecules (Brancaccio et al. 2013; Levine et al. 1994; Takahashi et al. 2010). Ablation of Gq activity in a subset of cells in the SCN produced marked changes across the SCN through changing expression of TTFL components (Brancaccio et al. 2013). The circadian impact of such perturbations is quite evident, but the second messenger systems are not a part of the core clock. Rather they are merely necessary for continuing clock function, not sufficient in themselves (O'Neill & Reddy 2011). Experiments using second messenger mutants must be interpreted with care due to the multiple off-target effects of disruption of second messengers. This mechanistic discrepancy must be examined carefully in novel mutant studies.

Mutations affecting SCN itself or output signalling can have wide ranging consequences for phenotypes across many peripheral tissues as synchrony is disrupted (Bechtold et al. 2010). For example, mutation of the SNAP25 protein (*Bdr*) primarily affects neurotransmitter release from vesicles involving the SNAP-SNARE complex. *Bdr* displays profound effects on circadian behaviour due to alteration of SCN output function (Oliver et al. 2012). Paracrine hormone *Vip* knockouts display many circadian disruptions due to weakening of the SCN synchrony itself without affecting

the oscillation of the core clock components, again affecting multiple outputs (Maywood et al. 2011) and *Opn4* knockout animals have reduced inner retinal sensitivity, circadian disruptions and an abnormal pupillary light response as well as being linked to development of Seasonal Affective Disorder (SAD) phenotypes all due to disruption of the iPRGC input to the SCN (Panda et al. 2002; Roecklein et al. 2009; MGI website).

Disruption of peripheral clocks (outputs of the pacemaker), have more specifically localised phenotypic consequences affecting multiple peripheral systems across the organism (Bechtold et al. 2010; Tokonami et al. 2014; Hastings et al. 2007; Lefta et al. 2011).

1.5.3: ENU mutants

Of the multiple ways used to generate genetic variants in mouse, ENU mutation has many advantages over alternative methods as explored in the following section.

ENU is an alkylating agent, and alkylations occur through transfer of an ethyl group to the nucleophilic site of the DNA base, which causes generation of mismatched base pairs (Justice et al. 1999). Mutations consist of mainly but not exclusively AT to TA transversions or AT to GC transitions (Barbaric et al. 2007). When injected intraperitoneally into male mice, ENU induces mutations randomly through the genome crucially affecting spermatogonial stem cells at a frequency of approximately 1 in 1000 gametes. Males undergo a period of sterility after which progenies can be generated, and heritable mutations can be investigated over subsequent generations. Mutations can be detected in the offspring of these male mice at a frequency of 1 in every 1.83Mbp of sequence (Keays, Clark, et al. 2007). The random nature of the event allows for the generation of mutants in any region of the animals' DNA, including uncharacterised regions as well as in characterised sequences containing known genes or regulatory sequences.

ENU can cause missense mutations (approximately 64%), nonsense mutations (approximately 10%) or splicing variants (approximately 26%) (Justice et al. 2000). This can lead to various phenotypes

including hypermorphs (gain of function), hypomorphs (loss of function), neomorphs (dominant gain of function), nulls and antimorphs (dominant loss of function) (Godinho & Nolan 2006; Quwailid et al. 2004). The subsequent gain or loss of function can be partial or complete and recessive or dominant in nature, with or without change in structure of gene product, or even entail truncation due to an early stop codon. This can be utilised in a varied approach to manipulating the function of a gene, and it is possible to generate an allelic series in a given gene which may not be possible with knockout animals. It also must be clarified which of these alterations has occurred when characterising and concluding findings using novel mutant models.

The Harwell ENU Archive

The Harwell ENU archive was generated by injection of male founder mice with an appropriate dose of ENU. Following a period of recovery G1 mutant offspring can be generated. Genetic material from the mutagenized male founder is archived freezing parallel sperm and DNA samples from G1 progeny of ENU-mutagenized animals (Fray 2009a; Fray 2009b). The 100000 sample DNA archive at MRC Harwell has successfully been used in gene driven approaches (reverse genetics). Animals at MRC Harwell are also tested in unbiased circadian locomotor screens of G1 animals for phenodeviants in order to identify potentially novel clock modifiers (forward genetics) (Acevedo-Arozena et al. 2008).

Genetic approaches to identifying novel mutants

The relative merits of reverse and forward genetics approaches are summarised in Table 3. Reverse genetic interference with gene function can be achieved in multiple alternative ways including gene-targeting, RNA interference, knock outs and most recently targeting with nucleases such as Transcription Activator-Like Effector Nucleases (TALENs) or Zinc-Finger Nucleases (ZFNs), and even CRISPR-Cas9 (Ran et al. 2013). As well as the relative simplicity and cost effectiveness of ENU, for the purposes of an unbiased mutation screen, and in looking at multiple alleles, ENU holds the advantage over these techniques and is therefore implemented in the current investigation.

PARAMETER	FORWARD GENETICS	REVERSE GENETICS
Phenotyping	Must use appropriate and high powered phenotyping to detect mutants	Mutation is in gene of interest, phenotype can be subtle
Dominant or Recessive?	Will only see phenotype in dominant animals unless phenotype G3 animals	Screen for mutant, can generate Het and Hom animals for phenotyping
Bias	Unbiased	Biased: target sequence investigated only
Genotyping	Gene must be mapped and mutation sequenced to develop an assay	Identification of mutants gives precise detail of nature of mutation to develop assay

Table 1.3: Advantages and disadvantages of forward and reverse genetics approaches to identifying novel mutants

1.5.4: Mutation detection

The nature of an archive screen guarantees transmission of mutations through the germline, the accurate detection of the mutation can be achieved using many techniques. Past screens have been performed using denaturing high-performance liquid chromatography (Quwailid et al. 2004) or temperature gradient capillary electrophoresis (TGCE) (Murphy et al. 2002), most recently a more sensitive heteroduplex detection assay has been used in high throughput screens (Anand et al. 2013). Detection of SNP mutations in mice can be complicated, and forward genetic approaches from the Harwell ENU archive begin with the identification of a phenotype. In the current investigation, SNPs are detected using a sensitive heteroduplex detection assay (Figure 1.3).

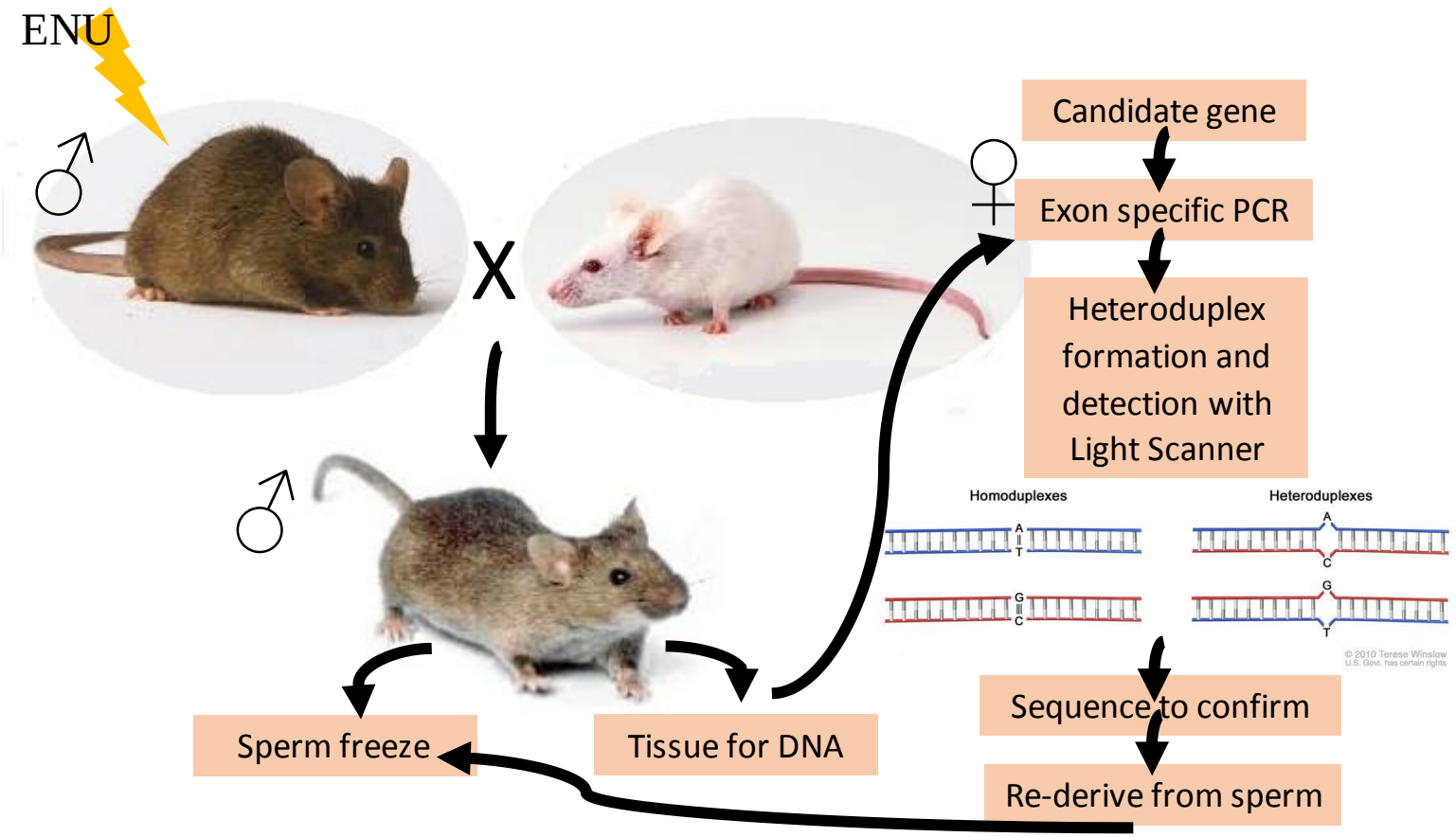

Figure 1.3: Schematic of Light Scanner screening and heteroduplex detection

ENU mutagenized male mice are bred with females to produce mutant G1 (Generation 1) offspring. Sperm is frozen from the G1 is frozen for use in In vitro Fertilisation (IVF) for re-derivation. DNA is frozen from the G1s. Screening is undertaken with exon-specific primers in a Light Scanner assay which identifies heteroduplexes. Heteroduplexes arise where mutations cause a mismatch in DNA sequence. These DNA strands melt faster than homoduplexes with complementary base pairs bound together. Upon identification, mutations are sequenced to confirm the base pair change and animals of interest re-derived by IVF

1.5.5: Forward genetic screening

The Harwell phenotyping pipeline is designed to identify novel mutations by screening for phenodeviants. It includes a circadian wheel running screen to identify individuals with changed locomotor activity, and investigate their circadian properties. The format of the wheel running screen is illustrated in the double plotted actogram (Figure 1.4). Briefly animals are singly housed in cages with running wheels, and their activity is recorded using these wheels. They are entrained to a light dark schedule of 12 hours of light followed by 12 hours of dark (LD). Once entrained, the animals are exposed to total darkness for 2 weeks (DD) which allows rhythms to free-run. Finally the animals are exposed to constant light (LL) to explore their response to light and continued behaviour in constant conditions. Currently animals are also being aged before being screened so any age-related development of circadian dysfunction is also under investigation (Oliver & Davies 2012). Circadian mutants identified using forward genetic techniques (from a screen looking for phenodeviants in circadian wheel running) include the *Afh* mutant and short circuit (Godinho et al. 2007; Bacon et al. 2004). The same screens used to identify phenodeviants in such high-throughput forward genetic screens will be used to screen for relevant circadian phenotypes in the novel mutants in the current investigation.

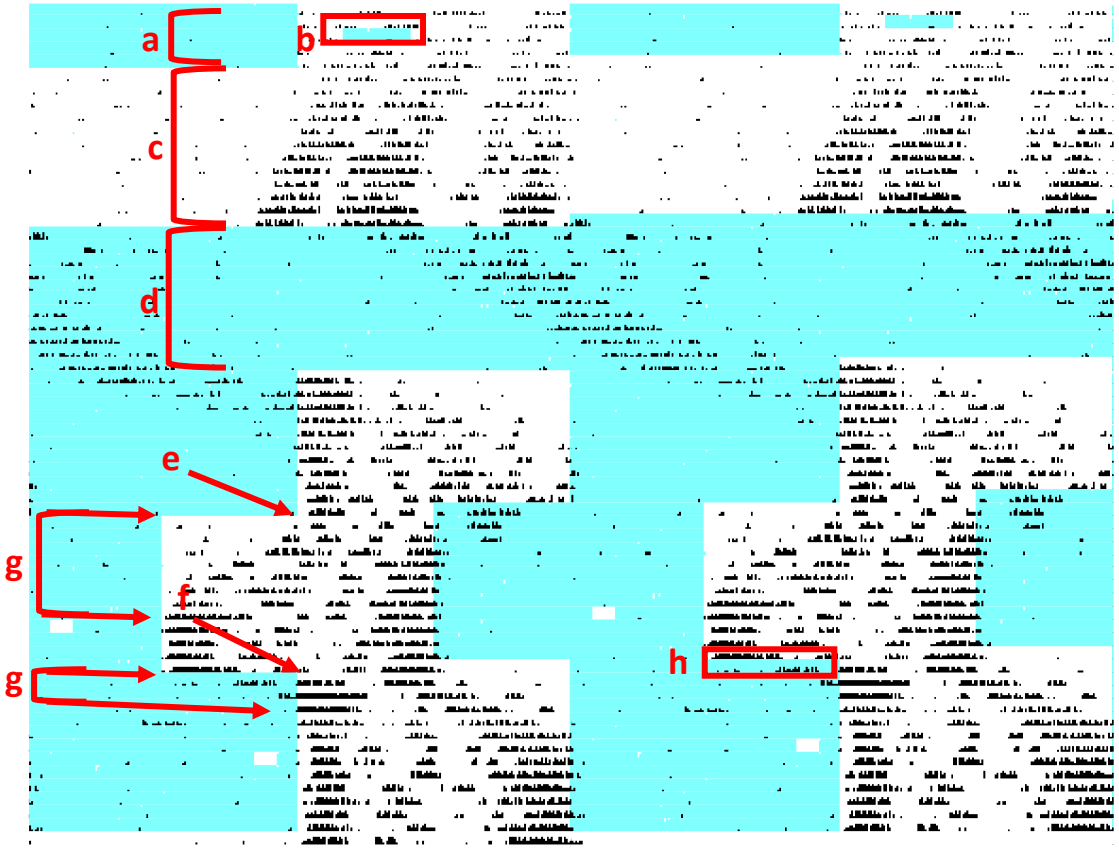

Figure 1.4: The wheel running screen

Animals are entrained to a light:dark (LD) cycle of 12 hours Light followed by 12 hours dark (a). During the LD screen, animals onset and activity levels are measured. On day 5 of the LD screen, a three hour light pulse is administered at ZT 14 (b). The activity of animals exposed to light during the dark phase is supressed due to a circadian phenomenon called masking. Next animals are allowed to free run in constant darkness (DD) to expose the endogenous rhythm generated by the SCN of the animal (c). And then the animals are exposed to constant light (LL) (d). Circadian period and length of activity is recorded through DD and LL. Animals are then allowed to re-entrain to LD, and the LD cycle shifted forwards by 6 hours (e) to examine the animals' response to a phase shift, followed by a 6 hour shift backwards (f). The number of days for the animal to re-entrain is measured (g), as well as the activity remaining out of phase with external light conditions for the backwards shift (h).

1.5.6: Cell based systems

The cell based system chosen to explore circadian function is of great importance and can impact the conclusions which can be drawn from the investigation. The choice of cell based system for circadian investigations is based on the cells' robustness in long-term recording or through treatment with chemicals such as transfection reagents, the achievable yield of overexpressed constructs, the availability of reporters for bioluminescent recordings and the circadian properties of the cells (Ramanathan et al. 2012).

In the current investigation, U2OS cells and rat-1 fibroblasts were used in compound screening due to the ability to record bioluminescent rhythms effectively, HEK293 cells for interaction studies due to their high tolerance for overexpression of constructs, and (despite the intensive nature of the work) organotypic SCN slices were used as an *ex vivo* SCN model as cell-cell interactions were maintained, and it was not possible to characterise the SCN-specific pacemaker or neural properties of SCN2.2 cells (Appendix 2).

1.5.7: Reporters

Reporters are essential to be able to quantify circadian output experimentally. Molecular circadian rhythms consist of a complex loop of gene expression and physiological effectors are regulated by the molecular clock. In historic circadian experiments, cells and tissues were looked at using samples from time points across the 24 hour circadian period, and markers such as mRNA probes were used to define the phase of oscillation of circadian clock (Millar et al. 1992). Gene expression levels can now be accurately quantified at time points using quantitative PCR techniques, although this is a highly invasive and labour intensive way to examine the clock. More recently still, circadian investigation has developed to monitoring circadian gene expression in real time using reporters such as luciferase, driven by the promoter regions of endogenously expressed circadian genes (Millar et al. 1992). Transient expression of reporters has been surpassed by stable cell line expression of

reporters and reporter animals (Ramanathan et al. 2012). Luciferase assays have been shown to be both accurate and easily quantified, tracked over long time periods and even imaged in individual cells over time (Yamazaki & Takahashi 2005; Welsh et al. 2005; Hastings & Herzog 2004; Hastings et al. 2005). Recent developments in technology even allow for the real time monitoring of circadian promoter driven luciferase activity *in vivo* in freely moving animals (Saini et al. 2013). Reporter cell lines as well as mice were utilised in the current investigation. As well as approaching the function of genes by mutation and so manipulation of their function, in this investigation, pharmacological manipulation was also undertaken to support circadian conclusions from *in vivo* and *in vitro* mutant assays. Of particular interest is the interaction of *Kdm1a* and *Kdm1b* genes and MAOIs (a subclass of antidepressant treatments) with respect circadian output. The use of screening and subsequent development of more specific compounds could contribute to the investigation of novel gene function in the clock.

1.6: Lysine specific Demethylases

As clock mechanisms are dynamic and complex, the identification and characterisation of novel regulators of the clock is of interest and importance in understanding the overall mechanisms at play. This investigation examines the role of putative regulators of the clock; lysine specific demethylases (LSDs).

LSDs are flavin adenine dinucleotide-dependent (FAD) amine oxidases. They have been characterised as histone modifying enzymes which affect gene transcription (Shi et al. 2004; Fang et al. 2010). 17 Lysine Specific Demethylase genes are expressed in humans, and of these, KDM1A (hereby referred to as LSD1) and KDM1B (hereby referred to as LSD2) are the most abundant and best studied.

1.6.1: LSD1

LSD1 was the first identified lysine demethylase (Shi et al. 2004). *Kdm1a* is expressed ubiquitously (Zhang et al. 2010; MGI website), plays wide ranging roles in development, cell cycle regulation and is over expressed in many cancer cell lines altering the expression of a wide variety of genes. LSD1 forms complexes with several histone modifying mediators including many HDACs, for example SIRT1 (Konovalov & Garcia-Bassets 2013; Suzuki & Miyata 2011). It has also been shown to play a role in neural systems including response to ischaemia, development of pyramidal cells and memory formation (Fuentes et al. 2012; Neelamegam et al. 2012).

LSD1 specifically demethylates di- and tri-methyl H3K4 residues in an FAD-dependent manner (Shi et al. 2004; Stavropoulos et al. 2006; Chen et al. 2006; Forneris et al. 2007; Culhane & Cole 2007). The LSD1 crystal structure has been elucidated. The LSD1 protein consists of an FAD cofactor binding domain, a SWIRM domain responsible for targeting of LSD1 to its appropriate substrates, a tower binding domain responsible for CoREST cofactor binding and a catalytic amine oxidase domain which mediates the demethylation reaction (Figure 1.5) (Stavropoulos et al. 2006; Chen et al. 2006).

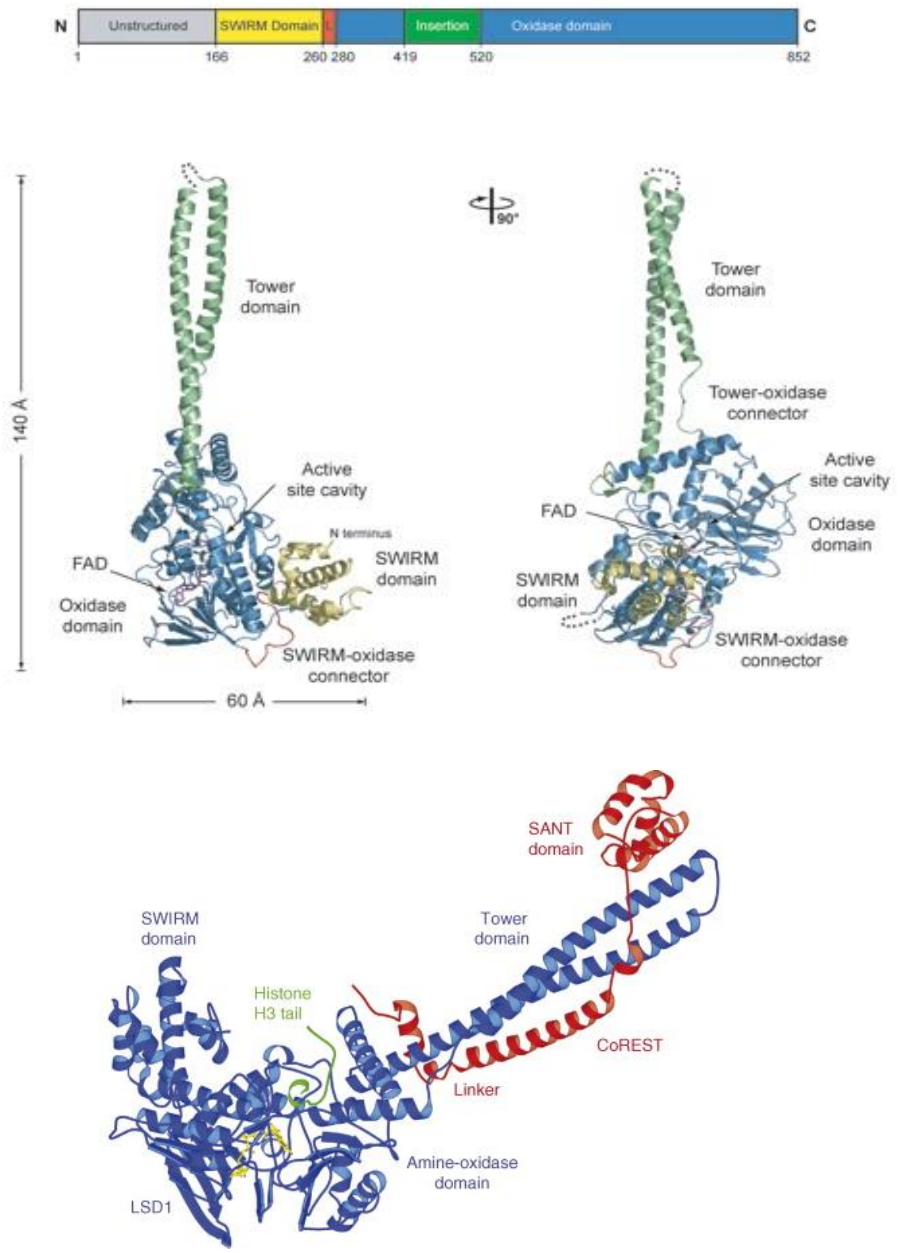

Figure 1.5: Structure of LSD1

The crystal structure of LSD1 has been fully elucidated. LSD1 has a SWIRM domain responsible for targeting LSD1 binding to histone H3K4, a catalytic amine oxidase domain and two cofactor binding sites, the C-terminal FAD binding domain and the tower domain responsible for CoREST binding. (Chen et al. 2006; Stavropoulos et al. 2006; Forneris et al. 2007)

1.6.2: LSD1 and CoREST

CoREST is the primary cofactor of LSD1 (Forneris et al. 2007). *CoREST (RCoR1)* is a member of the REST corepressor gene family and is essential for the repression of neuronal specific genes in non-neuronal cell lineages. The nuclear corepressor NCoR1, a protein related to CoREST, has no known circadian role but has been shown to bind to REV-ERBα (Kumar et al. 2010). CoREST acts as a part of the chromatin modifying RE-1 silencing transcription factor/neuronal restricted silencing factor REST:NRSF complex, some effects mediated in complex with LSD1 and BHC, and others independent of LSD1 (Lunyak et al. 2002; Humphrey et al. 2001; You et al. 2001; Hakimi et al. 2002). CoREST plays putative roles in Alzheimer's disease mechanisms and retinal growth cone development with regards neural functioning (Jarriault & Greenwald 2002; Baudet et al. 2011). CoREST is predicted to act as a scaffold for the assembly of repressor machinery (You et al. 2001; Humphrey et al. 2001) and it was shown that the SANT domain of CoREST is required for repressor function (You et al. 2001). CoREST binds to the tower domain of LSD1 and is essential in nucleosomal demethylation (Lee et al. 2005; Yang et al. 2006). CoREST binding acts structurally as a nanoscale binding clamp in order to improve LSD1 demethylase activity by increasing LSD1 stability (Baron & Vellore 2012; Shi et al. 2005). It must be considered in the following investigation that abolishing CoREST in cell systems should not impair all LSD1-mediated demethylation, merely reduce it.

1.6.3: LSD1 interactions

LSD1 acts in large chromatin modifying complexes, and the wide range of interactions of LSD1 must be considered in characterising exactly how it modifies chromatin affecting the clock.

LSD1 is regulated by its associated factors; positively by CoREST and negatively by BHC80 (Shi et al. 2005). It also interacts with SIRT1 (Mulligan et al. 2011), and has been shown to demethylate non-histone targets such as p53 and DNMT1 (Huang et al. 2007; Wang et al. 2009). Therefore when

manipulating LSD1 function, the activity of many LSD1-containing complexes may be affected which could influence epigenetic mechanisms or the clock.

1.6.4: LSD2

LSD2 was identified as a novel FAD-dependent demethylase (Karytinos et al. 2009). The LSD2 sequence is 18% homologous to that of LSD1 (Chen et al. 2006), and has also been shown to modulate gene expression through demethylation of H3K4 (Yang et al. 2010; Fang et al. 2010; Ciccone et al. 2009). LSD2, unlike LSD1, hasn't been shown to form complexes with histone deacetylases and has been shown to localise to chromosomes during mitosis, so may play a role in gene regulation during mitosis that LSD1 does not (Yang et al. 2010). LSD2 can repress transcription without its catalytic amine oxidase domain (Yang et al. 2010). LSD2 also plays a role in imprinting (Ciccone et al. 2009). Knockout animals are viable, although females exhibit reproductive deficits as oocytes from catalytic null mutant females exhibit suppression of vital imprinted genes which is lethal mid-gestation (Ciccone et al. 2009). Therefore it can be difficult to produce colonies for investigation (MGI website).

A Proline to Alanine mutation in human LSD2 has been identified in patients with gonadal dysgenesis (Personal Communication Dr A. Greenfield, MRC Harwell), and therefore this suggests that LSD2 plays a role in the reproductive system in humans. LSD2 is expressed more specifically in nervous tissue in embryo (including retina), and at low levels in the limbs, respiratory and reproductive and urinary systems (Visel et al. 2004), and as such might play a more specific and central role in rhythms. Its expression level in adult SCN has yet to be ascertained. These properties of LSD2 should be analysed in the investigation of its role in circadian behaviour.

1.6.5: Catalysis by LSD activity

LSD1 and LSD2 both act to oxidise an amine-methyl group on H3K4 utilising FAD as a cofactor (Figure 3.5) (Suzuki & Miyata 2011). LSD1 and LSD2 have both been shown to be inhibited by amine oxidase

inhibitors including tranylcypromine, a well-known antidepressant (Gooden et al. 2008; Binda et al. 2010; Suzuki & Miyata 2011). The existence of shared catalytic properties and shared cofactors allows for the molecular manipulation of catalysis by both LSD proteins simultaneously in *in vitro* and *in vivo* investigations, through FAD level manipulation or through administration of MAOIs such as tranylcypromine.

Both LSD1 and LSD2 have demethylase-independent roles (Yang et al. 2010; Nam et al. 2014), so it must be discerned whether the circadian effects of LSD mutations in the current investigation are independent of the catalytic demethylase activity (rather depend on substrate binding alone) or independent of histone function as discussed more thoroughly in Section 1.6.7.

1.6.6: ENU and LSDs

The *Kdm1a*$^{-/-}$ animal is embryonic lethal, due to gastrulation deficits (Wang et al. 2009) and *Kdm1b*$^{-/-}$ animals display reproductive deficits (Ciccone et al. 2009). In order to examine the role of LSD1 in circadian behaviour (an adult phenotype) LSD1 activity must be knocked down but not abolished (either a hypomorph or a gain of function alteration such as a neomorph or hypermorph), or be knocked out conditionally (in a tissue or time specific manner to avoid the developmental effect of its loss). Screening the Harwell ENU archive allows for hypothesis driven investigation of *Kdm1a* and *Kdm1b* genes and screening of specific domains of interest.

1.6.7: Histone modifiers

Histone function

Epigenetics (literally meaning 'above genetics') encompasses the study of regulation of gene expression via modification of its accessibility for transcription. Epigenetic histone modifications have been linked to circadian rhythmicity and entrainment (Masri & Sassone-Corsi 2010; Ripperger & Merrow 2011; Sahar & Sassone-Corsi 2012). Histone deacetylases (HDACs) such as SIRT1 play a role in regulating the core clock (Asher et al. 2008), and histone methyltransferase (HMT) MLL1 upregulates circadian gene expression by methylation of H3K4 (Katada & Sassone-Corsi 2010). However, at the outset of the current investigation no studies had examined the role of demethylases or LSDs in the clock. Transcriptional scaffold proteins known to regulate chromatin structure have also been shown to partially mediate the circadian negative feedback loop (Duong et al. 2011).

Histones function dynamically to modify the properties of the chromatin structure of DNA, thus regulating the expression patterns of genes. Histone modifications can have the effect of either loosening or tightening the wrapping of DNA about a histone, and as such make it more or less accessible to transcriptional machinery, and so directly impact on gene expression. The acetylation, methylation and phosphorylation state of histones at different residues can repress or enhance the expression of genes encoded by the DNA associated with that histone (Kubicek & Jenuwein 2004). Transcriptional regulators are also differentially recruited to sites to modulate gene expression depending on the structure of the chromatin wound around the histone. As well as histone manipulations, different combinations of histone variants, chromatin remodelling (energy-dependent movement of nucleosomes) and methylation of DNA itself can affect gene expression.

Histone acetylation

Histone acetylation is the most extensively studied of these modifications in circadian biology; acetylation at specific residues is traditionally associated with transcriptional activation and acetylation patterns have been linked to clock function (Etchegaray et al. 2003). CLOCK itself has been associated with histone acetyltransferase activity at histones H3 and H4 (Hirayama et al. 2007; Doi et al. 2006) as well as acetylating Lys537 of its binding partner BMAL1 (Hirayama et al. 2007). Modifiers external to the core clock can also regulate the clock by modifying histone acetylation. SIRT1 binds CLOCK and regulates deacetylation of BMAL1 as well as histones (Asher et al. 2008). SIRT1 has been shown to play a role in circadian regulation in vivo with liver-specific mutants (Nakahata et al. 2008). SIRT1 is of particular clinical relevance as it acts in an NAD+ dependent manner as a putative energy status sensor, and so might provide a mechanistic link as to why circadian disruption has metabolic repercussions (Asher et al. 2008).

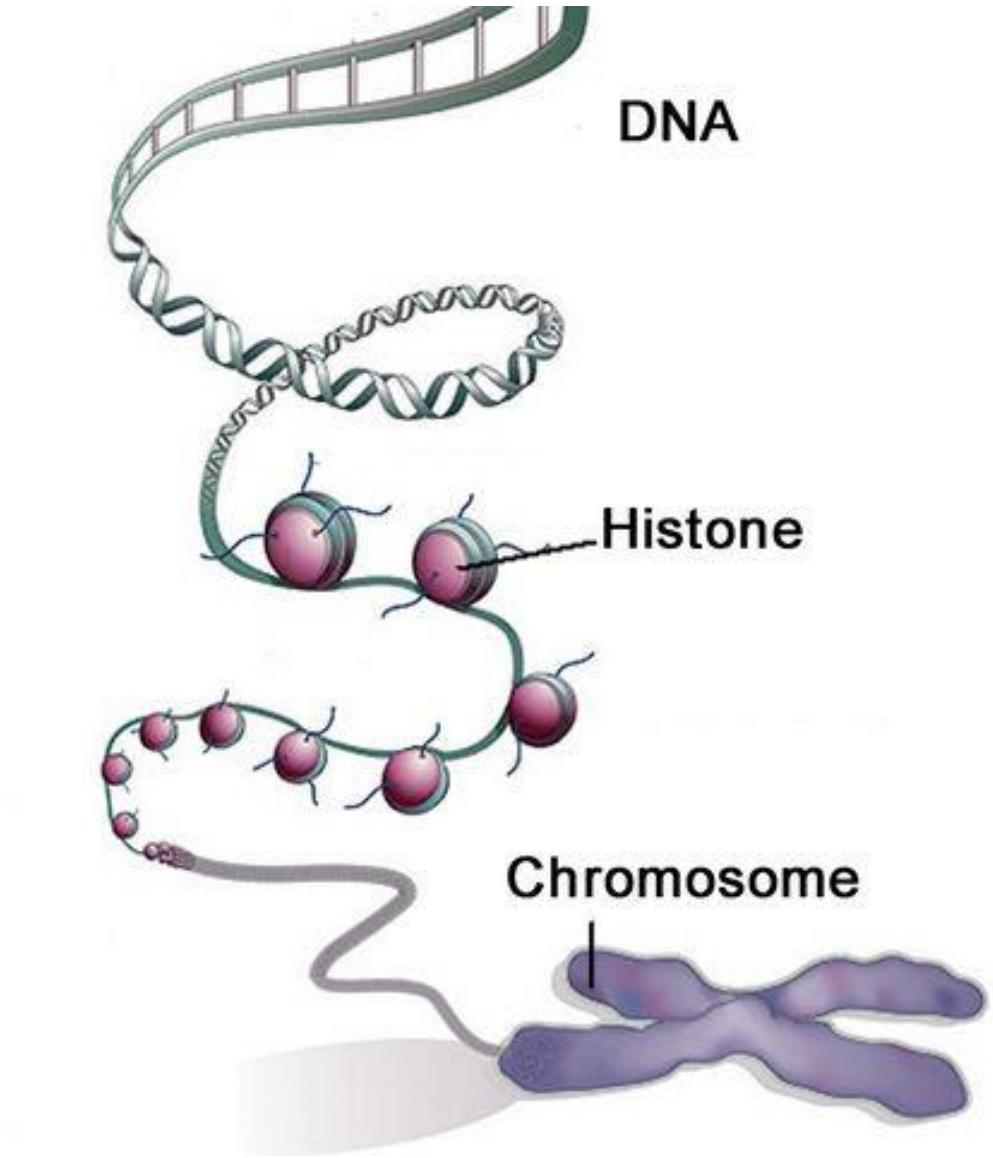

Figure 1.6: Histones are globular proteins that act to compact DNA sequence.

Histones oligomerise into octameric structures, the histone tails exposed on the surface, which can then be reached by modifier enzymes to phosphorylate, acetylate or methylate residues. Such post-transcriptional regulation modifies access of transcriptional machinery to the DNA, so controls gene expression.

DNA itself can be methylated (methylation characteristic of repression of gene expression) and is wound round the histone octamers in a string of DNA. Histones wind up together over H1 to form a structure called chromatin. Chromatin compresses further during mitosis to form chromosomes which can be replicated. Chromatin compacts to form denser heterochromatin in stable nuclei, denser areas being less accessible to transcriptional machinery and the genes contained therein less expressed than in the remaining euchromatin.

Image from http://becuo.com/histones

Histone methylation

As well as acetylation, histones can be mono, di- or tri-methylated at several distinct sites affecting histone function (tyrosine and lysine residues). Methylation of particular residues (unlike phosphorylation or acetylation) correlates strongly with the function of the histone, resulting in either an increase of gene expression or a decrease depending on the site (Kubicek & Jenuwein 2004). The role of demethylation in the clock has only been recently broached.

Some known circadian mechanisms have been linked to histone methylation states. Methylation of residues by MLL1 has been investigated and shown to promote trimethyl H3K4 (H3K4Me3) which activates expression of various circadian genes (Katada & Sassone-Corsi 2010). Methyltransferase EZH2 has also been shown to associate with CLOCK-BMAL1 complexes and mediates transcriptional repression at Period gene promoters. Period-associated protein WDR5 acts to modulate the methylation of lysines H3K4 and H3K9, mediating repression of *Per* and *Rev-erbα* gene expression (Brown et al. 2005). Jumonji-C domain containing demethylases have been shown to affect circadian function in *A. Thaliana* (Lu & Tobin 2011). JARID1a is involved in demethylating H3K4Me3 (DiTacchio et al. 2011) and moreover inhibits HDAC1 and activates CLOCK:BMAL1 mediated transcription in an unknown demethylase activity independent manner (DiTacchio et al. 2011).

LSD1 itself has been shown to play a PKCα-dependent role in phase resetting of the clock (Nam et al. 2014). A screen for LSD1-interacting proteins identified PKCα, and PKCα was confirmed to phosphorylate LSD1 on Serine 112. In the same study, co-immunoprecipitation (CoIP) experiments demonstrated that LSD1 binding to CLOCK:BMAL1 was affected by mutation of the phosphorylation site ($LSD1^{S112A}$), and $LSD1^{S112A/S112A}$ animals displayed a reduced rhythmicity in core clock gene expression and in phosphorylation of LSD1. Luciferase assays on *Per2* gene expression confirmed that LSD1 phosphorylation was necessary for its rhythmic expression in the SCN. Luciferase driven by E-box containing promoters was also disrupted in $LSD1^{S112A/S112A}$ animals, suggesting that LSD1 plays a role in recruitment of CLOCK:BMAL1 to E-box containing promoters (Nam et al. 2014)

There is also interplay between acetylation and methylation at specific sites on histones. Methylation patterns can direct acetylation surrounding the inactive portion of chromatin, and conversely acetylation has been shown to increase demethylation, and this has been specifically demonstrated at the H3K4 site (Cervoni & Szyf 2001; Maltby et al. 2012). MLL4 is a methyltransferase which has been shown to methylate H3K4, affected by histone acetylation (Nightingale et al. 2007). MLL1 methylates H3K4 and subsequently influences H3 acetylation (Katada & Sassone-Corsi 2010). This methyltransferase has been implicated in NFkB signalling (Wang et al. 2012) and more recently has been shown to play a role in regulation of the liver clock (Kim et al. 2014). The investigation of LSD mechanism therefore requires not only exploration of methylation of histone and other substrates, but investigation of acetylation and other associated histone changes.

DNA Methylation

DNA methylation affects gene expression, methylation of cytosine and adenine residues at specific DNA sites results mainly in silencing of expression, although the mechanism by which demethylation happens has not yet been elucidated. DNA methylation is employed in imprinted gene mechanisms (methylation marks which are carried through generations) and as such led to the idea that methylation might be permanent in nature until the recent identification of enzymes responsible for DNA demethylation (Shi et al. 2004). DNA methylation has more recently been shown to occur and possibly contribute to memory function and cognitive mechanisms (Day & Sweatt 2011) and has been shown to undergo dynamic changes (Day & Sweatt 2011) within a circadian time-frame (Brown et al. 2007). LSD1 activity is essential for maintaining DNA methylation through direct demethylation and stabilisation of DNA Methyltransferase 1 (DNMT1) (Wang et al. 2009). Therefore LSD1 may impact on DNA methylation through effects on DNMT1, which may mediate dynamic events such as circadian rhythms which must be considered during the course of the current investigation.

1.6.8: Aims

The circadian clock is complex and under several molecular levels of regulation. Although the core components of the clock are becoming ever better characterised, there is still the possibility that more regulators and components exist. The field of epigenetics has been expanding and techniques now allow for its manipulation and investigation in circadian research.

The identification and clarification of circadian mechanisms bears the potential for not only understanding the mechanism, but for intervention which could benefit people day to day; those suffering from circadian disorders, from psychological illness involving circadian disruption, from illnesses and syndromes with circadian elements and individuals required to adapt to rapid changes in circadian environments (for example, jet lag).

The roles of LSDs in circadian mechanisms are uncharacterised, but preliminary findings suggest they might play a role in clock regulation. The aim of the current investigation is to identify and re-derive ENU mutant models of LSD1 and LSD2 dysfunction and use these models to characterise the role of LSDs in the clock.

We hypothesise that LSD1 and LSD2 play a role in regulation of the molecular clock. This will be tested using in vitro characterisation of LSD-expressing constructs in cell-based assays, recording clock oscillations using luciferase reporters. A compound screen will be performed to confirm any findings. We hypothesise that LSD mutants can be identified through screening the Harwell ENU mutant archive and that upon rederivation the animals will survive and be viable. In this way we expect to be able to characterise the circadian phenotypes of the adult mutant animals. Animals will be assessed with various circadian screens and light dark manipulations, as well as looking at oscillation in *ex vivo* SCN slices and native gene expression in liver and SCN tissues.

The mutants will undergo a battery of behavioural tests to examine any other behavioural abnormalities, with special attention being paid to neurological considerations and circadian-related

syndromes which might relate to human disorders. The phenotyping battery will examine endophenotypes associated with depression primarily anxiety using open field, fear conditioning, startle response and social dominance, and secondarily tests of wellbeing such as digging and marble burying. To exclude any confounding behaviours motor ability, cognition and broad histology will also be assessed.

Chapter 2

METHODS

CHAPTER 2: Methods

2.1 Animals

2.1.1 Animal Husbandry

Animals were housed in the Mary Lyon Centre (Harwell) or The Department of Ophthalmology, Oxford University Ward 7 (John Radcliffe Hospital). Animals were kept in individually ventilated cages with ad lib access to food and water in a 12:12 light dark cycle, checked daily and cleaned regularly. Care of animals complied with the ASPA Act 1986 (Ammended 2012) and under guidance of the Medical Research Council 2013. Home office project licences 30/2686 and 30/3206 and personal licence 30/8882 detail all procedures followed. On the ward prior to circadian screening and throughout phenotyping, mice were weaned at 20 days of age and group housed in groups of 5 or less per cage. Following all experimental procedures and breeding, animals were culled according to Schedule 1 by cervical dislocation, in a designated area.

2.1.2 Screening the Harwell ENU Archive for ENU Mutants

In order to identify novel mutants using the Harwell ENU archive, heteroduplex screening was undertaken with the Light Scanner (Idaho Technology) (Quwailid et al. 2004). The Harwell ENU archive of DNA and corresponding sperm contains approximately 10000 frozen samples from ENU-mutagenised male F1 mice. For screening, samples are pooled into groups of 4 individuals and kept refrigerated at 4°C.

In order to amplify the DNA encoding the domains of interest and so search for mutations, PCR based assays amplifying exons 10, 11, 12 and 19 of LSD1 and 6, 7, 9 and 10 of LSD2 were developed. Light Scanner PCRs were developed as the heteroduplex detection discriminates between misaligned sequences as detailed previously (Section 1.5.4, Section 3.2). The DNA from G1 animals in the archive contains one allele inherited from the mutagenized founder, and one wild-type allele.

Therefore mismatched sequences form heteroduplexes which can be detected in the Light Scanner assay (Figure 3.7).

To develop the assay for heteroduplex detection in the exons of interest, the LS Grad PCR program (Table 2.7) was run using control (wild type C57BL/6) DNA at 5ug/ml in the (Table 2.2) using dark framestar 96-well plates (Cadema bioscience). Amplified exons were put through a Light Scanner analysis to check for a normal clear melting curve before running on 2% agarose gels to confirm amplification, clarify the exact annealing temperature and check for a strong, clear single band representing a single (specific) amplified product of an appropriate molecular weight.

Using the primers and PCR programs optimised for heteroduplex screening (LS51, LS56, LS60 and LS63) (Table 2.7), all pooled archive DNA samples were then screened for mutations in selected regions of LSD genes using the Light Scanner (Quwailid et al. 2004). Heterodimerisation of mutant sample DNA was identified as described in (Section 1.5.4). As potential outliers were identified, the individual DNAs comprising pooled samples were separately re-screened, and heteroduplexes confirmed (Section 1.5.4) (so confirming the individuals with mutations in LSD1 or LSD2). As well as confirmation using the Light Scanner, mutations were verified by sequencing.

***In silico* Analyses**

Wild type and mutant LSD1 and LSD2 sequences were entered into structure prediction software NFold3, Phyre, Polyphen and Sift for analysis (NFold3 website.; Phyre2 website.; Polyphen website; SIFT website.). Three dimensional Figures were generated using PyMOL (Pymol website).

2.1.3 Re-derivation of ENU mutant animals by IVF

Mouse lines containing mutations of interest were re-derived by IVF. Appropriate sperm samples from the Harwell FESA archive were used to fertilize C57BL/6 oocytes *in vitro*. Oocytes were then implanted into recipient females. Resulting offspring were screened using the Light Scanner for the mutation of interest and selectively bred until congenic (Table 2.1). (Acevedo-Arozena et al. 2008)

2.1.4 Backcrosses

Animals were backcrossed to a C57BL/6 background, and intercrossed after 2 generations (early backcross) and 5 generations (late backcross) to produce homozygote animals for phenotyping. The intercross progeny from early backcross animals (Table 2.1) were used for preliminary circadian screening. Intercross progeny from the late backcross (Backcross 5) (Table 2.1) were used for full circadian screening and detailed behavioural phenotyping. Breeding continued to congenicity (10^{th} backcross) (Table 2.1) for storage of mutant DNA and sperm sampling and archiving.

Backcross	Name of stage	Animals used for
IVF (1)	G1	Preliminary screen (2 animals to check for running), breed to generate mutant lines
2	Early backcross	Preliminary screen
5	Late backcross	Final screen
10	Congenic	Freeze down to store DNA and sperm

Table 2.1: Backcross stages

2.1.5 Genotyping

In order to collect DNA for genotyping, animals were ear clipped at weaning. DNA was extracted from the tissue by sodium hydroxide digest (adding 100µl 50mM NaOH and incubating at 90°C for 90mins using Ear Biopsy PCR program) before quenching with 10µl pH5 Tris-HCl and immediate use, storage at 4°C for up to a week or freezing at -20°C for any longer.

Per2:Luc Genotyping

For detection of the Per2::Luc gene, Per2:Luc Genotyping reaction mixture (Table 2.2) and primers (Table 2.4) was used and Per:Luc PCR program (Table 2.7) .

Heteroduplex Screen and Genotyping Primers

To detect heteroduplexes, primer pairs spanning the exon of interest plus an additional 30 bp either side were designed using the Light Scanner Primer design software and optimal detection of mutant samples ascertained using the LS gradient PCR (Table 2.7) (Section 2.1.1)

More genotyping protocols were developed in order to detect the mutation of interest in intercross cohorts. The Light Scanner heteroduplex assay is unable to discern homozygous sequences, as the sequences are complementary and align perfectly, so no heteroduplexes form and the melting temperature does not differ from wild type samples (Section 1.5.4). Primer design for pyrosequencing and qPCR was completed using Primer3 software. Pyrosequencing primers were developed against the sequence including the mutation of interest (biotin tags added to the reverse primer) and qPCR spanning an exon-exon junction for specificity. For the Light Scanner lunaprobe assay, the sequence surrounding the mutation of interest approximately 40bp in length is used in Light Scanner primer design software to design appropriate lunaprobes based on sequence composition and predicted melting curves. An average of 2 primer pairs were optimised for each mutation.

Heteroduplex Screen and Genotyping Assays

PCR programs for screening were Light Scanner based, LSD1 exon 10, 11 and 19 were screened with primers detailed in Table 2.4, using the LS60 PCR program (Table 2.7). Exon 12 was amplified with LSD1 E12 Fc and LSD1 E12 Rc primers (Table 2.4) using the LS56 PCR program (Table 2.7). LSD2 screening exons 6, 7 and 10 used primers LSD2 E6 F and LSD2 E6 R, LSD2 E7 F, LSD2 E7 R and LSD2 E10 F and LSD2 E10R respectively (Table 2.4) and the LS63 PCR program (Table 2.7), and exon 9 using LSD2 E9 Fd and LSD2 E9 Rd primers (Table 2.4) and the LS51 PCR program (Table 2.7). Initially genotyping was carried out using the same primers and programs as the screen (as heterozygotes can be detected using this assay).

For lunaprobe genotyping, E440G Reverse Probe and L491H Forward Probe primers (Table 2.4) were used in the Lunaprobe reagent mix (Table 2.2) and LS Lunaprobe PCR program (Table 2.7). Lunaprobe samples were analysed on the Light Scanner. For pyrosequencing based genotyping, forward, reverse and sequencing primers (Table 2.4) were used for each gene, and the Pyrosequencing reagent mix (Table 2.2) was amplified using the Pyrosequencing PCR program (Table 2.7). Pyrosequencing was performed by the GEMS department in MRC Harwell using specialised equipment.

PCRs

All PCR reactions were carried out using programmes listed in Table 2.7, on G-Storm PCR equipment, with the exception of pyrosequencing reactions which were cycled instead on Bio-rad tetrad machines.

DNA purification for PCR

When only very small tissue samples were available for genotyping, DNA was purified to maximise the efficacy of genotyping assays. DNA purification for PCR was performed according to

recommended Qiagen protocol. Briefly 5 volumes of buffer was added to one volume of DNA sample and acidified until pH drops below 7.5 with sodium acetate to allow optimal reaction conditions. 800µl reaction mixture was filtered through the QIAquick columns at a time until the whole sample had passed through the filter. Samples were washed through with 750µl buffer PE by centrifugation and DNA eluted in 50µl DEPC treated water again by centrifugation.

2.1.6 Sequencing

In order to sequence constructs for cloning or DNA from individuals to confirm mutations of interest, DNA was prepared for sequencing. DNA samples were diluted to 100ng/µl in RNAse-free DEPC water and the relevant primers added at 3.2pM/µl, before sending for sequencing by Source Bioscience. High-throughput sequencing was performed and analysed against mouse sequences from the Ensembl website using Lasergene software (DNASTAR).

2.1.7 Agarose gel electrophoresis

In order to visualise the size of PCR products in cloning and in confirming specific amplification by genotyping and screening primers, samples were run on agarose gels to separate products of varying molecular weights. 1.5% agarose gels are made using 1.5g agarose per 100ml TAE. Agarose is dissolved by heating the mixture and 1µl of GelRed per 10ml agarose was swirled in. The mixture was poured into a mould of appropriate dimensions with an appropriate comb and allowed to set. When set, the gel was released from the mould and placed in a Fisherbrand electrophoresis tank. The gel was loaded with an appropriate NEB ladder and samples mixed 1:1 with OrangeG loading dye. The tank was topped up with TAE buffer and sealed. A current (approximately 80V) was passed across the gel and before the dyefront reached the end of the gel, equipment was switched off and the gel removed for Image-Lab analysis using a Gel-Doc instrument (Bio-Rad).

2.2 Constructs

2.2.1 Rutherford Appleton Lab (RAL) cloning

DNA constructs were generated in the Oxford Protein Production Facility (OPPF) high-throughput cloning suite. For cloning in OPPF, primers were designed using software according to recommended primer design for the POPIN-J vector cloning protocol (OPPF website)

InFusion technology from Clontech was used to generate POPIN-J backbone N-terminal-GST-tagged constructs containing LSD1, LSD2, Per1, Per2, Cry1, Cry2, CLOCK and Bmal1 (See Appendix 1).

2.2.2 Site directed mutagenesis

In order to manipulate mutant LSD1 and LSD2 *in vitro*, constructs expressing the mutant versions were generated by site directed mutagenesis. Mutagenesis primers for each mutant construct were labelled by the gene name, followed by base pair change and then direction of primer annealing. For example, for the LSD1-E440G mutation, primers were labelled LSD1 E440G F and LSD1 E440G R. Constructs containing the LSD1 or LSD2 sequence to be mutated are mixed on ice according to the Mutagenesis reagent mixture (Table 2.2) with appropriate mutagenesis primers (Table 2.4) adding Pfu-polymerase last of all. They are processed using the MUTAGENESIS PCR program (Table 2.7) before the addition of the DpnI and final incubation at 37°C for 1 hr. The now mutagenized products are amplified by transforming into XL10 ultra competent cells and amplifying as normal. Products are sequenced to verify the success and specificity of the mutation.

2.2.3 LB plate preparation

Constructs were amplified by bacterial expression and growth of bacterial colonies required the use of lysogeny broth (LB) plates. Pre-autoclaved set LB agar was heated until no solid lumps remained and allowed to cool to room temperature. Appropriate antibiotics, typically 500µl 100mg/µl Ampicillin was added to 500ml of liquid LB and poured into 10cm dishes on a flat surface before allowing to set.

2.2.4 Transforming plasmids

In order to manufacture large numbers of plasmids for molecular work, competent cells were transformed and grown on LB plates. XL10 or DH5α competent cells were thawed from storage at -80°C and kept on ice from thereon, and SOC media pre-warmed to 37°C. For XL10 competent cells, 4µl of β-mercaptoethanol was added and stirred in to each aliquot and incubated for 10mins with frequent stirring before DNA was added. To each 50µl aliquot of cells, 1-10ng of plasmid DNA was added and mixed by gentle perturbation with a pipette tip. After 30mins incubation on ice, DH5α cells were shocked at 42°C for 20secs (30 for XL10 competent cells) and plunged back into ice. 950µl of warm SOC was added to the aliquot and the mixture incubated on a shaker at 37°C for one hr whilst the LB+ (Table 2.2) plates were warmed to 37°C in a static incubator. 200µl of the cell suspension were then plated onto each LB plate, and the remainder sealed and stored at 4°C in case a higher volume was required to generate colonies. The plates were incubated at 37°C overnight and the following day colonies were picked using a pipette tip for amplification of DNA. Plates were kept for up to 2 weeks for amplification of colonies. DNA amplified and purified from these plates by midiprep is utilised in transfection and overexpression experiments and periodically sent for sequencing to check the sequence encoded by the construct.

2.2.5 Plasmid culture and purification

Colonies picked from the LB plate were cultured to amplify constructs. They were dropped into 20ml liquid LB+ (Table 2.2). These were incubated overnight on a shaking incubator and the cloudy suspension used for DNA purification by Midiprep.

Midiprep was completed according to the protocol included in the Qiagen or Invitrogen kit (Table 2.5). Briefly, the bacteria were centrifuged to a pellet and the LB discarded. Bacteria were re-suspended and lysed to extract DNA and passed through a filter column. The filter was washed to clear cell debris and the DNA finally eluted with elution buffer. Isopropanol was then added to precipitate the DNA before high speed centrifugation pellets the material, which was finally washed

with ethanol and resuspended in RNAse and DNAse free water. The DNA was titred using the nanodrop (Thermo Scientific) and stored at 4°C for up to 2 weeks, or frozen for longer time periods.

2.3 Cell culture

2.3.1 Culture media

Cells were kept in media containing antibiotics to avoid infection of cultures and optimise experimental efficiency. Complete media consisted of 500ml DMEM, 5ml Penicillin-streptomycin and 50ml FBS mixed by inverting. McCoys used for U2OS cells was completed with 5ml Penicillin-streptomycin, 50ml FBS and 5ml L-glutamine.

2.3.2 Cell thawing and seeding

Cells used in tissue culture experiments were thawed rapidly. Upon removal from liquid nitrogen or -80°C storage, aliquots were added directly to 9ml pre-warmed complete media and plated into a T25 flask. After 24 hrs, media was aspirated and replaced with fresh complete media warmed to 37°C. When a confluent layer of cells coated the base of the flask, cells were split and maintained in T75 flasks or plated for experiments as required.

2.3.3 Cell splitting and culture maintenance

Cells were passaged as required to avoid overgrowth and to expand cultures for experiments. Culture media was aspirated and the adherent layer of cells washed with warm PBS thrice (swirled and discarded each time). 2ml 0.05% trypsin solution was added to the flask, and cells returned to the incubator for 5mins to allow detachment, and then the flask was swirled to dislodge the cells. Trypsin was quenched by addition of 8ml complete media. As required, cell number can be determined by adding 50µl cells to 50µl trypan blue and counted manually using a haemocytometer. For maintenance culture splitting, counting was not required but rather 1ml cell suspension added to 19ml fresh media and seeded in a fresh T75 flask. If cells were to be immunofluorescently analysed, a coverslip is placed on the base of the dry flask or dish, before addition of any media so no liquid infiltrates between the bottom of the coverslip and the flask and so no cells can adhere

between the two surfaces. Cells are periodically tested for infection using the MycoplasmaTest reagent mixture (Table 2.2) and PCR program (Table 2.7).

2.3.4 Cell freezing and storage

Cells were stored at -80°C when not actively in use. First cells were trypsinised as for splitting, and when quenched with complete media the suspension was divided between two falcon tubes. The tubes were centrifuged for 10mins at 1000rpm (until a pellet formed). Cells were then resuspended in freezing media (Table 2.2) and divided into 1ml aliquots in labelled cryotubes (4-6 per T75 flask of confluent cells). Aliquots were cooled rapidly and stored at -80°C or for longer periods of time in liquid nitrogen.

2.3.5 Extraction of Mouse Embryonic Fibroblasts

Embryonic fibroblasts were cultured from e14.5 embryos. Each culture dish was coated with 5mls PBS and 0.1% Gelatin (Invitrogen) to encourage fibroblasts adhesion to the surface of the dish. 25 ml of complete media supplemented with L-glutamine (25mls of 100X stock/ 500ml of media) was added to the dish and warmed to 37°C. Pregnant females were culled by cervical dislocation and dissected to remove the uterus and embryos which were then kept in PBS for microdissection. Embryonic head, internal organs and limbs were discarded. The tails were collected for genotyping. The remaining tissue was washed in PBS and bathed in trypsin. Tissue was crudely chopped with a scalpel and then homogenised by pipetting, and incubated for 10 mins with constant agitation in a 37°C water bath. The mixture was passed through a 10 ml syringe until well mixed. The entire mixture was then transferred to the pre-warmed tissue culture dish and incubated at 37°C. After 24hrs, debris was washed away from the cells by gently swirling with 10 ml warm PBS and the media refreshed. The MEFs were left to grow till they reached 85-90% confluence, after which they were split in 1:2 or 1:3 dilution in the same way as other cells maintained in culture (Section 2.3.3).

2.3.6 Lumicycle: bioluminescent cell rhythm recordings

The LumiCycle (Actimetrics) was used to investigate the effect of compounds and mutations on the clock by administration of a compound or by transfecting recombinant mammalian expression plasmids into the cell line and then imaging them in real-time. The U2OS and Rat-1 cell lines stably transfected with Per2:Luc (Per2 promoter driving luciferase transcription) were used for transfections and Rat-1 cells for compound screening. The stable cell lines were plated in 35mm dishes and were allowed to grow overnight at 37°C. The following day, cells would approximately reach 70-75% confluence and plasmids were transfected according to manufacturer's guidelines using the JetPrime 3.5mm Dish mixture (Table 2.2, Section 2.3.6). 24 hours after transfection, the cells were synchronised using forskolin (10μM final concentration) and left in the incubator for 2 hours.

During this time, the recording media (Table 2.2) was prepared in dark sterile conditions. 2 hours after synchronisation, the cell culture media was thoroughly removed using a Gilson pipette and 2mls of final recording media containing luciferin was added dropwise to each LumiCycle dish. The dishes were sealed immediately with a coverslip (VWR International Ltd.) and each dish was sealed with parafilm. It was important to ensure that there were no gaps left between the coverslip and dish itself as the luciferase count would then disrupt readings. Once sealed, the dishes were placed in the LumiCycle, and the luciferase counts were monitored over 5 days using the LumiCycle analysis software (Actimetrics). All graphs of data processed from the original traces include SEM error bars as appropriate.

2.3.7 Transfection

To artificially express circadian or LSD constructs in cells for molecular work, the cells were transfected using one of two reagents. All concentrations used according to table 2.2.

With Fugene: Fugene was added to warm media, mixed by vortexing and incubated for 5 mins at room temperature. DNA was then added to the mix and vortexed. Media on the dish/flask of cells (at 70% confluence) was replaced with incomplete media (with no antibiotics to increase

transfection efficiency), and the Fugene mix added dropwise with gentle swirling. Transfection time was at least 24hrs and reagent concentrations are listed in Table 2.2.

With JetPRIME™: DNA was mixed by vortexing with sodium chloride buffer at room temperature. JetPRIME™ reagent was then immediately added and vortexed once more. The mixture was incubated at room temperature for 15 mins and added dropwise to cells. Time until harvesting was 24 hours and reagent concentrations are listed in Table 2.2.

2.3.8 Protein extraction

Proteins were extracted from cell cultures to maximise the yield and allow for efficient pull down in immunoprecipitations. Cell lines were cultured in 10cm dishes for extraction purposes. Cells were washed twice in warm PBS to eliminate all residual media. 250µl of RIPA+ (Table 2.2) was added dropwise to each dish and incubated on ice for 30mins. The cells were scraped into a vessel for immediate use or storage.

2.4 Protein Work

2.4.1 Bradford assay

In order to immunoprecipitate proteins from cell cultures, the cells must be processed to extract the protein and the overall protein concentration of each sample calculated to normalise each pull down. Cell lysates were diluted 1:5 in RIPA buffer, and standard BSA solutions diluted in the same solution for calibration. BSA was serially diluted from a 2mg concentration through to 0.125mg and each solution vortexed to ensure consistency. 5µl of each blank (water), standard and sample were added to each well in a nunc 96 well dish, then 250µl of Bradford reagent added to each well. The plate was agitated at room temperature for 5mins and inserted into the µQuant plate reader (Biotech Instruments). Results were analysed using KC Junior software, a calibration curve formed and the data set and protocol recorded for future reference.

2.4.2 Immunoprecipitation (IPs)

To investigate binding partners of the LSD genes, cells were transfected to overexpress the LSD gene product along with circadian gene products tagged with epitopes which can be recognised by specific antibodies. The LSD is pulled down using antibodies to the tag or using LSD specific antibodies, and if the co-expressed circadian protein is bound to LSD, it will be precipitated along with the LSD. The purified proteins are then separated by tris-acetate gel electrophoresis, blotted and visualised by antibodies targeting the tags, and final detection by chemiluminescent or immunofluorescent labelling of the primary antibodies.

To firstly precipitate the protein of interest (LSD1 or LSD2), 250µg of transfected cell lysate made up to 250µl total volume with RIPA buffer was added to 20µl of Protein-G-Sepharose beads pre-washed in RIPA buffer. The mixture was continually inverted for 1 hr at 4 °C, the beads then pelleted by centrifugation and the supernatant extracted. The probe antibody was added to the supernatant at the appropriate concentration and rotated at 4°C for 24 hrs. 20µliters of new and washed Protein-G-

Sepharose beads were prepared and the overnight mixture added, and rotated at 4 °C for a further 2hrs. Finally the sample was centrifuged and the supernatant removed, and the complexes eluted from the beads using sample buffer and reducing agent. These samples were either used immediately or frozen at -20°C overnight before undergoing acrylamide gel electrophoresis, semi dry transfer and running on a western blot.

2.4.3 Tris-acetate gel electrophoresis

Protein samples from cell culture or from immunoprecipitation pull downs were mixed in with sample buffer (Table 2.2), and were heated to 90 °C for 10 mins to denature. If thawing from storage, 3µl of fresh reducing agent was added first. The gel was inserted into an Invitrogen tank which was filled with running buffer (Table 2.2). The comb was removed and the wells rinsed with 500µl of antioxidant. Samples were loaded into the wells and a 200V potential difference set up across the gel for an appropriate length of time for sample separation. The gel was removed from the tank and carefully from its casing and floated in transfer buffer ready for immediate semi-dry transfer.

2.4.4 Semi-dry transfer

The gel to be transferred was kept in transfer buffer whilst the transfer stack was prepared. Hybond membrane for ECL detection or low fluorescence PVDF for Fluorescent detection was cut to size and immersed briefly in methanol and water to activate for transfer. The tris-acetate gel floating in transfer buffer and membrane were loaded in a stack between filter paper soaked in transfer buffer, and sandwiched into the semi-dry transfer equipment (Bio-rad Trans-Blot). A 15V current was passed across the stack for 90mins and the membrane taken for western blotting.

2.4.5 Western blots

To visualise protein bands on membranes for immunoprecipitation or to check protein samples, the membrane was processed by western blot. The membrane was blocked and agitated for 1 to 24hrs

in 5% milk solution in PBST (Table 2.2) and primary antibody added for a further 2hrs at room temperature. The membrane was washed thrice with PBST and incubated for 2hrs in secondary antibody (in the dark if the secondary probe was fluorescent). For fluorescent processing, the membrane was then allowed to dry thoroughly in a light tight chamber, and visualised using LI-COR Biosciences Odyssey Infrared Imaging System software and equipment. In the case of ECL detection, rather the membrane was not allowed to dry out but instead coated in detection fluid as per protocol advised by ECL plus (Amersham biosciences) (Table 2.5). After 3mins incubation (in the dark) the blot was drained and wrapped in saran wrap and placed into the Chemidoc-It detection chamber and analysed using UVP software. ECL blots were kept refrigerated for up to 1 week for stripping and re analysis if required. All graphs of data include SEM error bars as appropriate. Data was processed as follows: bands quantified by selecting and measuring the density of the band in the region of interest and subtracting the recording from a neighbouring region of the same size (representative of the background of the blot) using ImageJ; for co-immunoprecipitation, interaction band intensity is normalised to the control band for each individual transfection (eg in the instance of an LSD1 HA- BMAL1 V5 interaction, the BMAL1 (67kDa) V5 band is normalised to the density of the LSD1 (90kDa) HA band for that sample); finally the test value is compared to the normalised value for the negative control (LSD1 HA-empty V5); average values across triplicated data is shown in the graph.

2.5 Tissue work

2.5.1 RNA extraction

For tissue collection to extract RNA for qPCR, animals were sacrificed according to schedule one guidelines in a laminar air flow cabinet. Tissue was collected as quickly as possible, always within 1hr of the ZT value, and was placed immediately on dry ice. Tissues were transferred to -80°C as quickly as possible.

50µg liver tissue was cut and weighed out using a fine balance (Primus Scientific) from the frozen sample and 0.5ml of trizol was added. Tissue was homogenised thoroughly with a pestle and left for 5 mins at room temperature. 100µl of chloroform was added and shaken vigorously before centrifuging at 12000xg for 15mins at 4 °C. The aqueous fraction (containing the RNA) was extracted and added to 250µl of isopropanol to precipitate the RNA, mixed by vortex. The mixture was incubated at room temperature for 10mins and then centrifuged for 10 further minutes at 12000xg. The liquid fraction was aspirated and the RNA pellet allowed to dry. The pellet was then washed with 500µl of 70% ethanol, and again dried before resuspension in RNAse-free water for use. This could be frozen down before processing.

For SCN punches (small tissue amounts) samples were just vortexed in trizol to avoid the tissue loss implicit in using a pestle.

RNA extraction using a Qiagen mini or micro extraction kit was performed as per recommended instructions, briefly the tissues were homogenised in trizol, the lysate centrifuged through the column, mixed with ethanol to precipitate RNA , centrifuged and washed with RW1 and twice with RPE wash buffer before eluting in RNase-free water.

2.5.2 RNeasy tissue processing, and DNase I protocol

RNA was purified before use in qPCR. DNase I stock was prepared by adding 550µl RNase-free water to each aliquot of DNase I. From this stock, 50µl aliquots are separated and either used immediately or stored at -20°C for future use.

Tissue was homogenised with trizol, and centrifuged for 3mins at maximum speed to pellet the debris. 1 volume of 70% ethanol was added to the sample lysate and the mixture pipetted directly into an RNeasy column, span at 8000xg for 15s and the flow through discarded. 350µl RW1 was added to the column, centrifuged at 8000xg and the flow-through discarded. 10µl DNase I solution was mixed with 70µl RDD buffer, the tube inverted and incubated in the RNeasy column for 15 mins. 350µl RW1 was added to the tube and again centrifuged at 8000xg. Flow through was discarded. The tube was then washed with buffer RPE as per the normal RNA extraction protocol and the sample processed as normal.

Quality of the resulting RNA was established using bioanalyzer software (Agilent). Gel dye-matrix mixture was injected to the bottom of the labelled wells on the chip cassette using a chip priming station and pressurised to fill the chip. Next RNA dye was added to each well, followed by ladder and samples. The chip was vortexed gently to mix and placed into the 2100 bioanalyzer and the electrophoresis program started.

2.5.3 cDNA synthesis

Superscript III synthesis kit was used for cDNA synthesis. Briefly, 1mg RNA was mixed with buffer and polymerase and incubated according to PCR program cDNA synthesis 1 (Table 2.7). RNAse H was added and the mixture incubated at 37°C for a further 20mins (cDNA synthesis 2, Table 2.7). cDNA was used immediately (Diluted 1 in 4 with water) for qPCR or stored at -20°C for future use.

2.5.4 qPCR

Primers were prepared at 2µM concentrations, and mixed with reagents as per Table 2.2 before PCR. Plates were heated gradually and analysed using a 7500 fast optical plate reader (Applied Biosystems). Quantification of each sample was achieved with the -2ΔΔCT method and constitutively expressed control RNA (GADPH for SCN analysis and actin for liver) were quantified and used for analysis. All graphs of data include SEM error bars as appropriate.

2.5.5 In Situ Hybridisation

In order to investigate the role of *LSD1* in gonadal development, it was necessary to examine the expression of female markers in male gonads to check for sex reversal. As tissue quantity at 14dpc is so little, it was necessary to visualise the expression of female markers using in situ hybridisation. 14dpc gonads were microdissected and stored in 100% methanol prior to *in situ* hybridisation. Gonads were rehydrated in series of methanol dilutions (75%, 50% and 25% for 5mins each) and washed twice with PBS for 5mins each. 6% H_2O_2 was added and incubated for 1hr to bleach the tissue, followed by three more PBS washes. The tissue was treated for 12mins with Proteinase K (Table 2.2) and for 5mins with glycine (Table 2.2) and washed twice more in PBS. Tissue was postfixed for 20mins in glutaraldehyde in PFA (Table 2.2) and washed twice more. Gonads were incubated for 2hrs in a humidified chamber at 70°C in prehyb solution before adding hyb solution (Table 2.2) and the denatured probe for an overnight incubation at 70°C. The following day samples were washed in Solution 1 (Table 2.2) twice for 30mins each at 70°C, solution 2 (Table 2.2) twice for 30mins each at 65°C and TBST (Table 2.2) thrice for 5mins each at room temperature. Tissue was pre-blocked in 10% sheep serum in TBST for 2.5hrs at room temperature. Embryo powder was activated in 1ml TBST at 65°C for 30mins. 10µl of sheep serum was added to each 1ml of TBST on ice, the activated embryo powder centrifuged to a pellet and excess TBST removed, and replaced with 1ml sheep serum block. 1µl anti-Digoxigenin-AP Fab fragments were added to each well and tissues incubated in the mixture on a rotor at 4°C overnight. The following day the tissue is washed multiple

times in TBST at room temperature, thrice for 5mins and 6 times for 1 hr and left in the final wash overnight. On the final day, NTMT (Table 2.2) was mixed fresh on the day and passed through a sterile filter. Tissue was washed for 10mins thrice in NTMT. 20µl NCIP was added to each 1ml of NTMT (Table 2.2) and the tissue bathed in the resulting stain in a glass dish for up to 2hrs in the dark (or until the stain becomes apparent when checked). The staining reaction was quenched when the stain was fully developed by washing four times in PBST and left to whiten for up to 3days in the dark. Tissue was then fixed for one hr with 4% PFA in PBS and either stored in PBST at 4°C or immediately visualised using a microscope. Probes were kindly given by Dr Nick Warr, MRC Harwell.

2.5.6 Histology

Gonads were taken from adult animals, and stored in bouins solution at room temperature until processing. Gonads were embedded in wax and cut to 3µm thick staggered Sections (60µm apart) before staining with H and E.

2.6 Imaging

2.6.1 Immunofluorescence

Imaging of construct expression in transfected HEK293 cells was used for co-expression analysis as well as to confirm efficacy in relation to immunoprecipitation preps. Constructs were tagged with epitopes which were then detected by specific antibodies which were detected with fluorescent secondary antibodies (Table 2.3). Coverslips were washed twice for 5mins with PBS in the dish before being fixed in 4% ice cold PFA in PBS for 15mins. The PFA was aspirated and the coverslip washed twice for 5mins with ice cold PBS. The coverslip was then washed once for 5mins in 0.2% Triton-X100 to permeabilise the cells, and thrice more with PBS. Coverslips were blocked for at least 2hrs at room temperature (or overnight at 4 °C) in 5% donkey serum, then placed on 50µl of primary antibody in block at the appropriate concentration (Table 2.3). This was incubated for 2hrs, washed thrice in PBS and then placed on 50µl of secondary antibody (Table 2.3), in a light tight chamber. Coverslips were then washed thoroughly with PBS and fixed in Prolong anti-fade with DAPI, and allowed to set overnight at room temperature before storage at 4°C or immediate microscopic analysis.

2.6.2 DiI Stain

DiI incorporates into the membrane of neuronal cells, and as such was employed in the characterisation of SCN2.2 cell cultures. Coverslips were prepared as for immunofluorescent analysis, and after blocking with donkey serum, DiI reagent was added to cover the surface of the coverslip. Liquid was then evaporated at 37 °C before flooding with PBS. This was allowed to incubate at 37 °C for a further 60mins in a dark chamber. Finally the coverslip was washed thrice with PBS for 5mins before fixing according to the remaining immunofluorescence protocol.

2.7 Circadian Screening

Animals were screened in many circadian based assays to assess the circadian system as is the aim of the current investigation. Tests were carried out on mice over 42 days old. *Kdm1a*$^{E440G/E440G}$ and *Kdm1a*$^{L491H/L491H}$ females and males were tested but no difference in phenotype was observed in circadian or behavioural testing so data presented is from both genders with the exception of social dominance, where exclusively males were used due to the nature of the test. In after-effect screening, *Kdm1a*$^{E440G/E440G}$ males were used due to a technical problem with the apparatus used when testing the female cohort. *Kdm1b*$^{T357M/T357M}$ females were used for circadian testing and males for behavioural testing in parallel due to time constraints for colony breeding. Animals were individually housed in cages equipped with running wheels with food and water provided ad libitum. The cages were kept in light tight ventilated chambers with up to 9 further cages of mice of the same gender, or 14 in the scantainer (Scanbur website). Animals were checked daily under infra-red light and cages cleaned weekly. Wheel-running recordings were made and analysed using ClockLab software (Actimetrics). All graphs of data include SEM error bars as appropriate.

2.7.1 LD and constant condition circadian screen

The first phase of the circadian screen was to check that the animals entrained to a normal 12:12 light-dark cycle. Following from this, a light pulse was administered in the dark phase to check if the animals had a normal light-induced suppression of activity (or masking response) as this masking response is indicative of normal photodetection and upregulation of immediate early gene expression in the SCN. Following the remainder of the LD schedule, animals were allowed to 'free run' in total darkness to investigate the nature of the endogenous circadian oscillations which maintain their rhythm in these conditions. And after 10 days the animals were exposed to constant light to investigate the reactive lengthening of circadian period by exposure of the SCN to light according to Aschoff's rule (Aschoff 1960). LL screening often also precipitates arrhythmia in animals such as clock mutant animals (Spoelstra et al. 2002). Animals were maintained in a 12:12 light dark

cycle (LD) with light at 100lux intensity for 7 days. A single 3hr light pulse was administered at ZT14 during the dark phase of day 5 of the screen. Following LD, animals were kept in constant darkness (DD) for 7-10 days before switching to constant light for the remaining 7 days of the screen. Analyses of data include wheel revolutions per day as a measure of activity in all conditions, percentage of nocturnal activity in LD cycles, percentage of activity in the masking 3 hr light pulse on day 5 of recording, length of circadian day (tau) and length of active phase (alpha) in DD and LL conditions indicative of how fast the circadian oscillator was ticking (and so driving behavioural outputs) in constant conditions, activity plots of LD days to investigate discrepancies in distribution of wheel running activity, and calculation of the phase angle of entrainment (phi) in LD. (Figure 2.1)

2.7.2 Phase shifting circadian screen

In order to assess how well the clock was able to entrain to changes in the light dark schedule, the animals were exposed to 6 hr shifts in the 12:12 light-dark cycle in a phase shifting screen. Animals were maintained in a 12:12 LD cycle and after 7 days the 12:12 cycle was shifted forwards by 6 hrs. After the cohort had re-entrained (approximately 11 days), the cycle was restored to the original 12:12 timing by delaying the light schedule by 6hrs. The screen was left for approximately 11 further days to allow animals to re-entrain. Percentage of the cohort able to re-entrain to the delay was calculated and the speed of entrainment to all phase shifts was also recorded both by summing up the number of days to entrain and by plotting the onset of activity as a function of time for each group.

2.7.3 Phase response curve circadian screen

It is the nature of the clock that light-induced expression of immediate early genes including *Per1* during the dark phase can shift the ensuing endogenous rhythm of the animal. It can shift the rhythm backwards if administered in early night and advance it if administered in late night, and this effect is dependent on the phase of the endogenous rhythm of Per1 expression in the SCN (Section 1.3.2). In order to investigate this mechanism in mutant animals, they were screened using

systematic light pulses at early and late time points during subjective night. From this data, a phase response curve was formulated and compared to that of wild-type animals.

Mice were maintained in constant darkness and when settled onto an endogenous tau, the relevant CT for a 15min light pulse was calculated by extrapolation of the current activity pattern of each mouse, before administering the pulse at approximately CT16 (early) and CT22 (late) to shift the onset of activity by manipulation of molecular entrainment mechanisms. The precise value of the CT varied as each shift occurred at the same time for the ten animals housed in the chamber together, and all animals had different endogenous rhythms. As such the CT was precisely recorded for each animal and analysed accordingly. The animals were left for approx. 11 days before the next light pulse to allow the circadian clock to re-establish a stable rest activity cycle. Data was analysed using ClockLab software, the lines of best fit generated extrapolated using the initial activity onset and the onset following stabilisation after the light pulse and the difference between the two recorded on the day after the light pulse to give a change of phase value. Stabilisation after the light pulse was only included in the analysis if the period was within 0.5hrs of the initial free running period. Phase shift values were plotted against CT of light pulses and grouped to generate phase response profile.

2.7.4 After effect circadian screen

In order to assess the reactive shortening or lengthening of endogenous rhythms in response to light-dark schedules (T cycles) shorter or longer than 24 hrs, animals were screened in an after-effect screen. The after-effects of exposure to such T-cycles lends insight as to the long term functioning of the SCN upon exposure to LD cycles (Pittendrigh & Daan 1976) (Section 5.8.4). Animals were housed in a custom built Scantainer and maintained in long (14:14) LD cycles, or 'T-cycles', until entrained. Animals were then left in DD for 7-11 days to observe the response to the entrainment period to the shortened day length. After a normal rest activity cycle was re-established, the animals were put into a short T-cycle (11:11) for up to 14 days before observing the effect of the 14:14 T cycle on circadian clock driven activity in DD. Percentage of animals able to entrain to each T-cycle was

recorded as well as time to re-entrain. Tau was also calculated for the 4 days immediately following the T-cycle and averaged to quantify the extent to which tau was lengthened or shortened by the preceding T-cycle. Previously, short T-cycles of 22 hours and long T-cycles of 26 hours were used to examine such after effect behaviour in wild-type mice (Azzi et al. 2014), but we found that female animals entrained to 28 hour cycles readily, so used 28 hour cycles in testing thereafter to exaggerate any detectable after effect.

2.7.5 Pupillometry

Pupillometry was performed on cohorts of 4 mice per group by Dr Gareth Banks at MRC Harwell. A high power white LED (Luxeon star) was used to generate the pupillary light reflex (light intensity of 14.4 log quanta/cm^2/s [169 µW/cm^2/s or 500 lux]). The pupillary response was recorded using a Prosilica near-infrared (NIR) sensitive CCD video camera (BRSL, Newbury, UK) positioned adjacent to the eye contralateral to the light source, allowing consensual light responses to be recorded. A NIR LED was used to illuminate the eye during dark periods. To take recordings, the mice were restrained by scruffing. Mice were dark adapted for at least 1 hour before recordings were made. All recordings were made between Zeitgeber times 4 and 8 (ZT4 and ZT8, where the onset of the light phase is defined as ZT0). The total recording time for each session was 30 seconds. A 2 second baseline measure was used to establish dark adapted pupil size. A 10-second light stimulus was then applied to elicit pupillary constriction. For a further 18 seconds, recordings were taken to monitor recovery in the absence of illumination. The camera was linked to a laptop via the National Instruments Measurement and Acquisition software (version 4.7.6). Data were collected using a custom made LabView application (Pothecary et al., manuscript in preparation), which also controlled the timing of both the light stimulus delivery and image recording, taking an image of the eye once every 0.2 seconds. ImageJ software (http://rsbweb.nih.gov/ij/) was used to establish the area of the pupil in each image, and the magnitude of the changes in pupil size was expressed as area relative to the fully dilated pupil from the dark adapted recording.

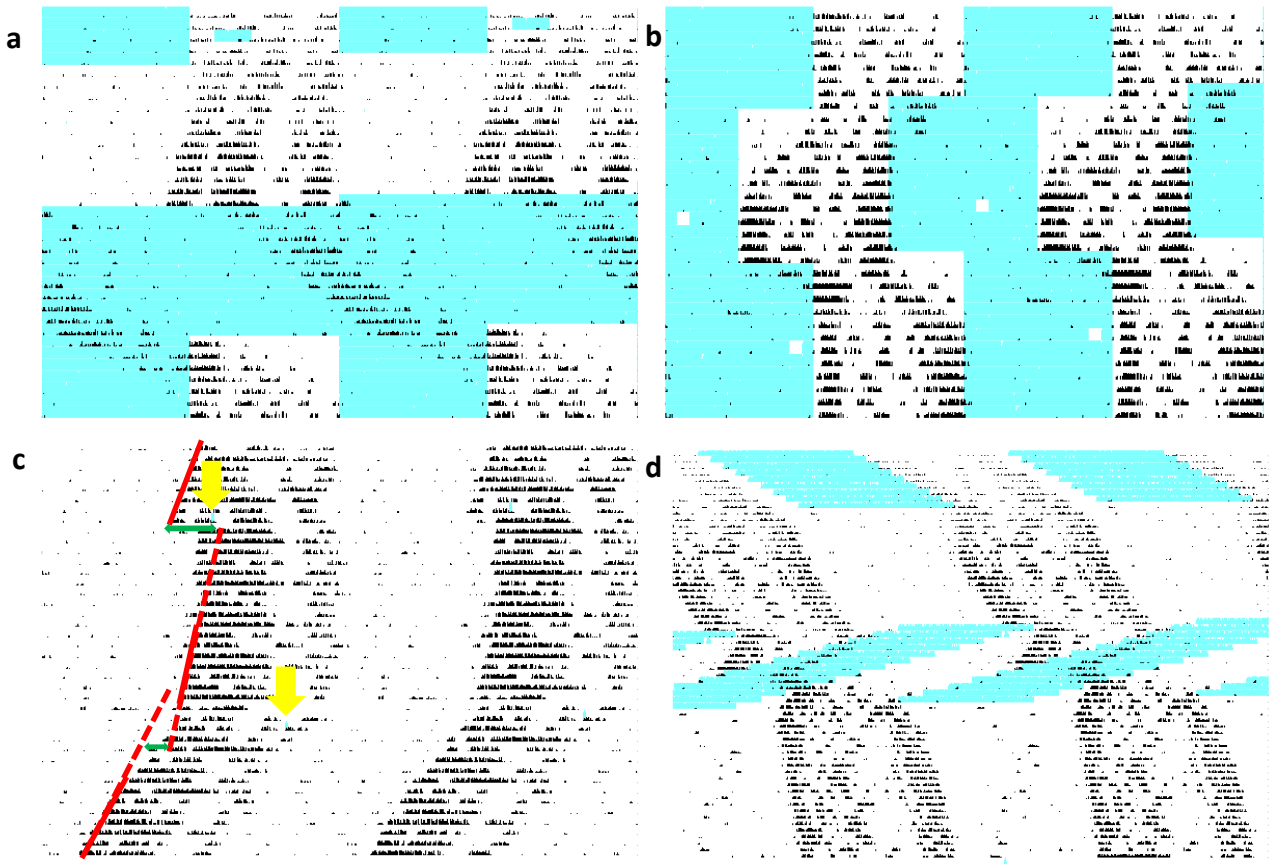

Figure 2.1: Actograms illustrating screen structures

a) LD and constant condition screen: Animals are entrained to 12:12 LD schedules then allowed to free run in constant darkness, followed by exposure to constant light (Figure 1.4, Chapter 5)

b) Phase shift screen: Animals are entrained to 12:12 LD cycles and upon entrainment, the LD cycle is shifted 6 hrs forwards and the ability of the animal to re-entrain tested, and then shifted 6 hrs backwards and again the ability of the animal to entrain is tested (Chapter 5).

c) Light pulse screen: Animals are kept in DD and light pulses of 15 mins administered in early and late subjective night (CT 16 and CT 20). Free running period of the animals is allowed to stabilise and the shift in phase on the day following the light pulse is measured (green arrows) to plot a phase-response curve.

d) After effect screen: Animals are entrained to a 28 hr LD schedule and then allowed to free run for 10 days, then entrained to 22 hr LD schedules and again allowed to free run. Free running period of animals is then measured after long and short T cycles, expecting to observe a lengthening after the long period and a shortening following the short T cycle (Pittendrigh & Daan 1976)

2.8 Behavioural phenotyping

Animals were put through a phenotyping pipeline designed to highlight any abnormal behaviours including traits linked to anxiety, depression and schizophrenia as well as examining cohorts for any deficits in motor behaviour, cognition or social interaction which might confound the results of the behavioural investigation. All tests were preceded by 15-30mins of acclimatisation to the testing room. All graphs of data include SEM error bars as appropriate.

2.8.1 Open field

The open field test is designed to allow free exploration of a novel and exposed environment and can be anxiogenic in some animal models (Prut & Belzung 2003). The open field test was performed on test-naïve animals to assess exploratory activity and anxiety in an exposed and novel arena. The mice were placed into a clean, grey, 72 x 72 x 33cm arena illuminated at 150-200lux, facing the corner and freely allowed to explore. Their response was tracked (Ethovision) for 20mins. Open field testing was performed over two trials on consecutive days allowing analysis of the exploratory behaviour on a second day so excluding any effect of the novel environment on the first days recording. Analysis included the latency to enter the centre of the arena (the more exposed and so anxiogenic area), time spent in the centre and overall distance moved.

2.8.2 SHIRPA

Animals were assessed by SHIRPA analysis for gross motor traits and behaviours which might confound the results of other experiments as previously described (Nolan et al. 2000; Rogers et al. 2001; Acevedo-Arozena et al. 2008). Breathing rate and activity in the viewing cylinder (Figure 2.2) were assessed by eye to determine anxiety responses, and posture and existence of any tremor scored to exclude any motor-neuron-like traits. A metal sheet was slid under the cylinder and the animal transferred to a white arena by removal of the sheet at a height of approximately 15cm and allowed to run freely. Response to transfer (freezing or hyperactivity) was recorded. In the arena,

gait was observed for analysis of coordination which might heavily influence wheel running screens. The mice were tested for hearing loss with a click box activated from 15cm above the animal (looking for a preyer reflex) and for general awareness and to an extent anxiety by recording response to approach from the front with a gloved hand. Next the animal was suspended by the tail to examine response which can be used to identify motor phenotypes (Figure 2.2). The animal was lowered gently onto a wire grate to examine for reaching and paw placement accuracy and when gripping the grate, gently pulled backwards to assess for gross strength discrepancies. The grate was elevated and inverted and the animal assessed for ability to remain suspended for 30secs. Then the grate was angled onto a flat surface at 80° and the animal allowed to climb down and grip and slipping recorded. The animal was lifted onto a wire suspended approximately 10cm above the arena and allowed to grasp with only its front paws. The animal was released and its ability to hang onto the wire and reach the safety of the edge of the wire scored, which gives another measure of coordination and strength. Lastly the animal was put into a clear perspex tube which was inverted and then its ability to right itself and escape the tube recorded (a test for vestibular defects).

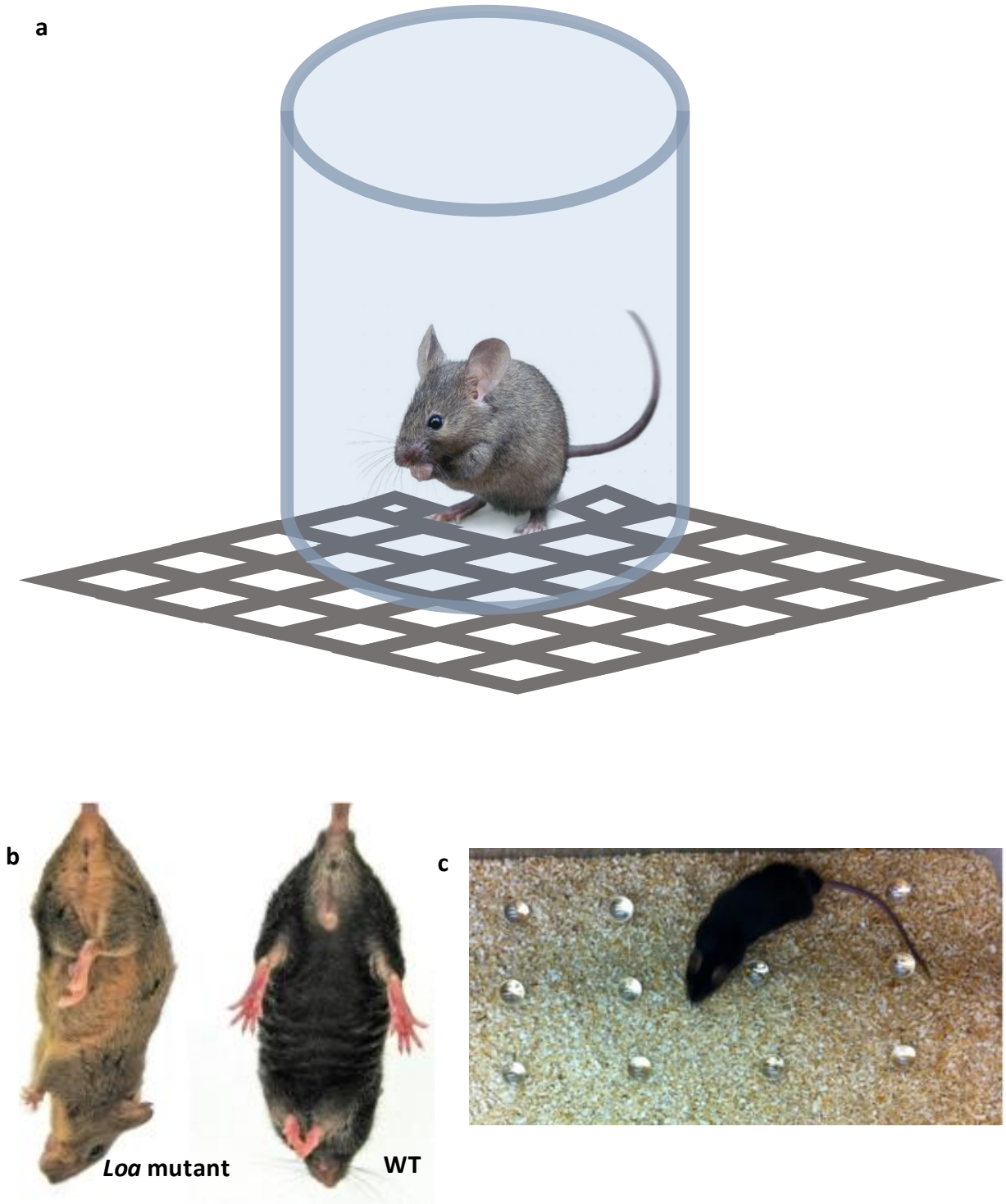

Figure 2.2: Phenotyping protocols

a) Animals are placed on a wire mesh and allowed to explore under a transparent viewing cylinder. Behaviour, breathing rate and any tremors or footfalls are monitored.

b) Tail suspension: Mice showing neurological deficits can be observed to limb grasp as shown (Animals shown here from (Sun et al. 2008)).

c) Marble burying: twelve marbles are arranged as shown on top of 5cm sawdust, the animal allowed to dig undisturbed for 20mins.

2.8.3 Marble burying

Marble burying tests ability to dig (so is used to identify animals with motor/coordination deficits) as well as the will to dig (which reflects the animals state of wellbeing) and response to a novel environment (such as neophobia) (Angoa-Pérez et al. 2013; Deacon 2006b). Animals were placed in a cage filled with 5cm of sawdust with 12 marbles arranged as in Figure 2.2. After 20mins, the animal was returned to the home cage and the marbles scored as buried when less than half of the edge of the marble is visible. Breakdown of part buried marbles was based on partial visibility or complete burial (no surface visible).

2.8.4 Digging

The digging test is an alternative more quantifiable way to test exploratory behaviour, wellbeing and response to novelty (however can be confounded by motor deficits more so than marble burying, so in this pipeline both techniques are used) (Deacon 2006a). Black plastic tubes (20cm long, 6.8cm diameter) were raised at one end by 3cm and closed at the other end. Tubes were filled with 175g food pellets and placed in the corner of a cage containing normal amounts of sawdust. Animals were left in the cage for 2hrs and then returned to the home cage, and the pellets remaining in the tube were weighed.

2.8.5 Spontaneous alternation

Alternation is a good predictor of cognitive capacity and short term memory (Hughes 2004). The T-maze is a black plastic structure, and was filled with a thin layer of sawdust to facilitate running. After 2 trials soiled sawdust from a cage of the opposite gender was used to increase the drive to explore and reduce trial length. Animals were placed in the start arm as shown in Figure 2.3 and allowed to explore freely. Once the animal has chosen a goal arm (the base of the tail has passed into the goal arm), the partition was closed and the animal held in that arm for 20secs. The partition of the chosen arm was raised and the animal allowed to return to the start arm, before removal

from the T maze (so as to avoid associating the removal with either goal arm which might affect the choice of the next trial). All partitions were raised, and the animal was then replaced as in Figure 2.3 and allowed to choose an arm based on the previous experience. Naturally a C57BL/6 mouse will explore one arm of the T maze and then alternate on the second placement approximately 75-80% (Bliss & Errington 1977; Deacon & Rawlins 2005; Deacon & Rawlins 2006) of the time, demonstrating an exploratory behaviour and retained memory of the familiar first arm.

2.8.6 Acoustic Startle and Pre-Pulse Inhibition (PPI)

The acoustic startle and PPI paradigm can be used to test for deficits in sensorimotor gating, which is an endophenotype of schizophrenia in man and in mouse models (Braff et al. 2001). Mice were enclosed in a Perspex tube and placed on a load cell platform and amplifier which recorded vibration as the animal moved (Med Associates Inc Equipment). The soundproofed door was secured shut. A series of 15 40ms 110dB white noises were played alone or preceded by a 65dB, 70dB or 75dB sound in pseudorandom order. The reflexive startle response was tracked throughout and after the series was completed, the mouse was returned to its home cage. The response to the pulse after a pre-pulse was expressed as a percentage of the response to the pulse alone (Nolan et al. 2000). Animals have lower startle responses after a pre-pulse, and deficits in this parameter have been shown to exist as an endophenotype in schizophrenia in man and in models such as Blind-Drunk (*Bdr*) (Jeans et al. 2007).

Figure 2.3: T-maze spontaneous alternation

The animal is placed facing the dead end at the foot of the T maze, and allowed to explore freely. The partitions (in blue) are closed and the animal explores the choice arm for 30 seconds. The animal is removed, the partitions removed and the animal replaced at the foot of the maze and allowed to choose once more, and whether the second arm is an alternation from the first choice arm is recorded. This two-part trial is repeated ten times for each animal.

2.8.7 Fear conditioning

Fear conditioning tests animals for contextual and cued conditioning, a test of memory based on the first trial. Fear conditioning was performed using the Freeze Monitor system (Ugo Basile) as previously described (Lassi et al. 2012). Briefly mice were placed in a wire grid arena in a sound-proof chamber illuminated at 23-26lux. They were exposed to a series of loud tones and associated shocks to condition to the experiment (animals were placed in the arena for a total of 616.5s, and a 5 second tone was played followed by a 0.5s shock at 150s, 305.5s and 461s). 24hrs after conditioning, the mice were placed in the same arena without tones or shocks for 300s (context trial) and returned to the home cage, and after at least 4hrs placed in a circular plexiglass arena scented with vanillin for 360s and exposed to tones but no shocks at 180s, 240s and 300s (cue trial). The activity of the mice in the arena was recorded by video tracking and immobility or freezing episodes quantified by Anymaze software. Increased freezing time in the context and cue trials is indicative of learning. Percentage of time spent freezing was calculated for each trial (split into two sections: before and during/after tones). The difference between percentage of time freezing in the context trial was compared to the percentage in the conditioning trial. The percentage time freezing in the second half of the cue trial is compared to the percentage in the first half of the trial.

2.8.8 Social dominance and recognition testing

In order to investigate social interaction of mice and confrontation-induced anxiety responses in the mutants, animals underwent a social dominance test. Animals were placed facing each other in opposite ends of a perspex tube. The tube is wide enough for one animal to pass through, but not for two. The mice are initially separated by clear perspex partitions. When both animals settled, the perspex doors were lifted and they were allowed to come into contact with one another. A win was defined as the animal pushing the opposite animal out of the tube, a lose if the animal was pushed from the tube. If an animal backed away with minimal contact it was noted down and no win was scored. Protocol adapted from (Messeri et al. 1975)

2.8.9 *Ex vivo*: SCN slices

In order to visualise the endogenous rhythm of the SCN in mutant animals, LSD mutant animals were crossed to m*Per2*:Luc reporter mice and *Kdm1a*$^{E440G/E440G}$; m*Per2*:Luc brains were taken along with *Kdm1a*$^{+/+}$; m*Per2*:Luc control brains for slice experiments. The SCN was extracted from mutant animals and the rhythm of *Per2::Luc* fusion reporter expression recorded through bioluminescent monitoring the luciferase reporter rhythm in a luciferin-containing preparation.

The brain was extracted from the animal taking care to avoid contact with the ventral surface of the brain. It was trimmed and sliced using a McIlwain tissue chopper to 300µm thickness. Slices were floated in ice cold Solution 1 (Table 2.2) and separated and the SCN identified manually using a microscope. The SCN was cut from the coronal Section using razor blades and transferred to a Millipore 22µm membrane with a pipette. The membrane was inserted into a 35mm diameter dish and the base filled with ice cold Solution 2 (Table 2.2). The dish was moved to an incubator kept humidified and at 37°C and allowed to settle for 2hrs, before the media was replaced with warmed Solution 3 (Table 2.2). The slice was incubated undisturbed, allowing for extra cells to slough away over the following week, and Solution 3 (Table 2.2) refreshed every 3 days before any recording was permitted. After 1 week or more, the slice was ready for recording. The media was removed and any excess aspirated from the base of the dish and replaced with pre-warmed Working Solution 4 (Table 2.2). The dish lid was discarded and replaced with a 35mm diameter coverslip, secured in place with parafilm to retain humidity in the dish. The dish was placed in the lumicycle (Actimetrics) which was kept at 37°C 3.5% CO2 in a sealed incubator. For recordings spanning multiple weeks, the media was refreshed approximately weekly. Data was analysed with Lumicycle analysis software (Actimetrics).

2.9 Table of Solutions

MIX	Reagent	Stock conc	ml/mg needed	Overall concentration
Solution 1 (sterile filtered)	GBSS Glucose MK801 MgCl2	- 250mg/ml 10mM 1:1000 150mM	47.5ml 1ml 0.5ml 1ml	 5mg/ml 0.1uM 3mM
Solution 2 (sterile filtered)	Solution 3 MK801 MgCl2	- 10mM 1:1000 150mM	24.25ml 0.25ml 0.5ml	 0.1uM 3mM
Solution 3 (sterile filtered)	EBM EBSS HiHS Glucose Glutamax Pen/Strep	- - - 250mg/ml - -	24.25ml 12ml 12ml 1ml 0.5ml 0.25ml	50% 25% 25% 10mg/ml 2% 1X
Solution 4 (sterile filtered)	Bicarb free DMEM $NaHCO_3$ Glucose HEPES Pen/Strep	- 3.5% w/v 250mg/ml 1M -	48.75ml 0.5ml 1ml 0.5ml 0.25ml	1X 0.035% 5mg/ml 0.01M 1X
Solution 4 (Working) (sterile filtered)	Solution 4 FBS B27 Glutamax Luciferin	- - - - -	9.29ml 0.5ml 0.1ml 0.1ml 10µl	 5% 1% 1% 0.1mM
LB+	Thick set LB Ampicillin	- 100mg/µl	500ml 500µl	 100mg/ml
RIPA	NaCl SDS Na-Deoxycholate NP40 Tris pH 7.5 H2O	Powder 10% 10% - 1M -	1.753g 2ml 10ml 2ml 10ml 176ml	0.15M 0.1% 0.5% 1% 0.05M
RIPA+	RIPA Protease inhibitor Phosphatase inhibitor	- 25X 10X	17ml 1ml 2ml	 1X 1X
Freezing media	Complete media DMSO	- -	9ml 1ml	 10%
Recording media (sterile filtered)	Phenol-free DMEM Glucose HEPES NaHCO3 Pen/Strep H2O	- Powder 1M 7.5% - -	1 bottle 4g 10ml 4.7ml 2.5ml To 1L	1X 0.004mg/ml 0.01M 0.00035% 1X
4% PFA fix	Paraformaldehyde PBS	- -	20g 500ml	4%
WB Blocking	PBST	-	100ml	

Solution	Skim Milk Powder	-	5g	5%
Running buffer	20X Tris Acetate buffer H2O	- -	50ml 950ml	1X
Transfer buffer	Tris Glycine SDS MeOH H2O	- - 10% - -	11.64g 5.88g 7.5ml 400ml 1592.5ml	0.005% 0.039M 0.0004% 20%
PBST	PBS Tween20	- -	500ml 0.5ml	 1%
ECL detection mix	Solution A Solution B	- -	975µl 25µl	
Fugene	Buffer Fugene DNA	 250ng/µl	276µl 18µl 6µl	
JetPrime 3.5cm dish	Buffer JetPRIME DNA	 250ng/µl	66.8µl 1.4µl 2.8µl	
JetPrime 10cm dish	Buffer JetPRIME DNA	 250ng/µl	480µl 15µl 20µl	
A overhangs	PCR product ATP 10X Buffer Taq MgCl2	10ng/µl 1mM 5U/µl 25mM	40.8µl 1µl 5µl 0.2µl 3µl	
Mutagenesis	Reaction Buffer dNTPs QuikSolution F Primer R Primer Plasmid H2O Pfu	 5mM 5mM 10ng/µl	5µl 1µl 3µl 2µl 2µl 1µl To 50µl 1µl	
TOPO cloning transformation (on ice)	PCR product Salt solution H2O TOPO vector		3µl 1µl 2µl 1µl	
cDNA synthesis	RNA RT enzyme RT Reaction mix H2O	1ug/µl	1µl 2µl 10µl 7µl	
Red dye PCR	cDNA F Primer R Primer Pfu Mastermix	1:4 1:10 1:10	1µl 1µl 1µl 0.1µl 6.9µl	
Gold PCR	MgCL2 10X buffer H2O	25mM	2µl 4µl 32µl	

	F Primer R Primer Taq	5uM 5uM 5U/µl	1µl 1µl 0.25µl	
Bioline PCR (Early Per2:Luc genotyping)	H2O Bioline Buffer dNTPs F Primer R Primer WT R Primer Mut MgCl2 Bioline Enzyme DNA	 5mM 5mM 5mM 20ng/µl	37.6µl 5µl 1.25µl 2µl 1µl 1µl 24µl 4.8µl 1µl	
Phusion flash PCR	Phusion Flash Mastermix H2O F Primer R Primer cDNA	 10mM 10mM 1:4	 6µl 4.8µl 0.3µl 0.3µl 0.6µl	
Realtime PCR	SYBR green F Primer R Primer cDNA H2O	 1:10 1:10 1:4	10µl 1µl 1µl 3µl 5µl	
LightScanner PCR	Hotshot LC green H2O F Primer R Primer DNA	 10mM 10mM 5ng/µl	5µl 1µl 1.8µl 0.2µl 0.2µl 2µl	
Pyrosequencing	Qiagen Master Mix H2O F Primer R Primer DNA	 10mM 10mM 5ng/µl	5µl 2.6µl 0.2µl 0.2µl 2µl	
Per2:Luc Genotyping	Hotshot F Primer R Primer WT R Primer Mut H2O DNA	 20mM 20mM 20mM 1:10	7.5µl 0.3µl 0.15µl 0.15µl 4.9µl 2µl	
In Situ Bleach	H2O2 PBST		2ml 8ml	
In Situ Proteinase K	ProtK stock PBST	10mg/ml	1µl 1ml	
In Situ Glycine	Glycine PBST		2mg 1ml	2mg/ml
In Situ Gluteraldehyde	Gluteraldehyde PFA Tween	25% 4% 10%	80µl 10ml 100µl	
Prehyb	Formamide SSC pH 4.5	 20X	25ml 12.5ml	

	H2O Tween Heparin	 10% 100mg/ml	12ml 500µl 25µl	
Hyb	Prehyb Yeast RNA Salmon Sperm DNA	 10mg/ml 10mg/ml	1ml 10µl 10µl	
In Situ Solution 1	Formamide SSC pH4.5 SDS H20	 20X 10%	10ml 4ml 2ml 4ml	
In Situ Solution 2	Formamide SSC pH4.5 H20	 20X	10ml 2ml 8ml	
TBST	NaCl KCl Tris pH7.5 Tween H2O	 1M 10%	0.8g 0.02g 2.5ml 1ml 96ml	
In Situ Preblock	Sheep Serum TBST	10%	1ml 9ml	
NTMT (filter through 0.2uM syringe filter)	NaCl Tris pH 9.5 MgCl2 Tween H2O	5M 1M 1M 10%	1ml 5ml 2.5ml 0.5ml 41ml	

Table 2.2 Table of Solutions

2.10 Table of antibodys

Antibody	Company (number)	Concentration		
		Western	CoIP	Immuno-fluorescence
Anti-MYC (rb)	Sigma (C3956)	1:1000	1:150	1:200
Anti-MYC (ms)	Invitrogen (13-2500)	1:1000	1:150	1:200
Anti-HA (rb)	Sigma (H6908)	1:1000	1:150	1:200
Anti-HA (ms)	Covance (MMS101R)	1:1000	1:150	1:200
Anti-V5 (ms)	Invitrogen (R96025)	1:5000	-	1:400
Anti-FLAG (ms)	Sigma (F3165)	1:500	1:50	1:100
Anti-Actin (rb)	Autogen (ACT822-A)	1:10000	-	-
Anti-LSD1 (rb)	Abcam (AB17721)	1:1000	-	1:200
Anti-LSD2 (rb)	Abcam (AB52001)	1:1000	-	1:200
Anti-Rabbit HRP	BioRad (170-6515)	1:10000	-	-
Anti-Mouse IgG Peroxidase	Sigma (A4416)	1:10000	-	-
Anti-rabbit Green (Licor)	Li-COR (925-32213)	1:10000	-	-
Anti-rabbit Red (Licor)	Li-COR (926-68073)	1:10000	-	-
Anti-mouse Green (Licor)	Li-COR (925-32212)	1:10000	-	-
Anti-mouse Red (Licor)	Li-COR (926-68072)	1:10000	-	-
Anti-Goat Red?	Li-COR (926-68074)	1:10000	-	-
AlexaFluor 488 (mouse, rabbit)	Invitrogen (A10684, A11070)	-	-	1:300
AlexaFluor 568 (goat, rabbit)	Invitrogen (A21069, A11057)	-	-	1:300
AlexaFluor 647 (mouse, goat)	Invitrogen (A21235, A21447)	-	-	1:300

Table 2.3 Table of antibodys

2.11 Table of Primers

S = Sequencing
C = Cloning
M = Mutagenesis
G = Genotyping
L = LightScanner
I = In Situ Probe
Q = qPCR

Primer name	Cat	5'-3' sequence
CRY1INTFOR	S	TCCCCTCCCCTTTCTCTTTA
CRY1INTREV	S	TGAGTCATGATGGCGTCAAT
CRY2INTFOR	S	TGAGAATGGGATTCCAGGAG
CRY2INTREV	S	AACAGCCTTGGGAACACATC
Cry1INTRev	S	CTGTTGATGCCCACGTT
Cry1INTFor	S	GAGCTGTAGCGGTGGAAA
Cry2INTRev	S	TGCCCACAGACGAGGAG
Cry2INTFor	S	AGAGCACTATCCAGTGGC
PlasCheckLSD1.HA_HAF	S	TACCCATACGACG
PlasCheckLSD1.HA_HAR	S	TGCATAATCTGGC
PlasCheckLSD1.HA_S1F	S	GGTAGAATAGACAGAG
PlasCheckLSD1.HA_S1R	S	CGAATAATATTCATCTTC
PlasCheckLSD1.HA_S2F	S	CGCCTTACAACAGCG
PlasCheckLSD1.HA_S2R	S	CTCTTGTAGATGCC
PlasCheckLSD1.HA_S3F	S	CAACGTCCTCAATAAT
PlasCheckLSD1.HA_S3R	S	GCTGAATGACAACC
PlasCheckLSD1.HA_S4F	S	GATCAGGATGATGAC
PlasCheckLSD1.HA_S4R	S	CAGGCACACATGAGTAG
PlasCheckLSD1.HA_S5F	S	TAGCAGGAGAAGCTGC
PlasCheckLSD1.HA_S5R	S	GAATGGCCAGGCACCG
PlasCheckLSD1.HA_EndF	S	CTGCACAGCAGT
LSD1 E10 F	L	CAGCTGGGCCATATATATGTG
LSD1 E10 R	L	AAGGAATCCCCGTTTTAGTTT
LSD1 E11 Fb	L	TGAATTGCTTTGCTATCGAGTATGA
LSD1 E11 Rb	L	TGACTGTTGAGGGCAGG
LSD1 E12 Fc	L	CTATTTAAGATTAAGCCACACTCATTTAT
LSD1 E12 Rc	L	ATTCTTAATGTCTGAGTTTCTCTCC
LSD1 E19 Fb	L	TAAAGTTATGTTTGCAACTTGGTGAT
LSD1 E19 Rb	L	GTAGCTGATGACATGGAGTTTC
LSD2 E6 F	L	AAGGTTAGGCCATCTATATTTGTC
LSD2 E6 R	L	AGATATGCTCCTGATACAGAGTGA
LSD2 E7 F	L	GGGAGGTATCATATTGAAAGAAAATGGA
LSD2 E7 R	L	TAGATGCTAGTCATTTACTTAGTGAACG
LSD2 E9 F	L	GCTTGCAGAGCTGCTTG
LSD2 E9 R	L	TGCTGCTGCTGCTGCTA
LSD2 E10 F	L	TATTGGTTACTTACTTTGTTGCTGT
LSD2 E10 R	L	CACCCAAAGGCAGAGCCTA
LSD2 Ex1 INTR	S	GAGAAAGCTCCAAATTGCTTCTC
LSD2 Ex21 INTF	S	TGCTGGTGAGGCAACA

LSD2 Ex6.7 F	S	AGAGTGTGGACCAGCAACGGCAAGACGGAG
LSD2 Ex6.7 R	S	CCTTCAGCAACGGAGGCTGGATGAGCAT
LSD2 Ex9.10 F	S	GCACCAGCACACATCGTGCCACCGTCACAG
LSD2 Ex9.10 R	S	CTAGCAGCTGCTAAGCCTGCTGGACCAG
LSD1 Ex1 INTR	S	CCGGCCTCGGTCCCAGCAGC
LSD1 Ex19 INTF	S	GCTTCGAGAAGCAGGAAGGATTG
LSD1 Ex10.11 F	S	GCTAGAAGCCACTTCTTACCTTAG
LSD1 Ex10.11 R	S	GATTGGCTTCCAATTCTTGAAG
E440G Reverse Probe	G	CTCTTTCAACTCCCCCTGAGTTTTCA[AmC3]
L491H Forward Probe	G	CTGACTGCCCACTGCAAGGTCA[AmC3]
LSD2 E9 M271T F	M	CTCTTCACTTGTCCTAGGCACGAACCGGTACTTCCAGCCG
LSD2 E9 M271T R	M	CGGCTGGAAGTACCGGTTCGTGCCTAGGACAAGTGAAGAG
LSD2 E9 N272S F	M	TTCACTTGTCCTAGGCATGAGCCGGTACTTCCAGCCGTTC
LSD2 E9 N272S R	M	GAACGGCTGGAAGTACCGGCTCATGCCTAGGACAAGTGAA
LSD2 E9 P281L F	M	CTTCCAGCCGTTCTACCAGCTCAACGAGTGTGGGAAAGCG
LSD2 E9 P281L R	M	CGCTTTCCCACACTCGTTGAGCTGGTAGAACGGCTGGAAG
LSD2 E10 T357M F	M	CTTTACTTCATGATGAGGAAAGGCCTC
LSD2 E10 T357M R	M	GAGGCCTTTCCTCATCATGAAGTAAAG
LSD2 E10 V366A F	M	GGCCTCATCAACACAGGCGCTCTCACGGTGGCAGCCGGCC
LSD2 E10 V366A R	M	GGCCGGCTGCCACCGTGAGAGCGCCTGTGTTGATGAGGCC
Per1 Luc Walk	S	CAATCACATGGTGACTCACAAC
ReverbaLuc Walk R	S	GTTTGGAAAGCCTTGTATGGC
ReverbaLuc Walk F	S	GACCTTACTGCTCCTCG
Per1 promoter F	S	ATTAAATTAGTCAGCC
Per1 promoter R	S	GGTGAAGAAGCCAC
Per2:Luc Genotyping P1	G	CTGTGTTTACTGCGAGAGT
Per2:Luc Genotyping P2	G	GGGTCCATGTGATTAGAAAC
Per2:Luc Genotyping P3	G	TAAAACCGGGAGGTAGATGAG
Nde1 F LSD1	C	TATGCCACCATGTTGTCTGGGAAGAAG
Xba1 R LSD1	C	CTAGACACCTCACATACTTGGGGACTG
Nde1 F LSD2	C	TATGCCACCATGGCCGCATCTCGAGGG
Xba1 R LSD2	C	CTAGACACCTCAACCGGGCCCAAAGGC
LSD1 E440G F	M	GAAGATAGTGAAAACTCAGGGGGAGTTGAAAGAGCTTC
LSD1 E440G R	M	GAAGCTCTTTCAACTCCCCCTGAGTTTTCACTATCTTC
LSD1 Ex11 smlAmplicon Geno F	L	TCCTGGTGAAGAGCAAGC
LSD1 Ex11 smlAmplicon Geno R	L	TGTTGAGGGCAGGCCGA
Per1 Promoter Walk R	S	CTACTACCACATAG
Per1 Promoter Walk2b R	S	GAATGAAATGTCTGC
Per1 Promoter Walk3 R	S	CTCAAGGATTTAGGTGTG
Per1 Promoter Walk4 R	S	GATCTTGGGAGAGGAATAC
Per1 Promoter Walk5 R	S	GTCCAGGGACCCTAGAGTGGTG
Per1 Promoter Walk6 R	S	CTGCGGAGTCTGCGCAGGCG
Per1 Promoter Walk7 R	S	CTCACTCTGTAGACTAGGC
Per1 Promoter Walk8 R	S	CAGAGATCCATATGCCAC
Per1 Promoter Walk9 R	S	GTCAGCTTTGCCTCATC
Per1 Promoter Walk10 R	S	CCTCTATCATTGTACTC
Per1 Promoter Walk11 R	S	CAAGAGGTGTGGGAAAC
Per1 Promoter Walk12 R	S	GATGGGAACCTCAGG
Per1 Promoter Walk13 R	S	CTATACAACACTCAAG

Luciferase Sequence INTRev	S	GTTCCATCTTCCAGCGGATAG
In Situ Probe LSD1 F	I	GGAAGCCAGGGATCGAGT
In Situ Probe LSD1 R	I	GAACAGCTGGTGGCTGCT
LSD2 pCM3 vector F	S	GAGGCAACAAACAGGC
Clock-Flg vector R	S	GTCCTTGTCATCTTCTTCC
Clock-Flg vector F	S	GCAACACCAGCCTCAGCAG
LV Per2Luc vector CMV F	S	CGCAAATGGGCGGTAGGCGTG
LV Per2Luc vector V5 R	S	ACCGAGGAGAGGGTTAGGGAT
Per2Luc Lvrev seq1	S	GAAGCCTACTAAAGCGTTCAG
Per2Luc Lvrev seq2	S	CTTGCTCTACATTTGGCCTGC
Per2Luc Lvrev seq3	S	GTTTCAGGGTTATAAGGACAG
Per2Luc Lvrev seq4	S	CTCAAGGTGAAATCCTGC
Per2Luc Lvrev seq5	S	GAGGTGATCCTCTATGTATG
Per2Luc Lvrev seq6	S	CTCAATGTGGCAGGAATC
Per2Luc Lvrev seq7	S	CCATGCACGACTGATCTG
Per2Luc Lvrev seq8	S	CAGATAGTAAACAGTCTCAGC
Per2Luc Lvrev seq9	S	GGAGCTAGTCCAGTAGCCAC
Per2Luc Lvrev seq10	S	CATTAGCTAGAAAGCAATC
Per2Luc Lvrev seq11	S	CCTCTGTGAAATATAAGG
Per2Luc Lvrev seq12	S	CAGCTTCAGACTTTG
Per2Luc Lvfor seq Luc INT	S	GTAACAACCGCGA
LVP2L Promoter_to_Luc F	S	GAGCGCGCAGCATCTTCATTG
LSD2 P196Ah P334Am F	M	TGCAAAGAAGCTCTCACCGCTCAGAAGTGCATTCCCC
LSD2 P196Ah P334Am R	M	GGGGAATGCACTTCTGAGCGGTGAGAGCTTCTTTGCA
LSD1 E440G Pyrosequencing F	G	AGGCTGCAAGAAAAGCATGT
LSD1 E440G Pyrosequencing R	G	Btn-ACACTGAATGCAAAGCTCTACCT
LSD1 E440G Pyrosequencing Seq	G	GAAGATAGTGAAAACTCAGG
LSD1 L491H Pyrosequencing F	G	TATCACAGCCGAGTTCCTGG
LSD1 L491H Pyrosequencing R	G	Btn-AGGCCGACACTGACCTTG
LSD1 L491H Pyrosequencing Seq	G	GGGACCTGACTGCCC
LSD2 P281L Pyro F	G	CTAGGCATGAACCGGTACTTCC
LSD2 P281L Pyro R*	G	Btn-CTCACGCACAGCGCTTTC
LSD2 P281L Pyro Seq	G	TCCAGCCGTTCTACC
LSD2 T357M Pyro F	G	AGATGCGTTCAGGAAGTGGA
LSD2 T357M Pyro R*	G	Btn-CGTGAGAACGCCTGTGTTGAT
LSD2 T357M Pyro Seq	G	GGAGAGGATTCTTTACTTCA
POPINJ Seq	S	AACGTATTGAAGCTATCCC
LSD1 qPCR F	Q	CTTTAGCTGAAGGCTTGGAC
LSD1 qPCR R	Q	CAATCACTTCACATCCTGAGG
LSD2 qPCR F	Q	AGCGCTTCTGAAAGATGTG
LSD2 qPCR R	Q	TTCATTGCAGAAGTGTTCCC
LSD1 L491H F	M	GCACAGGGACCTGACTGCCCACTGCAAG
LSD1 L491H R	M	CTTGCAGTGGGCAGTCAGGTCCCTGTGC
LSD1 qPCR F MCB	Q	CACAGCAGTCCCCAAGTATGT
LSD1 qPCR R MCB	Q	GCCTCTGCTGTCAAACTAGGA

Table 2.4 Table of Primers

2.12 Table of consumables and reagents

Reagent	Company	Order No.
10 ml Serological Pipettes	Greiner Bio-One	607180
100 mm Tissue Cµlture Dish	Greiner Bio-One	664160
100 bp Ladder	NEB	N0467S
1kb Ladder	NEB	N3232
25 ml Serological Pipettes	Greiner Bio-One	760180
35mm Tissue Culture Dishes	Greiner Bio-One	627160
5ml Serological Pipettes	Greiner Bio-One	606180
60mm Tissue Culture Dishes	Greiner Bio-One	628160
Agarose	Sigma	A9539
Albumin from Bovine Serum	Sigma	A2153
Amersham ECL Plus™ Western Blotting Detection Reagent	GE healthcare	RPN2132
Ampicillin	Sigma	A9518
Anti-Digoxigenin-AP, Fab fragments	Roche	11 093 274 910
β-mercaptoethanol	Sigma	M3148
Bacterial Grade Petri Dishes	VWR	82050-910
BIOTAQ Core Kit	Bioline	BIO-21071
Beetle Luciferin potassium salt	Promega	E1602
Blotting Paper, Extra Thick	Biorad	1703966
Bradford Reagent	Sigma	B6916
Calf Serum	Invitrogen / GIBCO	16010-159
Cell Scrapers	Greiner Bio-One	541070
Chloroform	BDH Chemicals	277106P
Complete, EDTA-free (Protease Inhibitor Cocktail Tablets)	Roche	11873580001
Cover-slips 22 X 22 mm	VWR	631-0124
dNTP 100mM Set	Invitrogen	10297-018
Denhardt's Solution	Serum Biotech	304205
Dexamethasone	Sigma	D4902-25MG
DH5α Competent Cells	Invitrogen	18265-017
DMEM (Dulbecco's Modified Eagle´s Medium)	GIBCO	3196-021
Dimethyl sulfoxide (DMSO)	Sigma	D2650
dNTP Mix 40mM	Bioline	BIO-39043
Donkey Serum	Sigma	D9663-10ml
DPBS (Dulbecco's Phosphate Buffered Saline)	Lonza	LONZ17-512F/12
DPX Mountant for Histology	BDH Chemicals	360294H
EBM	Sigma	B1522
EBSS	Sigma	E2888
Ethanol (EtOH)	Fisher Scientific	E/0650DF/17
Ethylenediaminetetraacetic Acid 99.995% (EDTA)	Sigma	431788
FG microplate LHS 96 well	Invitrogen	4346906
Foetal Bovine Serum	PAA Laboratories Limited	A15-010
Formamide	Sigma	F7508
Forskolin	Sigma	F6886
Fugene 6	Roche	11814443001
GBSS	Sigma	G9779

GelRed	Biotium	41003-1
GlutaMAX™-I Supplement, 200mM	Invitrogen	35050038
Glycerol	Fisher Scientific	G/0650/17
Glycine	Sigma	G7126
HEPES (1M solution)	Sigma	H0887
HindIII	NEB	R0104
HiMark Prestained Protein Standard	Invitrogen	LC5699
Hybond Blotting Paper	GE healthcare	RPN6101M
Hydrochloric Acid	Fluka	84436
Immidazole	Sigma	15513
Inoculation Loops	Sarstedt	203-10
Isopropanol	Fisher	P/7490/17
jetPRIME	POLYPLUS TRANSFECTION	114-15
Low-Fluorescence PVDF Transfer Membrane	Thermo Scientific	22860
Magnesium Chloride Hexahydrate	Sigma	M270
McCoy´s 5A Culture Media	PAA Laboratories Limited	E15-022
Non-essential Amino Acid Solution (100X)	Sigma	M7145
Methanol	Fisher Scientific	M/3950/17
MicroAmp FastOptical qRT-PCR plates	Applied Biosystems	403012
Midiprep	Invitrogen	K210014
MK801	Sigma	M107
NaCl	Sigma	S3014
NBT/BCIP Stock Solution	Roche	11 681 451 001
Nonidet P40 Substitute	Sigma	74385
NotI	NEB	R0189
NuPAGE® Antioxidant	Invitrogen	NP0005
NuPAGE® LDS Sample Buffer (4X)	Invitrogen	NP0007
NuPAGE® Novex 3-8% Tris-Acetate Gel 1.0 mm, 10 well	Invitrogen	EA0375BOX
NuPAGE® Novex 3-8% Tris-Acetate Gel 1.0 mm, 12 well	Invitrogen	EA03752BOX
NuPAGE® Novex 3-8% Tris-Acetate Midi Gel, 20W	Invitrogen	WG1602A
NuPAGE® Novex 4-12% Bis-Tris Gel 1.0 mm, 12W	Invitrogen	NP0322
NuPage® Sample Reducing Agent 10X	Invitrogen	NP0004
NuPAGE® Tris-Acetate SDS Running Buffer (20X)	Invitrogen	LA0041
OrangeG Loading Dye	NEB	B70225
Organotypic insert membranes	Millipore	PICMORG50
PCR plate Adhesive Seals	ThermoScientific	ab0558
Penicillin/Streptomycin	Lonza	DE17602E
Paraformaldehyde	Sigma	P6148-500g
PhosSTOP (Phosphatase Inhibitor Cocktail Tablets)	Roche	4906837001
Phusion Flash Polymerase Master Mix	Fisher Scientific	F-548L
Prolong gold Antifade Reagent with DAPI	Invitrogen	P-36931
Protein G Sepharose	Sigma	P3296
QIAfilter Plasmid Midi Kit	Qiagen	12243
Qiagen cDNA Synthesis Kit	Qiagen	210212
QIAquick Gel Extraction Kit	Qiagen	28704
QIAquick PCR Purification Kit	Qiagen	28104

Qiazol Reagent	Qiagen	79306
Qiagen RNase-free DNase kit	Qiagen	79254
Qiagen RNeasy mini plus kit	Qiagen	74134
SeeBlue® Plus2 Pre-Stained Standard	Invitrogen	LC592
SimplyBlue™ SafeStain	Invitrogen	LC6060
Skim Milk Powder	Sigma	70166-500G
SNAPid	Millipore	WAVDBASE
SNAPid Single Blot Holder	Millipore	WBAVDBH01
SOC outgrowth medium	NEB	B9020S
Sodium Acetate	Sigma	S2889
Sodium Deoxycholate >97%	Sigma	D6750
Sodium Dodecyl Sulphate >97%	Schwarz Mann Biotech	811036
Sodium Hydroxide ACS reagent, ≥97.0%, pellets	Sigma	221465
Steriflip falcon tubes	Millipore	FDR-140-030D
Superscript III First Strand QPCR Supermix	Invitrogen	11752050
T175 Flask with Filter Cap	Greiner Bio-One	660175
T25 Flask with Filter Cap	Greiner Bio-One	690175
T4 Ligase	NEB	M0202S
T4 Ligase Buffer	NEB	B0202S
T75 Flask with Filter Cap	Greiner Bio-One	658175
Taq mastermix for pyrosequencing	Qiagen	201445
Taq Master Mix II	Biogene	PCRM002D
Taqman Mastermix, Platinum	Invitrogen	11743-500
Thermo-Fast 96 Well Non-skirted, Natural PCR plate	Abgene	TUL-962-011N
TOPO TA Cloning kit (pCR® 2.1-TOPO®)	Invitrogen	K4600-01
Tris Base	Bio rad	161-0716
Tris-HCL	Promega	H5121
Trypan Blue	Invitrogen	15250-061
Trypsin-Versene (EDTA)	Lonza	733-1806
Tween®20	Sigma	P137-9
UltraPure DEPC-Treated Water	Invitrogen	750023
DNase I	Qiagen	74104/74106
Parafilm	Parafilm	PM992
Fast 96 well optical plate	Invitrogen	4346906
Microamp Optical Adhesive Film	Life Technologies Ltd	4360954
Nunc 96 well dish	Sigma	P8241

Table 2.5 Table of consumables and reagents

2.13 Table of constructs

Construct	Insert	Vector Backbone	Tags	Origin
Bmal1-V5-HIS	Full length mouse cDNA	pcDNA3.1	V5, HIS	Michael Hastings lab.
CoREST	Full length human cDNA	pcDNA3.1A	Myc	A kind gift from Gail Mandel
Cry1-HA	Full length mouse cDNA	pcDNA3.1	HA	Michael Hastings lab.
Cry2-HA	Full length mouse cDNA	pcDNA3.1	HA	Michael Hastings lab.
EV-HA	HA epitope only	pCI(modified)	HA	Yutaka Miura lab.
EV-LSD1	HA epitope only		HA	Hans Reinke lab.
EV-MYC	MYC epitope only	pCI(modified)	Myc	Yutaka Miura lab.
LSD1-(wt)-HA	Full length mouse cDNA	pMC3	HA	Hans Reinke lab.
LSD1-(E440G)-HA	Full length mouse cDNA	pMC3	HA	Hans Reinke lab.
LSD1-(L491H)-HA	Full length mouse cDNA	pMC3	HA	Hans Reinke lab.
LSD1-(E440G;L491H)-HA	Full length mouse cDNA	pMC3	HA	Hans Reinke lab.
LSD1-GST	Full length mouse cDNA	POPIN-J	GST	OPPF, RAL, Harwell
LSD2-(wt)-HA	Full length mouse cDNA	pMC3	HA	Hans Reinke lab.
LSD2-(M271T)-HA	Full length mouse cDNA	pMC3	HA	MRC Harwell (From Reinke construct)
LSD2-(V366A)-HA	Full length mouse cDNA	pMC3	HA	MRC Harwell (From Reinke construct)
LSD2-(P281L)-HA	Full length mouse cDNA	pMC3	HA	MRC Harwell (From Reinke construct)
LSD2-(N272S)-HA	Full length mouse cDNA	pMC3	HA	MRC Harwell (From Reinke construct)
LSD2-GST	Full length mouse cDNA	POPIN-J	GST	OPPF, RAL, Harwell
Per1-HA	Full length mouse cDNA	pcDNA3 vers.b	HA	Bert van der Horst lab ErasmusMC Rotterdam
Per2-HA	Full length mouse cDNA	pcDNA3 vers.b	HA	Bert van der Horst lab ErasmusMC Rotterdam
Per1-V5-HIS	Full length	pcDNA3.1	V5, HIS	Nolan lab MRC

	mouse cDNA			Harwell
Per2-V5-HIS	Full length mouse cDNA	pcDNA3.1	V5, HIS	Nolan lab MRC Harwell
Per2::Luc	Mouse Per2 promoter fused to firefly luciferase	PGL4	-	Meng lab, Manchester
Rev-erba-V5-HIS	Full length mouse cDNA	pcDNA3.1	V5, HIS	Nolan lab MRC Harwell

Table 2.6 Table of constructs

2.14 Table of PCR programs

Program Name	Program Number	Step/ Number of temperature step	Temp (°C)	Time/repeat number
CDNA synth 1		Heated lid	112	
		1	25	10:00
		2	50	30mins
		3	85	05:00
		Store	4	inf
cDNA synth 2		Heated lid	112	
		1	37	20:00
		Store	4	inf
EAR BIOPSY	4	Heated lid	112	
		1	95	90min
		Store	4	inf
HOTSHOT	5	Heated lid	110	
		1	98	00:10
		Start Cycle		30X
		2	98	00:01
		Gradient	55-70	02:00
		3	72	00:30
		EC		
		4	72	01:00
		Store	4	inf
LIGATE Overnight Cloning PCR	6	Heated lid	110	
		Start Cycle		16X
		1	14	1hr
		EC		
		Store	4	inf
LS 51	7	Heated lid	110	
		1	95	05:00
		Start Cycle		44X
		2	95	00:30
		3	51	00:30
		4	72	00:30
		EC		
		5	72	05:00
		Store	4	inf

LS 56	7	Heated lid	110	
		1	95	05:00
		Start Cycle		44X
		2	95	00:30
		3	56	00:30
		4	72	00:30
		EC		
		5	72	05:00
		Store	4	inf
LS 60	7	Heated lid	110	
		1	95	05:00
		Start Cycle		44X
		2	95	00:30
		3	60	00:30
		4	72	00:30
		EC		
		5	72	05:00
		Store	4	inf
LS 63	7	Heated lid	110	
		1	95	05:00
		Start Cycle		44X
		2	95	00:30
		3	63	00:30
		4	72	00:30
		EC		
		5	72	05:00
		Store	4	inf
LS GRADIENT		Heated lid	110	
		1	95	05:00
		Start Cycle		44X
		2	95	00:30
		Grad	50-80	00:30
		3	72	00:30
		EC		
		4	72	05:00
		Store	4	inf
LS LUNAPROBE		Heated lid	Off	
		1	95	02:00
		Start Cycle		80X
		2	95	00:30

		3	60	00:30
		4	72	00:30
		EC		
		5	95	00:30
		6	25	00:30
		7	15	00:30
		Store	4	inf
MUTAGENESIS		Heated lid	112	
		1	95	01:00
		Start Cycle		18X
		2	95	00:50
		3	60	00:50
		4	68	08:30
		EC		
		5	68	07:00
		Store	4	inf
MycoplasmaTest		Heated lid	112	
		1	94	01:00
		Start Cycle		35X
		2	94	00:30
		3	62	00:30
		4	72	00:30
		EC		
		5	72	03:00
		Store	4	inf
NEW HS GRAD		Heated lid	112	
		1	94	02:00
		Start Cycle		44X
		2	94	00:30
		Grad	65-80	00:30
		3	72	00:30
		EC		
		4	72	05:00
		Store	4	inf
PER2:LUC		Heated lid	112	
		1	95	01:00
		Start Cycle		35X
		2	95	01:00
		3	56	01:00
		4	72	01:00

		EC		
		5	72	07:00
		Store	4	inf
PHUSION		Heated lid	110	
		1	98	00:10
		Start Cycle		30X
		2	98	00:01
		3	45	00:05
		4	72	01:40
		EC		
		5	72	05:00
		Store	4	inf
Phusion grad		Heated lid	110	
		1	98	00:10
		Start Cycle		30X
		2	98	00:01
		Gradient	65-80	00:05
		3	72	01:40
		EC		
		4	72	05:00
		Store	4	inf
Pyrosequencing		Heated lid	112	
		Start Cycle		44X
		1	95	00:15
		2	60	00:15
		3	72	00:15
		EC		
		4	72	05:00
		Store	4	inf
Red mix Cloning PCR		Heated lid	112	
		1	94	02:00
		Start Cycle		44X
		2	94	00:30
		Grad	55-80	00:30
		3	72	00:30
		EC		
		4	72	05:00
		Store	4	inf
TaqGold Cloning PCR		Heated lid	112	

		1	94	05:00
		Start Cycle		30X
		2	94	02:00
		Grad	45-75	01:30
		3	72	03:00
		EC		
		4	72	10:00
		Store	4	inf

Table 2.7 Table of PCR programs

Chapter 3

IDENTIFICATION OF MUTANTS AND *IN SILICO* ANALYSIS

CHAPTER 3: Identification of Mutants and In Silico Analysis

3.1: Introduction

Upon initiation of the current investigation, the roles of LSD1 and LSD2 in circadian mechanisms had not been previously investigated. Rhythmic histone methylation had been demonstrated at the promoters of rhythmically expressed genes (Katada & Sassone-Corsi 2010). Historic evidence had suggested that MAOIs affected the clock in rodents (Section 1.6) (Montanaro et al. 1965; Snyder & Axelrod 1965) but it was unclear which targets of MAOIs were mediating these circadian effects (Duncan 1996; Weber et al. 2009). MAO-A and MAO-B inhibition could explain some circadian effects as monoamine metabolism (especially that of serotonin (Rea et al. 1994; Tominaga et al. 1992)) is known to affect the clock. Alternatively LSD1 and LSD2 may mediate (at least in part) the circadian effects of MAOIs (Menke et al. 2012). Both LSDs were known targets of the MAOI tranylcypromine (Binda et al. 2010) which has been shown to increase melatonin and affect sleep wake cycles previously (Oxenkrug et al. 1988). This led to the preliminary investigation of the role of LSD1 and LSD2 in the clock in the Reinke laboratory (Personal Communication Dr H. Reinke, Uni Düsseldorf, Ge).

To check if LSD1 expression was under circadian regulation, LSD1 expression was monitored in wild type mouse liver. Tissue was taken at ZT0, ZT4, ZT8, ZT12, ZT16 and ZT20 to examine LSD1 expression. It was observed that protein levels of LSD1 oscillate over 24 hours, displaying high expression levels in the light phase and low during the dark phase (Figure 3.1).

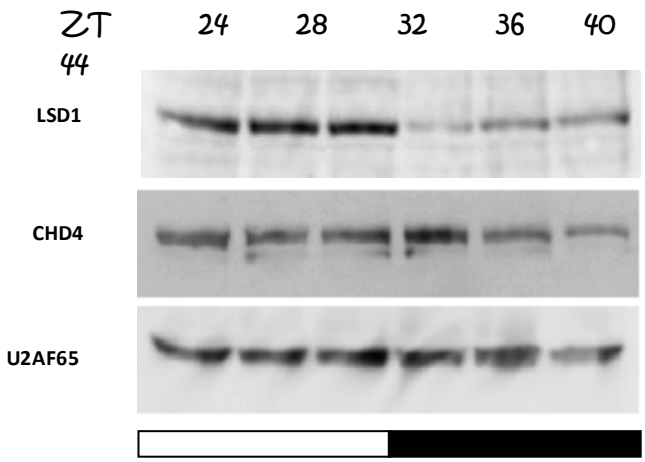

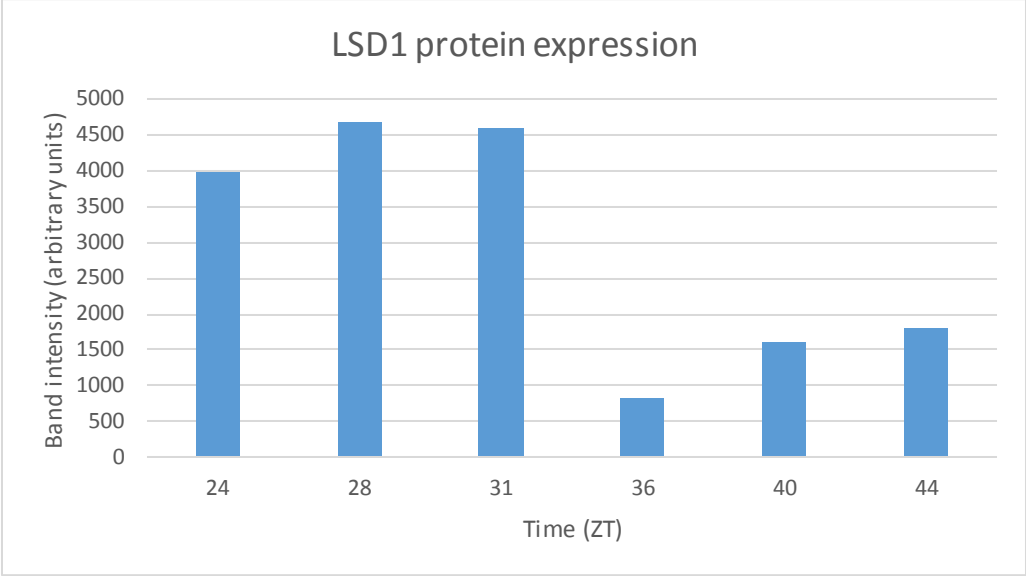

Figure 3.1: LSD1 protein expression in wild-type liver

Expression of LSD1 protein was analysed at four hour intervals over 24 hours by western blot using wild-type mouse liver. LSD1 protein was high during the light phase and low during the dark phase. (Personal Communication Dr H. Reinke, Uni Düsseldorf, Ge)

The use of knockout models was approached in the Düsseldorf lab to gather preliminary data which suggested LSD1 and LSD2 played a role in circadian mechanisms. However, circadian behaviour was not assessed *in vivo.*

LSD1 and LSD2 were identified as potential circadian regulators through cell-based work undertaken in the Reinke Laboratory (Personal Communication Dr H. Reinke, Uni Düsseldorf, Ge).

3.1.1: LSD1 and LSD2 siRNA knockdown

To investigate the roles of LSD genes in circadian rhythms, firstly the genes were knocked down. When siRNA directed against LSD1 was administered to NIH-3T3 cells transiently expressing a *Bmal1*:Luc reporter, circadian oscillations in luciferase (following precisely endogenous transcription of Bmal1) were observed to be dampened using several different variations in siRNA sequence (Figure 3.2a). Similarly, when LSD2 was knocked down, amplitude of these circadian oscillations was dampened (Figure 3.2a).

A further manipulation of circadian function was performed next, examining phase resetting of the oscillator. Knockdown (siRNA treated) cells were synchronised with dexamethasone and upon second synchronisation, the phase of *Bmal1*:Luc oscillation was shifted relative to control rhythms (Figure 3.2b). The investigation of phase shifts in this way can demonstrate the response of the molecular clock to perturbation as a cellular alternative to much a light pulse administered *in vivo*. Knockdown of LSD2 caused an advance in oscillations (shift forwards) and LSD1 a delay in circadian phase of oscillation, so perhaps the two genes have opposing roles in phase resetting the clock in response to glucocorticoid-mediated synchronisation. Phase resetting will be further explored *in vivo* in later chapters.

3.1.2 LSD1 knockout

Kdm1a$^{-/-}$ animals are embryonic lethal, but from the embryonic tissue, fibroblasts can be extracted and cultured in order to characterise this rhythmic expression. Both mRNA and protein expression of many of the core clock components oscillate over 24 hours in peripheral tissues. Knockout of LSD1 causes a change in expression of negative limb components of the molecular clock in peripheral fibroblasts, including *Per2* and *Rev-erbα* (Figure 3.3). *Kdm1a*$^{-/-}$ MEFs also displayed a lack of oscillation in the protein expression of *Rev-erbα* (Figure 3.4). This demonstrates that loss of LSD1 impacts on the expression of core circadian clock components in embryonic tissue. LSD1 may also play a role in adult rhythms, and the nature of these could be further examined in an adult system if one were available.

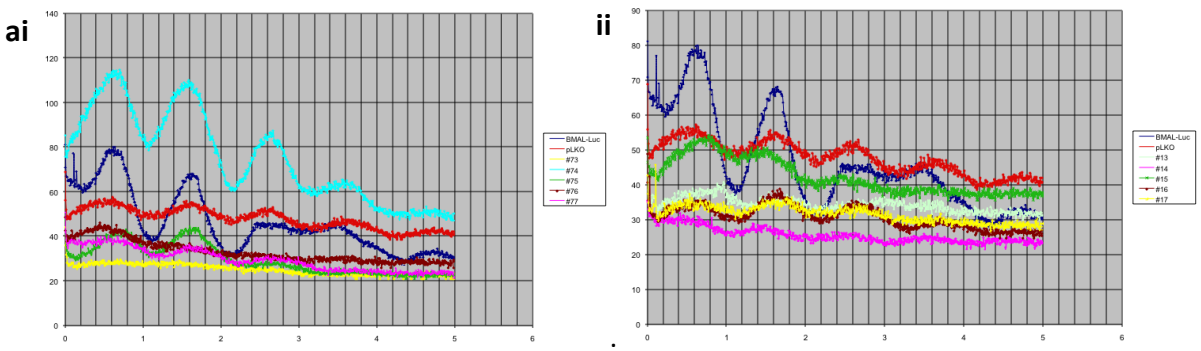

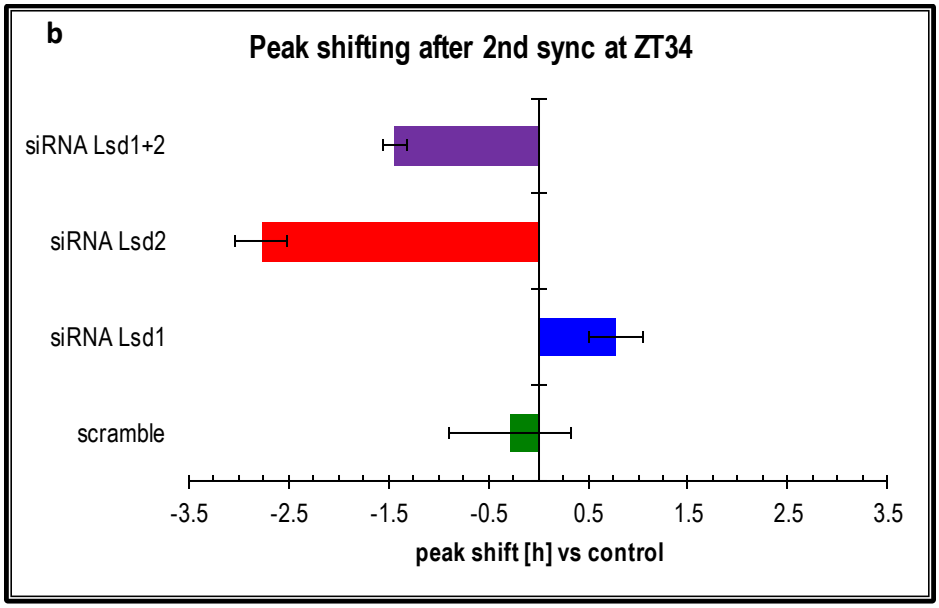

Figure 3.2: Knockdown of LSD1 and LSD2 by siRNA

a) Knockdown of i) LSD1 and ii) LSD2 by various siRNA constructs dampens circadian oscillation when compared to the oscillation of cells without siRNA knockdown (Dark blue traces) in *Bmal1*:Luc expressing NIH-3T3 cells (Personal Communication Dr H. Reinke, Uni Düsseldorf, Ge).

b) Knockdown of LSD1 and LSD2 affect the phase of oscillation in opposing directions after synchronisation with dexamethasone. The double knockdown displays a shift intermediate to the two single knockdown preparations. (Personal Communication Dr H. Reinke, Uni Düsseldorf, Ge)

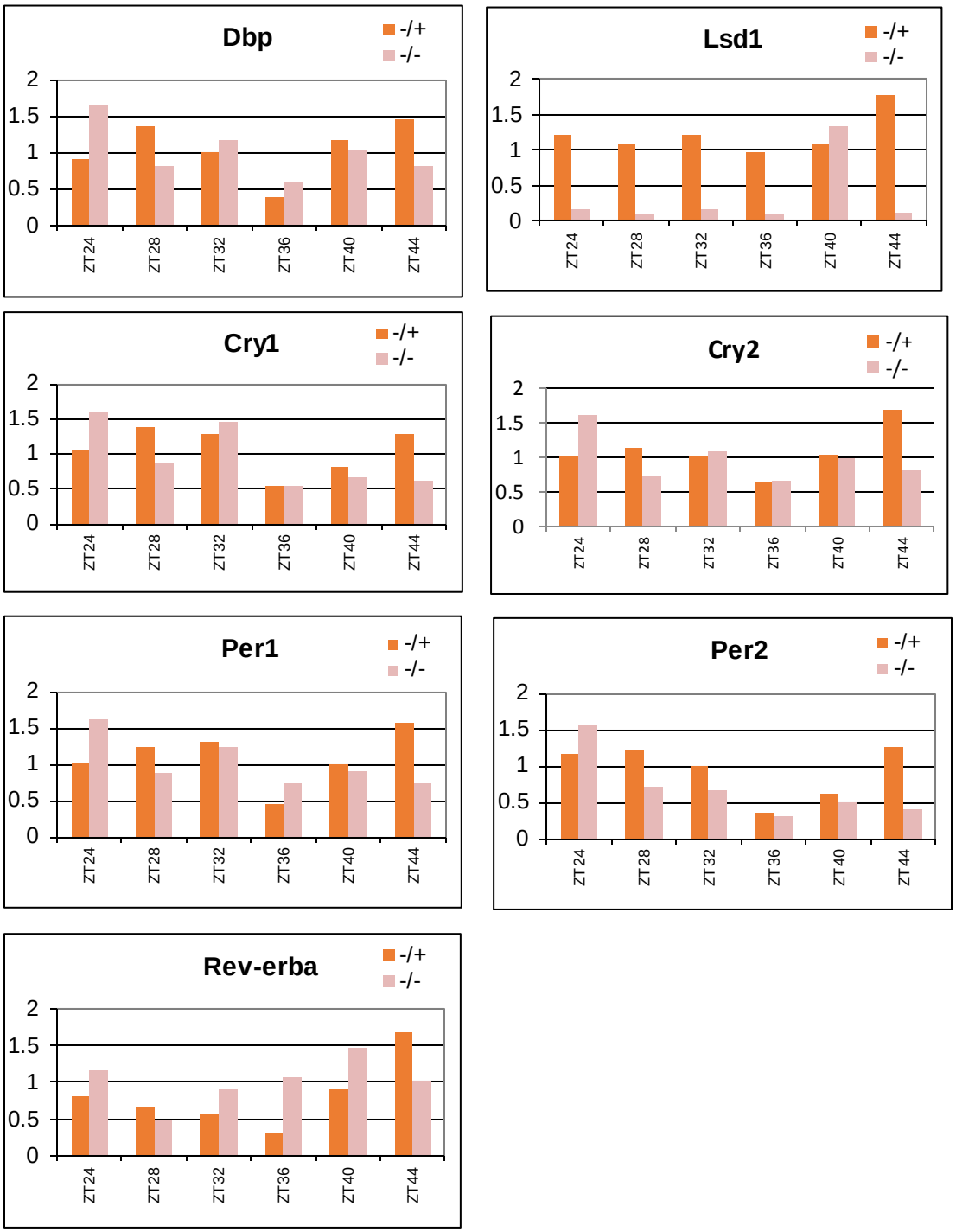

Figure 3.3: *Kdm1a*$^{-/-}$ MEF gene expression

Expression of circadian clock genes in MEF cells was measured at 4 hour intervals over 24 hours using real-time PCR. KDM1a$^{-/-}$ cells show changes in negative limb gene expression at ZT 24 and ZT44 (Personal Communication Dr H. Reinke, Uni Düsseldorf, Ge). All recordings were normalised to the expression of an unknown endogenous control. The aberrant expression of *Kdm1a* at ZT40 was due to a technical error.

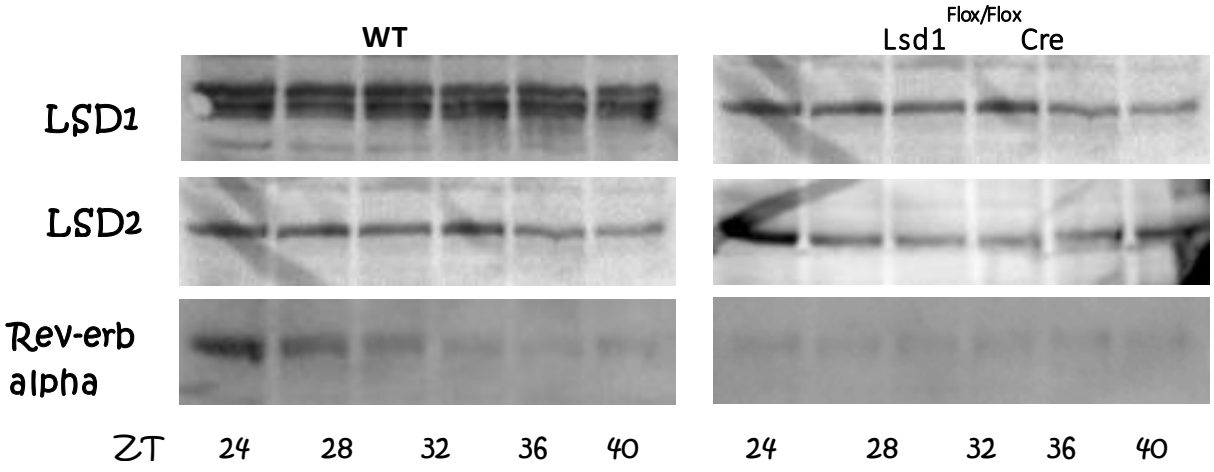

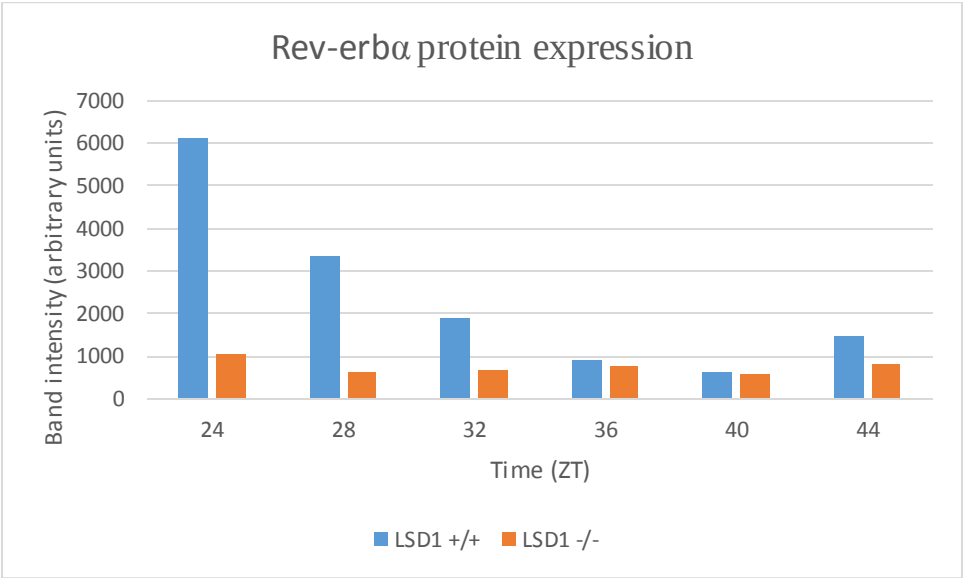

Figure 3.4: REV-ERBα protein expression

Expression of REV-ERBα protein was analysed at four hour intervals over 24 hours by western blot using LSD1 knockout liver. The oscillation of REV-ERBα protein was abolished in the knockout tissue. (Personal Communication Dr H. Reinke, Uni Düsseldorf, Ge). Blot quantified using ImageJ Software. Note that the protein expression of REV-ERBα is different to that of the gene expression in *Kdm1a*$^{-/-}$ MEFs (Figure 3.3).

3.1.3 Lysine specific demethylase mutants

LSD1 Knockout mice suffer from gastrulation defects which cause embryonic lethality before E5.5 (Wang et al. 2009). LSD2 knockout animals, although not embryonic lethal, display reproductive complications, with heterozygous offspring to homozygous mothers suffering embryonic lethality by E10.5 (Ciccone et al. 2009). Therefore when investigating circadian behaviour *in vivo*, an alternative model is required to allow efficient analysis of adult phenotypes (Justice et al. 1999). To cause a discernible change in LSD efficacy without risking the developmental deficits evident in knockout animals, a more subtle manipulation of gene function was sought. The approach utilised in the following investigation is that of ENU mutagenesis. ENU has been employed in the efficient generation of single residue mutants in MRC Harwell. This tool has been successfully used to identify novel mutants and characterise circadian components previously (Takahashi et al. 1994; Bacon et al. 2004). In the current investigation, I screen the Harwell ENU mutant DNA archive which contains the DNA of 10000 mutant individuals (Quwailid et al. 2004). The domains of interest in *Kdm1a* and *Kdm1b* were targeted for screening. The use of ENU mutants in circadian investigations is advantageous in that the mutant protein is expressed and its function can be studied. Knockout models can suffer from abnormal compensatory up-regulation of paralogues as the protein product is missing, and this can affect all roles of the gene in question throughout development through to the adult tissues. With regards circadian investigation, knockout of *Clock*, for instance, results in a rhythmic animal as NPAS2 compensates for the absent CLOCK in the SCN, whereas a point mutation of Clock in the *ClockΔ19* mutant produces a profoundly arrhythmic animal (King et al. 1997; Antoch et al. 1997).

In order to screen the Harwell ENU mutant archive, resources must be directed towards regions of interest in the LSD genes. To decide where in the gene would be best to screen in order to find a mutation, the functions of the domains of the two genes must be considered. Both LSD1 and LSD2 domains are well characterised (MGI website) and upon commencing this investigation the LSD1

crystal structure had been elucidated (Chen et al. 2006; Stavropoulos et al. 2006) (Figure 3.6) so prediction of its disruption aided with the choice of mutant for re-derivation and further investigation (Chen et al. 2006; Stavropoulos et al. 2006).

LSD1 is evolutionarily conserved, the first of the lysine specific demethylases to be identified (Shi et al. 2004). LSD1 is expressed in multiple tissues throughout development and into the adult animal (MGI website). LSD1 comprises several distinct domains (Figure 3.6). The SWIRM domain (named after the first three proteins it was identified in SWI3, RSC8 and MOIRA) is conserved in chromatin-remodelling proteins and in LSD1 is essential for catalysis (Stavropoulos et al. 2006), likely due its role in anchoring the histone tail (Tochio et al. 2006). The tower domain comprises two alpha helices structured together in an antiparallel coiled coil structure (Chen et al. 2006). Alpha helices are notably very stable structures, and point mutations are not often structurally disruptive (Personal Communication, Dr M. Simon, MRC Harwell). The tower domain plays a role in binding cofactors, most notably essential in binding CoREST (Chen et al. 2006; Yang et al. 2006; Nicholson & Chen 2009) which is an important cofactor of LSD1. CoREST has many chromatin-modifying roles and is a part of several complexes (Section 1.6.2), as well as being essential for the efficacy of LSD1 in demethylating nucleosomal substrates as well as playing a role in stabilising LSD1 (Chen et al. 2006). LSD1 contains a catalytic amine oxidase domain; demethylation of the substrate occurs through oxidation, formation of an imine intermediate and subsequent hydrolysis to an aldehyde (Binda et al. 2002; Shi et al. 2004). And finally LSD1 has a C-terminal FAD binding domain which is essential for binding of the FAD cofactor for its flavin-dependent amine oxidase catalytic activity (Stavropoulos et al. 2006; Shi et al. 2004).

Manipulations of various domains of LSD1 have been performed previously. Mutation of the tower domain at E413G and M448V have been shown to affect CoREST binding, decrease catalytic activity and consequential changes in gene expression in a previous mouse model (Nicholson et al. 2013). Unfortunately no circadian phenotype could be analysed using this mutant as it was lethal at peri-

natal stages due to a heart development defect (suggesting the loss of CoREST binding produced a hypomorph LSD1 model) (Nicholson et al. 2013). Mutations across the amine oxidase domain were analysed in a scintillation count-based assay of LSD1 demethylase activity using recombinant LSD1 in an *in vitro* experiment (Chen et al. 2006). Most of the mutations were shown to abolish demethylase activity but the mutation of two of the closer residues to the FAD binding domain did not cause a catalytic knockout (Chen et al. 2006) (Figure 3.5). In a separate study, residues across the domains of *Kdm1a* were mutated by site-directed mutagenesis, and the catalytic activity of LSD1 measured using H3K4 in a cell-free peroxidase assay (Stavropoulos et al. 2006). Mutations in the catalytic centre caused near total knock down of LSD1 activity, SWIRM domain mutants appeared to suffer either a complete loss of activity or no loss at all, and mutations in the C-terminal FAD-binding domain displayed either complete loss of activity or a partial knockdown (Stavropoulos et al. 2006). The tower domain also plays a known role in CoREST binding which is non-essential for but affects the efficiency of LSD1-mediated catalytic activity (Lee et al. 2005). (CoREST binding is essential for LSD1 in nucleosomal histone demethylation (Lee et al. 2005)). Therefore in the current investigation the Harwell ENU archive was screened for tower domain and FAD-binding domain mutants, as they are the most likely domains to yield an effect on gene expression without being a catalytic knockout not viable past gastrulation.

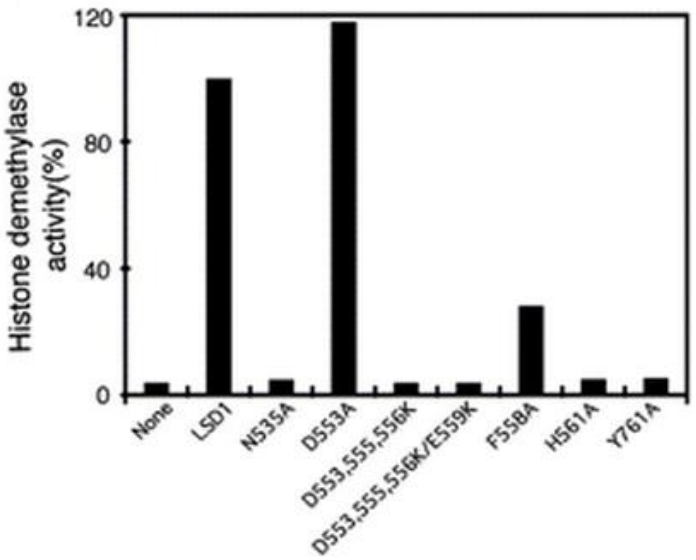

Figure 3.5: Demethylase activity of LSD1 mutants

The demethylase activity of LSD1 is abolished by mutation of crucial residues surrounding the catalytic groove. Recombinant LSD1 wild type and mutant protein was incubated with methylated H3K4 in a cell-free scintillation count assay. (Data from Chen et al. 2006).

LSD2 expression and domain functions are less well characterised. It is expressed across multiple tissues and in multiple cell lines regulating many actively transcribed genes (Fang et al. 2010). High expression is also seen in the oocyte, and supports the hypothesis that LSD2 plays a fundamental role in imprinting and early development (Ciccone et al. 2009). The LSD2 sequence is only 18% homologous to that of LSD1, but the two genes are structurally similar in that both the SWIRM and catalytic domains are expressed similarly (Chen et al. 2006), but the Tower domain is absent and rather a CW-zinc finger domain present in LSD2. This domain is responsible for binding to and reading the histone tail (He et al. 2010), so may be utilised in targeting LSD2 to its substrates. The domain shows much structural similarity to plant homeo domain fingers (PHD) which are very common motifs found in nuclear proteins acting on chromatin substrates (Bienz 2006). The SWIRM and CW-Zn finger domains were chosen for screening due to their roles in substrate binding and therefore prediction that mutation affecting their function might impact the appropriate targeting of LSD2 without directly affecting the catalytic demethylase activity itself.

The exons encoding the regions of interest, exons 10, 11, 12 and 19 of LSD1 and 6, 7, 9 and 10 of LSD2, were therefore identified as candidate regions in which to search for a phenotype affecting mutation whilst minimising the probability of lethality or breeding difficulties. These exons encode the Tower and FAD-binding domains of LSD1 and the SWIRM and CW-Zn finger domains of LSD2. An assay was developed to detect ENU mutations upon screening of the Harwell archive. Light Scanner analysis of DNA amplified from the archive samples detects discrepancies in the melting temperature of heteroduplexes formed when mutated residues anneal to wild type sequences and the resulting mismatch in DNA residues require less energy to separate than a complementary sequence (Quwailid et al. 2004). This chapter explores the preliminary data supporting the investigation of the circadian roles of LSD1 and LSD2, followed by the development of an assay to identify mutants and finally description of the process employed in identifying and choosing mutant models for re-derivation.

a

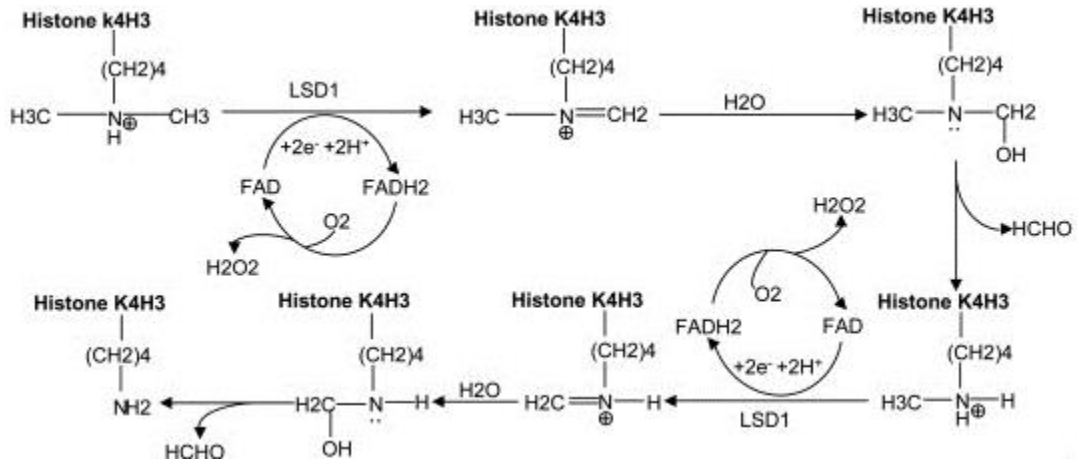

bi

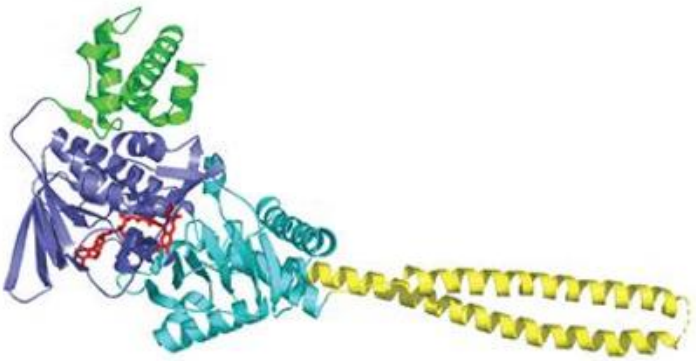

ii

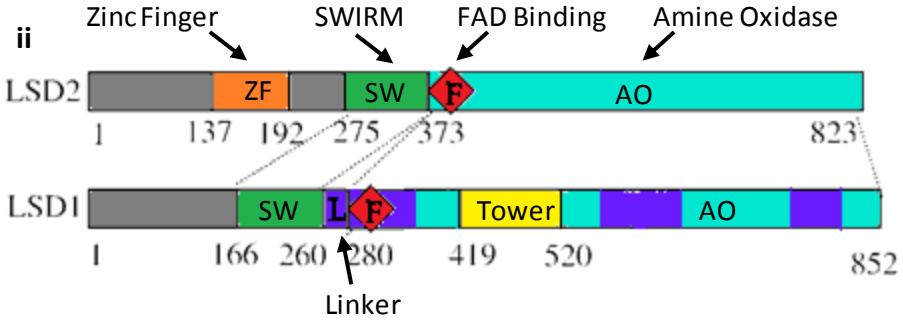

Figure 3.6: LSD1 and LSD2 catalytic mechanism and protein structure

a) Schematic of the postulated mechanism by which LSD1 acts to demethylate H3K4Me2 (from Shi et al. 2004)

b) i) Crystal structure of LSD1 (Chen et al. 2006) (not to scale)
ii) Differences between LSD1 and LSD2 sequences (Fang et al. 2010) Numbers depict amino acid residue number

3.2: Archive Screening

The preliminary analysis of LSD1 and LSD2 function *in vitro*, and the knockout phenotypes involving both genes indicate that the two genes could play a role in regulating the clock. Based on prior knowledge of the functional domains of both genes (Section 3.1.3), the Harwell ENU DNA archive was screened for mutations in exons encoding the tower and FAD-binding domains of LSD1 and SWIRM and CW-Zn finger domains of LSD2. Probes against the exons of interest were used in a LightScanner-based screen. Primers were trialled as detailed in table 3.1. The melting curves were analysed as illustrated in Figure 3.7. Briefly, when non-complementary mutant DNA anneals to a wild type sequence, a heteroduplex is formed. Heteroduplexes melt at a lower temperature than wild type sequences as less energy is required to separate the strands, and this produces a leftward shift in melting curve as demonstrated in Figure 3.7. After screening of pooled samples, the individual DNA constituting each pooled outlier sample was re-analysed with the same PCR to confirm which individual harboured the mutation, before the mutation itself was confirmed by sequencing (Table 3.2).

Exon	Primer F	Primer R	Amplify success	Annealing Temp (°C)
LSD1 Ex 10	CAGCTGGGCCATATATATGTG	AAACTAAAACGGGGATTCCTT	Y	60
LSD1 Ex 11	TGAATTGCTTTGCTATCGAGTATGA	TGACTGTTGAGGGCAGG	N	
	TGAATTGCTTTGCTATCGAGTATGA	CCTGCCCTCAACAGTCA	Y	60
LSD2 Ex 9	GCTTGCAGAGCTGCTTG	CAAGCAGCTCTGCAAGC	Y	51
LSD2 Ex 10	TATTGGTTACTTACTTTGTTGCTGT	TAGGCTCTGCCTTTGGGTG	Y	63

Table 3.1: Light Scanner Primer properties

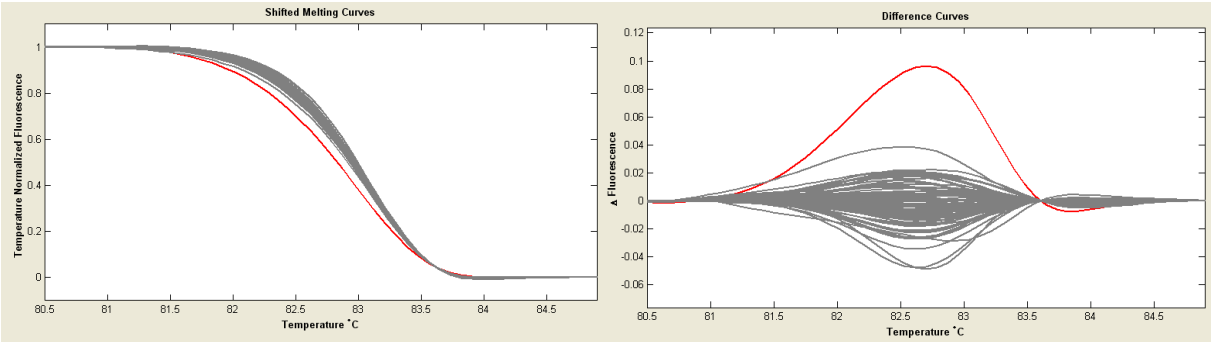

Figure 3.7: Light Scanner melting curves and the ENU archive screen.

Mutants were identified as illustrated here, a melting curve outlier was found in this plate. The curve produced by heteroduplex formation is shifted left in comparison to the remaining complementary sequences (melts at a lower temperature) (Figure 1.5). The second trace shows the same data but graphed as a difference curve.

Mutant	Wild-type sequence	Mutant sequence
LSD1- E440G	CAGCTGGGCCATATATATGTGTTGTCTCTTAC AGGCTGCAAGAAAAGCATGTCAAAGATGAGCA GATTGAACATTGGAAGAAGATAGTGAAAACTC AGGAGGAGTTGAAAGAGCTTCTTAATAAGGTA GAGCTTTGCATTCAGTGTTCTAAAAAACTAAA ACGGGGATTCCTT	CAGCTGGGCCATATATATGTGTTGTCTCTTAC AGGCTGCAAGAAAAGCATGTCAAAGATGAGCA GATTGAACATTGGAAGAAGATAGTGAAAACTC AGGGGGAGTTGAAAGAGCTTCTTAATAAGGTA GAGCTTTGCATTCAGTGTTCTAAAAAACTAAA ACGGGGATTCCTT
LSD1- L491H	TGAATTGCTTTGCTATCGAGTATGAAAATTTT TTACTTTTCCATCTTAGATGGTAAATTTGAAG GAGAAAATTAAAGAGCTCCATCAGCAATACAA AGAAGCTTCAGAAGTGAAGCCGCCCAGAGATA TCACAGCCGAGTTCCTGGTGAAGAGCAAGCAC AGGGACCTGACTGCCCTCTGCAAGGTCAGTGT CGGCCTGCCCTCAACAGTCA	TGAATTGCTTTGCTATCGAGTATGAAAATTTT TTACTTTTCCATCTTAGATGGTAAATTTGAAG GAGAAAATTAAAGAGCTCCATCAGCAATACAA AGAAGCTTCAGAAGTGAAGCCGCCCAGAGATA TCACAGCCGAGTTCCTGGTGAAGAGCAAGCAC AGGGACCTGACTGCCCACTGCAAGGTCAGTGT CGGCCTGCCCTCAACAGTCA
LSD2- C185C	TTTTTTGGCTTTTGGTTTTTGTTTTGTTTTGT TTTAAAAAGGGAGGTATCATATTGAAAGAAAA TGGACACCTAAGACTGTATGTTTTGAAAACAC TTAATTCAGACTTGGTTTTCTCTTGTAG**CCTG** **ACACCCCCGATCATTGTTCTTTCCCCGAGGAT** **CTG**GTGAGTACCTGTGTTCTGCATCAGAGTTA ACTTGGCCTTTCAAGATCCGTTCACTAAGTAA ATGACTAGCATCTATTTGGATGTACATCGAAG CCTTCTGACTTGAACATAGTGACTTCATTGTG AAAATACCCACAGTCATAGAT	TTTTTTGGCTTTTGGTTTTTGTTTTGTTTTGT TTTAAAAAGGGAGGTATCATATTGAAAGAAAA TGGACACCTAAGACTGTATGTTTTGAAAACAC TTAATTCAGACTTGGTTTTCTCTTGTAG**CCTG** **ACACCCCCGATCATTGCTCTTTCCCCGAGGAT** **CTG**GTGAGTACCTGTGTTCTGCATCAGAGTTA ACTTGGCCTTTCAAGATCCGTTCACTAAGTAA ATGACTAGCATCTATTTGGATGTACATCGAAG CCTTCTGACTTGAACATAGTGACTTCATTGTG AAAATACCCACAGTCATAGAT
LSD2- M271T	TGGCAAGAATCTTTACTCATTGGGCCGTCTTG GCCACCCCCTGTGTGTGTTGAGGACGTGCCCT CGTGAGTAGTGTGCACGTGTTTCTGGCTGTTT TGCAAGTCCCAGCTTGCAGAGCTGCTTGCCTG TGTGCCGTCAG**TCCTAGGCATGAACCGGTACT** **TCCAGCCGTTCTACCAGCCCAACGAGTGTGGG** **AAAGCGCTGTGCGTGAGGCCAGACGTGATGGA** **GCTGGATGAGCTCTACGAGTTCCCAGAGTATT** **CGCGGGACCCCACCATGTACCTGGCTTTGAGA** **AACCTCATCCTCGCACTGTGGTACACAAACTG** **CAAA**GTAAGTAAGAACGTAGCAGCAGCAGCAG CAGCAGCAGCGAGGAGAGGGCACCAGTGACTA ACGAGCAGAGTCGTCGGCCATGGTGACTAGCA AAGT	TGGCAAGAATCTTTACTCATTGGGCCGTCTTG GCCACCCCCTGTGTGTGTTGAGGACGTGCCCT CGTGAGTAGTGTGCACGTGTTTCTGGCTGTTT TGCAAGTCCCAGCTTGCAGAGCTGCTTGCCTG TGTGCCGTCAG**TCCTAGGCACGAACCGGTACT** **TCCAGCCGTTCTACCAGCCCAACGAGTGTGGG** **AAAGCGCTGTGCGTGAGGCCAGACGTGATGGA** **GCTGGATGAGCTCTACGAGTTCCCAGAGTATT** **CGCGGGACCCCACCATGTACCTGGCTTTGAGA** **AACCTCATCCTCGCACTGTGGTACACAAACTG** **CAAA**GTAAGTAAGAACGTAGCAGCAGCAGCAG CAGCAGCAGCGAGGAGAGGGCACCAGTGACTA ACGAGCAGAGTCGTCGGCCATGGTGACTAGCA AAGT
LSD2- N272S	TGGCAAGAATCTTTACTCATTGGGCCGTCTTG GCCACCCCCTGTGTGTGTTGAGGACGTGCCCT CGTGAGTAGTGTGCACGTGTTTCTGGCTGTTT TGCAAGTCCCAGCTTGCAGAGCTGCTTGCCTG TGTGCCGTCAG**TCCTAGGCATGAACCGGTACT** **TCCAGCCGTTCTACCAGCCCAACGAGTGTGGG** **AAAGCGCTGTGCGTGAGGCCAGACGTGATGGA** **GCTGGATGAGCTCTACGAGTTCCCAGAGTATT** **CGCGGGACCCCACCATGTACCTGGCTTTGAGA** **AACCTCATCCTCGCACTGTGGTACACAAACTG** **CAAA**GTAAGTAAGAACGTAGCAGCAGCAGCAG CAGCAGCAGCGAGGAGAGGGCACCAGTGACTA ACGAGCAGAGTCGTCGGCCATGGTGACTAGCA AAGT	TGGCAAGAATCTTTACTCATTGGGCCGTCTTG GCCACCCCCTGTGTGTGTTGAGGACGTGCCCT CGTGAGTAGTGTGCACGTGTTTCTGGCTGTTT TGCAAGTCCCAGCTTGCAGAGCTGCTTGCCTG TGTGCCGTCAG**TCCTAGGCATGAGCCGGTACT** **TCCAGCCGTTCTACCAGCCCAACGAGTGTGGG** **AAAGCGCTGTGCGTGAGGCCAGACGTGATGGA** **GCTGGATGAGCTCTACGAGTTCCCAGAGTATT** **CGCGGGACCCCACCATGTACCTGGCTTTGAGA** **AACCTCATCCTCGCACTGTGGTACACAAACTG** **CAAA**GTAAGTAAGAACGTAGCAGCAGCAGCAG CAGCAGCAGCGAGGAGAGGGCACCAGTGACTA ACGAGCAGAGTCGTCGGCCATGGTGACTAGCA AAGT
LSD2- P281L	TGGCAAGAATCTTTACTCATTGGGCCGTCTTG GCCACCCCCTGTGTGTGTTGAGGACGTGCCCT CGTGAGTAGTGTGCACGTGTTTCTGGCTGTTT TGCAAGTCCCAGCTTGCAGAGCTGCTTGCCTG TGTGCCGTCAG**TCCTAGGCATGAACCGGTACT** **TCCAGCCGTTCTACCAGCCCAACGAGTGTGGG** **AAAGCGCTGTGCGTGAGGCCAGACGTGATGGA** **GCTGGATGAGCTCTACGAGTTCCCAGAGTATT** **CGCGGGACCCCACCATGTACCTGGCTTTGAGA**	TGGCAAGAATCTTTACTCATTGGGCCGTCTTG GCCACCCCCTGTGTGTGTTGAGGACGTGCCCT CGTGAGTAGTGTGCACGTGTTTCTGGCTGTTT TGCAAGTCCCAGCTTGCAGAGCTGCTTGCCTG TGTGCCGTCAG**TCCTAGGCATGAACCGGTACT** **TCCAGCCGTTCTACCAGCTCAACGAGTGTGGG** **AAAGCGCTGTGCGTGAGGCCAGACGTGATGGA** **GCTGGATGAGCTCTACGAGTTCCCAGAGTATT** **CGCGGGACCCCACCATGTACCTGGCTTTGAGA**

	AACCTCATCCTCGCACTGTGGTACACAAACTG CAAAGTAAGTAAGAACGTAGCAGCAGCAGCAG CAGCAGCAGCGAGGAGAGGGCACCAGTGACTA ACGAGCAGAGTCGTCGGCCATGGTGACTAGCA AAGT	AACCTCATCCTCGCACTGTGGTACACAAACTG CAAAGTAAGTAAGAACGTAGCAGCAGCAGCAG CAGCAGCAGCGAGGAGAGGGCACCAGTGACTA ACGAGCAGAGTCGTCGGCCATGGTGACTAGCA AAGT
LSD2- T357M	AACGTAAAAATAAACTTTTAGCCCTAGTTTTT TGGTTTGTTTTTTATTGGTTACTTACTTTGTT GCTGTTGGTTTTGGTTTTGTTGTGAACACAGG AAGCTCTCACCCCTCAGAAGTGCATTCCCCAC ATCATTGTCCGGGGCCTTGTCCGCATCAGATG CGTTCAGGAAGTGGAGAGGATTCTTTACTTCA TGACGAGGAAAGGCCTCATCAACACAGGCGTT CTCACGGTGGCAGCCGGCCAGCATCTTCTTCC TAAACACTACCACAATGTAAGCAGCTGGATGT GCGGTAGGCTCTGCCTTTGGGTGTGATAAGAG ACTAGTGTGTTGCTATACTGGTACCAGATACT GCAGAAAC	AACGTAAAAATAAACTTTTAGCCCTAGTTTTT TGGTTTGTTTTTTATTGGTTACTTACTTTGTT GCTGTTGGTTTTGGTTTTGTTGTGAACACAGG AAGCTCTCACCCCTCAGAAGTGCATTCCCCAC ATCATTGTCCGGGGCCTTGTCCGCATCAGATG CGTTCAGGAAGTGGAGAGGATTCTTTACTTCA TGATGAGGAAAGGCCTCATCAACACAGGCGTT CTCACGGTGGCAGCCGGCCAGCATCTTCTTCC TAAACACTACCACAATGTAAGCAGCTGGATGT GCGGTAGGCTCTGCCTTTGGGTGTGATAAGAG ACTAGTGTGTTGCTATACTGGTACCAGATACT GCAGAAAC
LSD2- V366A	AACGTAAAAATAAACTTTTAGCCCTAGTTTTT TGGTTTGTTTTTTATTGGTTACTTACTTTGTT GCTGTTGGTTTTGGTTTTGTTGTGAACACAGG AAGCTCTCACCCCTCAGAAGTGCATTCCCCAC ATCATTGTCCGGGGCCTTGTCCGCATCAGATG CGTTCAGGAAGTGGAGAGGATTCTTTACTTCA TGACGAGGAAAGGCCTCATCAACACAGGCGTT CTCACGGTGGCAGCCGGCCAGCATCTTCTTCC TAAACACTACCACAATGTAAGCAGCTGGATGT GCGGTAGGCTCTGCCTTTGGGTGTGATAAGAG ACTAGTGTGTTGCTATACTGGTACCAGATACT GCAGAAAC	AACGTAAAAATAAACTTTTAGCCCTAGTTTTT TGGTTTGTTTTTTATTGGTTACTTACTTTGTT GCTGTTGGTTTTGGTTTTGTTGTGAACACAGG AAGCTCTCACCCCTCAGAAGTGCATTCCCCAC ATCATTGTCCGGGGCCTTGTCCGCATCAGATG CGTTCAGGAAGTGGAGAGGATTCTTTACTTCA TGACGAGGAAAGGCCTCATCAACACAGGCGCT CTCACGGTGGCAGCCGGCCAGCATCTTCTTCC TAAACACTACCACAATGTAAGCAGCTGGATGT GCGGTAGGCTCTGCCTTTGGGTGTGATAAGAG ACTAGTGTGTTGCTATACTGGTACCAGATACT GCAGAAAC
LSD2- A371A	AACGTAAAAATAAACTTTTAGCCCTAGTTTTT TGGTTTGTTTTTTATTGGTTACTTACTTTGTT GCTGTTGGTTTTGGTTTTGTTGTGAACACAGG AAGCTCTCACCCCTCAGAAGTGCATTCCCCAC ATCATTGTCCGGGGCCTTGTCCGCATCAGATG CGTTCAGGAAGTGGAGAGGATTCTTTACTTCA TGACGAGGAAAGGCCTCATCAACACAGGCGTT CTCACGGTGGCAGCCGGCCAGCATCTTCTTCC TAAACACTACCACAATGTAAGCAGCTGGATGT GCGGTAGGCTCTGCCTTTGGGTGTGATAAGAG ACTAGTGTGTTGCTATACTGGTACCAGATACT GCAGAAAC	AACGTAAAAATAAACTTTTAGCCCTAGTTTTT TGGTTTGTTTTTTATTGGTTACTTACTTTGTT GCTGTTGGTTTTGGTTTTGTTGTGAACACAGG AAGCTCTCACCCCTCAGAAGTGCATTCCCCAC ATCATTGTCCGGGGCCTTGTCCGCATCAGATG CGTTCAGGAAGTGGAGAGGATTCTTTACTTCA TGACGAGGAAAGGCCTCATCAACACAGGCGTT CTCACGGTGGCAGCTGGCCAGCATCTTCTTCC TAAACACTACCACAATGTAAGCAGCTGGATGT GCGGTAGGCTCTGCCTTTGGGTGTGATAAGAG ACTAGTGTGTTGCTATACTGGTACCAGATACT GCAGAAAC

Table 3.2: Sequencing results for mutants identified in the ENU archive screen.

Mutants were sequenced by Sanger sequencing (by GATC (LSD1) or Source Bioscience (LSD2)). Alignment using SeqMan (Lasergene) allowed the identification of the mutant sequences.

3.2.1: Mutation characteristics

Nine mutations were found as a result of the archive screen. Two non-synonymous mutations were found in the sequence spanning both exons 10 and 11 encoding the tower domain of LSD1, the *Kdm1a*^{E440G} mutation and *Kdm1a*^{L491H} mutation. One synonymous mutation (*Kdm1a*^{C185C}) was found in exon 7 of LSD2 encoding the CW-Zn finger domain of LSD2, and 5 mutations were found in exons 9 and 10 encoding the SWIRM domain of LSD2; *Kdm1b*^{M271T}, *Kdm1b*^{N272S}, *Kdm1b*^{P281L}, *Kdm1b*^{T357M} and *Kdm1b*^{V366A} (as well as one synonymous, *Kdm1b*^{A371A}) (listed in table 3.3). All mutations fell within highly conserved regions (Figure 3.8). The mutations found were of the expected frequency. On average one mutation is found in for every 1.83mb sequence screened (Keays, Clark, et al. 2007). It would be expected that for a screen spanning 1811 bases of DNA such as the one performed here, screening 10000 G1 animals (18mb of DNA) would yield 10 mutant hits. Here, 9 mutants were identified, in keeping with this prediction (Keays, Clark, et al. 2007) (Section 1.5.3).

As all mutations were found in highly conserved regions (Figure 3.8) and the amino acid changes resulting from each mutation were varied as shown in table 3.4, the mutations were next analysed *in silico* and also introduced into constructs using site-directed mutagenesis and analysed for circadian effects *in vitro*. Based upon the results from the following *in silico* tests, four mutant lines were re-derived from the archive by IVF.

Gene	Mutant	Residue Change		Amino Acid Change		Synonymous?	Deleterious?	Conserved?	Domain
		WT	Mut	WT	Mut				
LSD1	E440G	A	G	Glu (acidic)	Gly (nonpolar)	N	N	Yes	Tower
	L491H	T	A	Leu (hydrophobic)	His (basic)	N	N	Yes	Tower
LSD2	C185C	T	C	Cys	Cys	Y	-	Yes	CW-Zn finger
	M271T	T	C	Met (hydrophobic)	Thr (nucleophilic)	N	N	Yes except Xenopus	SWIRM
	N272S	A	G	Asp (amide)	Ser (nucleophilic)	N	N	Yes	SWIRM
	P281L	C	T	Pro (hydrophobic)	Leu (hydrophobic)	N	Y	Yes	SWIRM
	T357M	C	T	Thr (nucleophilic)	Met (hydrophobic)	N	Y	Yes except Xenopus	SWIRM
	V366A	T	C	Val (hydrophobic)	Ala (nonpolar)	N	N	Yes	SWIRM
	A371A	C	T	Ala	Ala	Y	-	Yes	Just after SWIRM

Table 3.3: Characteristics of the multiple LSD1 and LSD2 mutants identified in the Harwell ENU archive screen.

Mutations had various outcomes in the LSD1 and LSD2 genes, *in silico* predictions are needed to inform the decision as to which mutants are most appropriate for re-derivation.

Mutation	Wild type residue	Mutant residue
Kdm1a^{E440G} Acidic » Neutral	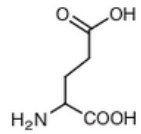 Glutamic Acid (Glu, E) MW: 129.12, pK_a = 4.07	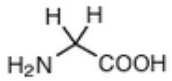 Glycine (Gly, G) MW: 57.05
Kdm1a^{L491H} Hydrophobic » Basic	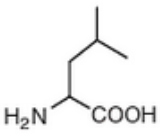 Leucine (Leu, L) MW: 113.16	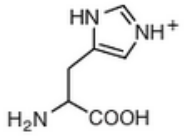 Histidine (His, H) MW: 137.14, pK_a = 6.04
Kdm1b^{M271T} Hydrophobic » Neutrophilic	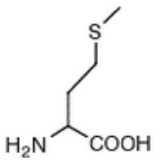 Methionine (Met, M) MW: 131.19	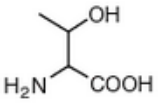 Threonine (Thr, T) MW: 101.11, pK_a ~ 16
Kdm1b^{N272S} Amide » Nucleophilic	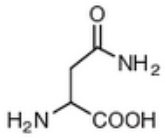 Asparagine (Asn, N) MW: 114.11	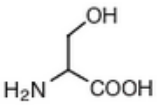 Serine (Ser, S) MW: 87.08, pK_a ~ 16
Kdm1b^{P281L} Hydrophobic » Hydrophobic	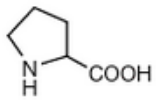 Proline (Pro, P) MW: 97.12	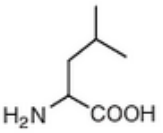 Leucine (Leu, L) MW: 113.16
Kdm1b^{T357M} Neutrophilic » Hydrophobic	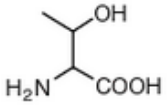 Threonine (Thr, T) MW: 101.11, pK_a ~ 16	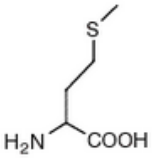 Methionine (Met, M) MW: 131.19
Kdm1b^{V366A} Hydrophobic » Neutral	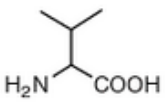 Valine (Val, V) MW: 99.14	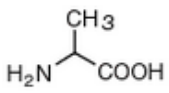 Alanine (Ala, A) MW: 71.09

Table 3.4: Amino acid changes resulting from mutations in LSD1 and LSD2

The 7 non-synonymous mutations result in changes to the amino acid encoded, and the properties of the amino acids are changed in each instance except the *Kdm1b*^{P281L} mutant.

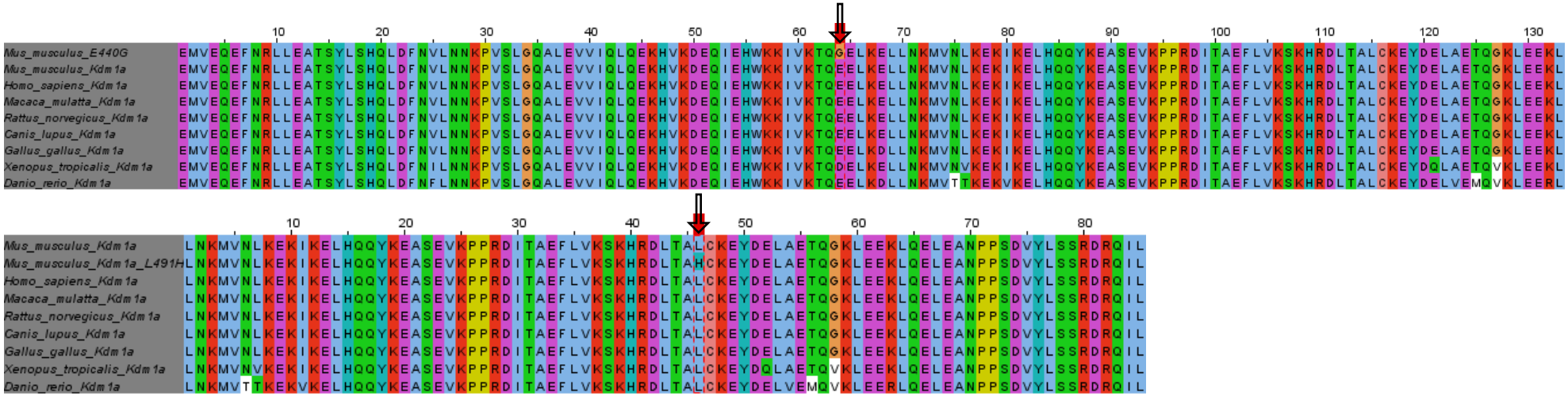

Figure 3.8: Conservation of mutations identified in the ENU archive screen. (*Kdm1a*)

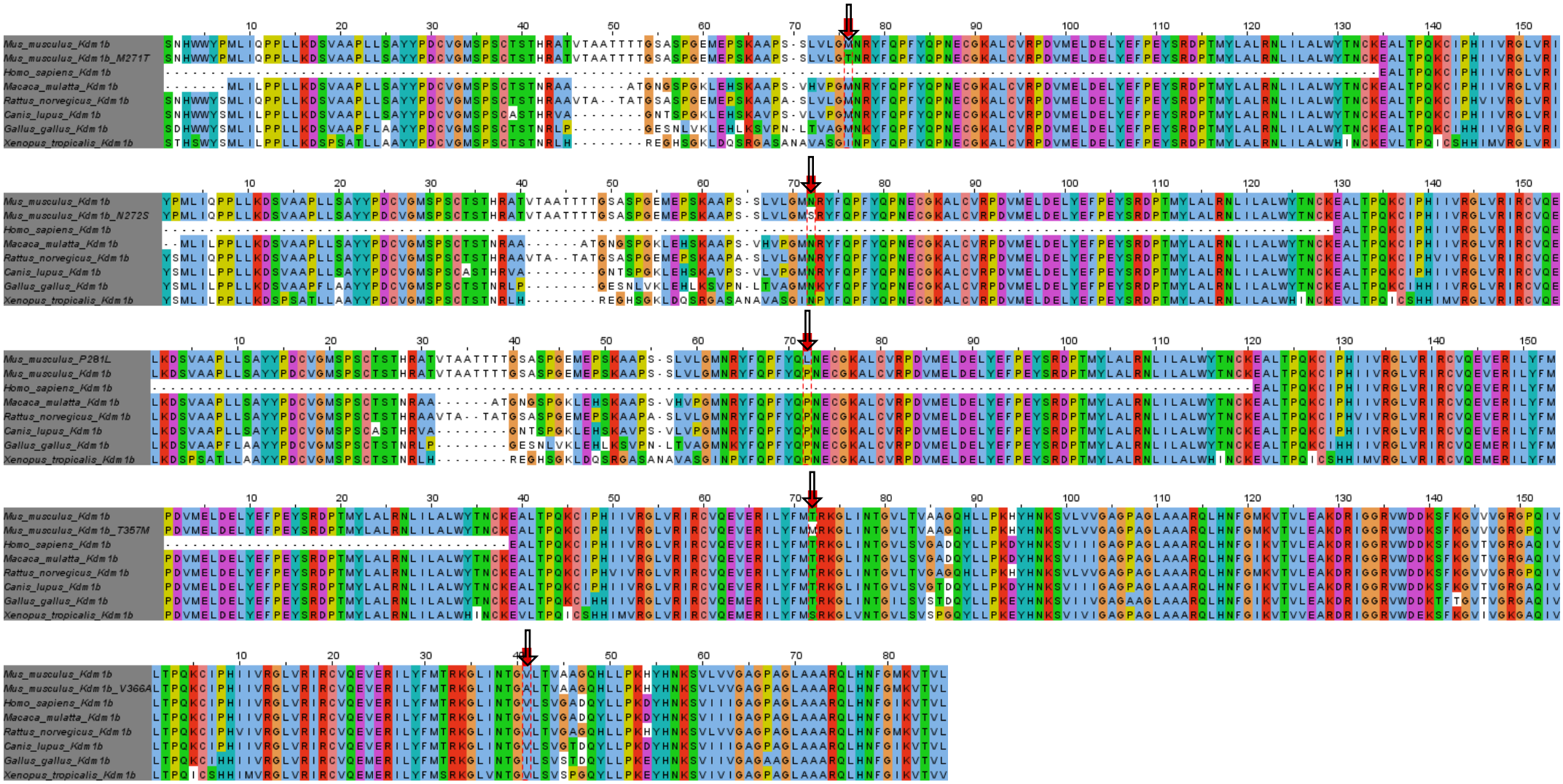

Figure 3.8: Conservation of mutations identified in the ENU archive screen. (*Kdm1b*)

Two mutations were identified in the tower domain of LSD1 and five in the SWIRM domain of LSD2. All four exons where mutations were identified are highly conserved across different species. As the primary human transcript does not contain all of the regions in which mutations were identified, there is no sequence shown for *Homo sapiens* in these diagrams. The secondary human transcript does contain these regions.

3.3: In Silico Data

Upon screening of the archive and sequencing of identified mutations, it was necessary to ascertain which mutations which would most likely yield a circadian phenotype upon re-derivation. Therefore mutated sequences were examined using multiple freely available *in silico* analyses predicting effects on resulting protein structure and function.

3.3.1: PolyPhen

Structural disruption of proteins can be predicted by various softwares based upon the known protein structure and the nature of the mutation. Firstly the mutations were put through analysis by Polyphen. Polyphen analysis demonstrated the likelihood of a structural disruption arising from any given mutation in a gene based on the known structures of human genes (Polyphen website). In the case of LSD1, both mutants were predicted to be benign and cause no disruption to protein structure. However, LSD2 mutants *Kdm1b*^{T357M} and *Kdm1b*^{P281L} seemed likely to cause protein structure disruption.

Mutant	Prediction	Available Data	Prediction Basis	Prediction data	Remarks
Kdm1a^{L491H}	Benign	Alignment structure	Alignment	PSIC score difference: 0.932	Closest contact with other chains: ILE 367B, distance 5.321 Å
Kdm1a^{E440G}	Benign	Alignment structure	Alignment	PSIC score difference: 0.496	Closest contact with other chains: ILE 352B, distance 3.316 Å
Kdm1b^{P281L}	Probably Damaging	Alignment structure	Alignment analysis HumDiv and HumVar	Scores 1.000, 0.999	
Kdm1b^{T357M}	Probably Damaging	Alignment structure	Alignment analysis HumDiv and HumVar	Scores 1.000, 0.939	
Kdm1b^{M271T}	Benign	Alignment structure	Alignment analysis HumDiv and HumVar	Scores 0.003, 0.003	
Kdm1b^{N272S}	Benign	Alignment structure	Alignment analysis HumDiv and HumVar	Scores 0.013, 0.006	
Kdm1b^{V366A}	Benign	Alignment structure	Alignment analysis HumDiv and HumVar	Scores 0.000, 0.000	

Table 3.5: Polyphen analysis of mutants identified in the ENU archive screen

All non-synonymous mutations were analysed using polyphen, and the *Kdm1b*^{P281L} and *Kdm1b*^{T357M} mutations were predicted to be probably damaging. (Polyphen website)

3.3.2: Phyre2 and Nfold3

Both Phyre2 (Söding 2005; Kelley & Sternberg 2009; Phyre2 website) and NFold3 (NFold3 website) analyses of protein structure use known protein database (pdb) structure scaffolds to predict the precise folded structure of the input sequence and give an estimate as to the confidence of how likely any given structure is to be correct.

LSD1

In the case of LSD1 (with an established crystal structure) confidence was 100% for both Phyre2 analyses and structures looked identical to *Kdm1a*$^{+/+}$ structure, as did the NFold3 prediction. (Figure 3.9, Figure 3.10)

LSD2

As the crystal structure of LSD2 has yet to be established, each mutant had different impact on the predicted structure. All mutations found in the archive screen were shown to affect the loop structure at the C terminal of LSD2, and the *Kdm1b*^{T357M} and *Kdm1b*^{P281L} mutations were disruptive to more central folding which might impinge on targeting or catalytic function. (Figure 3.11)

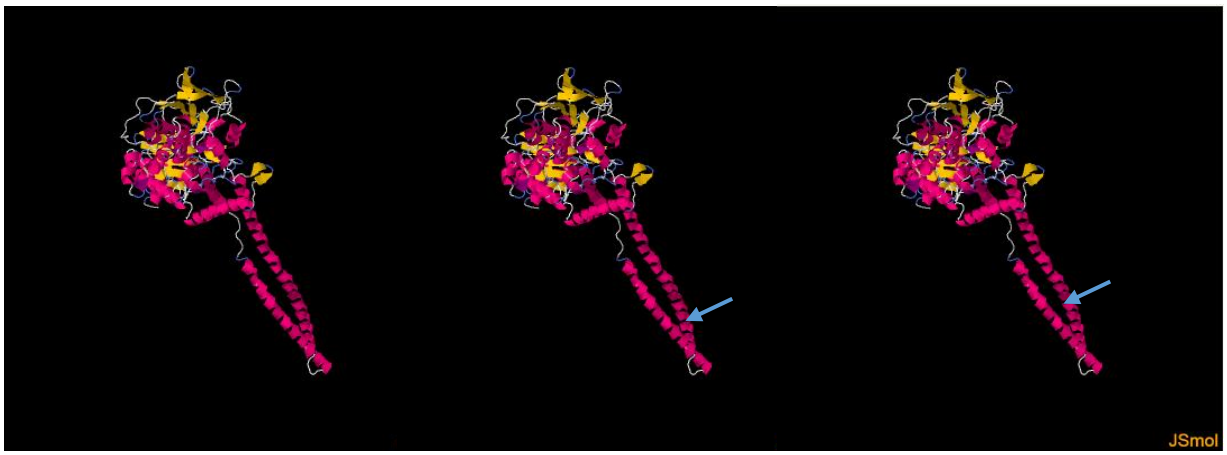

Kdm1a$^{+/+}$ *Kdm1a*^{E440G} *Kdm1a*^{L491H}

Figure 3.9: Phyre2 prediction of LSD1 mutant protein structure

The LSD1 mutations identified in the ENU archive screen were predicted to make no difference to the structure of the LSD1 protein product using Phyre2 software (Phyre2 website). Mutations highlighted with blue arrows.

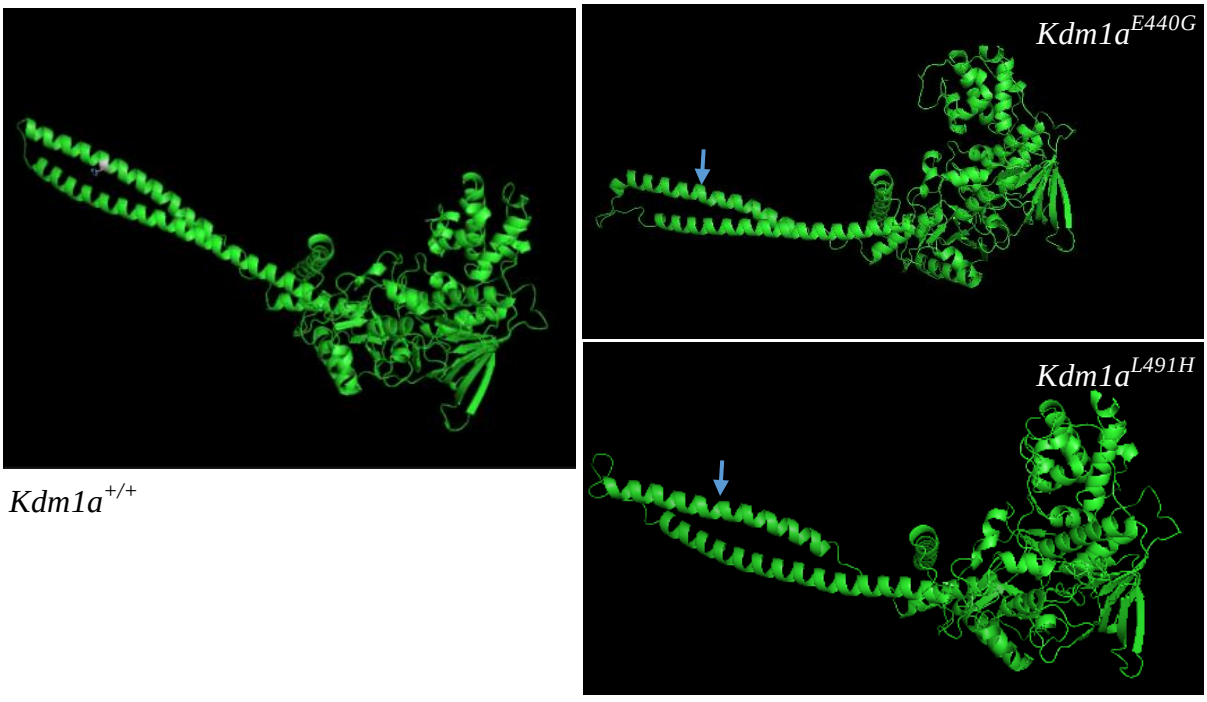

Kdm1a$^{+/+}$

Figure 3.10: Nfold3 prediction of LSD1 mutant protein structure

The LSD1 mutations identified in the ENU archive screen were predicted to make no difference to the structure of the LSD1 protein product using Nfold3 software (NFold3 website). Mutations highlighted with blue arrows.

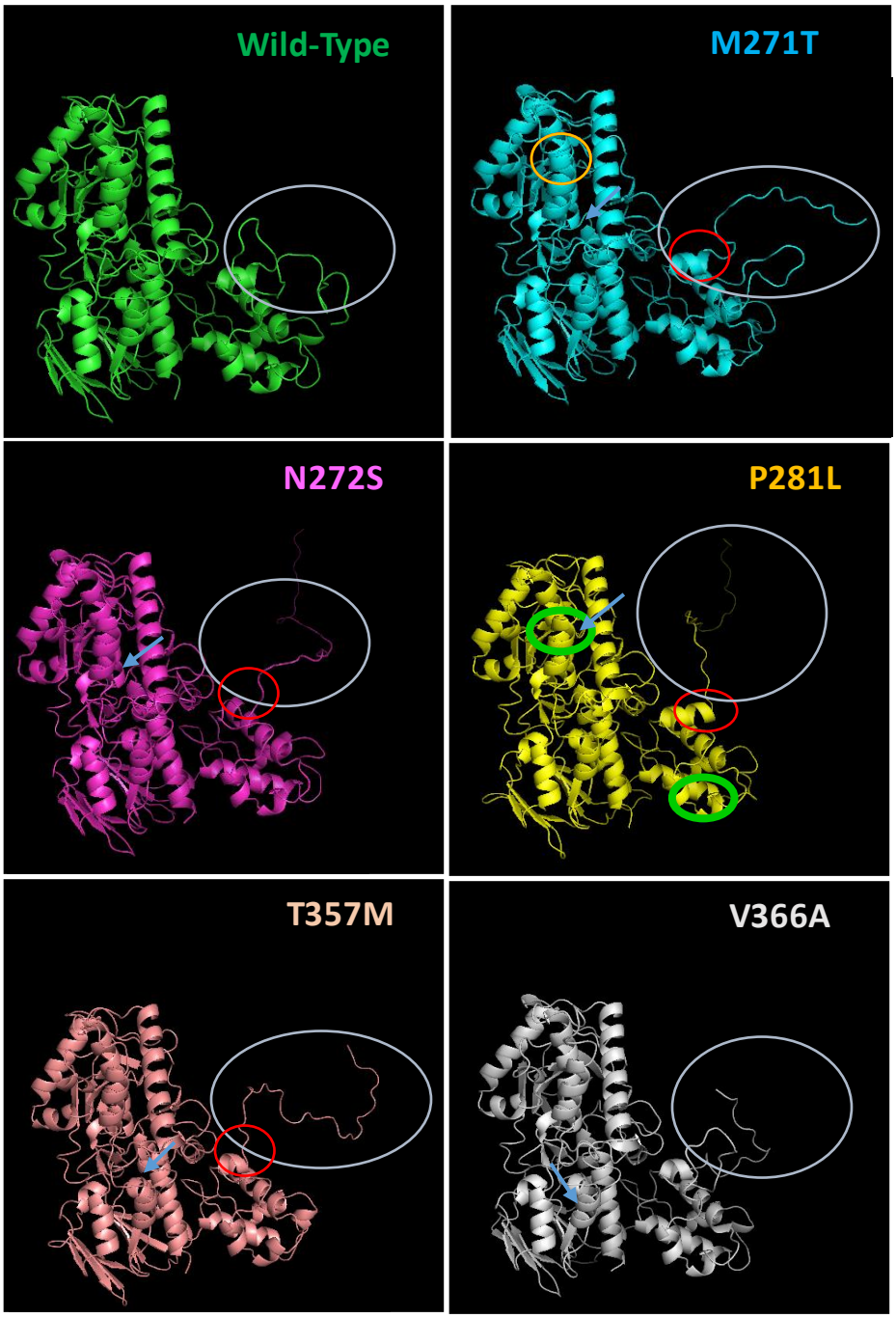

Figure 3.11: Nfold3-Predicted LSD2 mutant structure

LSD2 mutants identified in the ENU archive screen were analysed using Nfold3 (NFold3 website). All mutations were predicted to change the loop structure at the C terminal of LSD2 (grey circles), *Kdm1b*^{T357M} and *Kdm1b*^{N271S} shortened the final alpha helix (red circles). *Kdm1b*^{M271T} was predicted to disrupt one of the alpha helices in the centre of the protein structure (orange circle), and *Kdm1b*^{P281L} changed multiple alpha helices (green circles). Mutations highlighted with blue arrows.

3.3.3: SIFT

The final *in silico* analysis tool implemented in predicting LSD protein disruption was SIFT. SIFT analysis predicts likelihood of deleterious effects of human SNPs on protein structure. As the LSD2 *Kdm1b*^{N272S}, *Kdm1b*^{M271T} and *Kdm1b*^{P281L} mutations discovered through the archive screen are not in regions covered by the SIFT software, analysis was not performed. Contrary to the Nfold3 and Phyre data, the two LSD1 mutations were predicted to be deleterious, and the *Kdm1b*^{T357M} mutant was predicted to disrupt structure, discussed in section 3.4.4 (Table 3.6). Overall, the *in silico* analyses conducted here suggest that four mutations found in the archive screen would be valuable for rederivation and exploration of circadian phenotypes. Following this, *in vitro* work was undertaken to investigate which mutations caused molecular changes to the circadian mechanism before mutants were selected for rederivation.

Variation		Protein Sequence Change				Provean				SIFT prediction			
Row	Input	Protein ID	Position	Residue ref	Residue alt	SCORE	PREDICTION (cutoff=-2.5)	#SEQ	#CLUSTER	SCORE	PREDICTION (cutoff=0.05)	MEDIAN_INFO	#SEQ
1	ENSP00000349049 439 E G	ENSP00000349049	439	E	G	-4.09	Deleterious	121	30	0.100	Tolerated	2.95	91
2	ENSP00000349049 490 L H	ENSP00000349049	490	L	H	-2.54	Deleterious	121	30	0.170	Tolerated	2.94	91
3	ENSP00000297792 234 V A	ENSP00000297792	234	V	A	-0.66	Neutral	88	30	0.311	Tolerated	3.58	14
4	ENSP00000297792 225 T M	ENSP00000297792	225	T	M	-2.70	Deleterious	88	30	0.014	Damaging	3.58	14

Table 3.6: SIFT analysis of mutants identified in the ENU archive screen

Non-synonymous mutations were analysed using SIFT, and the *Kdm1a*^{L491H} *Kdm1a*^{E440G} *Kdm1b*^{T357M} mutations were predicted to be probably damaging. (SIFT website)

3.4: Discussion

3.4.1: Reverse genetics and ENU mutagenesis

ENU mutant models have been previously used in investigation of circadian functions (Acevedo-Arozena et al. 2008). ENU mutations in circadian genes can give information that alternative models would not yield (for instance, a knockout) (Table 1.2). *CLOCK* ENU gene mutants display circadian perturbations and arrhythmia whereas the knockout remains rhythmic. This is an artefact of knockout models as the gene product is missing entirely, and as such compensatory mechanisms are at play. *Npas2* is upregulated to compensate for the absence of CLOCK in the SCN, whereas the *CLOCK* gene product is present in the ENU mutant model, so *Npas2* is not upregulated despite the dysfunction of the CLOCK protein (King et al. 1997; Antoch et al. 1997). ENU mutants can be screened in a forward genetics or reverse genetics approach. The relative merits of each approach were discussed previously (Table 1.3). In the search for novel genes or gene mechanisms, forward genetic screening for phenotypes is unbiased. Although forward genetic screens have been used extensively to find novel mutants in phenotyping pipelines at MRC Harwell, reverse genetics are employed in the current search for a novel mutant as the genes of interest have already been established. In this investigation, the employment of a reverse genetics approach is still in some way unbiased as the screen focuses on known exons and domains of the *LSD* genes, but mutations found in the screen could affect any residue in the sequence. Any ENU mutations found through screening could result in increased or decreased functionality (for example loss of catalytic residues or modification sites), splicing variants or truncation of the target gene (Noveroske et al. 2000). Reverse genetics also has the advantage over forward genetics in speed of identification of novel mutants, and so this approach was taken in this investigation.

The success of the current archive screen reflected predicted success rates based on the frequency of mutations expected to be found in a given length of DNA code. ENU-induced mutations occur at a

frequency of 6×10^{-3} to 1.5×10^{-3} and as such it would be expected that one mutation would be functionally defective in every 175-655 gametes (Keays, Clark, et al. 2007). In the Harwell archive of DNA the dose of ENU used to generate the archive would be expected to yield one G1 mutant per 18mb DNA screened (Keays, Clark, et al. 2007). As 10000 DNA samples were screened over regions totalling 1811 base pairs, it would be expected based on previous findings that 10 ENU mutants would be found during the course of the screen, and in fact 9 mutants were identified in keeping with those predictions. The preliminary data *in vitro* initiated the search for mutant models of *LSD* gene function, an assay was then developed to identify mutants in regions of interest.

Nine mutants were identified and subsequently four were chosen for re-derivation based on the *in silico* analysis of the predicted structural consequences of the given mutations.

3.4.2: Preliminary work

Results from work completed in the Reinke laboratory (see Section 3.1) cumulatively suggest a role for LSD1 and LSD2 in clock mechanisms and support investigation of LSD roles in the clock in adult tissue *in vivo*. Knockdown of either LSD caused a dampening in circadian oscillation (Figure 3.2), LSD1 plays roles in gene expression modulation (Figure 3.3) (consistent with previous findings (Amente et al. 2013; Nicholson & Chen 2009; Nottke et al. 2009; Shi et al. 2004)), and conditional knockout of LSD1 caused a loss of REV-ERBα protein level oscillation in liver (Figure 3.4). These results are encouraging when investigating the role of LSD1 in circadian behaviour, as not only is circadian oscillation of *Bmal1* promoter-driven expression altered, a dampening of a core clock component at the protein level such as REV-ERBα suggests that LSD1 may affect expression of clock proteins over the 24 hour cycle in peripheral tissue, here liver specifically. The perturbation of gene expression need not affect protein oscillation (Vogel & Marcotte 2012), and this finding demonstrates that LSD1 disruption has functional implications for clock mechanisms at a translational as well as a transcriptional level. Bioluminescent data is collected using a circadian promoter driven luciferase assay, so follows and represents promoter-driven mRNA transcription patterns. It must therefore be

recognised that the dampening observed here could be caused by multiple general non-circadian effects on the cell. For example, global down-regulation of transcription or elongation factors, or global increase in expression of RNA-induced silencing complex (RISC) complexes might affect mRNA levels more globally. In this respect, the REV-ERBα protein data and the phase shift experiment support that LSD1 may be playing a role in CT-specific regulation of circadian gene products.

The shift in glucocorticoid-mediated phase shifting peak of *Bmal1* oscillation upon treatment with dexamethasone could be due to a role of LSD1 in phase resetting of the clock; a change in glucocorticoid response; or a change in circadian period but further experiments in this system are necessary to validate or disprove this hypothesis.

Knockdown of epigenetic regulators such as Histone deacetylases (HDACs) can also result in reduced circadian amplitude (Fogg et al. 2014), and mutation of *CLOCK* also dampens circadian rhythmicity by decreasing the efficiency of the CLOCK:BMAL1 dimer (King et al. 1997). Dampening of circadian rhythms such as the dampening in *Bmal1* promoter-driven luciferase expression observed in the current investigation (Figure 3.2) could therefore be mediated by a number of circadian modifications. LSD1 could be demethylating histones and affecting circadian transcription this way, or alternatively binding to another clock component and affecting its function in a demethylase dependent or independent way. The remaining investigation will examine the possible mechanisms at play in the siRNA knockdown of LSD1 and LSD2.

The current investigation of LSD function in the clock utilised ENU mutants as a novel model of LSD1 and LSD2 function which could yield adult circadian phenotypes. Care must be taken in interpretation of data from such novel investigations, however. When considering even direct manipulation of core clock components, a wide array of phenotypes is often evident in genetic models. Animals with disruption of Bmal1, for example, display disruptions in fertility, arthropathy, gluconeogenesis, lipogenesis and sleep wake cycles (Ko & Takahashi 2006). This single global disruption has a multitude of effects in many body systems which could be due to heterogeneity in

the role of the gene under investigation or due to knock-on effects of circadian disruption. Therefore pinpointing the circadian impact of the LSD disruption through *in vivo* phenotyping must be approached in a multidisciplinary manner and all eventualities in phenotypes should be considered.

3.4.3: Archive Screen

In order to identify new models of LSD1 and LSD2 disruption, reverse genetics screening of the Harwell ENU archive was employed. The archive screen for mutations in LSD1 and LSD2 successfully yielded several outliers in heteroduplex melting curve data. Through multiple rounds of analysis and confirmation by sequencing, two synonymous and seven non-synonymous mutations were identified across the areas of interest in the two genes (Table 3.3), in areas of high conservation (Figure 3.8). The changes to the encoded amino acids in the LSD1 and LSD2 mutants discovered in the archive screen were various, and most changed the wild type residue from one subgroup of amino acids to a separate group with distinct biochemical properties, so could putatively change protein function or structure.

Domains screened

The domains targeted for the archive screen were considered based on prior knowledge of function. Previous work on mutated LSD1 residues suggests that mutations in the catalytic centre cause a knock down of LSD1 activity (Stavropoulos et al. 2006). As demonstrated in Figure 3.12, this frequently leads to a 90% loss of catalytic efficacy and rarely leads to a partial knock down in activity which might therefore cause similar consequences to knockout, which would be undesirable in the context of the current investigation. The residues mutated in the SWIRM interface (in yellow on the diagram) are less likely to cause total loss of function, but the F179A, Q180A, I266A and S346A mutants appear to show no deterioration in efficacy at all and as such would be predicted not to display any phenotype if generated in a mutant line. Rather the most C-terminal residue mutants L819A and R824A which would lie in the FAD-binding domain had the effect of partial loss of efficacy (down to 60% of wild type) in this demethylation assay. In the case of LSD1, finding a partial knock

down of function might allow retention of enough LSD1 function through development for viability whilst also disrupting function enough to precipitate a phenotype in the adult. Therefore in the current investigation, the Harwell ENU archive was screened for mutations in exons 10, 11, 12 and 19 of *Kdm1a* encoding the tower and FAD-binding domains. Exons 6, 7, 9 and 10 of *Kdm1b* were screened encompassing the SWIRM and CW-Zinc finger domains which if disrupted might cause changes to its amine-oxidase catalytic activity. This was decided as the knockout is not lethal and LSD2 retains its repressive transcriptional regulatory function without amine-oxidase catalytic activity (Yang et al. 2010).

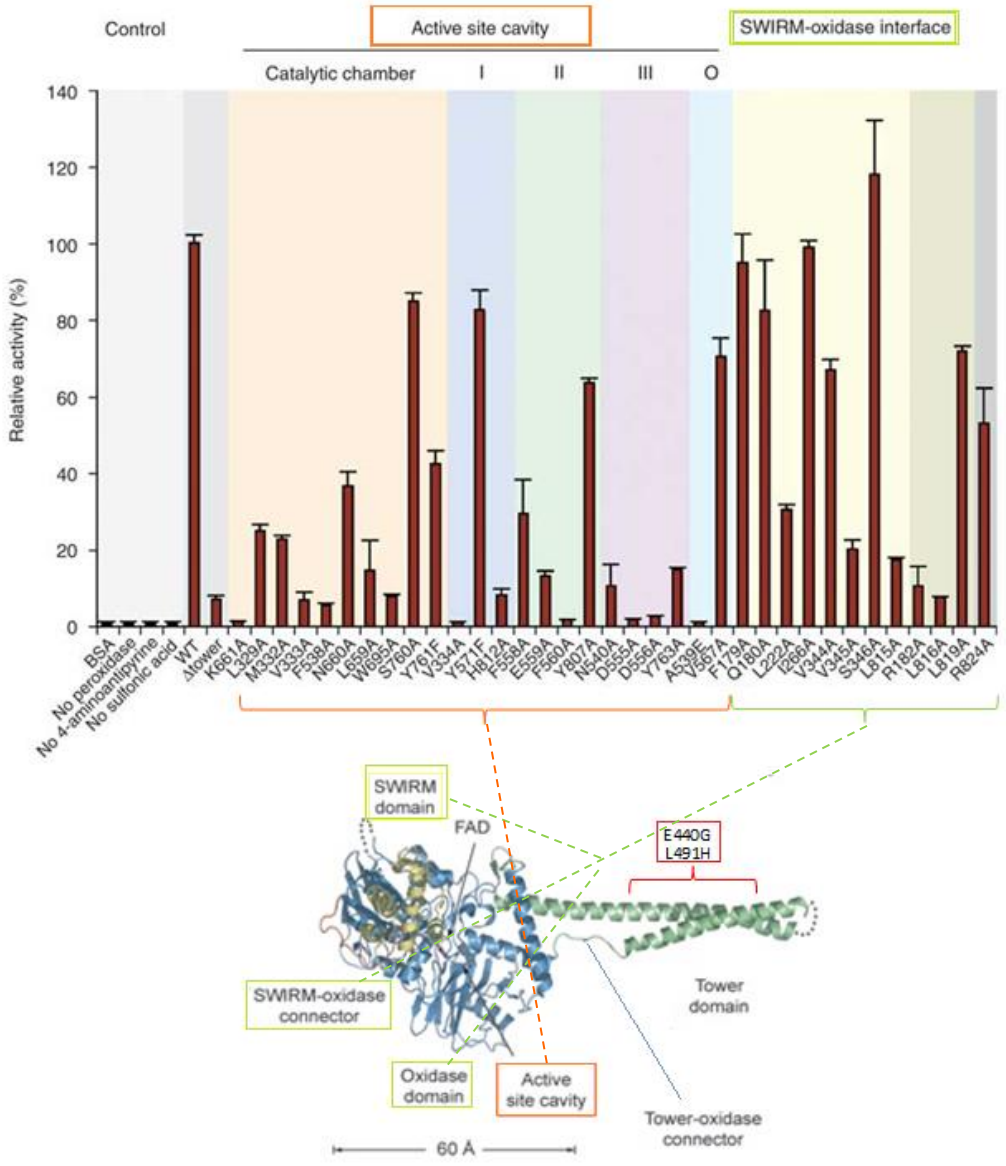

Figure 3.12: Activity of recombinant mutant LSD1

Recombinant LSD1 mutants were incubated in a cell-free photometric assay with methylated H3K4. Mutations in the catalytic and SWIRM domain are deleterious to LSD1-mediated demethylation. (Adapted from Stavropoulos et al. 2006),

3.4.4: Predicted Structural Disruption, and Re-derivation

Protein structure and mechanism prediction *in silico* has influenced previous transcriptomic investigations (Ng et al. 2007; Ueda et al. 2005). The manner in which LSD1 and LSD2 were predicted to be altered upon mutation were interpreted differentially; LSD1 disruption that might have led to a deficit in catalytic activity was avoided, whereas mutations which caused structural change in LSD2 were most likely to affect its activity and were considered most optimal. This is because *Kdm1b*$^{-/-}$ animals are able to survive to adulthood. As such if a mutation were found in the essential regions of LSD2, any deleterious impact caused by mutation would not necessarily be predicted to cause lethality.

Nfold3 and Phyre2 predictions confirmed that the *Kdm1b*^{T357M} and *Kdm1b*^{P281L} mutations were most likely to alter protein structure, and that the LSD1 mutations were not. Polyphen analysis supported the three-dimensional modelling software predictions. As SIFT analysis is based on human sequences rather than mouse, the results were less pertinent than earlier analyses for prediction of protein structure alterations in an ENU mouse model. Subsequently the *Kdm1a*^{E440G} and *Kdm1a*^{L491H} mutations and the *Kdm1b*^{T357M} and *Kdm1b*^{P281L} mutations in LSD2 were chosen for re-derivation.

Chapter 4

MOLECULAR CHARACTERISATION OF LSD FUNCTION IN THE CLOCK

CHAPTER 4: Molecular characterisation of LSD function in the clock

4.1: Introduction

In order to ascertain the function of novel genes in the circadian clockwork, a multitude of approaches can be employed. The activity of any gene can be isolated in cell-based systems and manipulated in several ways. *In vitro* experiments are often very specific in nature and in many cases the data more easily quantifiable than that acquired from *in vivo* investigations due to limitations posed by the living system used (for instance, visualising the activity of a brain area in a living animal is more technically demanding than if the brain slice or brain cells are isolated and output is measured *in vitro*).

For the current investigation, the LSD1 and LSD2 genes are expressed using constructs containing the mutated forms of the LSD genes (*Kdm1a*^{E440G}, *Kdm1a*^{L491H}, *Kdm1b*^{M271T}, *Kdm1b*^{N272S}, *Kdm1b*^{P281L}, and *Kdm1b*^{V366A} as the *Kdm1b*^{T357M} construct was unavailable). Using these mutated LSD constructs allows for interpretation of data in cellular assays where the gene function is perturbed in a specific way (here overexpression of genes containing a single nucleotide base change) (Picciotto & Wickman 1998). The conclusions we are then able to draw from the molecular results are expected to correspond to some extent with the physiology of the mutant animals as the mutation in question is identical to that present in the animals.

Molecular approaches can be used to monitor changes in circadian gene expression as a result of the LSD mutations *in vitro*. The protein product of the LSD gene can also be isolated and interactions with clock components and with chromatin investigated to determine exactly what role LSD1 and LSD2 play in clock regulation.

Promoters controlling the expression of clock genes are known to be differentially methylated and acetylated by multiple regulators which modulate the ticking of the clock (Etchegaray et al. 2003; Etchegaray et al. 2006; Ladurner 2003; Katada & Sassone-Corsi 2010; Ripperger & Merrow 2011). For

example, *Per1* and *Per2* promoter acetylation occurs in synchrony with transcription levels (Asher et al. 2008), and CLOCK has been shown to contribute to this acetylation pattern by heterodimerising with P300 (a transcriptional coactivator acting via acetyltransferase activity) and regulating recruitment of acetyltransferases (Etchegaray et al. 2003). Histone methylation at the *Dbp* promoter in particular is dynamic and clock dependent (Ripperger & Merrow 2011). Methylation events contribute to the regulation of the circadian clock at many other levels. DNA CpG island motif methylation has been shown to affect SCN plasticity in animals entrained to non-24 hour light dark cycles (Azzi et al. 2014). The methylation of messenger RNA has also been shown to modulate circadian function, and inhibition of METTL3 methyltransferase activity mediating mRNA methylation patterns causes elongation of circadian period (Fustin et al. 2013). Clock proteins are also modified directly, although as yet no methylation events have been examined with regards clock mechanism components. BMAL1 is acetylated on residue K537 (Hirayama et al. 2007). Acetylation increases recruitment of negative limb components and therefore transcriptional repression (Hirayama et al. 2007). CLOCK has been shown to deacetylate BMAL1 directly in a pulldown assay using overexpression in mammalian cells (Hirayama et al. 2007). SIRT1 also promotes deacetylation and degradation of PER2 (Asher et al. 2008). Histone acetylation has also been shown to impact on DNA methylation by DNMT1 (Cervoni & Szyf 2001), demonstrating a complex and dynamic interplay between epigenetic mechanisms which can affect circadian oscillation.

LSD1 and LSD2 were initially identified as histone demethylases (Shi et al. 2004; Ciccone et al. 2009), but both play demethylase-independent roles (Nam et al. 2014; Nicholson & Chen 2009), so all functions of the mutant LSD constructs may impact on *in vivo* phenotypes that will be observed using the ENU mutant animals. The LSDs have both been shown to specifically demethylate mono-methylated and di-methylated histone H3K4 (Shi et al. 2004; Yang et al. 2010). As investigation has delved further into the action of LSD1, it has become apparent that it is required to maintain DNA methylation (Wang et al. 2009), and that it also acts on non-histone substrates including DNMT and p53 (Nicholson & Chen 2009). Disruption of LSD1 function has previously been associated with vital

functions in development, cancer and memory (Fuentes et al. 2012; Han et al. 2014; Nicholson et al. 2013; Nottke et al. 2009; Scoumanne & Chen 2007; Amente et al. 2013; Wang et al. 2011; Baron et al. 2011; Lynch et al. 2012; Clinical-Trial website; Neelamegam et al. 2012). LSD2 has not been shown to influence DNA methylation outside of imprinting mechanisms, and has no identified non-histone targets (Ciccone et al. 2009). Knockout studies of LSD2 demonstrate its importance in reproduction (Ciccone et al. 2009), and its role in imprinting is well established (Ciccone et al. 2009).

Considering the extent to which the characterisation of the epigenetic mechanisms modulating the circadian clockwork has expanded, investigation into the role of demethylases in the molecular clock have only recently been considered. Demethylase JARID1A was shown to bind to and activate CLOCK:BMAL1 by regulation of histone methylation at the *Per2* E-box promoter (DiTacchio et al. 2011). During the course of this study, the circadian role of the more abundant and well-characterised LSD1 was investigated (Nam et al. 2014). In order to investigate the role of LSD1 in the clock, LSD1 regulation by protein kinase PK1C was disrupted. The $Kdm1a^{S112A}$ mutant (disruption of a phosphorylation residue essential to LSD1 function) displayed dampened circadian rhythmicity and impaired phase resetting of the clock in response to light (Nam et al. 2014). LSD1 phosphorylation correlated with its ability to bind to CLOCK and BMAL1 directly as shown by immunoprecipitation of endogenous LSD1 using MEFs, suggesting that it might exert its phase resetting effects on the clock via direct interactions with CLOCK and BMAL1. This binding is independent of the demethylase activity of LSD1.

The molecular properties of LSD1 and LSD2 in relation to the clock are henceforth investigated with a view to re-derivation of relevant identified novel mutants by IVF and then to tease apart the function of each gene in the clock machinery.

4.2: Overexpression of LSD1 and LSD2

Disruption of the two histone modifier genes *Kdm1a* and *Kdm1b* would be expected to alter the expression of many genes through changes in histone methylation patterns. LSDs demethylate mono-methylated and di-methylated H3K4 (Shi et al. 2004). H3K4 methylation impacts on the expression of several circadian clock genes (Xydous et al. 2012; Katada & Sassone-Corsi 2010; Wang et al. 2012). *Kdm1a* and *Kdm1b* also demethylate other protein substrates (such as p53 and DNMT1 (Nicholson & Chen 2009)) and play demethylase-independent roles in the clock (Nam et al. 2014), so gene expression could also be affected in alternative ways.

In order to examine circadian properties of the *Kdm1a* and *Kdm1b* mutations identified earlier in the Harwell ENU archive screen (Chapter 3), constructs were generated by site directed mutagenesis (Section 2.2.2). The constructs were subsequently artificially overexpressed in cell cultures and their circadian properties compared to cells transfected with the wild-type construct (Section 2.3.6).

4.2.1: LSD1 and LSD2 mutant rhythms

Firstly, potential direct effects of LSD mutations on circadian rhythms were examined, for comparison with results from the knockdown siRNA cells in the Reinke lab (Personal Communication Dr H. Reinke, Uni Düsseldorf, Ge) (Section 3.1).

Rene Linka (Dr H. Reinke lab Düsseldorf) transfected mutant $Kdm1a^{E440G}$ and $Kdm1a^{L491H}$ constructs (generated in the MRC Harwell lab) into NIH-3T3 cells, and the expression of clock gene mRNA was investigated using real time PCR. Downregulation of expression of multiple clock genes in unsynchronised cells was observed (Personal Communication Dr H. Reinke, Uni Düsseldorf, Ge). In the case of $Kdm1a^{L491H}$ *LSD2, Cry2, Per2, Dbp* and *Rora* are downregulated and *Bmal1* upregulated, whereas for $Kdm1a^{E440G}$ overexpression, *LSD2, CLOCK, Bmal1, Cry2, Per2, Dbp, Rora* and *Rev-erbα* are all downregulated. All downregulation of circadian clock genes by the $Kdm1a^{E440G}$ mutation was by at least 50% (except *Bmal1* which was only downregulated by 30%). Gene expression was less

extensively downregulated by the overexpression of the *Kdm1a*^{L491H} mutation, perhaps suggesting that the *Kdm1a*^{E440G} mutation evokes more substantial circadian changes *in vitro*.

Next, LSD1 and LSD2 mutant constructs were transfected into stably transfected *Per2*:Luc reporter containing cell lines (both Rat-1 fibroblasts and U2OS cells) and bioluminescent reporter recording utilised to assess how each mutant altered the amplitude, phase and period of *Per2* expression. Recordings were performed and confirmed in triplicate.

Figure 4.1 shows that the period of cells transfected with mutated constructs were different to wild type. This suggests that mutations change the period of the molecular circadian clock in cell lines so they may be associated with a circadian mechanism. To check for effects of overexpression of the LSD constructs without mutations in cell cultures, the period of LSD1 transfected Rat-1 cells was compared to untransfected control cultures, and overexpression alone did not alter circadian period ($p=0.2151$ by ANOVA) (Figure 4.1a). While the overexpression of LSD1 mutations *Kdm1a*^{L491H} and *Kdm1a*^{E440G} caused a shortening of circadian period relative to overexpression of *Kdm1a* (by 20 minutes and 51 minutes respectively), mutation *Kdm1b*^{P281L} lengthened the period of the clock from 21.2 to 22.1 hours ($p=0.0002$ for LSD1 constructs, $p=0.0291$ for LSD2 constructs by ANOVA).

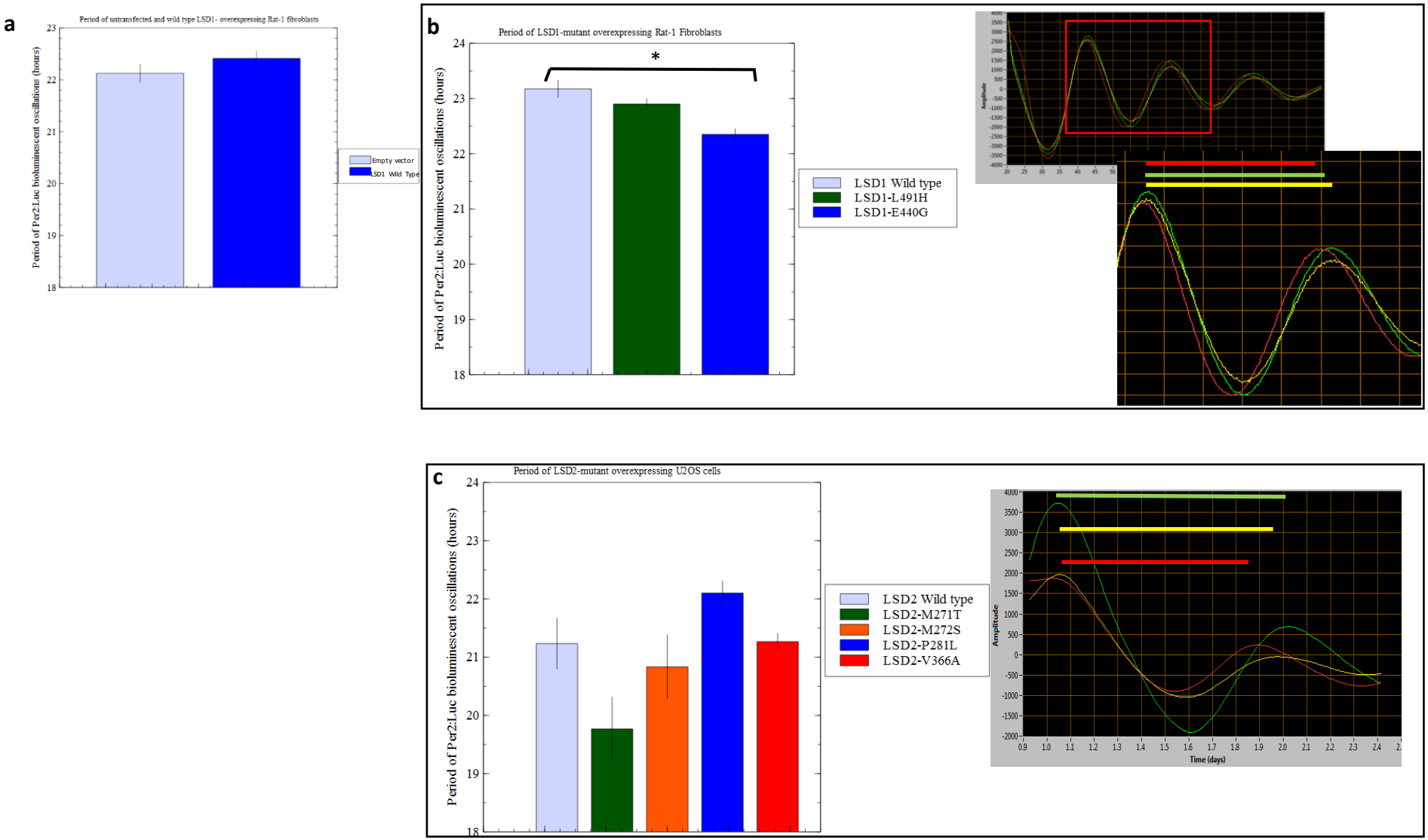
a
Period of untransfected and wild type LSD1- overexpressing Rat-1 fibroblasts
Period of Per2:Luc bioluminescent oscillations (hours)
Empty vector
LSD1 Wild Type
b
Period of LSD1-mutant overexpressing Rat-1 Fibroblasts
Period of Per2:Luc bioluminescent oscillations (hours)
*
LSD1 Wild type
LSD1-L491H
LSD1-E440G
c
Period of LSD2-mutant overexpressing U2OS cells
Period of Per2:Luc bioluminescent oscillations (hours)
LSD2 Wild type
LSD2-M271T
LSD2-M272S
LSD2-P281L
LSD2-V366A
Amplitude
Time (days)

Figure 4.1: Overexpression of LSD1 mutant and LSD2 mutant constructs in fibroblast cells

Both *Kdm1a*^{E440G} and *Kdm1a*^{L491H} constructs cause a shortening of circadian period in fibroblasts. *Kdm1b*^{P281L} overexpression lengthens the period and *Kdm1b*^{M271T} shortens the period of fibroblasts.

a) Expression of LSD1 in rat-1 fibroblasts did not change circadian period significantly (for untransfected cells period was 22.13 ±0.17, LSD1 transfected cells 22.41 ±0.15, p=0.215113)
b) LSD1 mutant constructs change circadian period (wild type 23.18 ±0.15, *Kdm1a*^{E440G} 22.35 ±0.10, *Kdm1a*^{L491H} 22.90 ±0.09, ANOVA p= 0.000195) (*Kdm1a*^{L491H} p=0.1260, *Kdm1a*^{E440G} p=0.0129), *Kdm1a*$^{+/+}$: Yellow trace, *Kdm1a*^{E440G}: red trace, *Kdm1a*^{L491H}: green trace. Yellow, red and green bars show the length of one cycle from peak to peak of expression for comparison.
c) LSD2 mutant constructs change circadian period (wild type 21.23 ±0.43, *Kdm1b*^{M271T} 19.77 ±0.55, *Kdm1b*^{P281L} 22.10 ±0.21, ANOVA p=0.029082. When individual data was assessed, the effect was not significant (*Kdm1b*^{M271T} p=0.1031, *Kdm1b*^{P281L} p=0.1458), *Kdm1b*$^{+/+}$: Yellow trace, *Kdm1b*^{M271T}: red trace, *Kdm1b*^{P281L}: green trace. Yellow, red and green bars show the length of one cycle from peak to peak of expression for comparison.

Measurements repeated in triplicate, each experimental group consisted of n=3 dishes. Period differences analysed by student T-test. (*p<0.05, **p≤0.005, ***p≤0.001)

4.2.2: LSD1 Co-Immunoprecipitation

As the LSD genes are both histone modifiers, they are frequently found in large chromatin-modifying complexes (Section 1.6.1) (Yang et al. 2006). As well as binding to many chromatin-modulating partners, LSD1 has been shown to demethylate non-histone substrates (Nicholson & Chen 2009), so interactions with core clock protein products was initially investigated to ascertain whether LSD1 can bind to circadian proteins in the first instance. Subsequently, the nature of the interaction must be established to determine the role of clock binding, whether LSD1 binds and modulates clock proteins directly, in a demethylase-dependent or demethylase-independent manner, or whether clock components bind to LSD1 as a part of a larger complex which then acts to modify chromatin in a circadian-regulated manner.

In order to assess any direct protein-protein interactions involving LSDs and clock machinery, constructs containing epitope tagged cDNA encoding LSDs and molecular clock components were co-transfected into HEK293T cells. Cells were harvested after 24 to 48 hours and the constructs isolated using anti-tag antibody-mediated pull-down (Section 2.4.2). Any interacting partners of the isolated protein are co-immunoprecipitated as they remain bound together. The two proteins were then separated by electrophoresis on a tris-acetate gel, transferred to a PVDF membrane and blotted (Sections 2.4.3, 2.4.4 and 2.4.5). Finally the clock construct pulled down with the LSD was detected with a probe antibody (Section 2.4.2).

LSD1-HA constructs were used for most of the interaction studies. However, in order to examine some clock components which were contained in HA-tagged constructs (in particular CRY1 and CRY2), LSD1-GST constructs were generated using a high-throughput cloning pipeline (Appendix 1). Each CoIP was performed in triplicate with negative controls as indicated.

The efficiency of construct overexpression in HEK293 cells was also confirmed by double antibody labelling and immunofluorescence, and images qualitatively checked for co-localisation (Section 4.2.3).

4.2.2.1 Wild-type LSD1 interactions with clock components

The interaction of LSD1 with clock components was unknown at the outset of the current investigation. More recently the interaction of LSD1 with the CLOCK:BMAL1 heterodimer has been established using co-immunoprecipitation assays (Nam et al. 2014). Therefore in the current investigation, constructs expressing wild-type LSD1 were overexpressed with several constructs encoding major core clock components in turn.

Firstly, the LSD1-HA construct was used in HA pull downs with PER1-V5, PER2-V5, CLOCK-FLAG, BMAL1-V5 and REV-ERBα-V5. The clock components were detected with antibodies against the V5 and FLAG epitope tags. LSD1 interacts with all of the listed components of the core clock (Figure 4.2a). The strength of interaction was observed to vary, the strongest interaction detected with CLOCK (although multiple bands were present due to the FLAG antibody), followed by BMAL1 and PER2 and the weakest interactions with PER1 and REV-ERBα. The quantification of such interactions is qualitative as factors such as the integrity of the binding and whether the binding is direct or indirect can affect the intensity of the band measured on the CoIP blot.

With regards *Cry* genes, only HA epitope tagged constructs were available. Therefore, the *Kdm1a* and *Kdm1b* genes were cloned into GST tagged vectors (Appendix 1) and interactions with CRY1 and CRY2 were investigated by GST pull down. Because often multiple bands were observed on blots for FLAG-tagged constructs, the interaction of CLOCK was re-trialled using a CLOCK-HA construct. LSD1 was shown to interact with both CRY2 and to a lesser extent, CRY1, and its interaction with CLOCK was confirmed (Figure 4.2b).

4.2.2.2 Wild-type LSD2 interactions with clock components

The interaction of LSD2 with core clock components has never previously been investigated. LSD2 demethylates H3K4 utilising the same catalytic mechanism as LSD1, and is 18% identical in sequence

to *LSD1*. Therefore, the non-histone binding and demethylation effects of LSD1 could be shared with its paralog LSD2.

In order to investigate what clock components LSD2 interacts with, LSD2 was immunoprecipitated in a similar manner to LSD1 (Section 4.2.2.1). It was shown that LSD2 interacts with CRY1, CRY2 and BMAL1 (Figures 4.2a, 4.3). This suggests that LSD2 plays a different role in the clock to LSD1.

a

Construct	1	2	3	4	5	6	7	8	9	10	11	12	13	14
Ladder														
Empty-HA	+							+						
LSD1-HA		+	+	+	+	+	+		+	+	+	+	+	+
empty-V5		+							+					
CoREST-Myc	+		+					+		+				
CLOCK-Flg				+							+			
BMAL1-V5					+							+		
PER1-V5						+							+	
PER2-V5							+							+

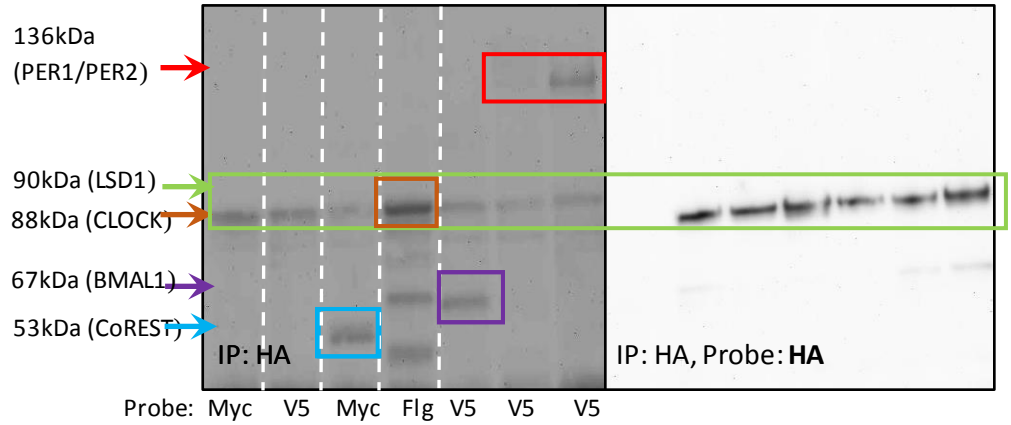

Figure 4.2: Co-immunoprecipitation of clock proteins using LSD1 and LSD2 protein overexpressing cells

a) LSD1 pulldown with HA antibody precipitated CLOCK, BMAL1, PER1, PER2, and REV-ERBα

White dashed lines indicate where blot was cut for detection of bands with the respective probe antibodies before being re-aligned for imaging.

Blots representative of experiments repeated in triplicate.

b

Construct\Lane	1	2	3		4	5	6
Ladder				+			
LSD1-GST	+	+	+				
LSD2-GST					+	+	+
Empty-HA	+				+		
Cry1-HA		+				+	
Cry2-HA			+				+

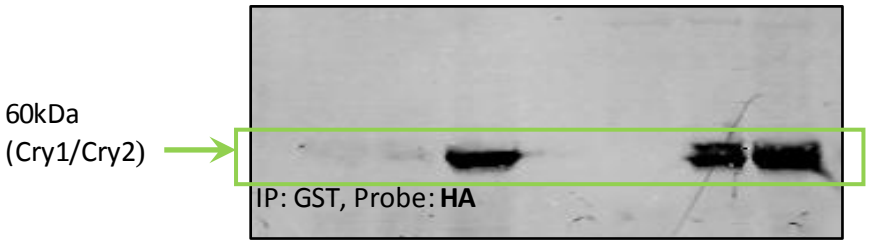

Figure 4.2: Co-immunoprecipitation of clock proteins using LSD1 and LSD2 protein overexpressing cells

b) Pulldown of LSD1-GST construct precipitated CRY1 and CRY2 suggesting interaction between LSD1 and multiple components of the core clock. LSD2-GST pulldown precipitated CRY1 and CRY2 also.

Blots representative of experiments repeated in triplicate.

Construct\Lane	1	2	3	4	5	6
Ladder	+					
H2O		+				
LSD2-GST			+	+	+	+
Bmal1-V5			+			
Per1-V5				+		
Per2-V5					+	
CLOCK-V5						+

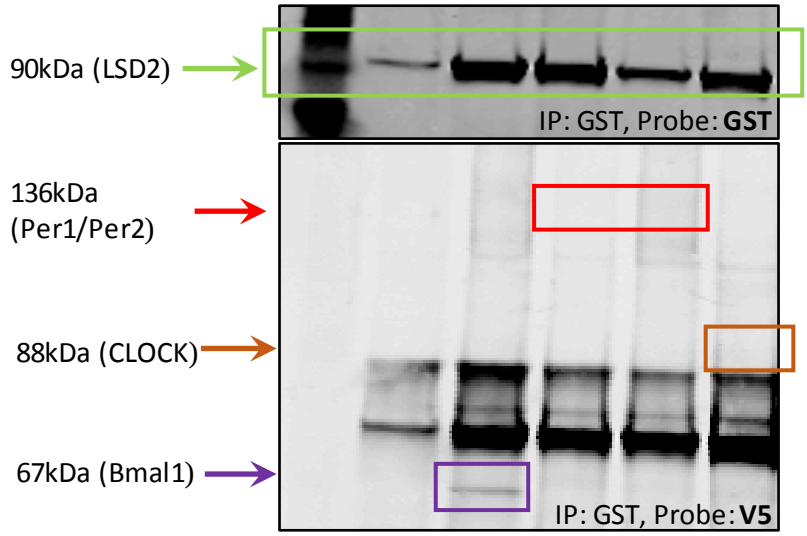

Figure 4.3: Co-immunoprecipitation of clock proteins using LSD2 gene construct pull down

LSD2 pulldown with a GST antibody precipitated BMAL1 and not PER1, PER2 or CLOCK, suggesting that LSD2 interacts with specific components of the clock. Band in lane 2 due to pipetting spill-over. Bands between 88kDa and 67kDa non-specific antibody binding.

Blot representative of experiments repeated in triplicate.

4.2.2.3 CoREST influence on LSD1 interactions

LSD1 activity is modulated by interaction with its cofactor, CoREST (Shi et al. 2005). LSD1 binds to CoREST via the tower domain, and it has been shown that this interaction is essential for nucleosomal demethylation and increases the efficacy of LSD1 at H3K4 (Shi et al. 2005). To investigate the effect of the presence of CoREST on the interaction of LSD1 with circadian components, triple transfection of LSD1-HA, CoREST-myc and REV-ERBα-V5 was performed and the interaction was quantified. The presence of CoREST was shown to non-significantly almost double the yield of REV-ERBα upon LSD1 pull down (Figure 4.4).

The interaction studies presented here have demonstrated that LSDs interact with clock components (Sections 4.2.2.1 and 4.2.2.2), and that LSD1 interaction with clock proteins can be influenced by its interaction with its cofactor (Section 4.2.2.3). Next, the effect of mutations on cofactor and clock component interactions will be examined. Mutation of the tower domain would be predicted to primarily disrupt cofactor binding. However, the direct impact of tower mutations on clock protein binding must also be ascertained (Section 4.4).

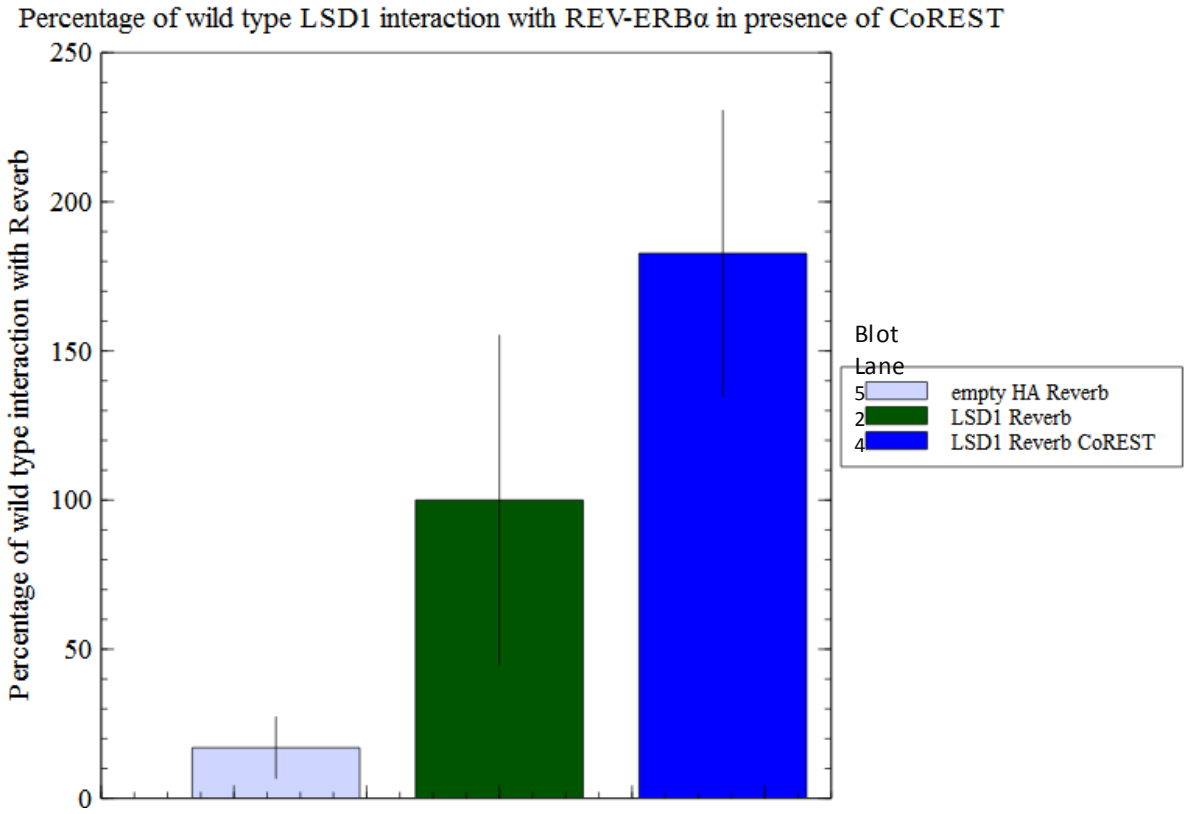

Construct\Lane	1	2	3	4	5
Ladder			+		
LSD1-HA	+	+		+	
REV-ERBα-Flg		+		+	+
CoREST-myc				+	
Empty-HA					+

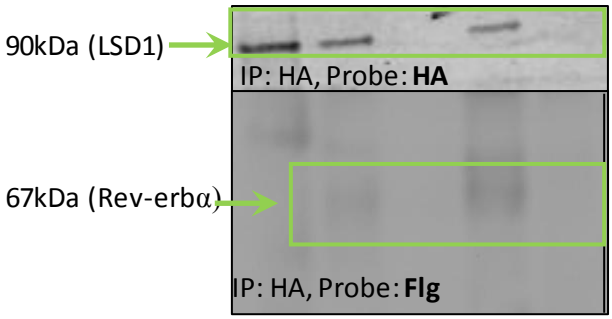

Figure 4.4: Co-immunoprecipitation of REV-ERBα using LSD1 in presence and absence of CoREST

CoIP for KDM1A HA pulls down more REV-ERBα upon cotransfection with CoREST (182.5% of the band observed in the absence of CoREST)

Blot representative of experiments repeated in triplicate.

No significant difference by ANOVA ($P<0.275$)

4.2.2.4 Mutant LSD1 interactions with clock components

The effect of LSD1 mutations on interactions with CoREST and with clock proteins which were established earlier (Figure 4.2) was also assessed. CoIP experiments were performed using cells co-transfected with constructs expressing LSD1 along with CoREST and individual clock components BMAL1, CLOCK, PER1 and PER2.

Mutant constructs failed to interact with CoREST (no interaction was detectable using KDM1A^{L491H} pulldown, and only 2.3% of the control interaction was detected using KDM1A^{E440G} pulldown) (Figure 4.5). This is consistent with the hypothesis that the two mutations which lie in the tower domain have affected the functionality of the domain in CoREST binding.

Mutated constructs interacted weakly with CLOCK (Figures 4.6a and 4.6c), and KDM1A^{E440G} decreases interaction with BMAL1 whereas KDM1A^{L491H} has no effect on the strength of interaction with BMAL1 (Figures 4.6b and 4.6d). The direct interactions of LSD1 with both BMAL1 and CLOCK have recently been independently established by the Reinke lab (Personal Communication Dr H. Reinke, Uni Düsseldorf, Ge) and by Nam et al. 2014. Immunoprecipitation of LSD1 mutant constructs yielded no PER1 protein, and immunoprecipitation of the KDM1A^{E440G} mutant yielded 71% less PER2 protein (Figure 4.7).

The differences between interactions of KDM1A^{L491H} and KDM1A^{E440G} suggest that the two mutants interact differentially with the clock components. The weaker interaction of KDM1A^{E440G} and KDM1A^{L491H} mutants with clock components disruption of the established direct LSD1 interaction with CLOCK or BMAL1 or the PER or CRY proteins (Figure 4.2a). Alternatively, pulldown may be weaker due to the disruption of LSD1 mutant binding to CoREST established earlier (Figure 4.5). As the cells in this experiment are transfected with LSD constructs and clock component constructs for overexpression but are not also transfected with CoREST (so expression is native to the HEK293 cells), the interaction detected by CoIP is likely to be direct in nature, but using CoREST knockout cells for this CoIP would test this hypothesis.

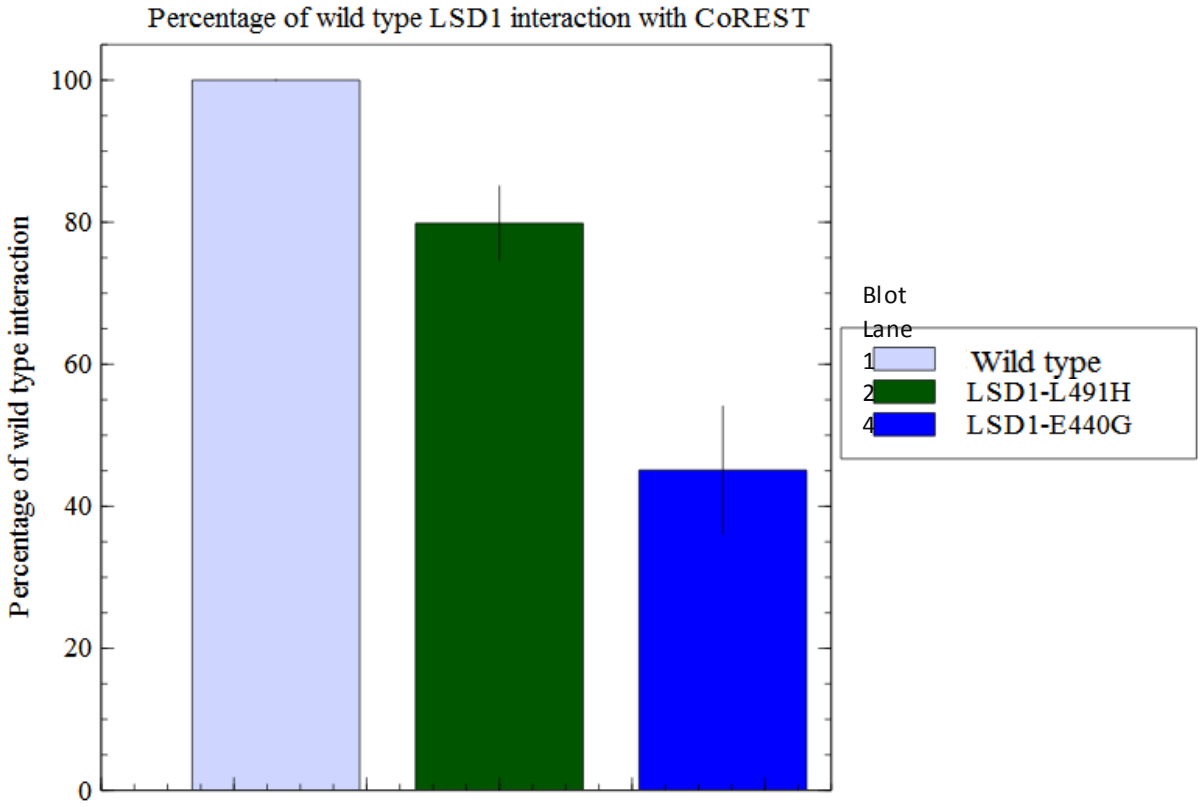

Construct\Lane	1	2	3	4	5	6	7	8
Ladder								
LSD1-HA	+				+			
LSD1-L491H-HA		+				+		
LSD1-E440G-HA				+				+
CoREST-myc	+	+	+	+	+	+	+	+
Empty-HA			+		+		+	

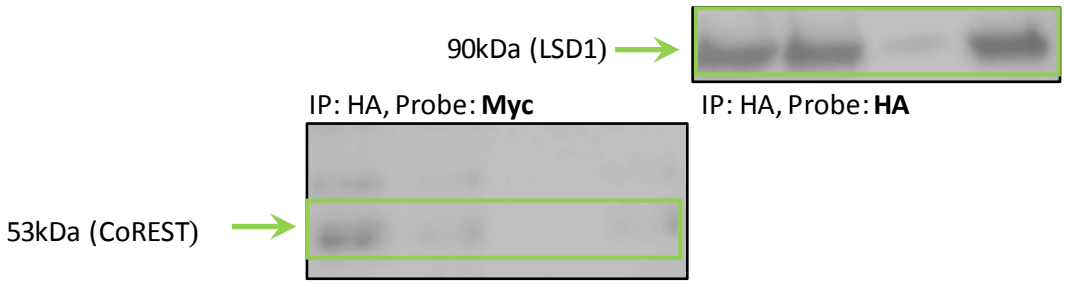

Figure 4.5: Co-immunoprecipitation of CoREST using KDM1A^{L491H} and KDM1A^{E440G} gene construct pull down

CoIP for KDM1A^{E440G} and KDM1A^{L491H} HA pull down less CoREST than wild type constructs (79.9% p= 0.0018 and 44.5% p= 0.0003 respectively). Blots repeated in triplicate, graph depicts averaged data. Data analysed by Student t test

a

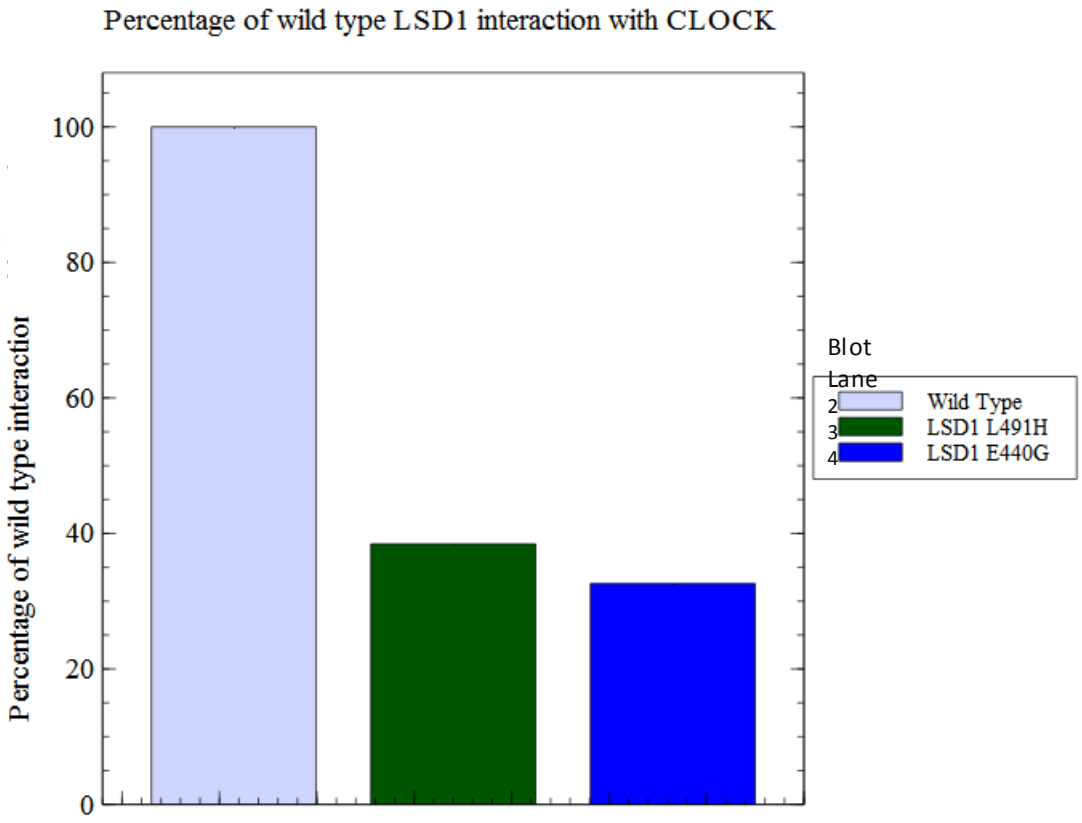

b

Construct\Lane	1	2	3	4	5		6	7	8	9
Ladder	+						+			
LSD1-HA		+						+		
LSD1-L491H-HA			+						+	
LSD1-E440G-HA				+						+
Empty-HA					+					
CLOCK-Flg		+	+	+	+			+	+	+

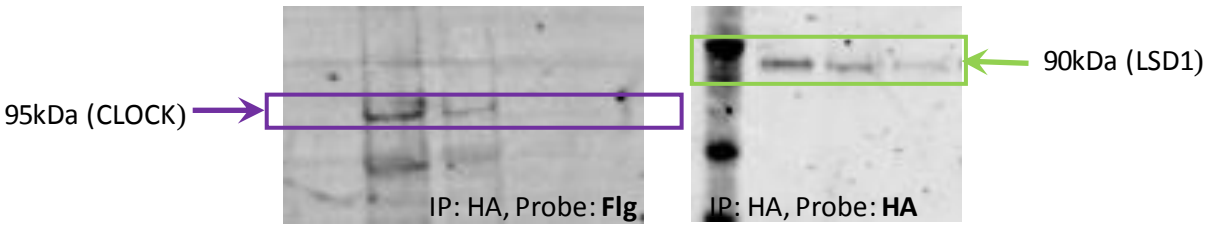

Figure 4.6: Co-immunoprecipitation of CLOCK and BMAL1 using KDM1A^{L491H} and KDM1A^{E440G} constructs

a/b) CoIP for KDM1A^{E440G} and KDM1A^{L491H} HA pull down less CLOCK than wild type constructs (38.5% and 32.6% respectively)

Blot not replicated. Data analysed by Student t test.

c

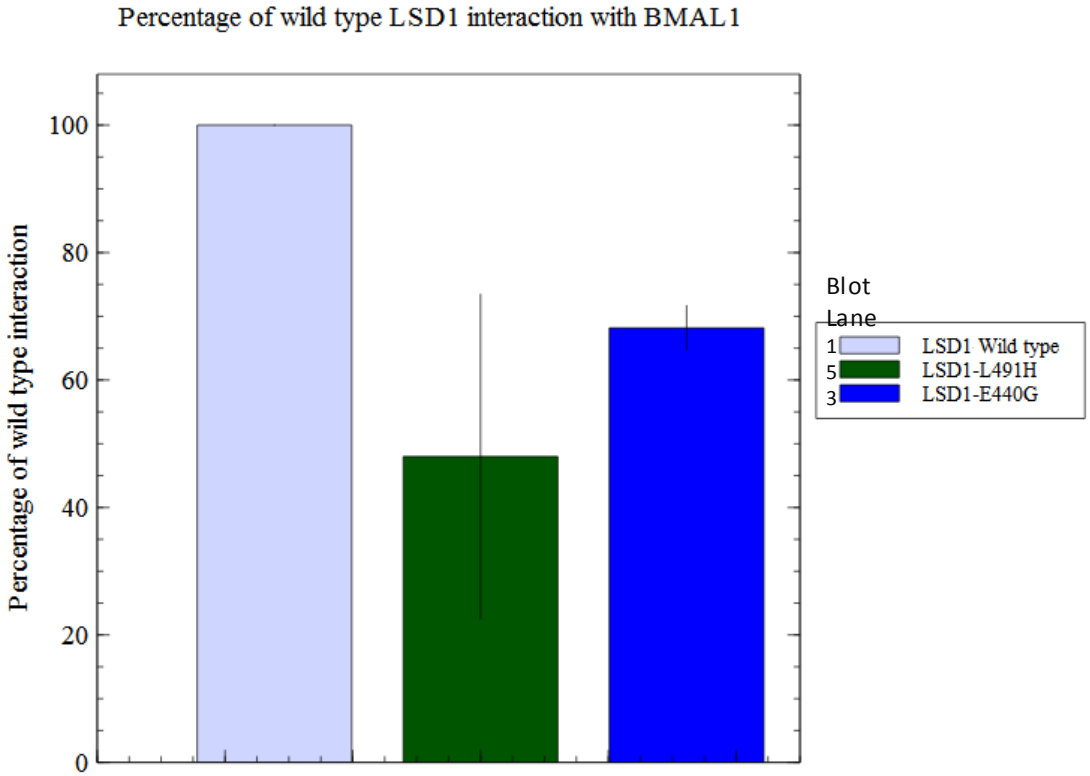

d

Construct	1	2	3	4	5	6	7		9	10	11	12	13	14	15	16
Ladder																
LSD1-HA	+	+							+	+	+					
LSD1-L491H					+	+								+	+	
LSD1-E440G			+	+								+	+			
Empty-HA							+									+
CoREST-myc (+)											+					
BMAL1-Flg	+		+		+		+		+			+		+		+
Empty-Flg		+		+		+				+			+		+	

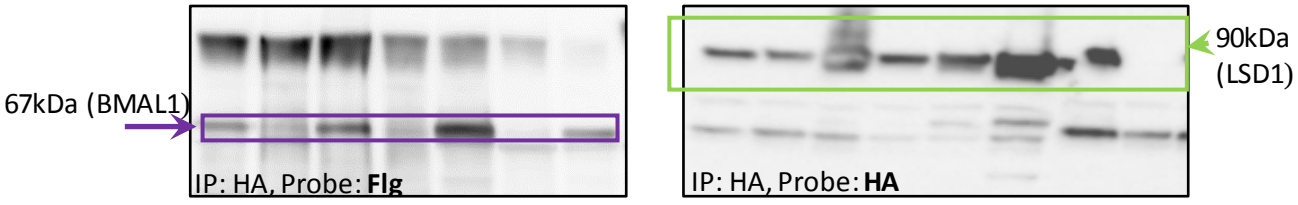

Figure 4.6: Co-immunoprecipitation of CLOCK and BMAL1 using KDM1A^{L491H} and KDM1A^{E440G} constructs

c/d) CoIP for KDM1A^{E440G} HA and KDM1A^{L491H} HA pull down a non-significant amount less BMAL1 than wild type constructs (38.3% of wild type p=0.23, 69.0% p=0.285, respectively)

Blots repeated in triplicate, graph depicts averaged data. Data analysed by Student t test.

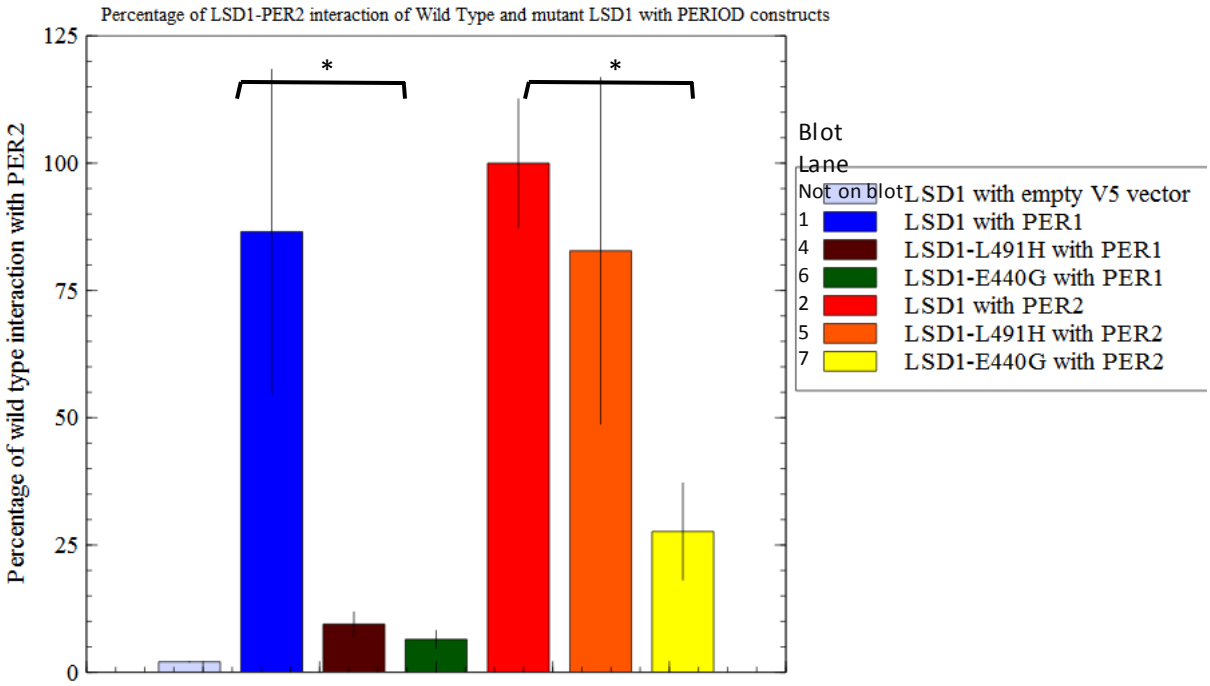

Construct\Lane	1	2	3	4	5	6	7
Ladder							
LSD1-HA	+	+	+				
LSD1-L491H-HA				+	+		
LSD1-E440G-HA						+	+
Bmal-V5 (pos)			+				
Per1-V5	+			+		+	
Per2-V5		+			+		+

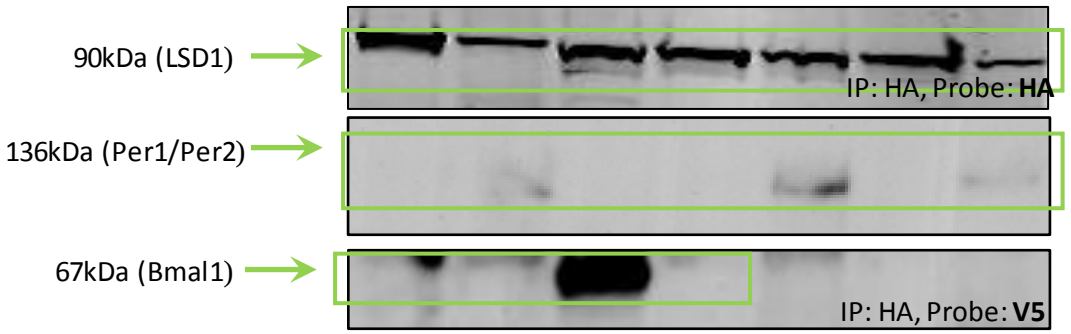

Figure 4.7: Co-immunoprecipitation of PER1 and PER2 using KDM1A^{L491H} and KDM1A^{E440G} constructs

KDM1A^{L491H} and KDM1A^{E440G} HA pull down yield less PER1 protein than wild type (9.52% p=0.0521 and 7.01% p=0.0457 respectively). KDM1A^{L491H} and KDM1A^{E440G} HA pull down yield less PER2 than wild type constructs (81.17% p=0.6515 and 26.98% p=0.0037 respectively)

Blots repeated in triplicate, graph depicts averaged data. Data analysed by 2-way ANOVA.

4.2.3: Immunofluorescent analysis of LSD transfections with clock constructs

To ascertain the efficacy of transfections used in CoIP experiments, immunofluorescent staining was carried out. Investigations showed the transfections to be effective, and double staining shows the subcellular localisation of each construct. LSDs display a nuclear pattern of expression (as expected for a histone modifying protein (Bradley et al. 2007; Shi et al. 2004)) and KDM1A^{E440G}, KDM1A^{L491H} and KDM1B^{P281L} mutations do not alter the efficiencies of the construct transfections or their subcellular localisation (Figure 4.8).

Colocalisation of LSD1 with binding partners was also demonstrated using immunofluorescent staining. CoREST, BMAL1, PER1, PER2 and REV-ERBα localise to the nucleus with LSD1 (Figures 4.9, 4.10). CLOCK did not localise in the nucleus in this experiment (Figure 4.11), variation could be due to the Flag labelled CLOCK construct in use as the other clock constructs were detected with V5 or HA antibodies. As the FLAG antibody had not been verified in immunofluorescent staining previously, CLOCK localisation could not be confirmed.

Co-localisation of LSDs with the clock protein constructs supports the hypothesis that they might directly interact with core clock components. CLOCK localisation is discussed in more depth later (Section 4.4.2).

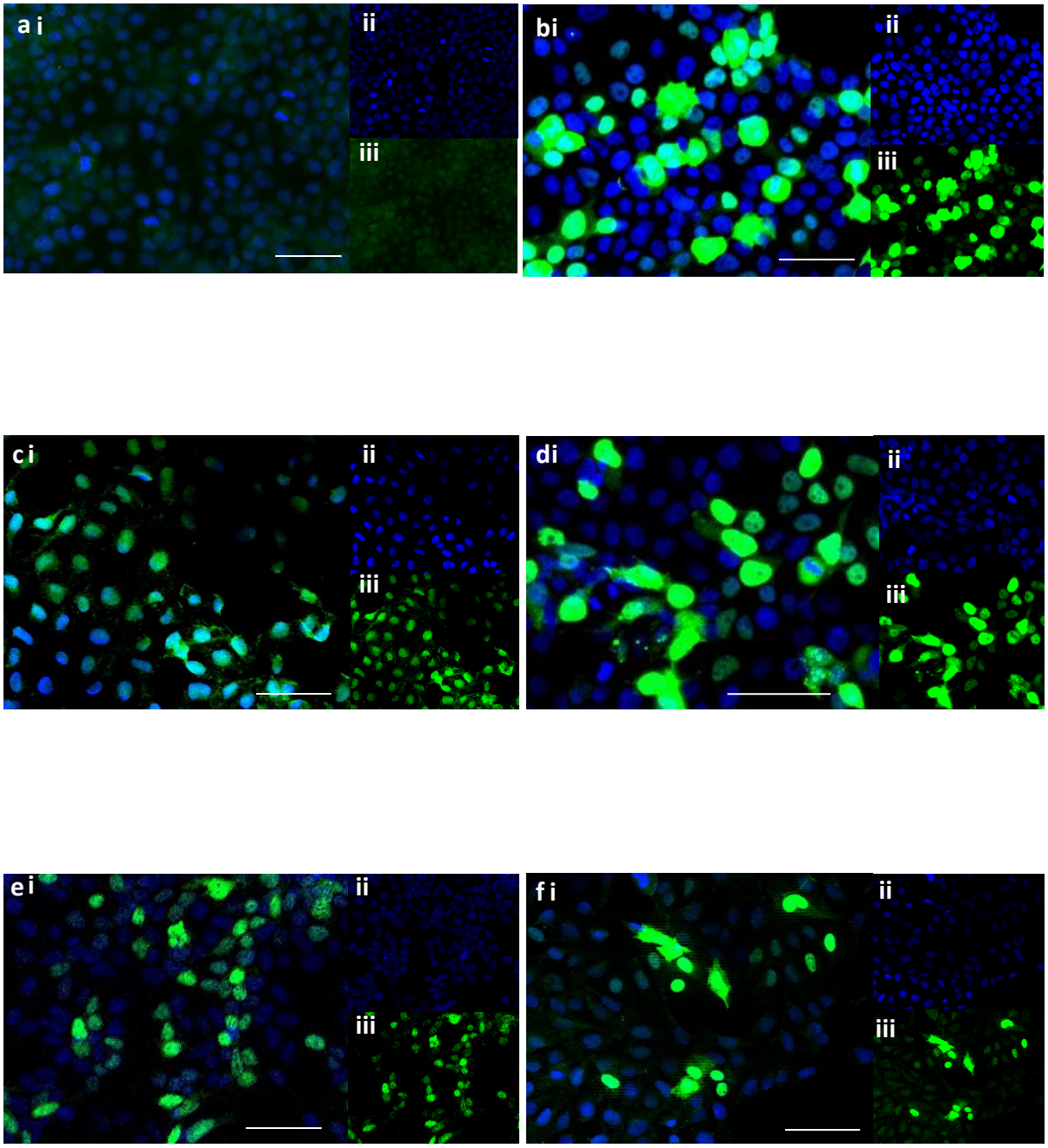

Figure 4.8: Subcellular localisation of overexpressed LSD constructs

LSD1 and LSD2 display nuclear and extranuclear localisationwhen HA-tagged constructs were transfected into HEK293 cells using JetPrime. Scale bars = 50µm.

a) Untransfected, b) LSD1, c) LSD2, d) *KDM1A*^{E440G}, e) *KDM1A*^{L491H}, f) *KDM1B*^{P281L}
i) Merge, ii) DAPI, iii) HA Green

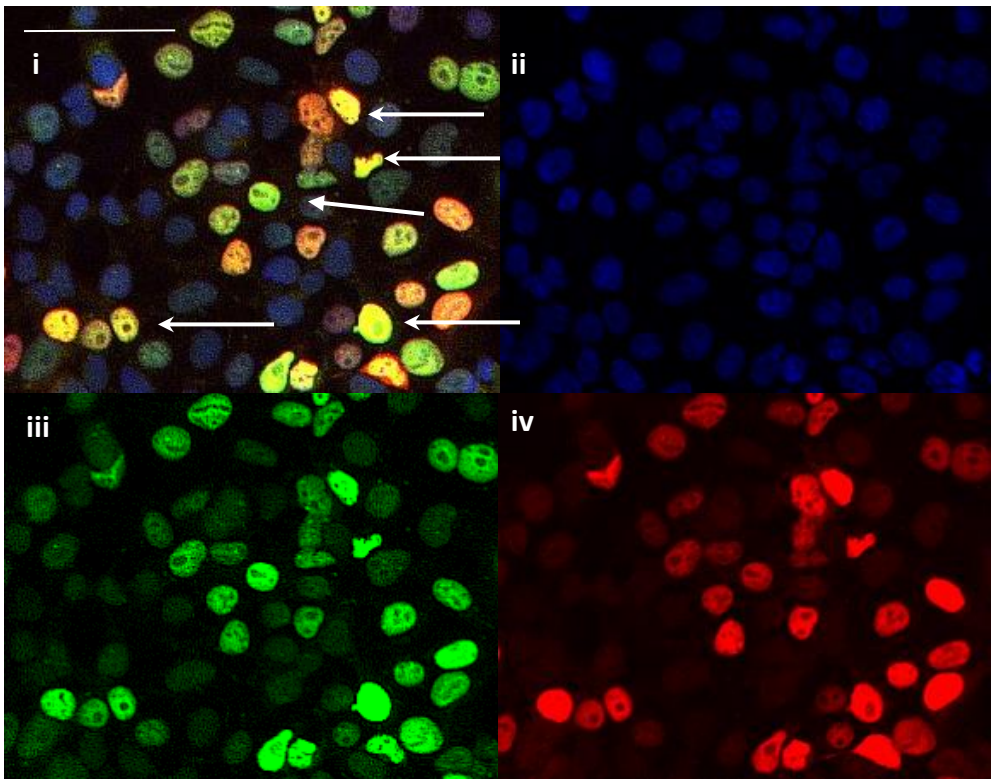

Figure 4.9: Subcellular localisation of overexpressed LSD1 and CoREST

HEK293 cells were cotransfected with LSD1-HA and CoREST-myc constructs. The image demonstrates colocalisation of LSD1 and CoREST in the nucleus (white arrows). Scale bar = 50µm.

i) Merge, ii) DAPI, iii) Myc Green (CoREST), iv) HA Red (LSD1)

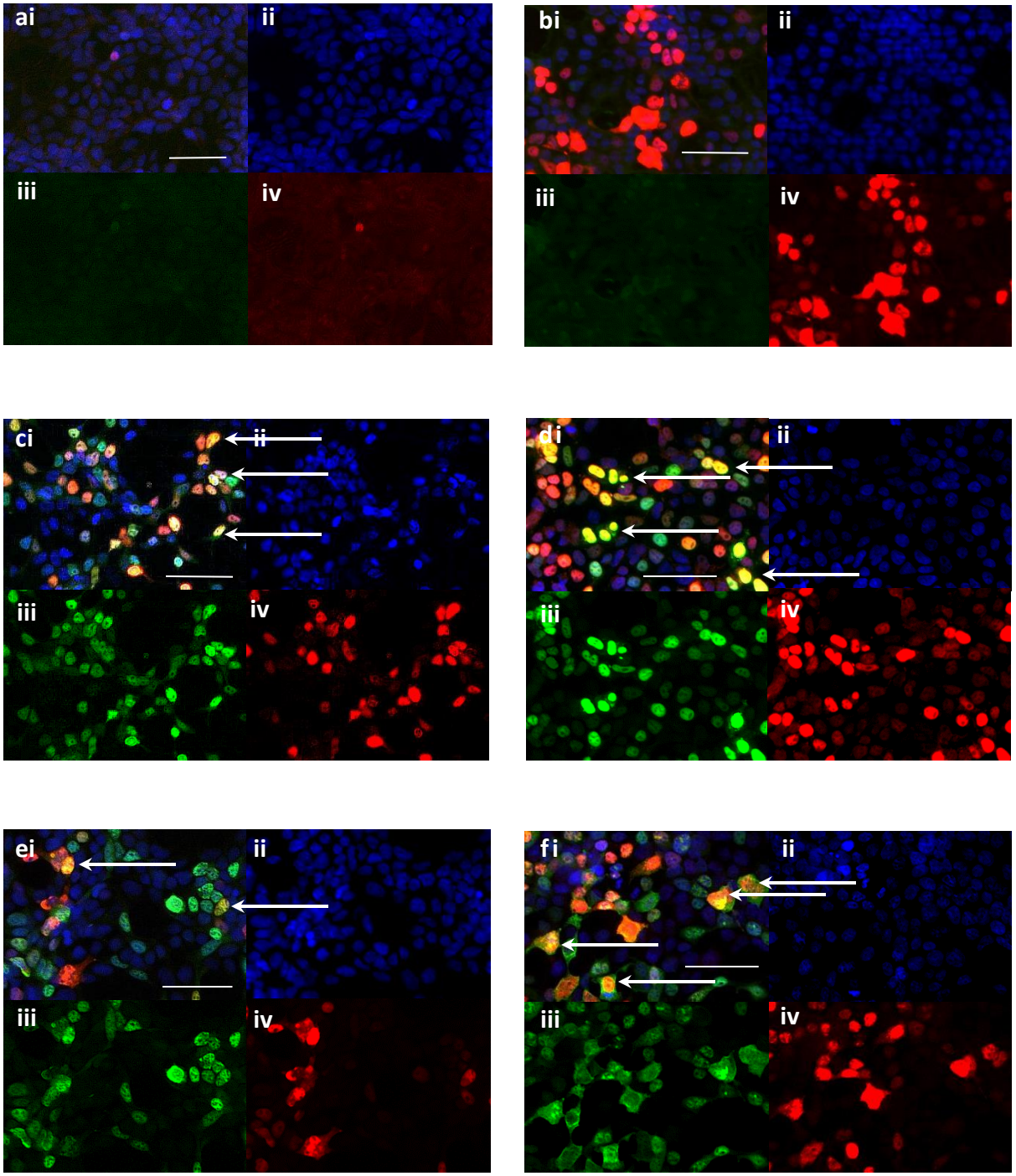

Figure 4.10: Subcellular localisation of overexpressed LSD1-HA and clock protein-V5 constructs

HEK293 cells were cotransfected with LSD1-HA and clock component-V5 constructs. The image demonstrates colocalisation of LSD1 and clock components in the nucleus (white arrows). Scale bars = 50µm.

a) Untransfected, b) LSD1 alone, c) BMAL1 , d) Rev-erbα, e) Per1, f) Per2,
i) Merge, ii) DAPI, iii) HA Red, iv) V5 Green

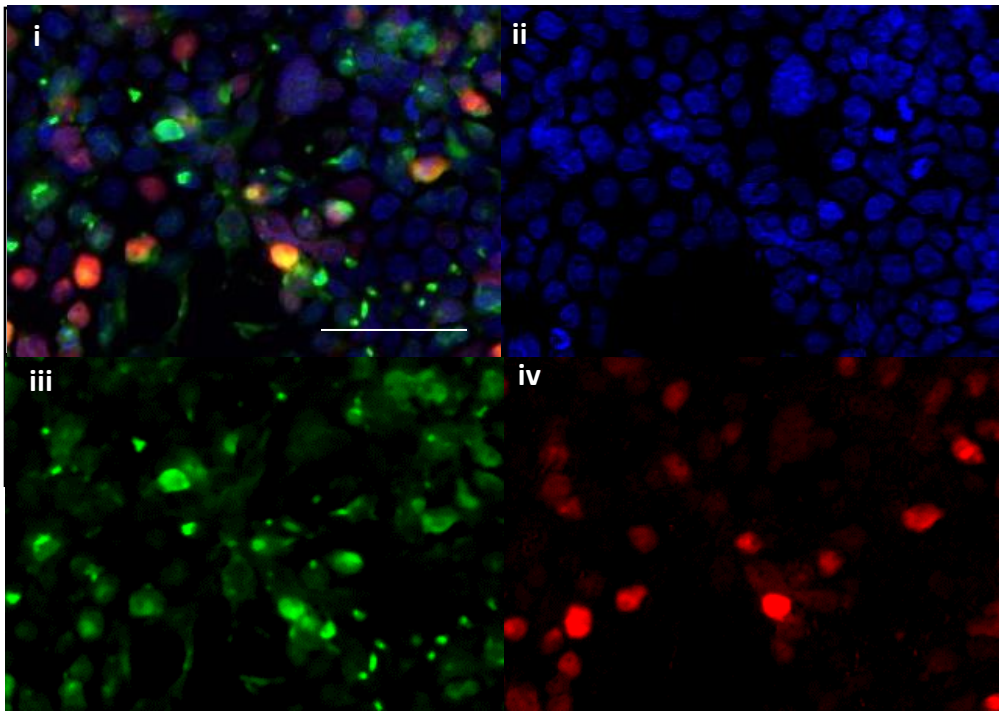

Figure 4.11: Subcellular localisation of overexpressed LSD1-HA and CLOCK-FLAG construct

HEK293 cells were cotransfected with LSD1-HA and CLOCK-FLAG constructs. The image fails to reaveal colocalisation of LSD1 and CLOCK in the nucleus. CLOCK staining appears to be cytoplasmic. Scale bar = 50µm.

i) Merge, ii) DAPI, iii) FLAG Green, iv) HA Red

4.3: LSD1 mutant Chromatin-Immunoprecipitation Data

After establishing the interactions of LSD1 with core clock proteins, the binding of LSD1 mutant proteins to H3K4 (its known target (Shi et al. 2004; Stavropoulos et al. 2006; Forneris et al. 2007)) was investigated and any epigenetic effect resulting from changes to LSD1-mediated H3K4 demethylation established. It will be valuable to ascertain whether it is affecting circadian mechanisms through interaction with clock proteins, perhaps through direct demethylation of those components or alternatively by modification of histone methylation (involving demethylation of H3K4) at circadian promoters. Methylation at H3K4 is a marker of activation of gene expression (Katada & Sassone-Corsi 2010). LSD1 acts to demethylate H3K4Me2 and H3K4Me1 thus supressing gene expression at associated promoter regions.

To investigate whether the demethylase activity of LSD1 at circadian sites might be contributing to changes in clock gene expression, chromatin immunoprecipitation (ChIP) was performed to complete the molecular investigation presented in the current chapter. *Kdm1a*$^{E440G/E440G}$ animals are used and extensively characterised in Chapter 5, but in this section ChIP was performed using MEFs. MEFs were harvested from mutant animals (Section 2.3.5) and heterozygous littermate animals used as a control (as heterozygote animals do not display circadian phenotypes) at E14. ChIP was performed by Rene Linka in the Reinke Lab, Düsseldorf, Germany. A gene with a robust circadian expression pattern, CCG *Dbp*, was chosen for chromatin pull-down investigation.

LSD1 knockout MEFs display an increase in marker H3K4Me2 at 4 marker regions (the promoter, exon 1, intron 1 and exon 4) at the *Dbp* gene locus (Personal Communication Dr H. Reinke, Uni Düsseldorf, Ge, Figure 4.12a). The CLOCK:BMAL1 heteroduplex binds all of these sites excluding the exon 4 sequence. The final region in exon 4 showed no change in the *Kdm1a*$^{-/-}$ MEFs which could be because CLOCK:BMAL1 only plays a role in LSD1 binding to the first three regions (Personal Communication Dr H. Reinke, Uni Düsseldorf, Ge). The increase in methylation of the *Dbp* promoter, exon 1 and intron 1 would suggest an increase in activation of gene transcription (so an increase of

Dbp expression) which is inconsistent with the findings acquired with RTPCR of circadian genes in NIH-3T3 cells (Personal Communication Dr H. Reinke, Uni Düsseldorf, Ge, Section 4.2.1). This may be due to differences between the two systems, for example in the NIH-3T3 cells, mutant LSD1 protein is overexpressed whereas in MEFs, LSD1 is expressed natively.

Next, the effect of the *Kdm1a*$^{E440G/E440G}$ on demethylation of H3K4 methylation at the *Dbp* locus was compared to the effect of the *Kdm1a*$^{-/-}$. Two *Kdm1a*$^{E440G/E440G}$ MEF samples displayed the same pattern of enrichment as the *Kdm1a*$^{-/-}$ samples (Figures 4.12c and 4.12d), albeit at a nonsignificant level, however one sample displayed the inverse (Figure 4.12b). This individual variation might be due to incomplete cell lysis or the over-dilution of a sample which would affect the result.

Taken together, *Kdm1a*$^{E440G/E440G}$ samples showed a non-significant increase in H3K4Me2 (which might suggest a deficit in demethylation at this site) but this was not statistically significant for any of the four sites (p=0.719, 0.832, 0.602 and 0.519, Figure 4.12e). ChIP experiments often require the processing of many cells to collect robust data due to the sensitive nature of the procedure (Collas & Dahl 2008). If such variability was observed in 3 samples here, then analysing more samples in future work will clarify the effect of *Kdm1a*$^{E440G/E440G}$ on H3K4 methylation marks at the *Dbp* locus.

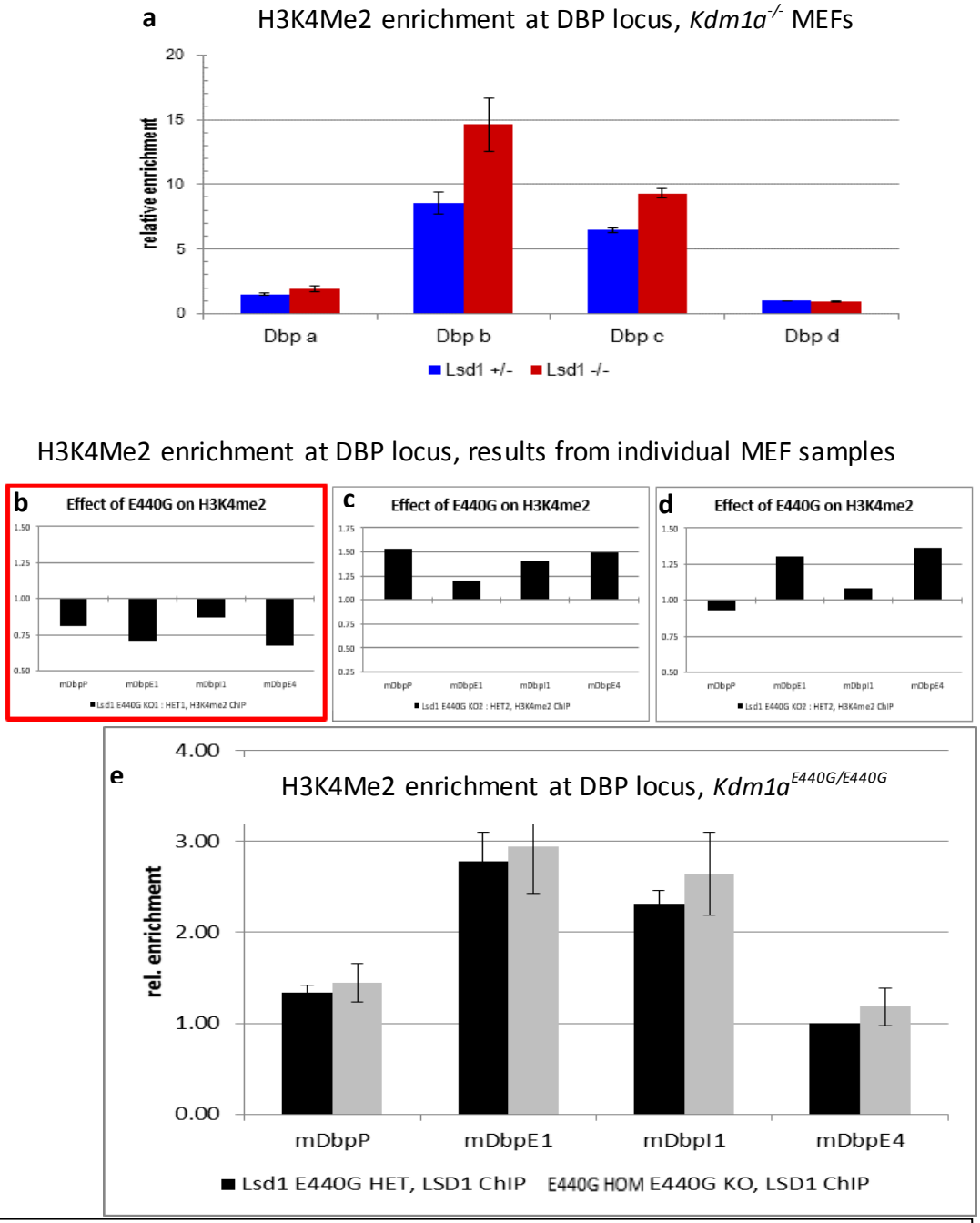

Figure 4.12: Chromatin immunoprecipitation: enrichment of H3K4Me2 at the *Dbp* locus

a) *Kdm1a*$^{-/-}$ MEFs show increased K4Me2 (indicating the lack of LSD1 presence, so no demethylase activity) at all 4 target points at the *Dbp* locus

b, c, d) Individual data from *Kdm1a*$^{E440G/E440G}$ MEFs show varying effects on K4Me2 enrichment at the *Dbp* locus (trace b an decrease and traces c and d increases)

e) Overall *Kdm1a*$^{E440G/E440G}$ MEFs show non-significant increases of K4Me2 at the *Dbp* locus (heterozygous MEFs 1.33 ±0.07, 2.77 ±0.28, 2.31 ±0.13, 1.00 ±0.00 at each region and homozygous MEFs 1.44 ±0.18, 2.94 ±0.45, 2.64 ±0.40 and 1.18 ±0.18 at each region. p=0.719, p=0.832, p=0.602 and p=0.519 respectively)

n=3 heterozygote and n=3 homozygote MEF samples. Data was analysed by student T-test

LSD1 binding at the locus was next examined to see whether demethylation is dampened due to a lack of binding rather than a catalytic defect in mutant samples. If LSD1 fails to bind the locus effectively, it could account for the nonsignificant decrease in demethylation observed at this site. LSD1 is not enriched upon pulldown in *Kdm1a*$^{-/-}$ MEFs because LSD1 is absent (Figure 4.13a). However, in the case of *Kdm1a*$^{E440G/E440G}$ mutants, a non-significant decrease in binding was observed at all sites (p= 0.985, 0.337, 0.358 and 0.130, Figure 4.13e). Binding was varied across samples, especially at the first site (Figures 4.13b, 4.13c, 4.13d). This may be a consequence of the rhythm of LSD1 binding over circadian times so more samples need to be analysed in future.

As binding is not significantly decreased at any sites (Figure 4.13e), the trend towards decreased ability of the *Kdm1a*$^{E440G/E440G}$ mutant to demethylate these sites (Figure 4.12) may be due to catalytic dysfunction rather than decreased binding. It appears that the *Kdm1a*^{E440G} mutation does not impair LSD1 binding at circadian loci, but could impact LSD1 function although more samples would need to be tested in future experiments to verify whether this trend were an effect. This might go some way towards explaining the circadian effects of *Kdm1a*^{E440G} *in vitro*.

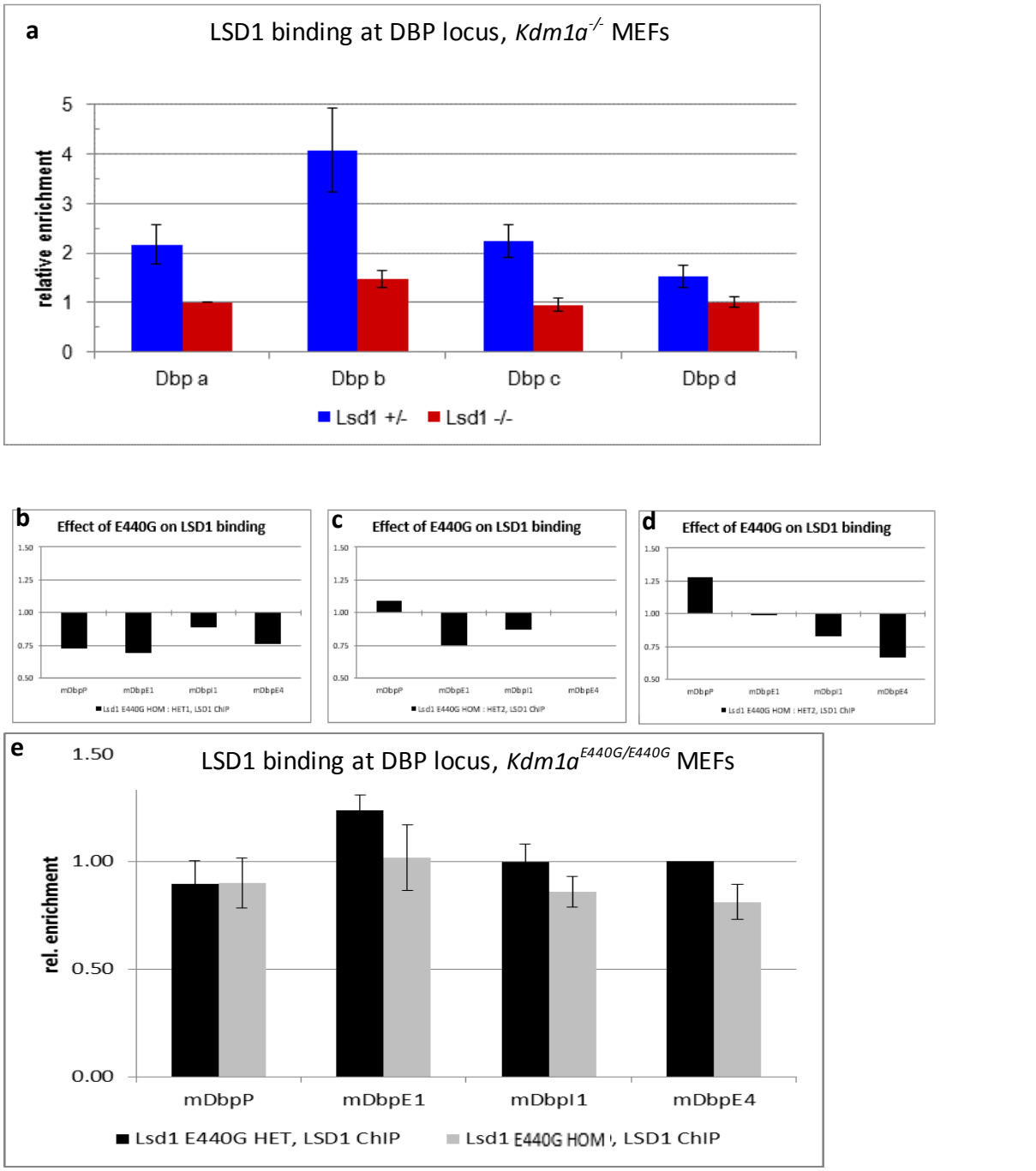

Figure 4.13: Chromatin immunoprecipitation: enrichment of LSD1 binding at the Dbp locus

a) *Kdm1a*$^{-/-}$ MEFs show decreased binding at the *Dbp* locus

b, c, d) Individual data from *Kdm1a*$^{E440G/E440G}$ MEFs show effects on LSD1 enrichment at the *Dbp* locus, mainly a trend towards decreased binding

e) Overall *Kdm1a*$^{E440G/E440G}$ MEFs show a non-significant decrease in binding at the *Dbp* locus (heterozygous MEFs 0.90 ±0.09, 1.24 ±0.06, 1.00 ±0.07, 1.00 ±0.00 at each region and homozygous MEFs 0.90 ±0.10, 1.02 ±0.13, 0.86 ±0.06 and 0.81 ±0.07 at each region. p= 0.985, 0.337, 0.358 and 0.130 respectively)

n=3 heterozygote and n=3 homozygote MEF samples. Data was analysed by student T-test

4.4: Discussion

LSD1 and LSD2 interact with the core clock in multiple ways. As mutations of the two genes cause different circadian consequences in overexpressing cells and each gene binds to different clock components, it is likely the two genes play separate roles in the clock and that the different mutations affect clock interactions differentially. Although protein binding and methylation of circadian loci are affected by mutation of LSD1 (Figures 4.5, 4.6, 4.7, 4.12 and 4.13), the interaction of LSD1 with clock components could be direct or indirect in nature. Interaction could be due to either clock component binding to and regulating LSD1 or LSD1 binding to and regulating of clock components. Therefore the nature of the interactions will require further analysis to clarify this.

4.4.1: Bioluminescent Recordings and Real Time data

Overexpression of mutant LSD1 caused a shortening of circadian period in comparison to LSD1 wild type in HEK293T cells (Figure 4.1). The shortened period observed in the mutant expressing cells could be due to numerous core clock alterations either independent of or involving the LSD1-CoREST interaction. As the two mutations were shown in *in silico* analyses to impact minimally on protein structure (Section 3.3), and as both lie in the cofactor binding tower domain of LSD1, it was hypothesised that effects observed resulting from these mutations may be due to cofactor binding discrepancies.

LSD1 is known to bind and demethylate mono- and di-methylated residues at histone sites H3K4 and H3K9 (Nicholson & Chen 2009). LSD1 is also confirmed to interact with multiple large histone modifying complexes such as with REST and CoREST (Shi et al. 2005), with Mi-2 and NuRD (Wang et al. 2009) and with SIRT1 and HDACs (Mulligan et al. 2011), as well as extensive binding of many other partners in a cell specific manner (Yokoyama et al. 2014). In order to ascertain by which route the LSD mutations are affecting the clock in the overexpression system, two lines of investigation were undertaken. Firstly, interaction and co-localisation studies were performed in order to investigate any direct binding which could contribute to direct demethylation or demethylation-

independent interactions. Secondly in order to clarify the demethylase activity of the *Kdm1a*$^{E440G/E440G}$ mutant, ChIP experiments were performed examining the *Dbp* site using both H3K4Me2-specific antibodies to examine demethylation and LSD1-specific antibodies to examine LSD1 binding.

4.4.2: Co-Localisation and Co-Immunoprecipitation

LSD1 localisation is primarily nuclear (staining is brightest in the nucleus); this is its site of enzymatic activity demethylating histones and modifying chromatin structure (Shi et al. 2004). LSD1 localisation has been linked to carcinogenesis; in healthy mammary epithelial cells LSD1 is expressed around the periphery of the nucleus and upon chemical induction of carcinogenesis LSD1 is up-regulated in the nucleus (Bradley et al. 2007). In HEK293T cells transfected with LSD1 constructs, LSD1 was mostly detected in the nucleus (Figure 4.8).

Colocalisation of clock constructs was observed as CoREST and BMAL1 labelling overlapped with LSD1 in nuclei which supports incidence of direct interaction (Figures 4.9 and 4.10), whereas in the case of CLOCK, localisation appeared not to coincide with LSD1 in this overexpressing system (Figure 4.11). It has been shown that CLOCK does not translocate into the nucleus unless co-transfected with BMAL1, which might explain this pattern of staining (Kondratov et al. 2003). Co-immunoprecipitation data indicated an interaction of LSD1 with the same clock components as immunofluorescent slides as well as with CLOCK (Section 4.2). Taken together, these data suggest that there is an interaction of LSD1 with BMAL1, PER1, PER2, CRY1, CRY2, REV-ERBα and CLOCK, concurring with results observed in the Reinke lab (Personal Communication Dr H. Reinke, Uni Düsseldorf, Ge). In the case of CLOCK, manipulation of LSD1 structure in the Reinke lab abolished pull down in CoIP assays, suggesting a direct interaction involving the C-terminal (Figure 4.14).

The evidence of an interaction between LSD1 and REV-ERBα (or indeed CLOCK or BMAL1) could go some way to explain the results in Section 3.1 which show a loss of REV-ERBα oscillation in LSD1 knockout MEFs. LSD1 could play a role in expression, transport, stabilisation, methylation states or

any number of other roles affecting REV-ERBα protein oscillation as measured in the knockout tissue, but further work will be necessary to truly test this hypothesis.

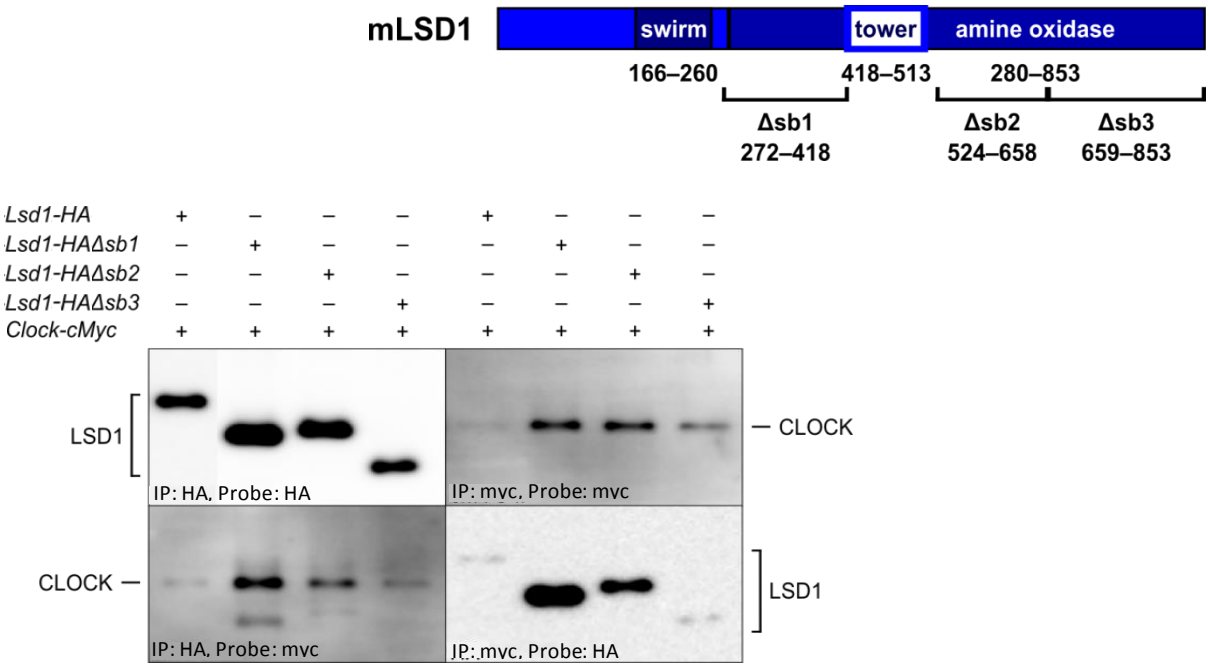

Figure 4.14: Co-immunoprecipitation of CLOCK using LSD1 mutant constructs

Ablation of the C-terminal residues 659 to 853 reduces its ability to bind to CLOCK and so reduces the precipitation of CLOCK upon LSD1 pulldown, and of LSD1 upon CLOCK pulldown. Ablation of residues 271-418 and 524-658 do not interfere with CLOCK pulldowns. (Personal Communication Dr H. Reinke, Uni Düsseldorf, Ge)

Some experimental limitations must be considered in interpretation of the data presented here. In order to ascertain the localisation of LSD1 and clock components transfected cells were double labelled with fluorescent antibodies against the epitope tags associated with the constructs of interest. This labelling can be of limited quantitative use in analyses due to the variability between the antibodies utilised, artefacts due to the effect of overexpressing constructs in HEK293T cells on expression of other interacting partners, co-expressed constructs and tag-tag interactions as well as limitations in ability to process fluorescent output (bleeding of fluorescence across the wavelengths produced by the two co-expressed constructs). The variation in brightness of staining is a qualitative indicator of the variation in expression levels of LSD1, indicative of the unsynchronised nature of the cells in the staining protocol. The caveats to staining protocols are further discussed in section 8.4.2.

CoIP experiments are used to assess whether two proteins interact. Measurements are qualitative as so many factors might influence the strength of the bands observed and precise quantification of interaction between any two proteins requires further investigation (Lee et al. 2013). Recently CoIP interactions have been monitored using single-molecule real time recordings (measuring fluorescent fusion reporters at high resolution) which could give more precise data on LSD interactions with clock components if utilised in future (Lee et al. 2013). In the current investigation, tagged vectors were used and overexpressed in HEK293 cells and some care must therefore be taken in interpreting the data. Firstly, empty vectors expressing the tag without LSD1 or LSD2 were used to control for any potential interactions between the tag and the clock protein pulled down. Secondly, the HEK293T cells used for transfection also express clock components endogenously as well as other transcripts which could be responsible for LSD or clock regulation which may affect CoIP interactions and so confound results. Any interaction detected may or may not be effected through an intermediary or linker protein, and this possibility cannot be completely excluded while intermediate proteins are expressed endogenously in the cell system. All relevant interacting partners which might affect the interaction in question can only be eliminated in a cell-free purified protein interaction study. Thirdly, the interactions of overexpressed constructs are required to be sufficiently strong to

withstand the CoIP experimental procedure, and the tag must be readily detectable in complex in order to ascertain accurately the existence and semi-quantitative strength of the interaction. Antibodies to the native proteins could be used to mitigate against the inability to detect an epitope tag in complex if there was difficulty in detection of the CoIP. And finally it must be considered that when transcripts are overexpressed in a system, their localisation and levels may not be true to the endogenous state, the overexpression itself may affect these parameters, and this will affect interactions if considering the remaining endogenously expressed binding partners which might be involved in a complex. In order to overcome this complication, antibodies against native clock components need to be utilised in both the pulldown and the probe of protein samples.

Further Experiments

Some of these experimental limitations could be overcome with further molecular work, and the nature of the interactions discovered here require further biochemical analysis for full elucidation of their functional implications. Whether LSD is regulating its binding partners by direct methylation or by a demethylase independent interaction, or whether clock proteins are regulating LSD demethylase localisation is yet to be examined. If the clock proteins bind LSDs and act to regulate them in some way (by modulating shuttling or localisation for example), the difference between clock protein interactions observed for each mutant construct could be due to differential regulation of the two genes by clock components which could affect H3K4 methylation patterns. It would be hypothesised that LSD2 is regulated by CRYs and BMAL1 only, whereas LSD1 is under regulation by several components of the clock. Alternatively, and more likely, the binding of clock components could indicate a role of the LSD genes in demethylating and affecting the clock component function in some way. In which case the pull downs completed here indicate that LSD1 binds to and putatively regulates more components of the clock than LSD2.

Quantification of these interactions by using purified proteins in cell-free assays would more precisely describe the interactions in question. LSD1 has been shown to act in large histone

modifying complexes with multiple regulatory binding partners (Nakamura et al. 2002). It could be discerned whether the interactions of LSD1 with clock proteins are direct or indirect by examining what is pulled down in complex with LSDs by mass spectrometry. CoIP could be used to confirm whether the LSD interaction with clock proteins was dependent on other members of the complex by knockdown of those other binding partners using siRNA. If interactions were still evident upon knockdown of other members of the LSD1 complex (for example CoREST), it would support the hypothesis that the LSD interaction with the clock component was direct in nature. FRET microscopic analysis of cells could also be employed to identify whether the proteins in question are within 50Å of each other and are therefore in proximity for direct interaction.

CoREST is the major cofactor of LSD1 (Lee et al. 2006; Karytinos et al. 2009). Previous studies in HeLa cells found that CoREST binding increases the stability of LSD1, increasing protein product levels in cells fivefold when compared to RNAi knockdown cells (Shi et al. 2005). Upon cotransfection with CoREST, the interaction of LSD1 with REV-ERBα is increased (Section 4.2.2.3). Although the interaction with REV-ERBα does not increase fivefold, the mechanism by which CoREST is increasing the strength of the interaction may be down to its effect on LSD1 stability. Alternatively, CoREST is increasing the efficiency of binding of LSD1 to REV-ERBα. Whether the interaction at hand is direct or indirect in nature is unclear, however as LSD1 and REV-ERBα are both being overexpressed it does support the hypothesis that the interaction is direct in nature, as indirect interaction would require sufficient expression of the third interacting partner.

Although the interactions of LSDs with clock proteins can be very precisely characterised, the function underlying the interactions needs to be clarified. Whether LSDs are acting as regulators or whether circadian components regulate LSDs could be tested using methylation assays. It would be expected that if the LSDs bind to and therefore act as regulators of the clock components, disruption of LSD binding to the clock proteins might alter LSD-mediated methylation. Direct methylation of the clock proteins would indicate a direct regulation of clock components, whereas methylation of

histones associated with clock gene promoters would indicate LSD binding to clock proteins is associated with epigenetic modulation of circadian mechanisms. Assaying the methylation of proteins purified from CoIP cell lysates could be used to investigate this hypothesis, or alternatively performing mass spectrometry on the proteins purified from CoIP cells to detect any difference in methylation on the clock proteins. Conversely, if the clock is regulating LSDs in some way then the methylation of H3K4 substrates could be examined in a clock component mutant model to ascertain whether the clock component is regulating LSD1 or LSD2. Therefore methylation assays would be valuable as a tool to measure LSD activity levels at H3K4 in teasing this apart in future.

4.4.3: Chromatin-Immunoprecipitation

ChIP of *Kdm1a*$^{E440G/E440G}$ MEFs showed a non-significant decrease in enrichment of LSD1 binding at *Dbp* loci and a non-significant increase in enrichment of H3K4Me2 (Figures 4.12 and 4.13), both to a lesser extent than the effects observed in ChIP of knockout cells. These two observations do not rule out the hypothesis that in *Kdm1a*$^{E440G/E440G}$ cells, LSD1 binding is reduced which in turn causes a reduction in demethylation and so dimethylated H3K4 is increased at these loci, but more samples must be tested to verify this trend.

The deficits of mutant LSDs in binding and demethylation of H3K4 could be due to a decrease in CoREST binding (Figure 4.5) or cofactor independent in nature, and CoREST inhibition or knockdown is required to test this hypothesis. Loosening of nucleosomal chromatin might change the efficiency of the crosslinking step and alter the pull down in this experiment. CoREST is essential for and LSD1-mediated nucleosomal demethylation (Yang et al. 2006), therefore the structure of the nucleosomes could be affected in mutants which might alter the pull down.

The changes in methylation mark enrichment observed in knockout cells were more pronounced than the changes seen in homozygote mutant cells, but as enrichment was not statistically significant the theory that the *Kdm1a*^{E440G} mutation is deleterious to LSD1 demethylation of H3K4 at circadian loci has yet to be verified. The trend towards a decrease in demethylation could be

partially attributed to the non-significant decrease in LSD1 binding (Figure 4.13). In the knockout cells from the Reinke lab, LSD1 fails to bind any loci as it is not expressed, and demethylation is at its lowest (Figures 4.12a and 4.13a) suggesting there is not much redundancy in the system and that LSD1 is responsible for H3K4 demethylation at these sites.

For full characterisation of the activity of LSD1 at these loci, monomethyl marks also need to be examined. Due to its partial loss of function as seen in the H3K4Me2 ChIP (Figure 4.13), monomethyl marks would also be expected to be increased in mutant cells, and increased more in knockout cells. To elucidate the functional consequences of loss of this demethylation, subsequent mRNA expression and protein expression must be characterised, so RNA levels of *Dbp* are examined later in this investigation.

The ChIP results presented here cannot explain or clarify any demethylase-dependent or demethylase-independent direct binding effects of LSD1 mutations on the clock machinery, but does suggest that the circadian effects of the *Kdm1a*^{E440G} mutation could be mediated by a decreased efficacy in LSD1 binding and demethylation of chromatin at circadian loci (Figures 4.12 and 4.13). Methylation assays and ChIP across many other circadian regions (genes and promoter or enhancer sites) would be valuable in full characterisation of how the LSD1 mutation is affecting circadian gene expression as only *Dbp* was examined here. The *Dbp* loci were chosen for this investigation due to the reliable nature of its oscillatory expression. It would be expected that if LSD1 were affecting clock gene expression by demethylation of histone targets that ChIP of knockout or mutant MEFs at other circadian loci would reveal increased monomethylation and demethylation compared to wild type. Native ChIP in various tissues could also be used to show tissue-specific changes in methylation and chromatin binding.

4.4.4 Summary

Although the nature of the interactions of the two LSD genes with core clock components and their activity at circadian loci require further clarification, the molecular work thus far suggests that both

genes play a role in the circadian clockwork. Therefore it is pertinent to examine circadian characteristics *in vivo* using ENU mutant mouse lines. The choice of mutant LSD1 and LSD2 genes chosen for re-derivation was based on the *in silico* analysis discussed previously (Chapter 3), and the molecular work presented in this chapter. The *Kdm1a*^{E440G} and *Kdm1a*^{L491H} mutants alter circadian function *in vitro*; both caused a shortening of circadian period when overexpressed (Figure 4.1), both affected the ability of LSD1 to bind to CoREST as observed in Co-IP experiments (Figure 4.5), and the mutations also affect the interaction of LSD1 with clock components (the KDM1A^{E440G} mutation more so than the KDM1A^{L491H} mutation) (Figures 4.6 and 4.7). The *KDM1A*^{E440G} mutation was then tested in ChIP experiments and results show a promising trend which could suggest that the mutation impacts on the ability of LSD1 to demethylate its H3K4 target at circadian promoters (Figure 4.12). This decrease in demethylation could be attributed to impaired LSD1 binding at these sites and both ChIP findings require analysis of more sample in future to verify the findings presented here. Given the circadian effects of the mutations observed *in vitro*, the corresponding mutant mouse lines were selected for re-derivation and *in vivo* circadian characterisation.

LSD2 mutants were chosen for re-derivation based on the *in silico* data presented in chapter 3 along with the finding that circadian period increased upon overexpression of *Kdm1b*^{P281L} in fibroblast cells. Of the 5 mutations, two were predicted to be deleterious to protein folding; *Kdm1b*^{P281L} and *Kdm1b*^{T357M}. The *Kdm1b*^{P281L} construct when transfected into cells caused a lengthening of circadian period (Figure 4.1), and *Kdm1b*^{T357M} was one of just two of the mutations identified in the archive screen to lie in a region present in the primary human transcript. SIFT analysis also confirmed that the *Kdm1b*^{T357M} mutation would be predicted to disrupt protein structure (Table 3.6). Therefore these two mutants were re-derived by IVF for *in vivo* circadian analysis.

Chapter 5

LSD1 AND LSD2 MUTANT CIRCADIAN PHENOTYPES

CHAPTER 5: LSD1 and LSD2 Mutant Circadian Phenotypes

5.1: Introduction

In order to characterise the roles of *Kdm1a* and *Kdm1b* genes *in vivo*, it was necessary for animals to be reared to adulthood, so mutant lines were sought to bypass the embryonic stage difficulties (including lethality in the case of $Kdm1a^{-/-}$) encountered in the case of knockout animals (Macfarlan et al. 2011). The adult animals (of 40 days of age and above) were housed individually and underwent circadian phenotyping analysis by wheel running. Wheel running behaviour has long been the gold standard for circadian phenotypic output in rodents (Pittendrigh & Daan 1976). Ability to entrain, free running rhythm in DD and LL and phase resetting in response to light pulses can be assessed *in vivo* with wheel running by manipulating light dark schedules (Pittendrigh & Daan 1976).

$Kdm1a^{E440G}$, $Kdm1a^{L491H}$, $Kdm1b^{P281L}$ and $Kdm1b^{T357M}$ mouse lines (chosen as per Chapter 3) were re-derived by IVF from founder sperm samples. BALB/c x C3H background founder mutant animals were crossed to C57BL/6 due to the strong circadian wheel-running behaviour characteristic of the strain (Jackson website). IVF was performed using C57BL/6 female eggs and animals were subsequently backcrossed. At backcross 2, animals were intercrossed to produce homozygous individuals and preliminarily screened. Early backcross animals showed circadian phenotypes as detailed in Figure 5.1 and Figure 5.5. Animals at early stages of breeding still have a high proportion of BALB/c x C3H genetic background material, and the mutation causes phenotypic changes which are readily observed on this background when mutant animals were compared with wild type littermate controls. At backcross 5 when the animals are considered to have reached a high level of congenicity, the two lines with the most striking circadian phenotypes observed at backcross 2 ($Kdm1a^{E440G}$ and $Kdm1b^{T357M}$) were intercrossed once more and fully phenotyped for circadian (Chapter 5) and other behaviours (Chapter 6). The later backcross animals displayed more subtle circadian phenotypes, indicating that the phenotype observed in the earlier animals was altered by the C57BL/6 background.

Kdm1a$^{E440G/E440G}$ backcross 2 animals showed a trend towards lengthened period in constant darkness (Figure 5.1), anticipation of lights on and a lack of masking, whereas *Kdm1a*$^{L491H/L491H}$ animals display period lengthening in constant light, and masking deficits (Figure 5.1). In the screens of late backcross animals, masking effects were still prominent in *Kdm1a*$^{E440G/E440G}$ animals, but the difference initially observed in period was not evident on a C57BL/6 background (Figures 5.2, 5.3). Backcross 5 *Kdm1a*$^{L491H/L491H}$ animals behaved comparably to littermate controls in LD and DD, demonstrating a shorter tau and shorter alpha in LL (Figure 5.4). In the case of *Kdm1b*$^{T357M/T357M}$, splitting in constant light conditions observed in early cohorts (Figure 5.5) was no longer apparent upon screening of later backcrosses (Figure 5.6).

5.2: Circadian Wheel Running Screen

Cohorts of LSD mutant animals were screened for wheel running behaviours including LD activity patterns, response to light-induced suppression of activity in LD (masking), free running period (tau) in constant dark (DD) and constant light (LL), and length of activity (alpha) in DD and LL (Figure 1.4).

Firstly animals were screened at backcross 2 to C57BL/6 in order to explore circadian perturbations. Then at backcross 5 to C57BL/6, animals were again screened more extensively in order to examine the effect of the LSD mutations on a strain background closer to C57BL/6 where mutations may have different phenotypic outcomes due to strain differences between this and the Balb/c X C3H founder. Strain differences could be due to different penetrance on each background or due to different enhancer or suppressor mechanisms in the strains.

5.2.1.1: Circadian Parameters at Backcross 2 for *Kdm1a*$^{E440G/E440G}$ and *Kdm1a*$^{L491H/L491H}$ animals

The LSD1 mutant circadian phenotypes observed at backcross 2 to C57BL/6 are detailed in Figure 5.1. *Kdm1a*$^{E440G/E440G}$ mice displayed a trend towards a 20 minute lengthening of period in constant darkness, anticipation of lights on in LD and running was not supressed by the light pulse. To test

light induced masking in the animals, they are exposed to a 3 hour light pulse as described previously (Figure 1.4b).

Backcross 2 *Kdm1a*$^{L491H/L491H}$ animals displayed less circadian phenotypes than the *Kdm1a*$^{E440G/E440G}$ animals. They displayed a significant 27 minute longer free running period than control animals in constant light (p=0.0113) (Figure 5.1). After backcrossing, mutants ran with a trend towards a shorter period than wild type (Figure 5.4).

5.2.1.2: Circadian Parameters at Backcross 5 for *Kdm1a*$^{E440G/E440G}$ and *Kdm1a*$^{L491H/L491H}$ animals

Intercross animals from backcross 5 to C57BL/6 display no significant difference in free running period or length of active phase between *Kdm1a*$^{E440G/E440G}$ and control animals (Figure 5.2). Overall activity levels and pattern on LD days was similar between *Kdm1a*$^{E440G/E440G}$ mutants and their littermate controls, onset coincided with lights off in both cases so anticipation is not observed in the animals after backcrossing (Figure 5.3). The percentage of total running occurring in the light phase on LD days was significantly higher for *Kdm1a*$^{E440G/E440G}$ animals than controls (8.1% compared to 4.4% p=0.046092), and the percentage of wheel running activity which occurred during the masking light pulse when compared to normal days showed a trend to be higher than that of wild type animals (p=0.087997) Figure 5.3. This weak response to the light pulse (which supresses the activity of wild type animals) could be due to poor light detection in mutant animals, poor ipRGC function or altered SCN response to the light pulse. Anticipation of lights off was observed for *Kdm1a*$^{E440G/E440G}$ (Figure 5.3) but littermate controls displayed some tendency towards anticipating lights off as well.

Kdm1a$^{L491H/L491H}$ animals displayed a significantly shorter circadian period and length of active phase under LL conditions (p=0.0399 and p= 0.044481 respectively) (Figure 5.4). This shorter period is the opposite to the significant effect seen in earlier backcross *Kdm1a*$^{L491H/L491H}$ animals (Figure 5.1).

The apparent changes from the circadian phenotypes initially observed at backcross 2 in both mutant lines may be due to background strain effects as discussed in Section 8.5.1 (Jackson website).

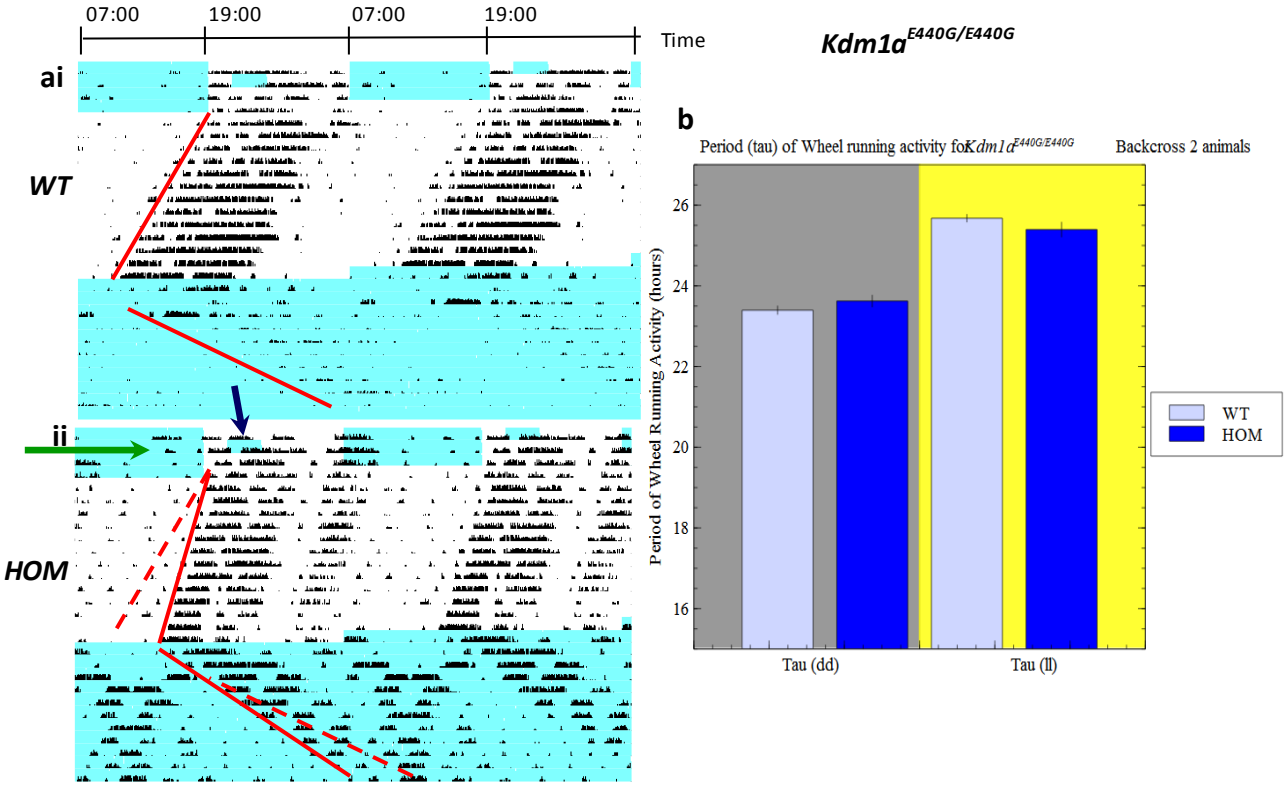
07:00
19:00
07:00
19:00
Time
ai
WT
ii
HOM
Kdm1a E440G/E440G
b
Period (tau) of Wheel running activity for Kdm1a E440G/E440G
Backcross 2 animals
Period of Wheel Running Activity (hours)
26
24
22
20
18
16
WT
HOM
Tau (dd)
Tau (ll)

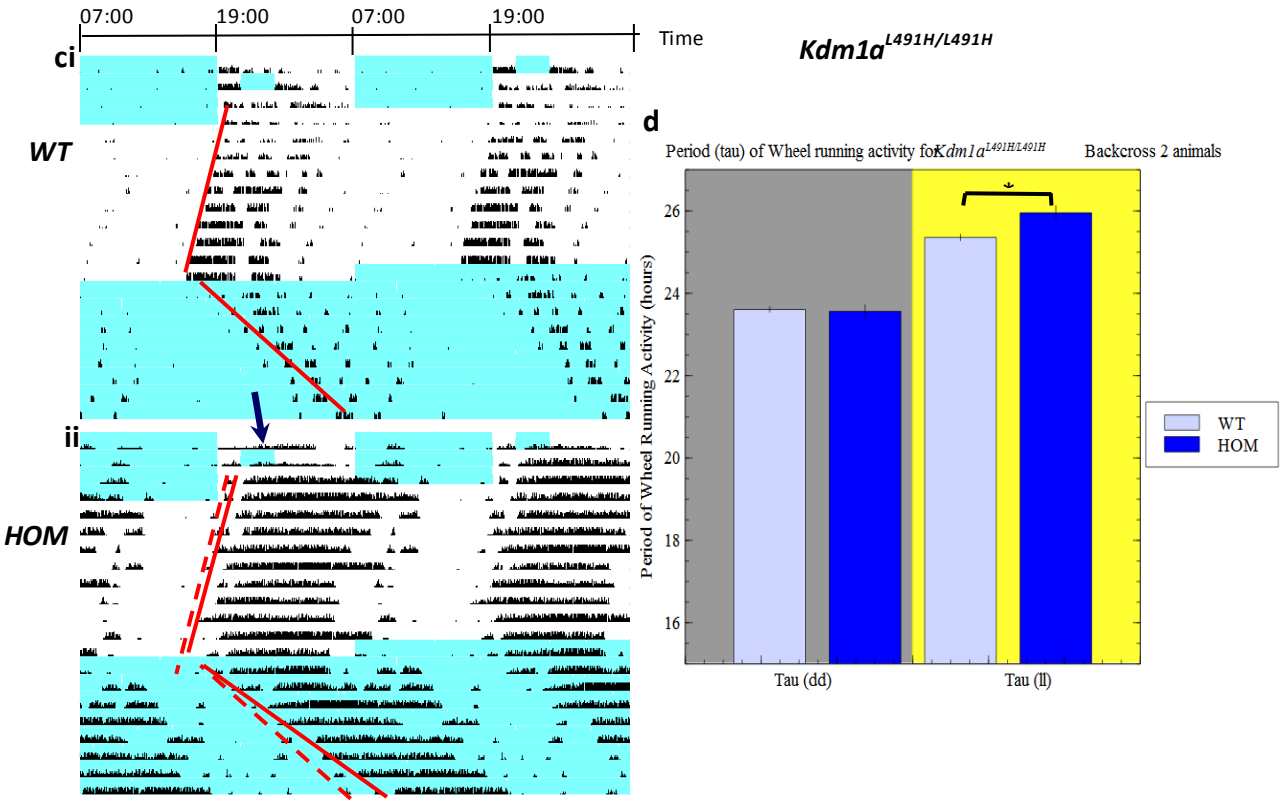
07:00
19:00
07:00
19:00
Time
ci
WT
ii
HOM
Kdm1a L491H/L491H
d
Period (tau) of Wheel running activity for Kdm1a L491H/L491H
Backcross 2 animals
Period of Wheel Running Activity (hours)
26
24
22
20
18
16
WT
HOM
Tau (dd)
Tau (ll)

Figure 5.1: Phenotypes of *Kdm1a*$^{E440G/E440G}$ and *Kdm1a*$^{L491H/L491H}$ mutants at backcross 2

a) *Kdm1a*$^{E440G/E440G}$ actogram showing anticipation of lights off (green arrow) and impaired masking (blue arrow) in response to the light pulse i) *Kdm1a*$^{+/+}$, ii) *Kdm1a*$^{E440G/E440G}$

b) *Kdm1a*$^{E440G/E440G}$ animals displayed a trend towards period lengthening (20 minutes) in DD (Wild type 23.40 ±0.10, homozygote 23.62 ±0.14, p=0.6249), and a 20 minute shortening of period in LL (Wild type 25.68 ±0.09, homozygote 25.40 ±0.18, p=0.2422).

c) *Kdm1a*$^{L491H/L491H}$ actogram showing longer period in LL and impaired masking (blue arrow) in response to the light pulse i) *Kdm1a*$^{+/+}$, ii) *Kdm1a*$^{L491H/L491H}$

d) *Kdm1a*$^{L491H/L491H}$ animals showed non-significant trends towards a 6 minute longer free-running period in DD (Wild type 23.61 ±0.07, homozygote 23.56 ±0.16, p=0.7049), and a significant 27 minute lengthening of period in LL (Wild type 25.34 ±0.08, homozygote 25.95 ±0.18, p=0.0113).

Red lines denote onset of activity used to determine circadian period. Dashe d lines denoting wild type onsets are placed on mutant traces for ease of comparison to mutant onset.

N=6 wild type and n=15 homozygote *Kdm1a*^{E440G} backcross 2 intercross animal, n=5 wild type and n=6 homozygote *Kdm1a*^{L491H} backcross 2 intercross animals. Period length was analysed by student T test. (*p<0.05, **p≤0.005, ***p≤0.001)

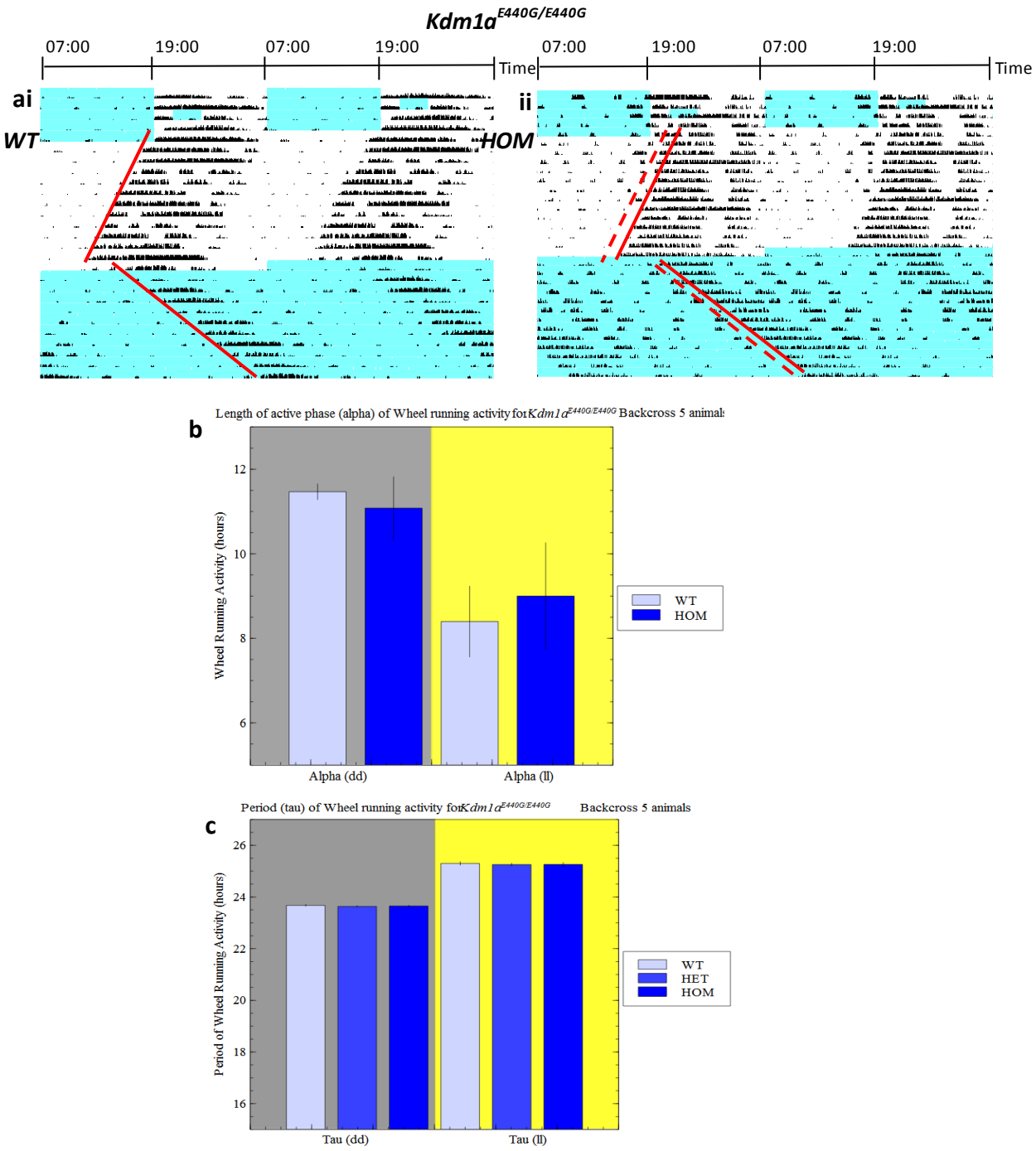

Figure 5.2: Phenotypes of *Kdm1a*$^{E440G/E440G}$ animals at backcross 5

a) Actogram showing representative activity of *Kdm1a*$^{E440G/E440G}$ animals. In both DD and LL, mutant animals displayed no significant difference to wild type animals in circadian period or in length of activity (alpha) i) *Kdm1a*$^{+/+}$, ii) *Kdm1a*$^{E440G/E440G}$. Red lines denote onset of activity used to determine circadian period. Dashed lines denoting wild type onsets are placed on mutant trace for ease of comparison to mutant onset.

b) Graph to show Alpha dd (Wild type 11.47 ±0.18, homozygote 11.08 ±0.74, p=0.2276) and Alpha ll (Wild type 8.39 ±0.84, homozygote 9.00 ±1.26, p=0.3392)

c) Graph to show Tau dd (Wild type 23.68 ±0.03, heterozygote 23.63 ±0.03, homozygote 23.64 ±0.03, p=0.5569) and Tau ll (Wild type 25.30 ±0.06, heterozygote 25.25 ±0.05, homozygote 25.26 ±0.08, p=0.7610)

N=20 wild type and n=20 homozygote *Kdm1a*^{E440G} backcross 5 intercross animals. Period length and alpha were analysed by student T test.

a

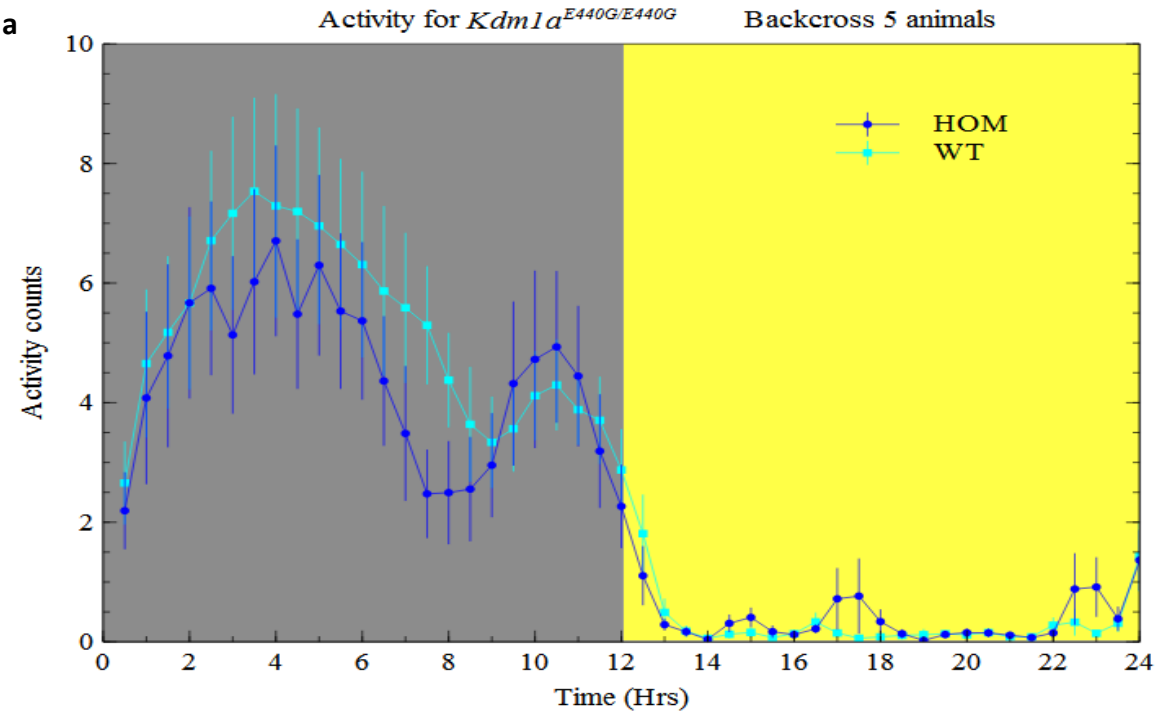

b

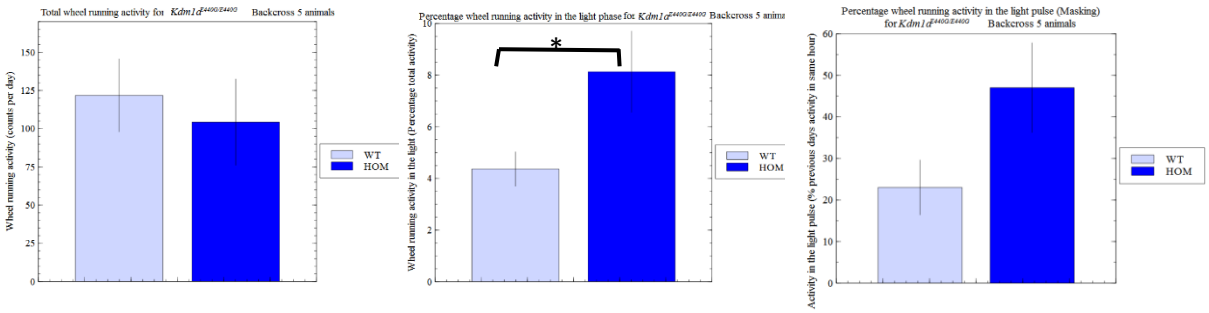

Figure 5.3: Wheel running activity of *Kdm1a*$^{E440G/E440G}$ backcross 5 animals in LD

a) *Kdm1a*$^{E440G/E440G}$ animals show a similar distribution of activity in wheel running screens over the LD cycle, but run more in the lights on phase, and with a more pronounced biphasic distribution of running (Analysed with RM ANOVA p= 0.507 F(2.172, 71.687)).

b) Total activity of mutant animals is similar to that of wild type animals (Wild type 121.78 ±23.79, homozygote 104.29 ±28.11, p=0.645175)

c) *Kdm1a*$^{E440G/E440G}$ animals run more in the light phase of the LD cycle than *Kdm1a*$^{+/+}$ animals (Wild type 4.37 ±0.66, homozygote 8.13 ±1.57, p=0.046092)

d) *Kdm1a*$^{E440G/E440G}$ animals show a trend towards higher activity than control animals during the light pulse compared to activity measured on non-light pulse days, therefore an impaired masking in response to the light pulse during LD (Wild type 23.02 ±6.57, homozygote 47.03 ±10.77, p=0.087997)

N=20 wild type and n=20 homozygote *Kdm1a*^{E440G} backcross 5 intercross animals. Activity parameter data was analysed by student T test. (*p<0.05, **p≤0.005, ***p≤0.001)

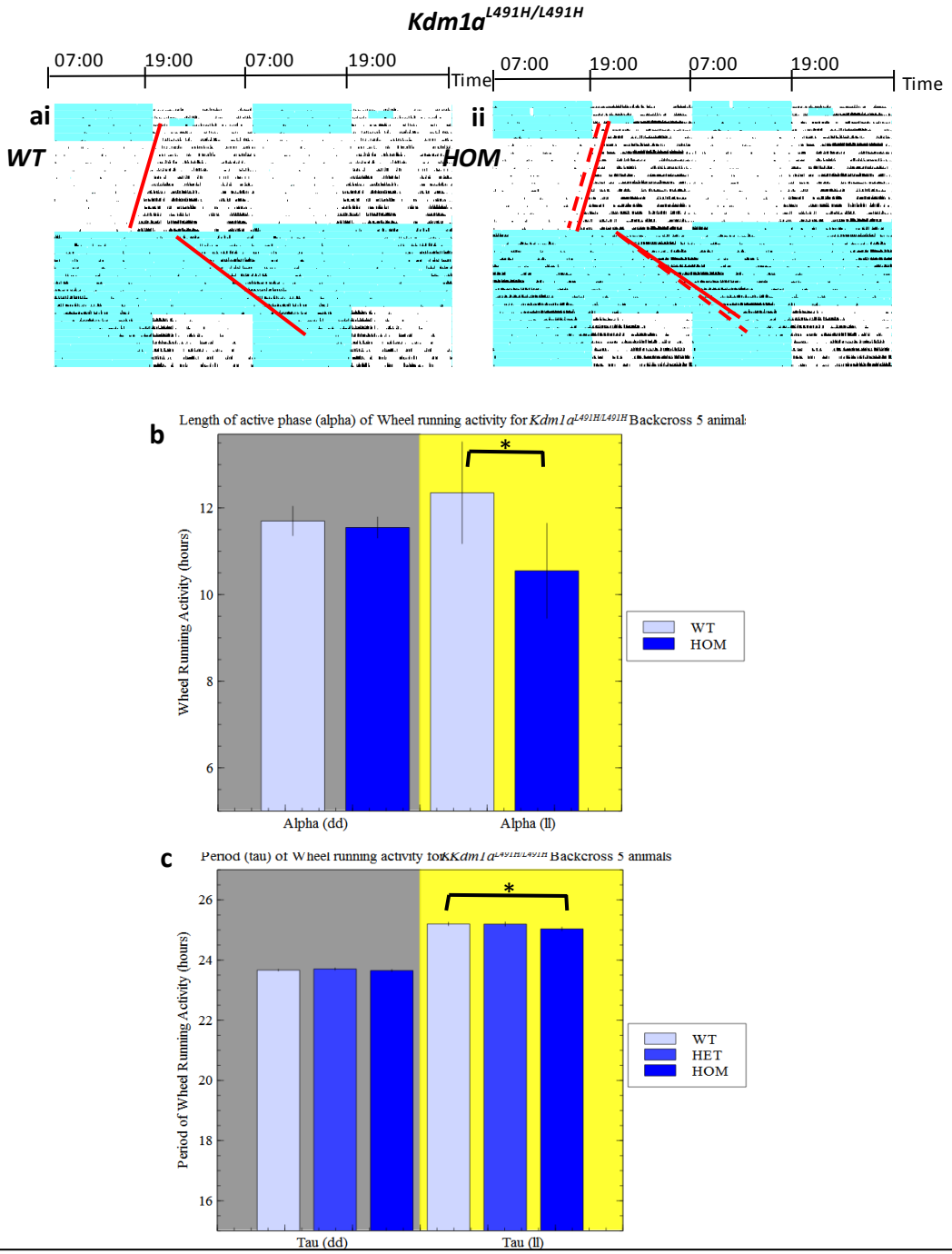

Figure 5.4: Phenotypes of *Kdm1a*$^{L491H/L491H}$ animals at backcross 5

a) Actogram showing representative activity of *Kdm1a*$^{L491H/L491H}$ animals. In DD, mutant animals displayed no significant difference to wild type animals in circadian period or in length of activity. In LL, period is 10 minutes shorter than wild type animals and alpha 1.8 hours shorter. i) *Kdm1a*$^{+/+}$, ii) *Kdm1a*$^{L491H/L491H.}$ Red lines denote onset of activity used to determine circadian period. Dashed lines denoting wild type onsets are placed on mutant trace for ease of comparison to mutant onset.

b) Graph to show Alpha dd (Wild type 11.70 ±0.34, homozygote 11.55 ±0.24, p=0.38334) and Alpha ll (Wild type 12.35 ±1.17, homozygote 10.55 ±1.09, p=0.044481)

c) Graph to show Tau dd (Wild type 23.67 ±0.03, heterozygote 23.71 ±0.03, homozygote 23.65 ±0.03, p=0.7825) and Tau ll (Wild type 25.20 ±0.05, heterozygote 25.20 ±0.07, homozygote 25.04 ±0.06, p=0.0399)

N=10 wild type and n=10 homozygote *Kdm1a*^{L491H} backcross 5 intercross animals. Period and alpha were analysed by student T test. (*p<0.05, **p≤0.005, ***p≤0.001)

5.2.2.1: Circadian Parameters at Backcross 2 for *Kdm1b*$^{T357M/T357M}$ and *Kdm1b*$^{P281L/P281L}$ animals

No differences from wild type animals were detected in tau DD or tau LL in either of the LSD2 mutants. Taus of *Kdm1b*$^{T357M/T357M}$ animals were 23.523 in DD and 25.354 in LL in comparison to *Kdm1b*$^{+/+}$ animals 23.581 and 25.261 respectively (Figure 5.5). Taus for *Kdm1b*$^{P281L/P281L}$ animals were 23.702 in DD and 25.134 in LL in comparison to littermate controls (23.593 and 24.896 respectively) (Figure 5.5).

Phenotypes which were observed in wheel running included an apparent lack of masking for both LSD2 mutant lines. In the case of *Kdm1b*$^{P281L/P281L}$ animals displayed running during the inactive phase. *Kdm1b*$^{T357M/T357M}$ animals displayed splitting in LL in 87.5% of animals compared to littermate controls where split rhythms could be detected in just 20% of animals. (Figure 5.5 p=0.229134)

5.2.2.2: Circadian Parameters at Backcross 5 for *Kdm1b*$^{T357M/T357M}$ animals

Kdm1b$^{T357M/T357M}$ activity levels were similar to control animals during the LD Section of the screen, and activity patterns were similar across the 24 hour day (Figure 5.6). *Kdm1b*$^{T357M/T357M}$ animals displayed normal masking and had free running periods and lengths of active phase similar to controls in both DD and LL (p=0.253229 and p=0.217888 respectively). The animals did not display splitting behaviour in LL conditions. The lack of circadian phenotype observed in these animals could be attributed to diluting out unrelated mutations by selective breeding, or more likely due to background effect similarly to the LSD1 mouse data.

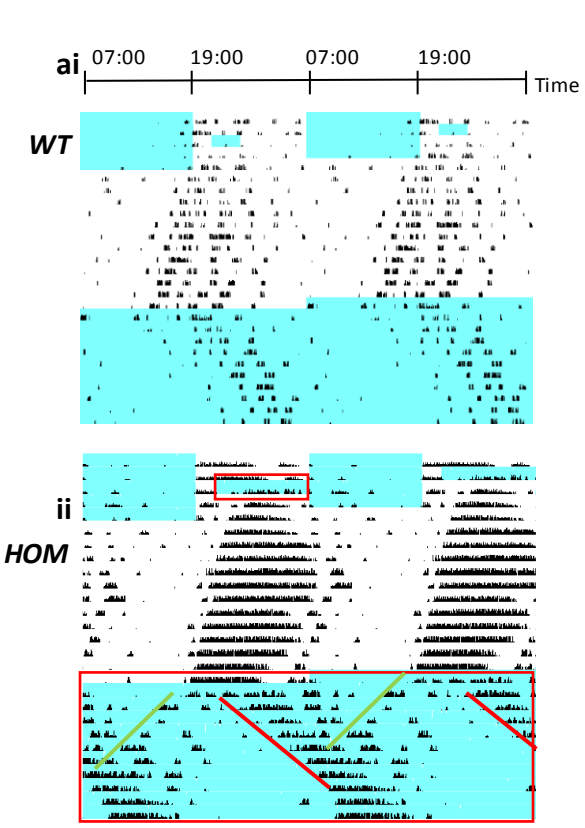
ai
07:00
19:00
07:00
19:00
Time
WT
ii
HOM

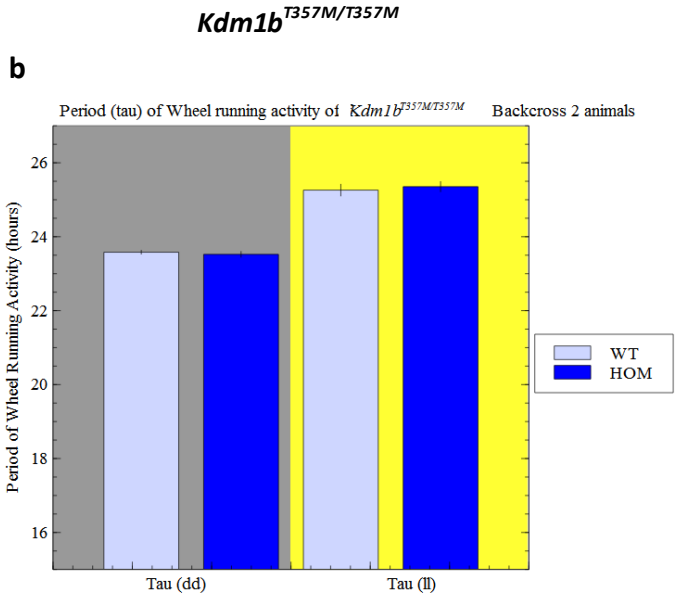
Kdm1b T357M/T357M
b
Period (tau) of Wheel running activity of Kdm1b T357M/T357M Backcross 2 animals
Period of Wheel Running Activity (hours)
26
24
22
20
18
16
Tau (dd)
Tau (ll)
WT
HOM

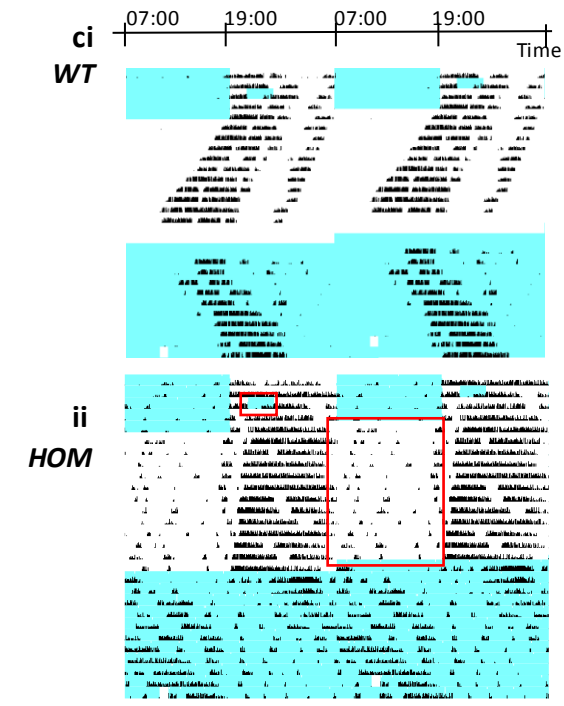
ci
07:00
19:00
07:00
19:00
Time
WT
ii
HOM

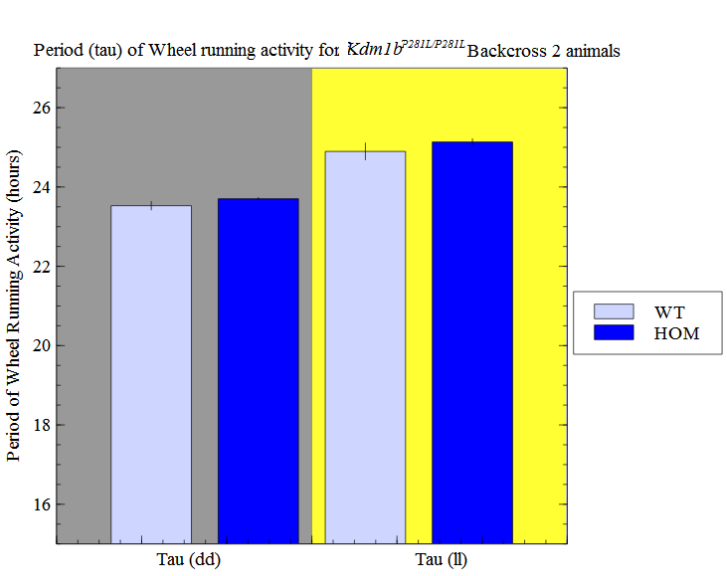
Kdm1b P281L/P281L
d
Period (tau) of Wheel running activity for Kdm1b P281L/P281L Backcross 2 animals
Period of Wheel Running Activity (hours)
26
24
22
20
18
16
Tau (dd)
Tau (ll)
WT
HOM

e

Kdm1b$^{T357M/T357M}$ mutation	Animals displaying splitting behaviour (%)
Wild type	20% ±13.33
Heterozygous	61.11% ±11.8
Homozygous	87.5% ±12.5

Figure 5.5: Phenotypes of *Kdm1b*$^{P281L/P281L}$ and *Kdm1b*$^{T357M/T357M}$ mutants at backcross 2

a) Actograms showing phenotypes of i) wild type, and II) *Kdm1b*$^{T357M/T357M}$ animals at backcross 2. 87.5% of mutant animals displayed splitting in LL (red and green lines highlight the two activity onsets) as well as reduced suppression of activity by the light pulse (red boxes). Light pulse in this trace is longer than 3 hours due to a fault in equipment (light timer), not representative of whole data. Data affected by such faults were excluded from analysis.

b) Graph of circadian period of *Kdm1b*$^{T357M/T357M}$ animals at backcross 2. Homozygous animals displayed no change in circadian period in comparison to wild type in DD (Wild type 23.58 ±0.05, homozygote 23.52 ±0.07, p=0.536273) or in LL (Wild type 25.26 ±0.15, homozygote 25.35 ±0.13, p=0.624072)

c) Actograms showing phenotypes of i) wild type, and ii) *Kdm1b*$^{P281L/P281L}$ animals at backcross 2. Intermittent running throughout subjective day was seen in mutant animals as well as a reduced light-induced suppression of activity (red boxes)

d) Graph of circadian period of *Kdm1b*$^{P281L/P281L}$ animals at backcross 2. Homozygous animals displayed a near significant 12 minute lengthening of free-running period in DD (Wild type 23.53 ±0.10, homozygote 23.70 ±0.03, p=0.061341) and no change in period compared to wild type in LL (Wild type 24.90 ±0.21, homozygote 25.13 ±0.08, p=0.229134)

e) *Kdm1b*$^{T357M/T357M}$ backcross 2 animals displayed splitting behaviour in LL (Wild type 20% ±13.33, heterozygote 61.11% ±11.8, homozygote 87.5% ±12.5, p=0.229134)

N=11 wild type n=18 heterozygote and n=9 homozygote *Kdm1b*^{T357M} backcross 2 intercross animals. N=5 wild type n=17 heterozygote and n=9 homozygote *Kdm1b*^{P281L} backcross 2 intercross animals. Period and splitting were analysed by student T test.

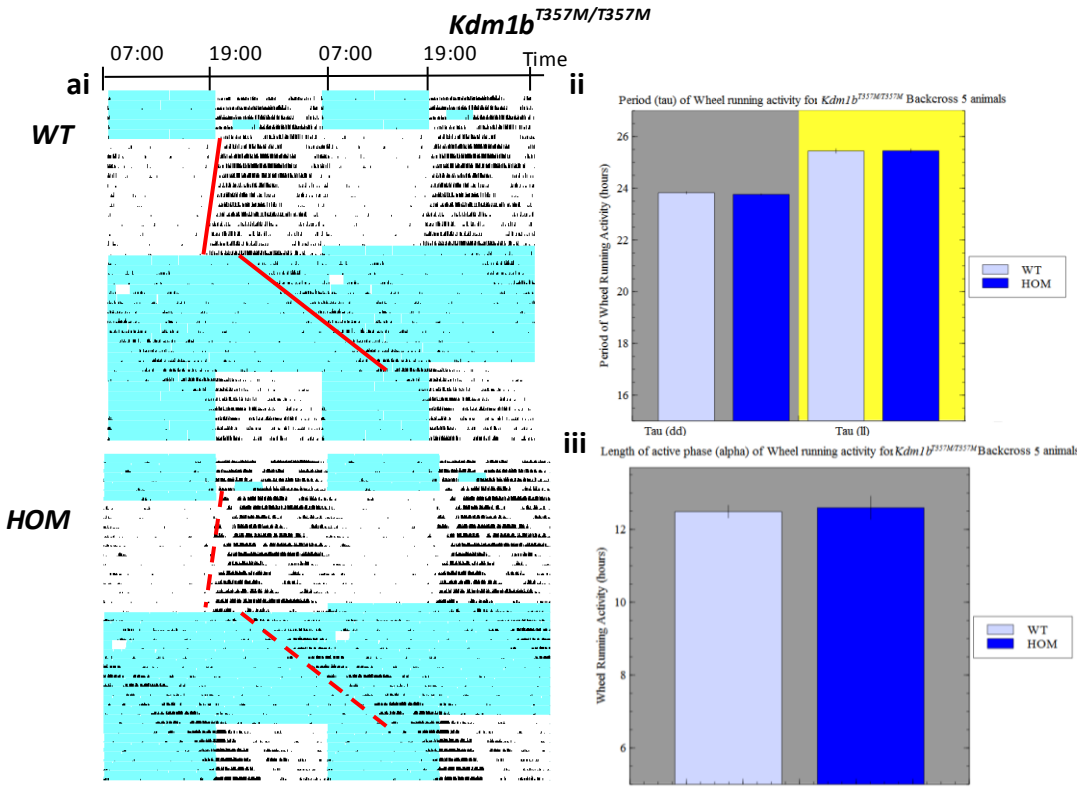
Kdm1b T357M/T357M
07:00
19:00
07:00
19:00
Time
ai
WT
HOM
ii
Period (tau) of Wheel running activity for Kdm1b T357M/T357M Backcross 5 animals
Period of Wheel Running Activity (hours)
26
24
22
20
18
16
WT
HOM
Tau (dd)
Tau (ll)
iii
Length of active phase (alpha) of Wheel running activity for Kdm1b T357M/T357M Backcross 5 animals
Wheel Running Activity (hours)
12
10
8
6
WT
HOM

b

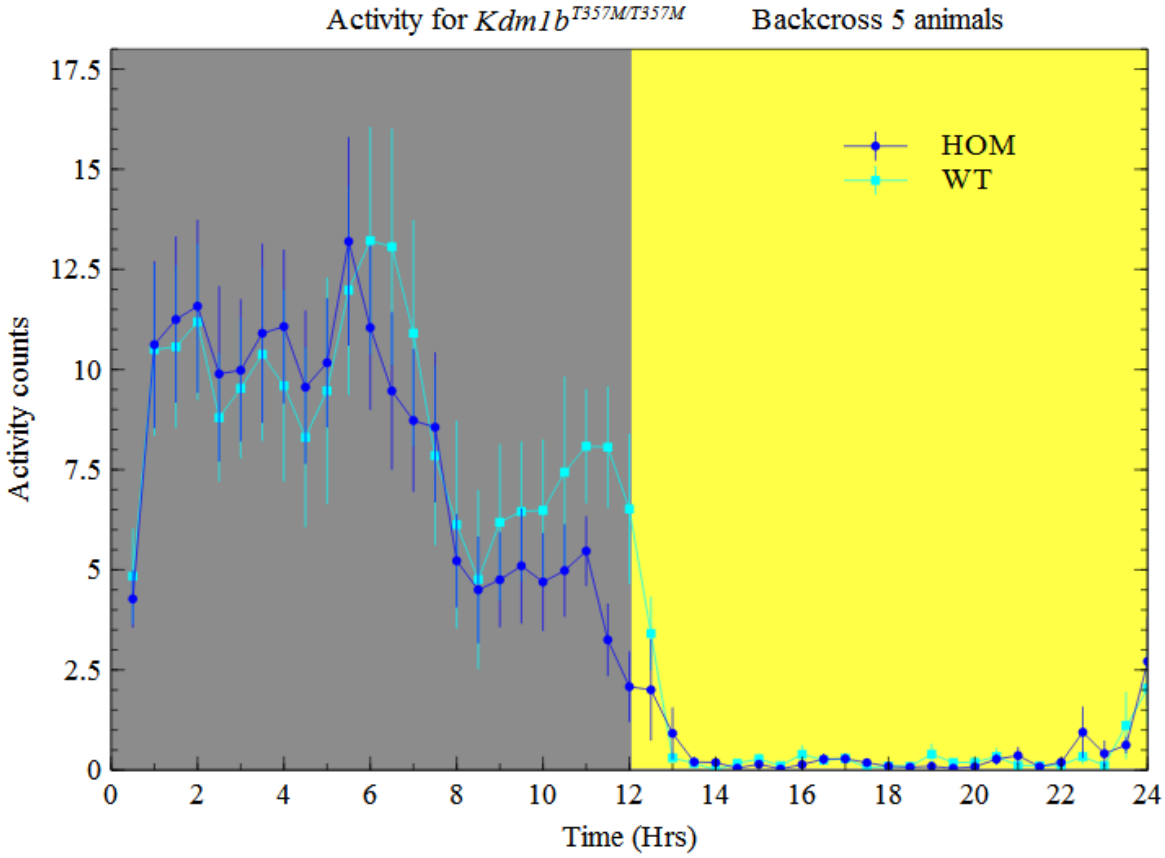
Activity for Kdm1b T357M/T357M
Backcross 5 animals
HOM
WT
Activity counts
17.5
15
12.5
10
7.5
5
2.5
0
0
2
4
6
8
10
12
14
16
18
20
22
24
Time (Hrs)

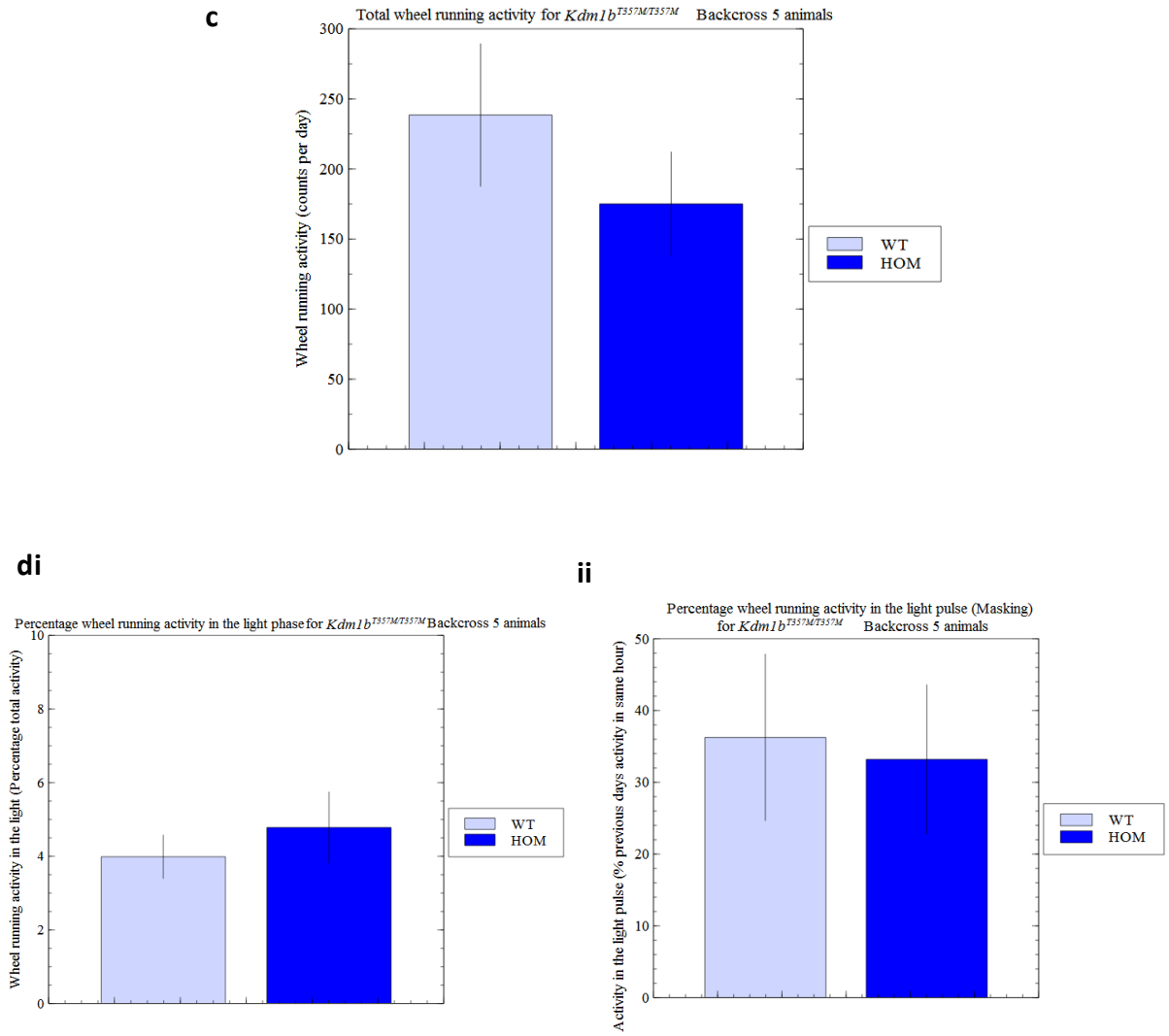

Figure 5.6: Wheel running activity of *Kdm1b*$^{T357M/T357M}$ backcross 5 animals in LD

a) i) Actogram and graphs to show homozygote *Kdm1b*$^{T357M/T357M}$ animals display no significant difference in ii) circadian period in DD or LL (Wild type 23.83 ±0.04, homozygote 23.76 ±0.02, p=0.253229 and Wild type 25.44 ±0.08, homozygote 25.45 ±0.07, p=0.217888 respectively) or iii) alpha in DD (Wild type 12.49 ±0.17, homozygote 12.60 ±0.31, p=0.769131)

b) Mutant animals show a similar distribution of activity in wheel running screens over the LD cycle, with the exception of the last hour before lights on (RM ANOVA p=0.610, F (4.260, 72.425))

c) Total activity of mutant animals is the same as wild type animals (Wild type 238.5 ±50.7, homozygote 175.1 ±36.9, p=0.319)

d) i) Homozygote *Kdm1b*$^{T357M/T357M}$ animals run no more in the light phase of the LD cycle than *Kdm1b*$^{+/+}$ animals (Wild type 3.99 ±0.59, homozygote 4.78 ±0.96, p=0.501) ii) and also show no difference in light induced masking (Wild type 36.26 ±11.6, homozygote 33.19 ±10.4, p=0.846)

N=10 wild type and n=10 homozygote *Kdm1b*^{T357M} backcross 5 intercross animals. Period, alpha and activity parameter data was analysed by student T test.

5.3: Jet Lag Paradigm

In order to assess the molecular effects of *Kdm1a*^{E440G} and *Kdm1b*^{T357M} on circadian mechanism *in vivo*, homozygous animals were subjected to various additional circadian paradigms. Firstly animals were phase advanced by 6 hours, and after re-entrainment phase delayed by 6 hours to assess ability to entrain and speed of entrainment in response to phase shifts, similar to the effects of jet lag. Both *Kdm1a*$^{E440G/E440G}$ and *Kdm1b*$^{T357M/T357M}$ animals demonstrated the ability to re-entrain to both shifts as efficiently as wild type littermate controls. This shows that both animals have the capability to entrain normally to shifts in the LD cycle (Figure 5.7). Even though overall patterns of re-entrainment were not statistically different for either mutant line, separate analysis of the delay of *Kdm1b*$^{T357M/T357M}$ animals on day 1 of re-entrainment was significantly different to wild type animals ($p=0.04$). Upon closer examination of actograms, it can be seen that the onset of activity of wild type animals following a phase delay was weak before lights off, and that the major bout of activity began much later than the weak running in the light phase. Considering this observation, the first major bout of activity of *Kdm1b*$^{T357M/T357M}$ animals is much earlier than littermate controls, indicating that they take longer to re-entrain to the phase delay (Figure 5.7).

5.4: Phase Response Curve

To assess the ability of light to reset the circadian pacemaker, animals were kept in constant darkness, and 15 minute light pulses administered at CT 16 and CT 22 during the active phase. Onset of activity was then allowed to stabilise and the shift in phase response to early and late light pulses analysed for *Kdm1a*$^{E440G/E440G}$ and *Kdm1b*$^{T357M/T357M}$ animals as described previously (Figure 1.4). *Kdm1a*$^{E440G/E440G}$ animals showed no significant difference in response to the light pulses compared to wild type demonstrating that their ability to reset in response to light pulses is intact (Figure 5.8). *Kdm1b*$^{T357M/T357M}$ animals displayed a greater shift in response to the late light pulse than wild type (Figure 5.8). The phase shift of wild type animals in response to the ZT22 light pulse in this instance was unexpectedly small. A change in response to the late light pulse might suggest that LSD2 plays a

role in regulation of the clock, which affects the late part of circadian oscillation more than the early part. This results in disruption of the phase resetting response to late light pulses but not those earlier in the circadian cycle similar to the *Cacna1c* mutant (Schmutz et al. 2014) (discussed in section 5.8.3.3). As LSD2 mutants have not been shown to display a deficit in circadian masking in response to a 3 hour light pulse (Figure 5.6dii) or any deficits in pupillary light response (Figure 5.12), LSD2 is likely to act downstream of the light detection event so may be affecting phase resetting in the SCN (discussed in section 5.8.3).

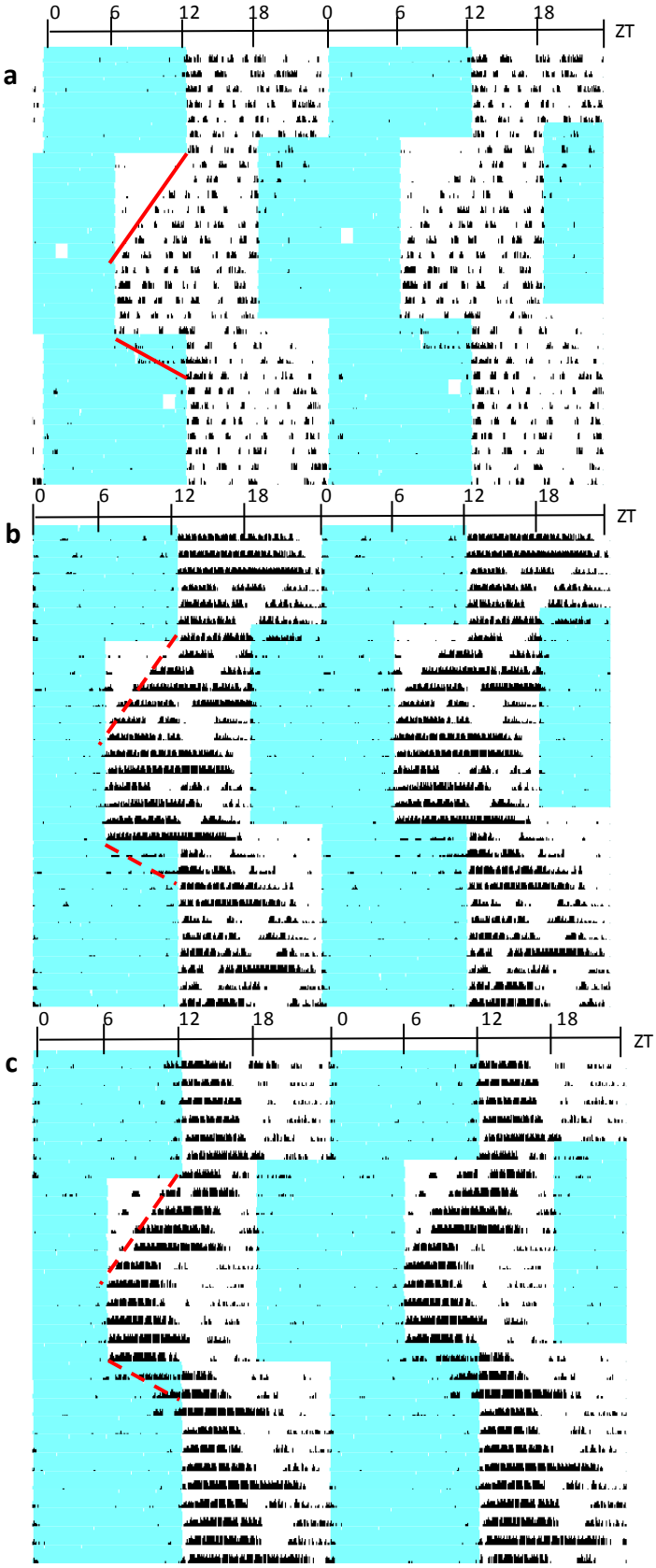

***Kdm1a*$^{E440G/E440G}$**

littermate control (WT)

***Kdm1a*$^{E440G/E440G}$**

***Kdm1b*$^{T357M/T357M}$**

d

***Kdm1a*$^{E440G/E440G}$**

e

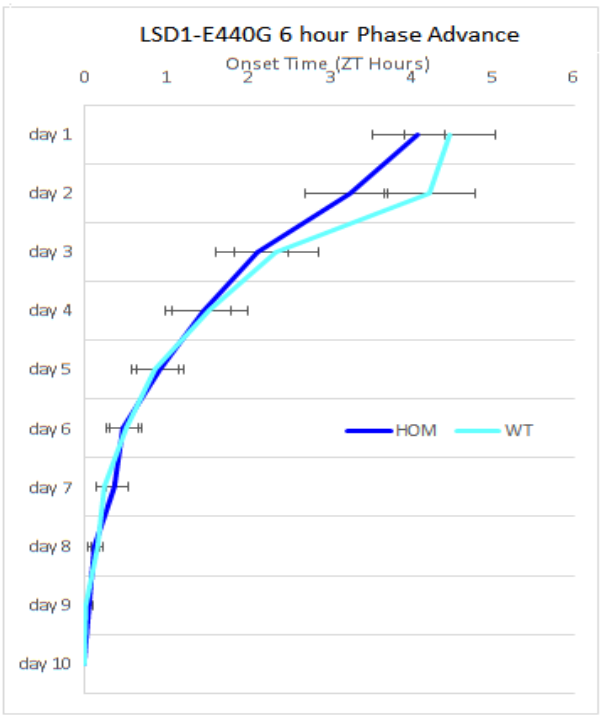

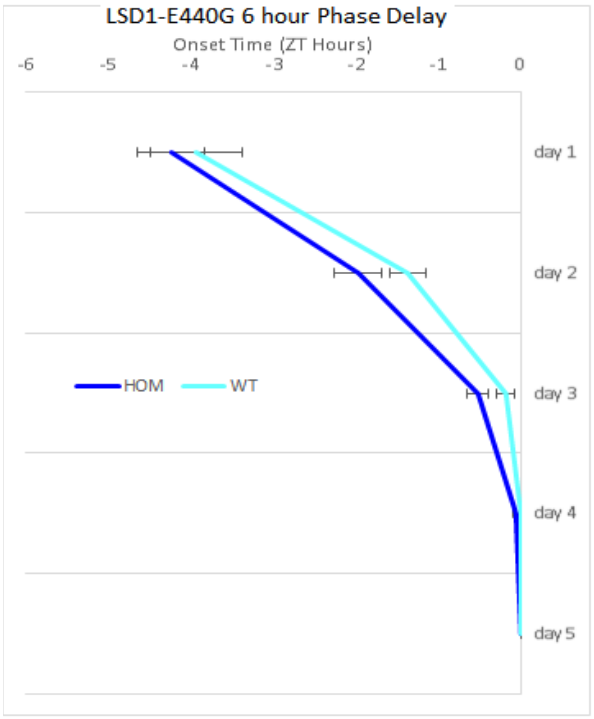

***Kdm1b*$^{T357M/T357M}$**

f

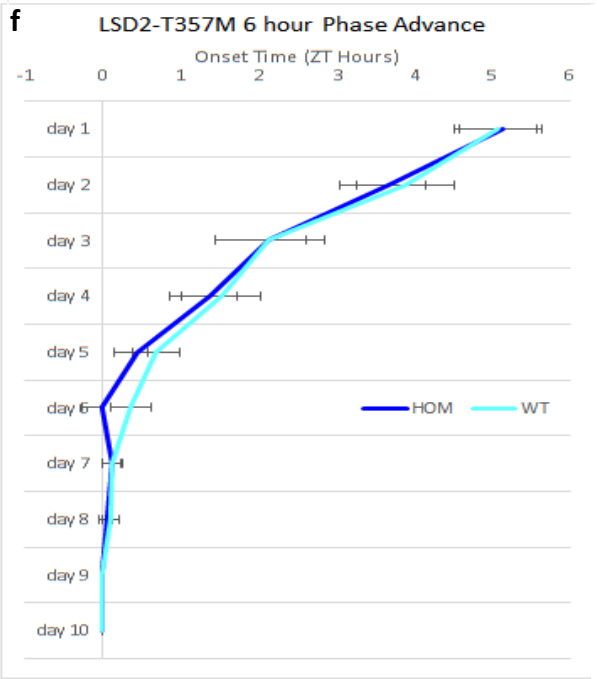

g

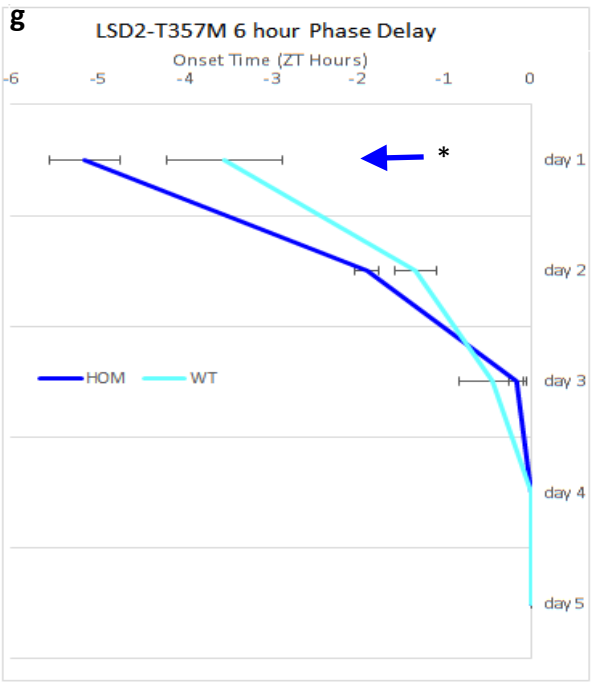

Figure 5.7: Jet lag shift of 12:12 LD cycles in *Kdm1a*$^{E440G/E440G}$ and *Kdm1b*$^{T357M/T357M}$ animals

Kdm1a$^{E440G/E440G}$ animals show no difference in re-entrainment to 6 hour advance or 6 hour delay in light dark cycle. *Kdm1b*$^{T357M/T357M}$ animals show a change in re-entrainment after phase delay.

a), b), c) Kdm1a$^{+/+}$ animal (control trace), *Kdm1a*$^{E440G/E440G}$ and *Kdm1b*$^{T357M/T357M}$ actograms

d) *Kdm1a*$^{E440G/E440G}$ response to 6 hour advance shift, effect of genotype p=0.19 F(1,260)=1.70, interaction of genotype with time p=0.75 F(9,260)=0.65

e) *Kdm1a*$^{E440G/E440G}$ response to 6 hour delay shift, effect of genotype, p=0.30 F(1,150) =1.10, interaction of genotype with time p=0.44 F(4,150)=0.94

f) *Kdm1b*$^{T357M/T357M}$ response to 6 hour advance shift, p=0.34 F(1,126) =0.94, interaction of genotype with time p=0.99 F(8,126)=0.13

g) *Kdm1b*$^{T357M/T357M}$ response to 6 hour delay shift, p=0.11 F(1,56) =2.59, interaction of genotype with time p=0.09 F(3,56)=2.27, blue arrow p=0.043 for day 1 by Student T-test

Red lines denote onset of activity used to determine circadian period. Dashed lines denoting wild type onsets are placed on mutant trace for ease of comparison to mutant onset.

N=10 wild type and n=10 homozygote *Kdm1a*^{E440G} backcross 5 intercross animals, n=10 wild type and n=10 homozygote *Kdm1b*^{T357M} backcross 5 intercross animals. Phase shift responses were analysed by two-way RMANOVA and post hoc Tukey test. (*p<0.05, **p≤0.005, ***p≤0.001)

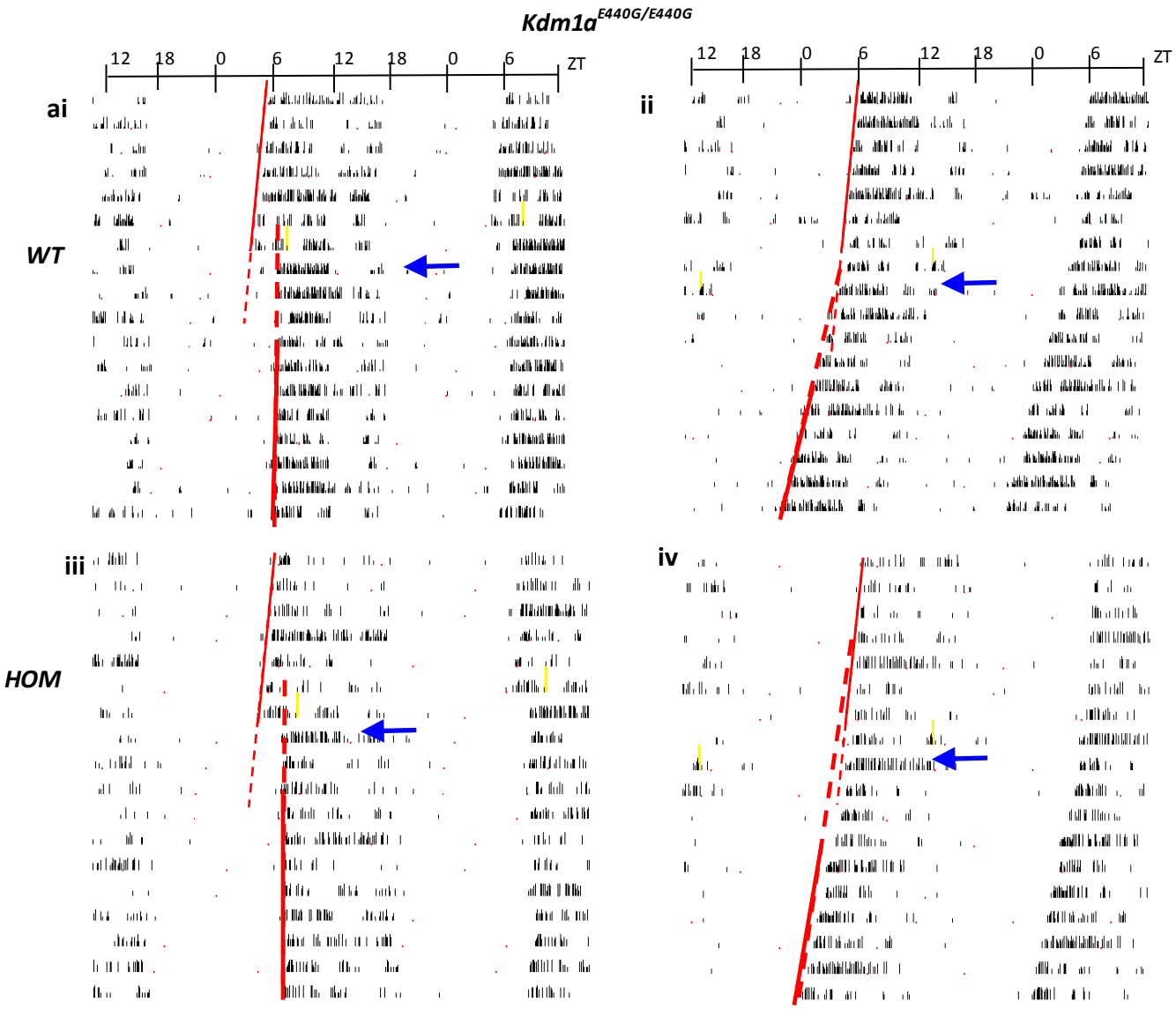
Kdm1a E440G/E440G
12 18 0 6 12 18 0 6 ZT
ai
ii
WT
iii
iv
HOM

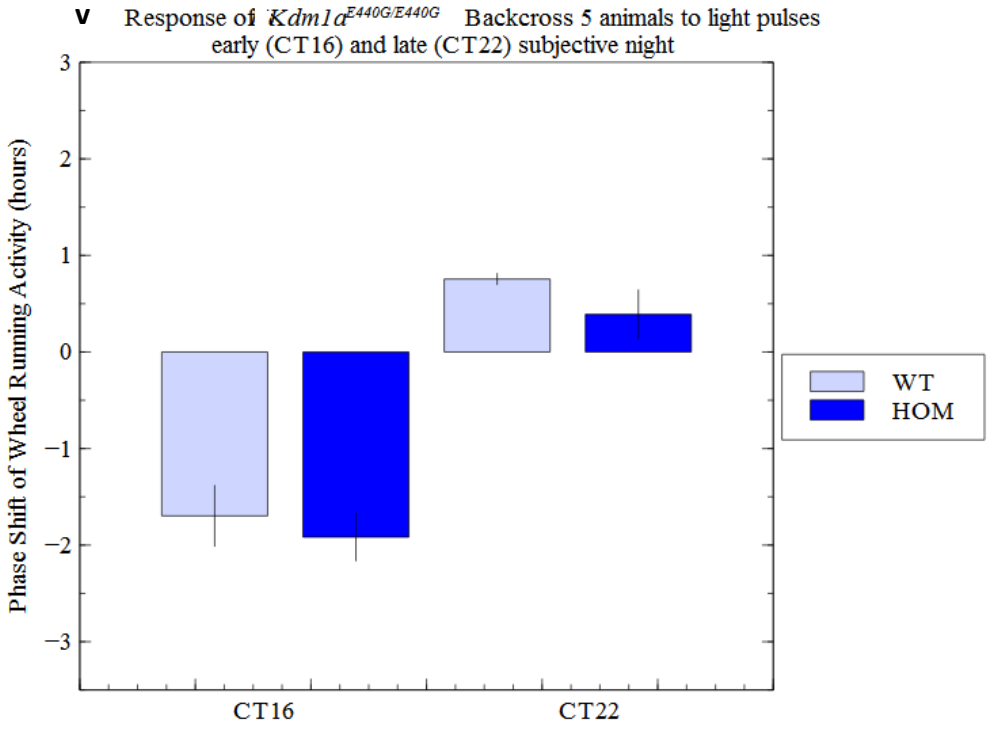
v
Response of Kdm1a E440G/E440G Backcross 5 animals to light pulses
early (CT16) and late (CT22) subjective night
Phase Shift of Wheel Running Activity (hours)
3
2
1
0
−1
−2
−3
CT16
CT22
WT
HOM

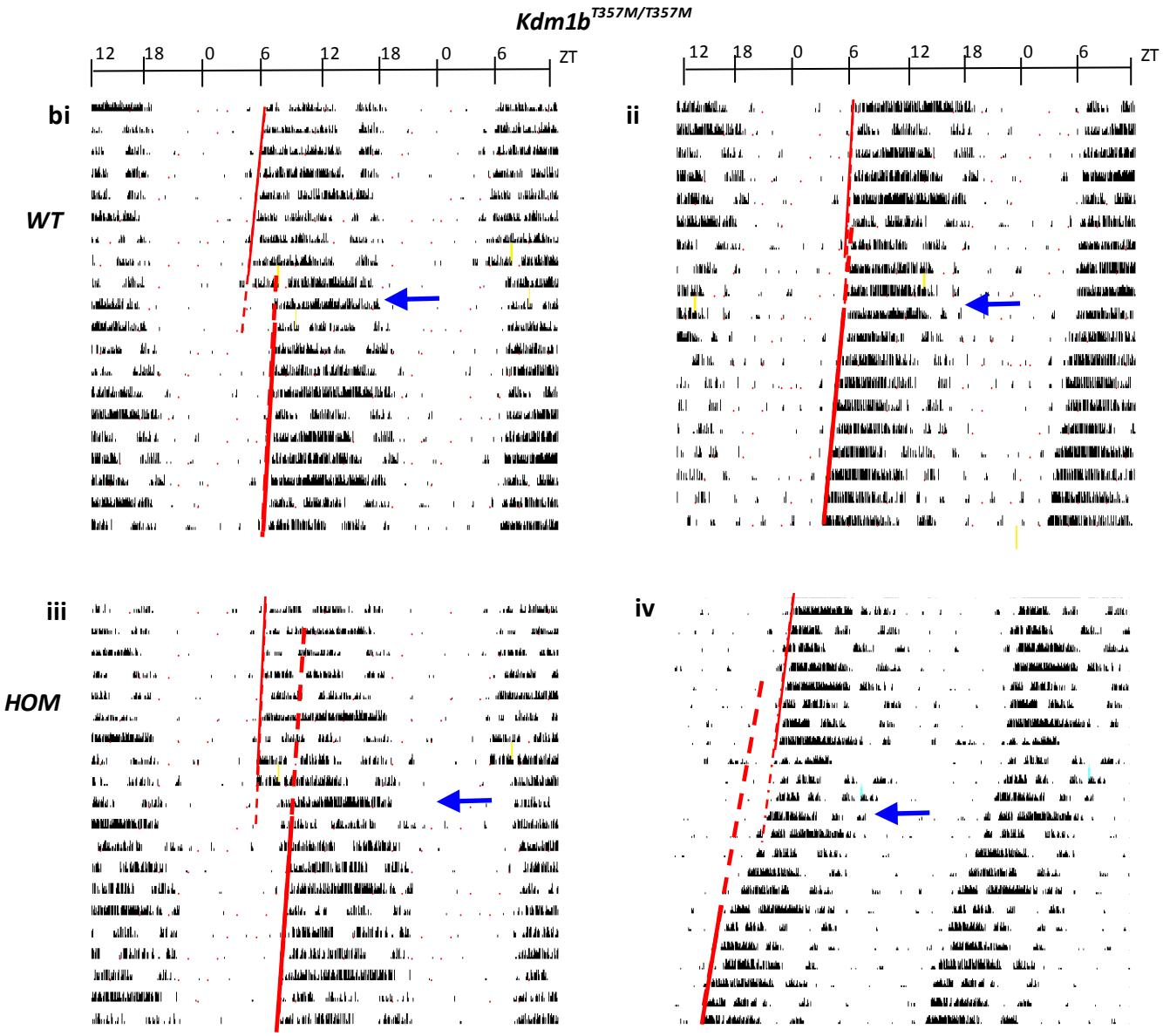
Kdm1b T357M/T357M
12 18 0 6 12 18 0 6 ZT
bi
WT
ii
12 18 0 6 12 18 0 6 ZT
iii
HOM
iv

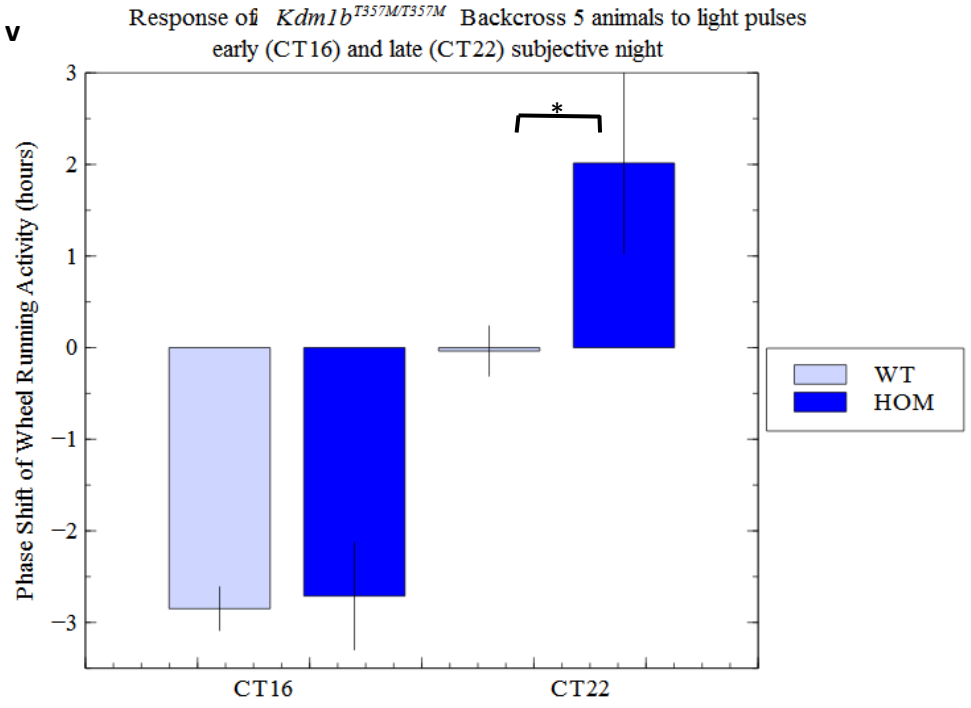
v
Response of Kdm1b T357M/T357M Backcross 5 animals to light pulses
early (CT16) and late (CT22) subjective night
Phase Shift of Wheel Running Activity (hours)
3
2
1
0
−1
−2
−3
*
CT16
CT22
WT
HOM

Figure 5.8: Phase responses of *Kdm1a*$^{E440G/E440G}$ animals and *Kdm1b*$^{T357M/T357M}$ animals

No difference was observed in *Kdm1a*$^{E440G/E440G}$ response to the light pulse compared to wild type animals. *Kdm1b*$^{T357M/T357M}$ displayed a greater shift in response to the late light pulse than wild type. Thin red lines show onset of activity before the light pulse, thick lines after the light pulse. Lines are dotted to show extrapolated onset, and blue arrows show which day the shift in phase was measured on (immediately following the day of the light pulse).

a) *Kdm1a*$^{E440G/E440G}$ phase response curve i) wild type early time point, ii) wild type late time point, ii) homozygote early time point, iv) homozygote late time point, v) graphical representation (early time point wild type -1.70 ±0.31, homozygote -1.92 ±0.24, p= 0.589366, late time point wild type 0.76 ±0.06, homozygote 0.39 ±0.25, p=0.34371)
b) *Kdm1b*$^{T357M/T357M}$ phase response curve i) wild type early time point, ii) wild type late time point, ii) homozygote early time point, iv) homozygote late time point, v) graphical representation (early time point wild type -2.85 ±0.24, homozygote -2.71 ±0.58, p= 0.799052, late time point wild type -0.04 ±0.27, homozygote 2.02 ±0.99, p=0.023437)

N=10 wild type and n=10 homozygote *Kdm1a*^{E440G} backcross 5 intercross animals, n=10 wild type and n=10 homozygote *Kdm1b*^{T357M} backcross 5 intercross animals. All animals exposed to either 2 or 4 light pulses, and data excluded if onset following the light pulse did not re-stabilise or if circadian period after the light pulse deviated from that before the light pulse by more than 0.5 hours as in both instances extrapolation could not be performed. Phase resetting responses were analysed by student T test. (*$p<0.05$, **$p\leq0.005$, ***$p\leq0.001$)

5.5: Aftereffects (T-Cycles)

Aftereffects are changes in free-running circadian period elicited by exposure of animals to T cycles of periods shorter or longer than 24 hours. In response to entrainment to an 11:11 LD T cycle (short T cycle), animals are expected to free run in DD with a shorter period than if entrained to normal 24 hour LD. Conversely in response to a long T cycle of 14:14, animals are expected to run with a longer period than after 12:12. The responses of *Kdm1a*$^{E440G/E440G}$ and *Kdm1b*^{T357M} animals did not differ significantly from their wild-type littermate controls in response to either 22 or 28 hour long T cycles (11:11 or 14:14 LD cycles) (Figures 5.9 and 5.10).

5.5.1: Aftereffects *Kdm1a*^{E440G}

Whereas wild type *Kdm1a*$^{+/+}$ animals displayed a free-running period of 24.01 hours after exposure to 22 hour T-cycles, *Kdm1a*$^{E440G/E440G}$ animals tended towards shorter periods of oscillation at 23.97 hours (p=0.412) (Figure 5.9ai). After 28 hour T cycles the free running period of wild type animals was 24.11 hours, *Kdm1a*$^{E440G/E440G}$ ran with a shorter period of 24.02 hours (p=0.275) (Figure 5.9aii). These effects are far from significant, and the limitations to interpretation of the data are discussed later (section 5.8.4).

5.5.2: Aftereffects *Kdm1b*^{T357M}

After 22 hour T-cycles, it is expected that the free running period of wild type *Kdm1b*$^{+/+}$ animals is shorter than after 24 hour T cycles. After short T-cycles, *Kdm1b*$^{T357M/T357M}$ activity only oscillated with a 23.92 hour period whereas the *Kdm1b*$^{+/+}$ animals ran with a period of 23.75 hours, but this result was not statistically significant (p=0.333) (Figure 5.10aii). *Kdm1b*$^{T357M/T357M}$ animals did run with a similar period after 28 hour T-cycles to that of wild type animals (23.97 compared to the control 23.98 hour period p=0.913) (Figure 5.10aii) (discussed in section 5.8.4).

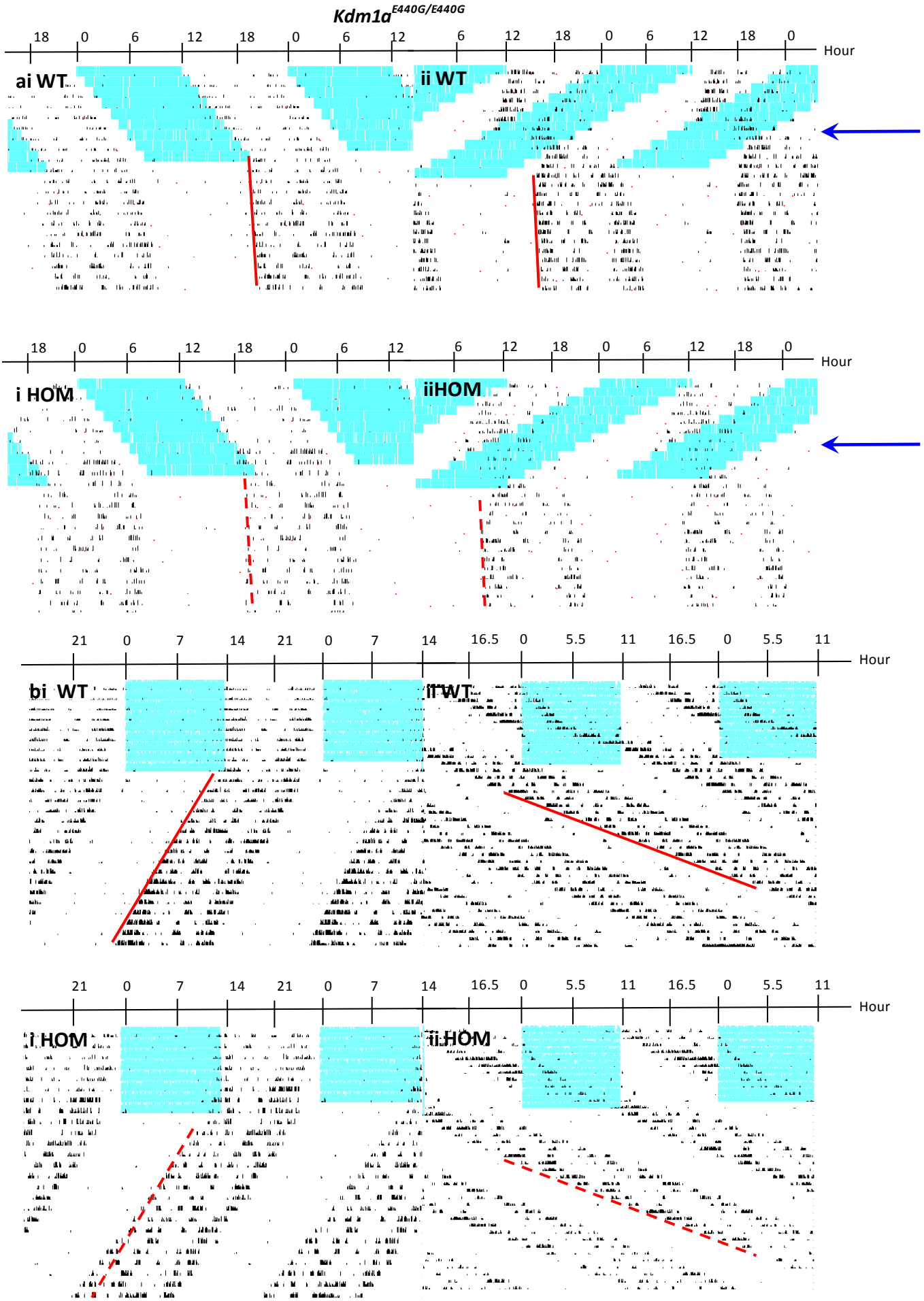
Kdm1a E440G/E440G
18 0 6 12 18 0 6 12 6 12 18 0 6 12 18 0
Hour
ai WT
ii WT
18 0 6 12 18 0 6 12 6 12 18 0 6 12 18 0
Hour
i HOM
iiHOM
21 0 7 14 21 0 7 14 16.5 0 5.5 11 16.5 0 5.5 11
Hour
bi WT
ii WT
21 0 7 14 21 0 7 14 16.5 0 5.5 11 16.5 0 5.5 11
Hour
i HOM
ii HOM

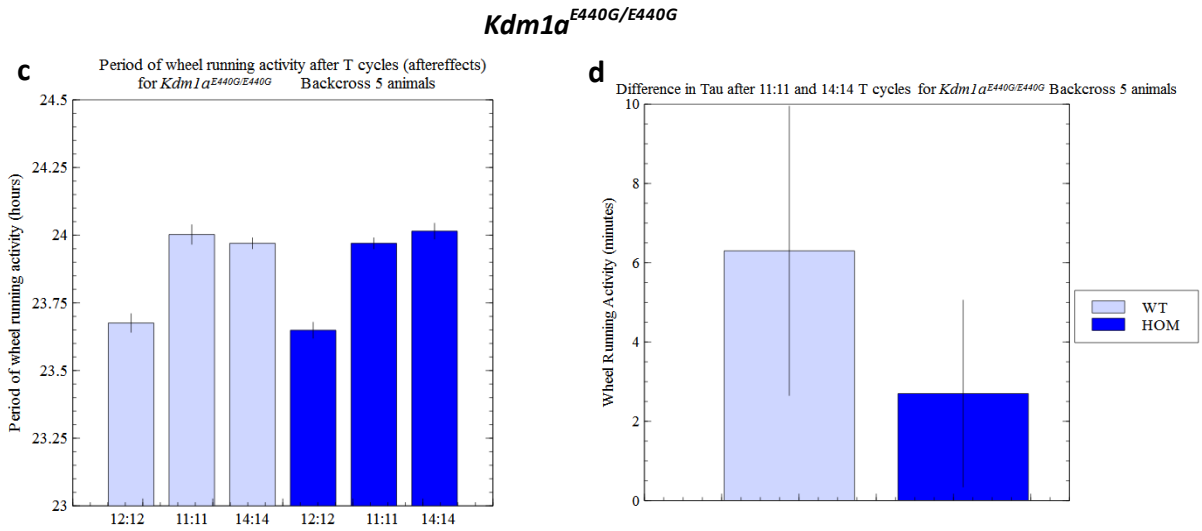

Figure 5.9: Response of *Kdm1a*$^{E440G/E440G}$ animals to non-24 hour LD cycles

a) Actograms demonstrating similarities between *Kdm1a*$^{+/+}$ and *Kdm1a*$^{E440G/E440G}$ animals after i) long and ii) short T-cycles. Activity is plotted as a 24 hour double plotted actogram. Blue arrow shows that neither wild type nor homozygous animals entrained to 11:11 cycles.

b) Actograms demonstrating similarities between *Kdm1a*$^{+/+}$ and *Kdm1a*$^{E440G/E440G}$ animals after i) long and ii) short T cycles. Long T cycle traces are plotted as double plotted 14:14 actograms, short as 11:11 actograms

c) Free running period was analysed after LD schedules of different lengths. *Kdm1a*$^{+/+}$ free running period after a 12:12 schedule is 23.68 ±0.03, after an 11:11 LD schedule is 24.00 ±0.04, and after 14:14 LD is 23.97 hours ±0.02. The exposure of the animals to T cycles failed to produce the expected aftereffect period changes, and as such data from the mutant animals cannot be interpreted as intended. *Kdm1a*$^{E440G/E440G}$ after effects were not significantly different to *Kdm1a*$^{+/+}$, 23.65 ±0.03, 23.97 ±0.02 and 24.02 ±0.03 respectively. The difference between genotypes in short T cycles, p= 0.412 and in long T cycles p=0.275

d) As *Kdm1a*$^{+/+}$ animals did not respond to the T-cycles by shortening or lengthening period as expected, the difference between the long and short T-cycle after effects was analysed. *Kdm1a*$^{E440G/E440G}$ animals still did not show any significant difference to wild type animals (wild type 6.13 hours ±3.65, homozygote 2.7 hours ±2.35 p=0.407499)

Red lines denote onset of activity used to determine circadian period. Dashed lines denoting wild type onsets are placed on mutant trace for ease of comparison to mutant onset.

N=10 wild type and n=10 homozygote *Kdm1a*^{E440G} backcross 5 intercross animals. Changes in period were analysed by student T test.

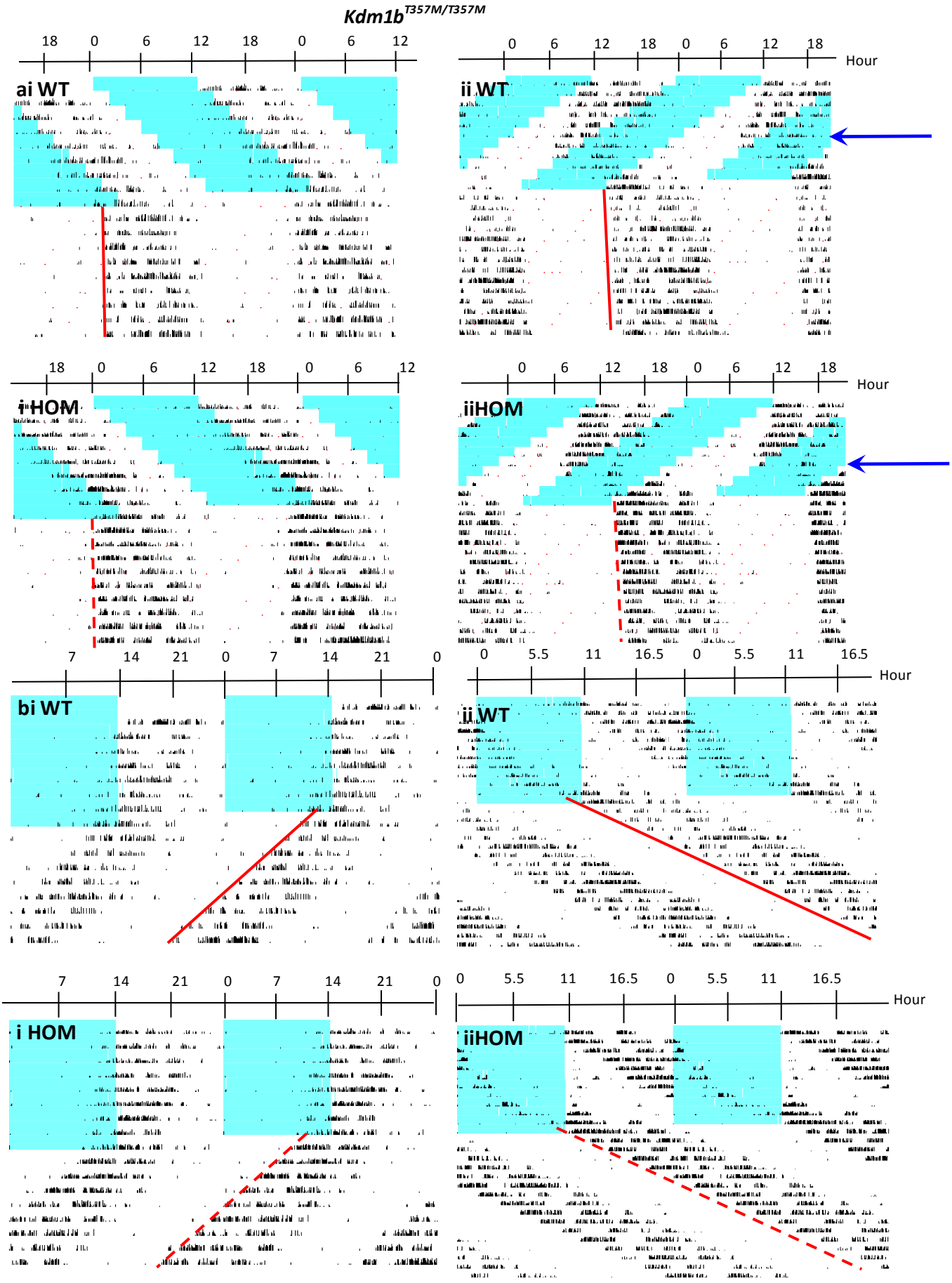
Kdm1b T357M/T357M
18 0 6 12 18 0 6 12
ai WT
0 6 12 18 0 6 12 18
Hour
ii WT
18 0 6 12 18 0 6 12
i HOM
0 6 12 18 0 6 12 18
Hour
ii HOM
7 14 21 0 7 14 21 0
bi WT
0 5.5 11 16.5 0 5.5 11 16.5
Hour
ii WT
7 14 21 0 7 14 21 0
i HOM
0 5.5 11 16.5 0 5.5 11 16.5
Hour
ii HOM

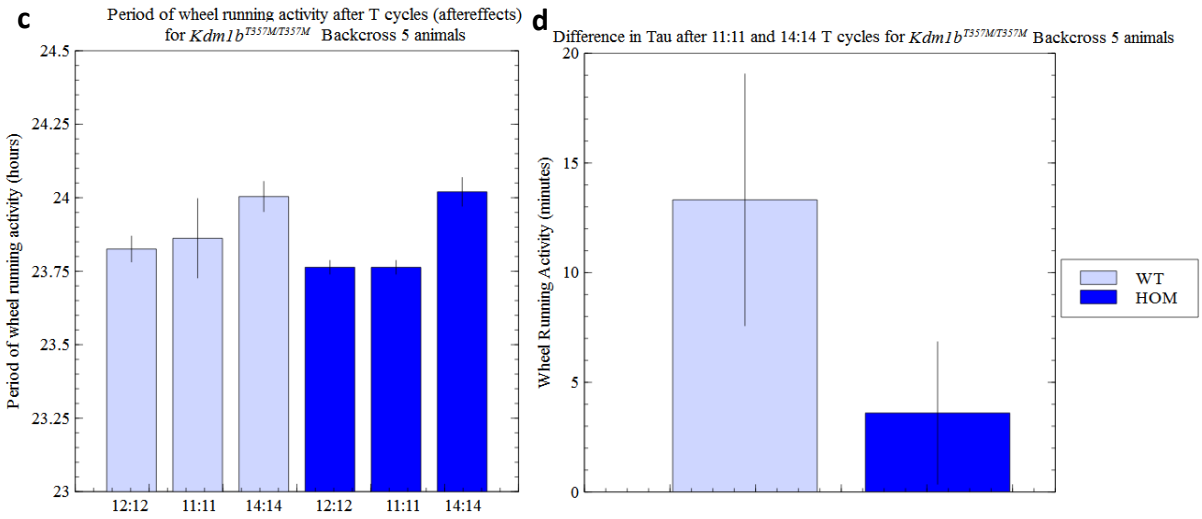

Figure 5.10: Response of *Kdm1b*$^{T357M/T357M}$ animals to non-24 hour LD cycles

a) Actograms demonstrating similarities between wild type and homozygous animals after i) long and ii) short T-cycles. Activity is plotted as a 24 hour double plotted actogram. Blue arrow shows that neither wild type nor homozygous animals entrained to 11:11 cycles.

b) Actograms demonstrating similarities between *Kdm1b*$^{+/+}$ and *Kdm1b*$^{T357M/T357M}$ animals after i) long and ii) short T cycles. Long T cycle traces are plotted as double plotted 14:14 actograms, short as 11:11 actograms

c) Tau DD was analysed after LD schedules of different lengths. *Kdm1b*$^{+/+}$ free running period after a 12:12 schedule is 23.83 ±0.04, after an 11:11 LD schedule is 23.86 ±0.13, and after 14:14 LD is 24.00 hours ±0.05. The exposure of the animals to T cycles failed to produce the expected aftereffect period changes, and as such data from the mutant animals cannot be interpreted as intended. *Kdm1b*$^{T357M/T357M}$ after effects were not significantly different to *Kdm1b*$^{+/+}$, 23.76 ±0.02, 23.97 ±0.06 and 24.02 ±0.05 respectively. For short T cycles, p= 0.333 and long T cycles p=0.913

d) As *Kdm1b*$^{+/+}$ animals did not respond to the T-cycles by shortening or lengthening period as expected, the difference between the long and short T-cycle after effects was analysed. *Kdm1b*$^{T357M/T357M}$ animals still did not show any significant difference to wild type animals (Wild type 13.32 hours ±5.73, homozygote 3.60 hours ±3.24 p=0.213171)

Red lines denote onset of activity used to determine circadian period. Dashed lines denoting wild type onsets are placed on mutant trace for ease of comparison to mutant onset.

N=10 wild type and n=10 homozygote *Kdm1b*^{T357M} backcross 5 intercross animals. Changes in period were analysed by student T test.

5.6.1: Pupillometry *Kdm1a*^{E440G}

In order to investigate whether a discrepancy in photodetection between the mutant and wild type groups was implicated in the masking phenotype of *Kdm1a*$^{E440G/E440G}$ animals, pupillary light response (PLR) was examined (Figure 5.11). There was no major difference in pupil constriction in mutant animals in trials 2-4 so no apparent problem with the PLR. In trial 1, however, mutant animals displayed less constriction than controls, suggesting hypersensitivity or over-reflexiveness which could be linked to anxiety in the strains, a decrease in constriction as seen here would indicate an increased anxiety level in the mutant animals, but as the effect is not sustained over the trials, this effect needs verifying by testing animals in a stressed and non-stressed state. This result also suggests that the lack of ability of *Kdm1a*$^{E440G/E440G}$ animals to mask wheel running in response to the masking light pulse is not affected at the level of retinal sensitivity to light.

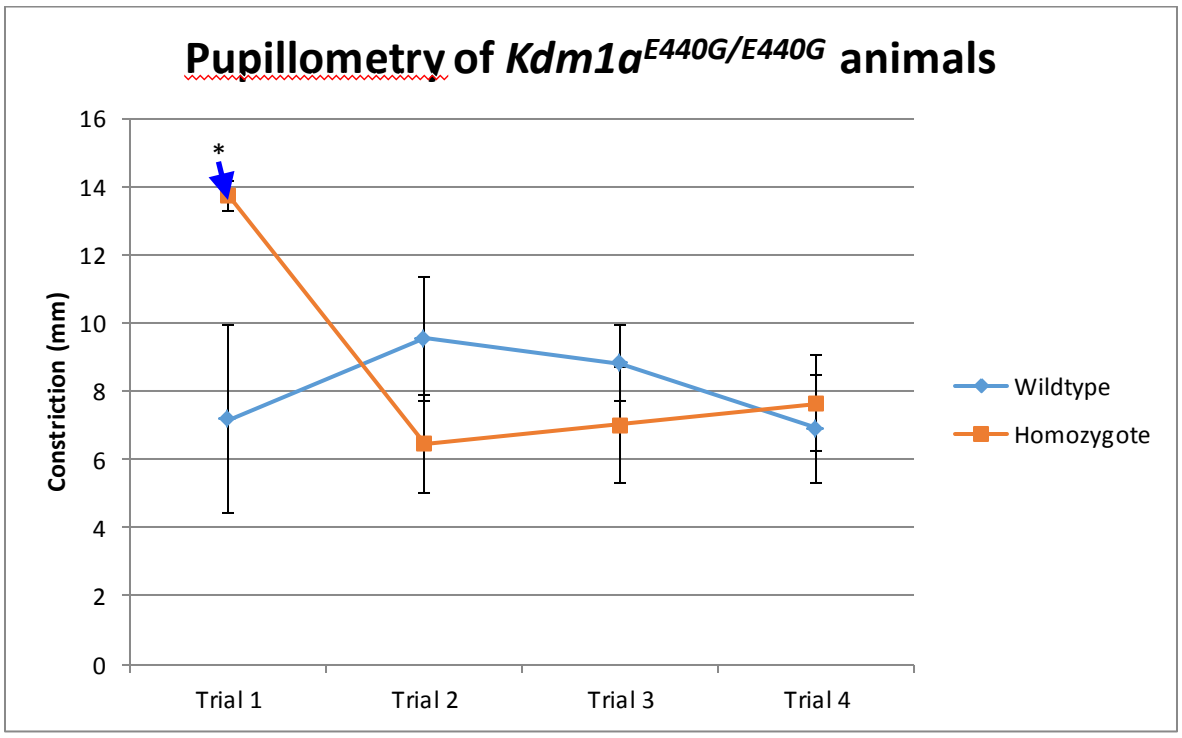

Figure 5.11: Pupillary light response of *Kdm1a*$^{E440G/E440G}$ animals

Upon administration of light to the contralateral eye, homozygote animals initially show a reduced constriction in comparison to wild type animals (p=0.039 by student T-test). In following trials pupillary constriction is similar in the two groups (constriction for wild type was 7.17 ±2.77, 9.54 ±1.83, 8.81 ±1.12 and 6.90 ±1.59 on respective trials, and for homozygotes 13.72 ±0.43, 6.46 ±1.45, 7.02 ±1.70 and 7.63 ±1.41). Overall the genotypes were not statistically different from one another (RM ANOVA p=0.601, F(0.282)) N=3 wild type and n=4 homozygote *Kdm1a*^{E440G} backcross 5 intercross animals for every trial. (*p<0.05, **p≤0.005, ***p≤0.001)

5.6.2: Pupillometry *Kdm1b*^{T357M}

Kdm1b$^{T357M/T357M}$ animals did not display any difference in PLR to that of controls (Figure 5.12). PLR is an example of a non-image forming function of the retina and non-image forming pathways are involved in phase resetting mechanisms. Therefore the PLR was examined to investigate whether the change in phase response to the late light pulse in *Kdm1b*$^{T357M/T357M}$ animals found earlier (Section 5.4) was due to a deficit in retinal function or due to impairment downstream of the retina. The lack of difference in PLR suggests that the *Kdm1b*^{T357M} mutation is impacting phase response downstream of the retinal input pathway.

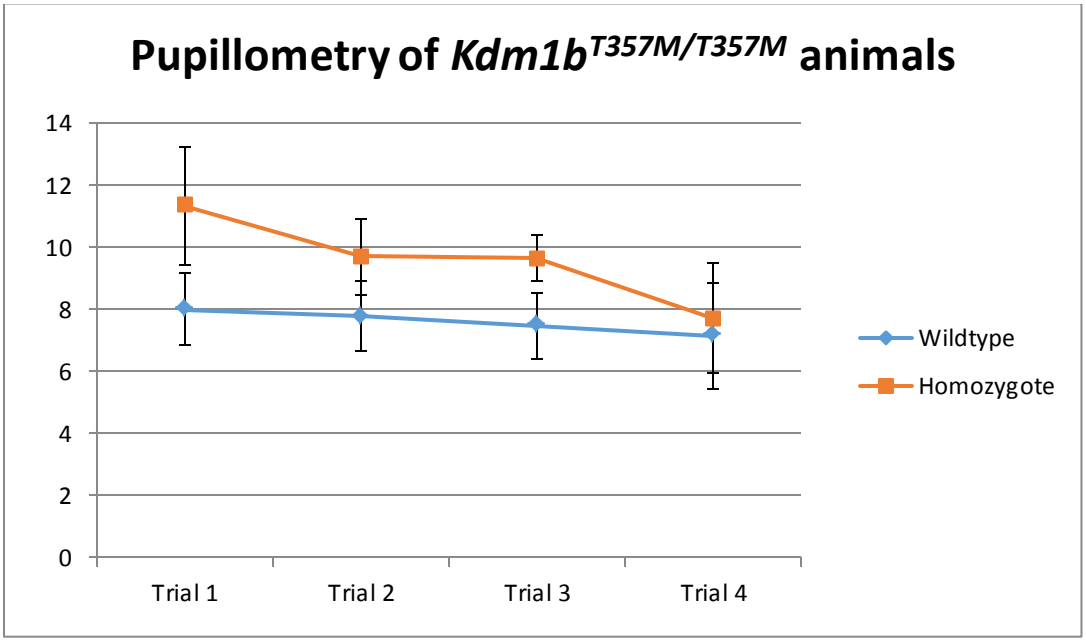

Figure 5.12: Pupillary light response of *Kdm1b*$^{T357M/T357M}$ animals

The pupil constriction observed in response to light is not statistically different between the homozygotes and wild type animals (constriction for wild type was 7.99 ±1.15, 7.79 ±1.14, 7.47 ±1.06 and 7.16 ±1.71 on respective trials, and for homozygotes 11.35 ±1.90, 9.71 ±1.21, 9.66 ±0.72 and 7.72 ±1.76) (RM ANOVA genotype p=0.062, F(1,24)). N=4 wild type and n=4 homozygote *Kdm1b*^{T357M} backcross 5 intercross animals.

5.7: *Ex vivo* data

In order to further elucidate how molecular clock mechanisms were affecting *in vivo* behavioural outputs of the clock, molecular work was undertaken using native tissue from the mutant animals and comparing gene expression to littermate controls. This lends insight into what molecular mechanisms might be at play affecting *in vivo* observations of mutant animals.

5.7.1: Tissue RNA Expression

Tissues taken from *Kdm1a*$^{E440G/E440G}$ animals at ZT intervals 4 hours apart were analysed by RNA extraction followed by real time qPCR analysis of clock gene expression. Liver *Bmal1* and *Per1* were shown to oscillate statistically normally in *Kdm1a*$^{E440G/E440G}$ homozygotes. *Cry1* oscillation was statistically significantly advanced but expression levels appeared normal (Figure 5.13). *Bmal1* and *Dbp* expression curves appeared shifted, and the expression of Dbp was significantly lower in *Kdm1a*$^{E440G/E440G}$ MEFs than wild type at ZT7 ($p=0.000001$). The subtlety of the change in *Dbp* expression does not correlate with the decrease in LSD1 binding or demethylation observed earlier (Section 4.3). It would be expected that an increase in H3K4 methylation at the *Dbp* locus would increase *Dbp* expression as an association between methylation at this site and transcriptional activation has been previously established (Metzger et al. 2010).

To investigate whether LSD1 plays a central role in SCN pacemaker tissue, RNA extracted from SCN tissue was examined. In SCN samples, samples were far smaller than the liver samples analysed previously. As such they were analysed with a pico kit (Table 2.5), and upon data cleaning, more samples were excluded on the basis of poor quality RNA. The variation in each of the data points at each timepoint was much higher than in liver due to the size of the tissue sample, and all wild type data points taken at the timepoint ZT13 were excluded from the analysis due to the variation between individuals at this timepoint (Figure 5.14) Error bars are substantial due to this variation. No gene expression patterns were clearly cyclic in the SCN unlike those observed in liver. It was observed that *Kdm1a*$^{+/+}$ animals do not display any significant oscillation in *Bmal1*, *Cry1* or *Kdm1a*

and therefore the difference between wild type and homozygous animals was not ascertained from this data. In the case of *Dbp* oscillation, *Kdm1a*$^{E440G/E440G}$ animals display a non-significant shift in onset of expression and a decrease in total expression which could be consistent with liver gene expression data. (Figure 5.14)

Figure 5.13: Real time analysis of circadian gene expression in liver tissue from *Kdm1a*$^{E440G/E440G}$ animals

In Liver, both wild-type and homozygous animals display cycling in the *Bmal1, Cry1, Per1* and *Dbp*. In this experiment, *Kdm1a* expression was not observed to cycle in wild type or homozygous animals. Homozygous animals displayed expression patterns statistically similar to wild type in the case of the core clock genes *Per1, Bmal1* and *Dbp (*P=0.596, F (1.601, 4.803)=0.501, P=0.427, F (1.752, 5.257)=0.965, p=0.426, F (1.013,3.040)=0.849). *Cry1* patterns were significantly different to one another (P=0.03, F (2.343, 7.029)=5.807), and a phase advance was evident in the peak of expression. In the case of *Dbp*, homozygous animals appear to display a a narrower peak of expression, and the peak of *Bmal1* expression appears phase advanced in homozygotes, similar to the *Cry1* shift although these observed effects were not statistically different. Upon closer individual analysis of *Dbp* expression data from liver at ZT7, mutants showed a decrease in expression which was found to be significant by t-test (p=0.000001)

N=3 for each genotype at each timepoint. All expression data quantified against actin expression in liver tissue. Data was analysed with two way RM ANOVA (*p<0.05, **p≤0.005, ***p≤0.001)

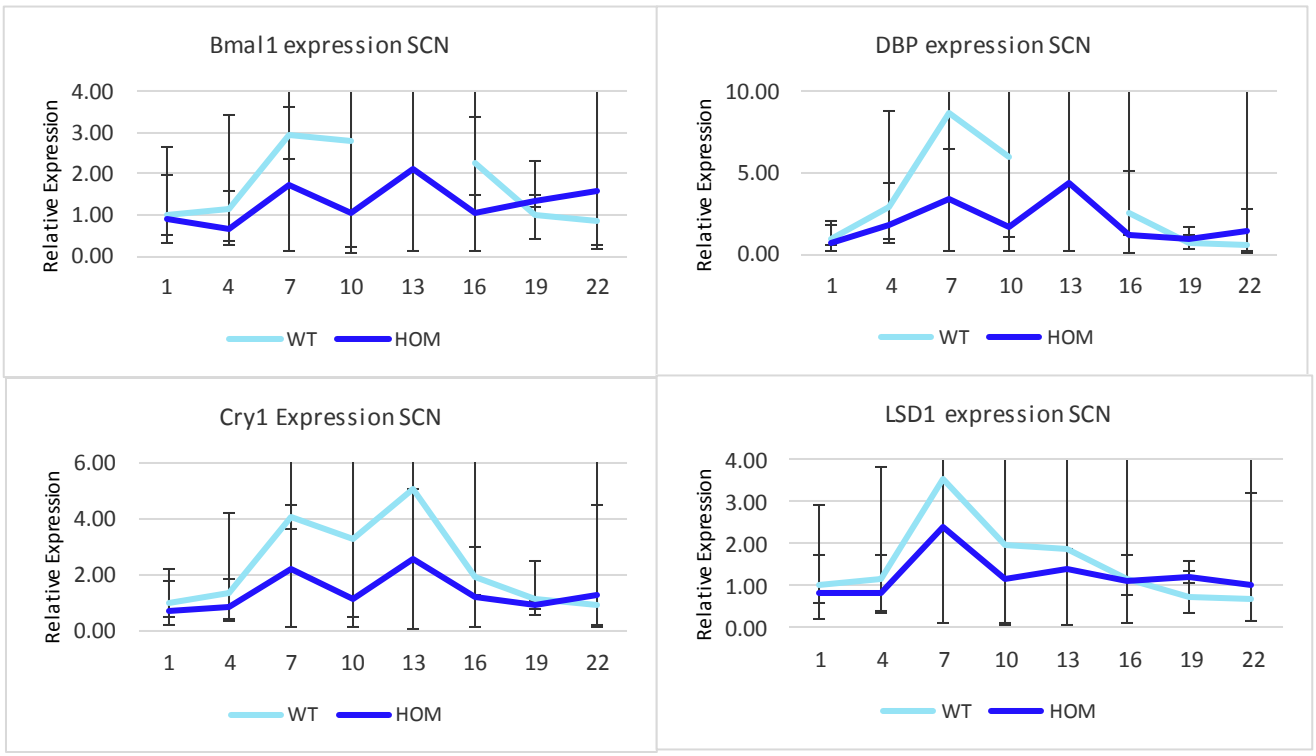

Figure 5.14: Real time analysis of circadian gene expression in SCN tissue from *Kdm1a*$^{E440G/E440G}$ animals

The expression of *Bmal1, Cry1*, *Dbp* and *Kdm1a* was examined in the SCN. The data was highly variable due to the exclusion of many samples from the analysis based on RNA quality. No oscillation was observed in any gene except *Dbp*. The shifts in *Cry1, Bmal1 and Dbp* expression observed in liver are not observed in real time data acquired using SCN tissue. Differences between mutant and wild type controls were not able to be discerned.

N=3 for each genotype at each timepoint, multiple samples excluded from analysis due to poor quality RNA. All expression data quantified against GADPH expression in SCN tissue. There was not enough data to conduct ANOVA

5.7.2: Organotypic SCN slice culture

To examine whether the differences in tau observed in the *Kdm1a*^{E440G} wheel running assay was as a result of SCN function directly, *ex vivo* SCN slices were examined. *Kdm1a*$^{E440G/E440G}$ animals were crossed to m*Per2*:Luc reporter mice to generate animals heterozygous for the reporter gene but homozygous for the *Kdm1a*^{E440G} mutation, as well as wild-type littermate controls carrying the reporter alone. The stability of bioluminescent recording from SCNs from m*Per2*:Luc animals was previously ascertained (Section 7.3).

The *Kdm1a*$^{E440G/E440G}$ mutant SCN oscillated with a shorter period of 23.35 in comparison to the *Kdm1a*$^{+/+}$ 23.66. This result does not concur with *in vivo* wheel running rhythm observations where the animals free-ran with a period 20 minutes longer than wild type. Neither of these trends reaches significance, and the SCN slice experiment would benefit from increasing the number of samples tested upon breeding a bigger colony (Figure 5.15).

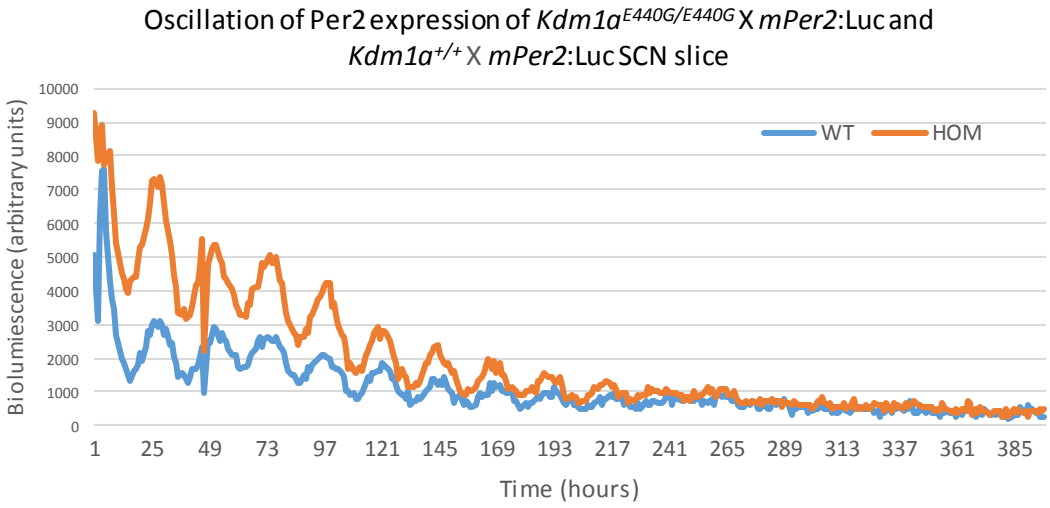

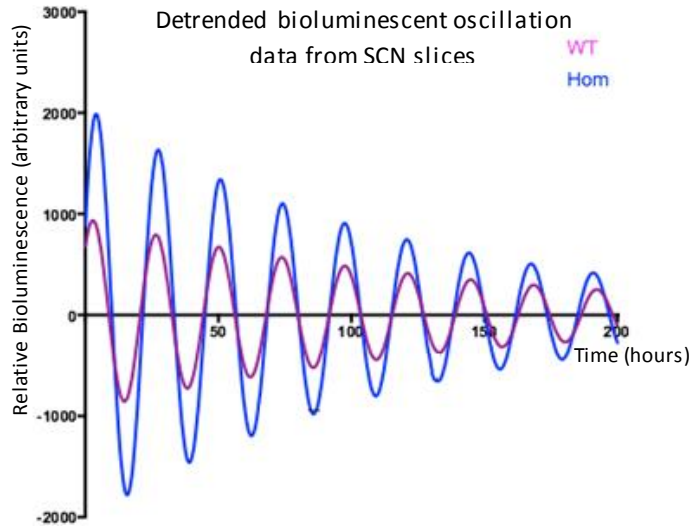

Best-fit values	WT	HOM
Baseline	3.036	11.05
Amplitude	-950.9	-2047
Wavelength (Period, hours)	23.66	23.35
Phase shift	3.927	3.583
Frequency	0.04226	0.04283
Half life	143.7	118.1

Figure 5.15: Oscillation of *Kdm1a*$^{E440G/E440G}$ X m*Per2*:Luc animal SCN slices

Kdm1a$^{E440G/E440G}$ animals were crossed to m*Per2*:Luc reporter animals and the SCNs extracted from individuals heterozygous for the m*Per2*:Luc reporter gene. SCN slices were taken and the bioluminescent rhythms recorded using a luminometer. The *Kdm1a*$^{E440G/E440G}$ animal does not display a difference in Per2 driven luciferase oscillation when compared to the *Kdm1a*$^{+/+}$ slice.

a) Raw data (Pierre modified best fit sine wave)
b) Detrended data

N=1 wild type and n=1 homozygote *Kdm1a*^{E440G} both heterozygous for the mPer2:Luc reporter organotypic slices. There was not enough data to conduct ANOVA

5.8: Discussion

5.8.1: Circadian parameter screen results

The activity measured in circadian wheel-running screens was analysed as a reliable output marker for circadian rhythmicity (Pittendrigh & Daan 1976). Results from circadian phenotyping are summarised in Table 5.1. Activity was initially assayed in early backcross animals to ascertain any phenodeviance in the mutant lines when compared with wild type littermate control cohorts. Activity was assessed in 12:12 light dark cycles (LD), constant darkness (DD), constant light (LL) and in response to a masking light pulse (Figure 1.4).

Wheel running assays in initial mutant screens showed that LSD1 and LSD2 mutants displayed abnormalities including anticipation of lights off (Figure 5.1a), masking deficits in response to a 3 hour light pulse (Figure 5.1a), and split rhythms in LL (Figures 5.5a and 5.5e) which were not observed in animals after further backcrosses to C57BL/6.

The difference between phenotypes seen in intercross animals from early and late backcrosses is evidence of the effect of different genetic backgrounds on a single mutation. In early backcrosses, naturally ENU-derived mutant lines carry multiple mutations, ENU inducing one mutation approximately every megabase of DNA sequence (Quwailid et al. 2004). With each generation of breeding to an inbred strain (in this case Balb/c X C3H to C57BL/6), two effects are seen in the genetics of the offspring. Firstly and most likely, the effect of the mutation in question may be much more readily observed at one backcross than another due to the differences in background strain. Different background strains have inherently different circadian properties (Banks et al. 2015) and in fact, tau in constant darkness varies widely across different inbred strains (Ebihara et al. 1978; Schwartz & Zimmerman 1990). And secondly, as generations pass the proportion of offspring genome contributed by the ENU-mutagenised founder animal is decreased and therefore the activity of ENU mutated genes which are not related to the selected LSD gene mutations could be more prominent on a C57BL/6 background or unmasked as other ENU mutations are selected

against in breeding, and subsequently be acting to modify circadian parameters. Conversely, phenotypes caused by the LSD mutations observed on a Balb/c X C3H background may be masked by naturally occurring but unknown C57BL/6 alleles in later backcrosses. Such modifier alleles could be sought with screens for linkage disequilibrium (Rogers et al. 2004). In this investigation, therefore the initial circadian observations can be explained by these two phenomena: background effects and the effect of modifiers on mutations unrelated to the gene of interest. The higher level of variability witnessed in data from the initial screen can also be attributed to the two effects at play, as the population of LSD mutants were more heterogeneous than they are in later backcrosses. The two effects could be teased apart experimentally by breeding the mutant animals back onto a Balb/c X C3H background. If the phenotype observed in early backcrosses were rescued by this breeding, the backcross 2 animal phenotype which was not observed in later backcrosses could be attributed to background effects, and if not then the phenotype observed in backcross 2 animals was due to a separate ENU mutation which was selected out of the backcross 5 animals.

Mutant	BC	♂/♀	Test	Result	Figure
Kdm1a$^{E440G/E440G}$	2	♂/♀	Initial screen	Anticipation of lights off	5.1a, 5.1b
				Masking ↓	
				TauDD ↑ (20min)	
				TauLL↓ (20min)	
Kdm1a$^{L491H/L491H}$	2	♂/♀	Initial screen	Masking ↓	5.1c, 5.1d
				TauDD ↑ (6min)	
				TauLL ↑ (27min) p=0.011	
Kdm1a$^{E440G/E440G}$	5	♂/♀	Initial screen	AlphaDD and AlphaLL ND	5.2a, 5.2b
				TauDD and TauLL ND	5.2a, 5.2c
				Activity distribution ND	5.3a
				Total activity ND	5.3b
				Running in the light phase ↑ p=0.047	5.3c
				Masking ↓	5.3d
Kdm1a$^{L491H/L491H}$	5	♂/♀	Initial screen	AlphaDD ND and AlphaLL ↓ (1.8hr) p=0.044	5.4a, 5.4b
				TauDD ND and TauLL ↓ (10min) p=0.040	5.4a, 5.4c
Kdm1b$^{T357M/T357M}$	2	♂/♀	Initial screen	Masking ↓	5.5a, 5.5b
				TauDD and TauLL ND	
				Splitting ↑	5.5a, 5.5e
Kdm1b$^{P281L/P281L}$	2	♂/♀	Initial screen	Punctate running in light phase	5.5c, 5,5d
				TauDD ↑ (12min) and TauLL ND	
Kdm1b$^{T357M/T357M}$	5	♂	Initial screen	AlphaDD, AlphaLL, TauDD and TauLL ND	5.6a
				Activity distribution ND	5.6b
				Total activity ND	5.6c
				Running in the light phase ND	5.6d
				Masking ND	
Kdm1a$^{E440G/E440G}$	5	♂/♀	Jet lag screen	ND	5.7b, 5.7d, 5.7e
Kdm1b$^{T357M/T357M}$	5	♂	Jet lag screen	Day 1 delay↓ p=0.043	5.7c, 5.7f, 5.7g
Kdm1a$^{E440G/E440G}$	5	♂/♀	Phase response screen	ND	5.8a
Kdm1b$^{T357M/T357M}$	5	♂	Phase response screen	Shift in response to late light pulse ↑ p=0.023	5.8b
Kdm1a$^{E440G/E440G}$	5	♂	After effect screen	NA	5.9
Kdm1b$^{T357M/T357M}$	5	♂	After effect screen	NA	5.10
Kdm1a$^{E440G/E440G}$	5	♂/♀	Pupillometry	Constriction on trial 1 ↓ p=0.039	5.11
Kdm1b$^{T357M/T357M}$	5	♂	Pupillometry	ND	5.12

Table 5.1: Summary of circadian phenotyping data

BC: Back cross; ND: No difference, NA: Not applicable (data not effective)

Table 4. Published τ of inbred mouse strains

Str [a]	τ_{DD}[a]	τ[b]	Reference
C57BL/6	23.77	23.59	Ebihara et al., 1978
		23.73	Possidente and Stephan, 1988
		23.28[c]	Ebihara et al., 1988b
		23.52[d]	Abe et al., 1989
AKR/J	23.52	23.5[d]	Possidente et al., 1982
DBA/2J	23.46	23.31	Possidente and Stephan, 1988
C57BL/10	23.43	23.47	Ebihara et al., 1978
		23.9[d]	Possidente et al., 1982
		23.5	Welsh et al., 1986
		23.30	Possidente and Stephan, 1988
A/J	23.37	22.9[d]	Possidente et al., 1982
BALB/c	22.94	23.4[c]	Haus et al., 1967
		22.7[d]	Possidente et al., 1982
		22.90	Possidente and Stephan, 1988

[a] Values taken from the present study.
[b] Values taken from previous studies.
[c] Value of τ obtained in blinded mice.
[d] Value of τ obtained in mice maintained in constant dim red light.

Figure 5.16: Variability of natural circadian free running period of inbred mouse strains (from Schwartz & Zimmerman 1990)

5.8.2: Jet Lag

Kdm1a$^{E440G/E440G}$ and *Kdm1b*$^{T357M/T357M}$ animals' ability to reset the clock to a new LD schedule was tested. The LD cycle was either delayed by or advanced by 6 hours from an initial period of photo-entrainment (jet-lag paradigm). *Kdm1a*$^{E440G/E440G}$ animals performed as well as wild type controls in the jet lag paradigm. Successful re-entrainment requires fully functional photoreception and processing as well as elasticity in the master clock in order to re-entrain to the new schedule (which is heavily influenced by the rigidity of neural coupling in the SCN (Hatori et al. 2014)). It can be concluded that the *Kdm1a*$^{E440G/E440G}$ mutants tested show the capacity to re-entrain in a similar manner to wild type animals and as such display no overt deficits in photoreception or pacemaker elasticity, suggesting that neuronal coupling in the SCN is intact (Figure 5.7). Many mutants with profound circadian deficits display the ability to re-entrain to this paradigm (Section 8.5.4) and as such the circadian role of LSD1 cannot be dismissed on this basis.

With regards the *Kdm1b*$^{T357M/T357M}$ data, although animals showed no statistical difference in the number of days taken to re-entrain or the pattern of re-entrainment, on day 1 of re-entrainment they shift significantly less than wild type animals ($p=0.04$). *Kdm1b*$^{T357M/T357M}$ animals do appear to run more in the process of re-entrainment when actograms are considered, and if the onset of activity were analysed differently (the major bout of activity being used as a measure of daily activity onset rather than the first bout of activity as was analysed here and previously (Jagannath et al. 2013)), it is apparent that these animals take longer to re-entrain to the phase delay where wild type animals entrain nearly immediately (Figure 5.7).

5.8.3: Phase Response Curve

In order to assess phase-resetting in mutant animals, animals were kept in DD and light pulses administered during subjective night. The resulting phase shift in activity following the light pulses was assessed. Phase resetting requires functional photodetection, direct ipRGC-mediated retinal input to the SCN and subsequent immediate early gene induction as well as the ability of the SCN

itself to re-entrain to a new phase of activity without the constant cycling of an external cue such as light. Phase response analyses for *Kdm1b*$^{T357M/T357M}$ animals revealed a greater shift in response to the late light pulse (Section 5.8.3.2) whereas *Kdm1a*$^{E440G/E440G}$ animals responded similarly to wild type animals (Section 5.8.3.1) (Figure 5.8).

5.8.3.1: Response to light in LSD1 mutants

Early backcross *Kdm1a*$^{E440G/E440G}$ animals display anticipation of lights off, deficits in masking responses to light, and late backcross animals display a deficit in masking as well as increased running in the light phase. Anticipation in LD cycles is impaired in other mutants such as the Histidine Decarboxyllase (*HDC*) knockout, which displays altered sleep cycles due to the role of histaminergic neural networks in arousal (Parmentier et al. 2002) so perhaps LSD1 plays a role in circadian arousal. *HDC-ΔBmal1* animals have a gain of function in histaminergic transmission as BMAL1 is necessary for the oscillation of histaminergic cells (Yu et al. 2014). The *HDC-ΔBmal1* line suffers from fragmented sleep, so perhaps this could be investigated in *Kdm1a*$^{E440G/E440G}$ animals. It would be interesting to compare the phenotypes of *Kdm1a*$^{E440G/E440G}$ and *HDC-ΔBmal1* animals in LD and LL.

5.8.3.2: Response to light pulses in LSD1 mutants

The lack of difference between LSD1 mutant and wild type animal response to light pulses is surprising as it has been previously demonstrated that LSD1 plays a role in phase resetting (Nam et al. 2014). The discrepancy between the phenotypes arising from the *Kdm1a*^{E440G} allele discussed here and the *Kdm1a*^{S112A} allele used in the aforementioned study are likely due to the different functional impact of the two mutations. Whereas the *Kdm1a*^{S112A} allele ablates a phosphorylation site, the *Kdm1a*^{E440G} allele disrupts the tower domain of LSD1 leading to decreased cofactor binding. The Nam et al. study showed that LSD1 binds to the *Per1* promoter region in response to CT14 light pulses and that phosphorylation of LSD1 is induced by light pulses at both CT14 and CT22. Animals with a mutation of the LSD1 phosphorylation site are less responsive to these phase resetting cues,

and the light induced IEG-mediated upregulation of *Per1* expression in SCN (essential for phase resetting (Albrecht et al. 1997)) is reduced in these animals. The lack of discrepancy between the *Kdm1a*$^{E440G/E440G}$ mutants examined here and wild type animals would suggest that these mutations are unlikely to be affecting the phosphorylation of LSD1 in response to the light pulses and that the decrease in CoREST binding (Section 4.2.2.4) that has been shown to be caused by the mutation does not affect phase resetting function in these animals. It could, however, contribute to downstream functions such as the underlying *Per1* promoter binding in response to light as the masking response to the LD light pulse is impaired in the *Kdm1a*^{E440G} animals (and *Kdm1a*^{L491H} at backcross 2). Therefore rather than looking at phase resetting, the lack of masking in response to the light pulse could be examined to ascertain which downstream mechanism is perturbed by the *Kdm1a*^{E440G} or *Kdm1a*^{L491H} alleles.

The lack of effect of mutations on light pulse responses in constant conditions was not mirrored when considering light pulses administered to supress activity during the dark phase of LD cycles. *Kdm1a*$^{E440G/E440G}$ animals showed a lack of light pulse-mediated suppression of activity in LD (masking) (Figure 5.2a). *Kdm1a*$^{E440G/E440G}$ animals also displayed a higher percentage of running being distributed in the light phase in LD (Figure 5.3c). Masking occurs when the normal activity output governed by the circadian rhythm maintained by the central oscillator is masked by light and the activity of the animal is decreased during a period of time that the animal would be highly active (Aschoff 1999). This could be explained by light induction of immediate early gene expression in the SCN. Subsequently SCN output is altered inappropriate to the subjective time of day masking the true circadian rhythm of the animal (Smale et al. 2003). The lack of masking taking effect in the *Kdm1a*^{E440G} mutants indicates that the central rhythm is somehow not overridden by the masking light pulse, perhaps due to the output of the central pacemaker being more robust than wild type animals (for example increased neural coupling therefore lack of elasticity in SCN activity), or perhaps due to differences in non-image forming retinal processing. A deficit in retinal function would be expected to cause impairment of the pupillary light response. As pupillometry

measurements were no different between *Kdm1a*^{E440G} mutants and controls (except for a slight impairment in the first trial) the photoreception of the light pulse is unlikely to contribute to this effect (Figure 5.11). The mutation is therefore more likely affecting a process downstream of the light detection event where PLR and phase resetting mechanisms diverge. The precise molecular events subsequently evoked in the SCN such as IEG up-regulation have yet to be investigated but might resolve what mechanism LSD mutation is affecting with regards the masking effect. The normal phase response following nocturnal light pulses but lack of masking makes for an interesting investigation into what part of the light-response is being affected by the *Kdm1a*^{E440G} mutation. Perhaps IEG upregulation would be expected to be intact in the animals and rather the *Kdm1a*^{E440G} mutation is affecting neural processing downstream from IEG expression (which would be different after a 3 hour masking light pulse to a 15 minute phase resetting light pulse).

5.8.3.3: Response to light pulses in LSD2 mutants

Kdm1b$^{T357M/T357M}$ animals displayed a greater shift in phase of activity than wild type animals in response to the late light pulse (Figure 5.8). The phase shift of wild type animals in this instance was unexpectedly small and could be perceived as absent in the graphical representation (Figure 5.8av). However, as multiple animals were tested the phase shift may not have been absent rather the responses of individuals averaged out to no shift. Regardless of the reason for this afrtefact, the response of the mutant animals was significantly different to wild types. Homozygous animals did not display any perturbation in response to the early light pulse (Figure 5.8), any deficit in circadian masking in response to the three hour light pulse (Figure 5.6a) or any change in pupillary light response (Figure 5.12). Although the *Cacnac1* mutant displays a similar phenotype to the *Kdm1b*$^{T357M/T357M}$ animals (Schmutz et al. 2014), the mechanism by which each mutation takes effect is different between the two models. The *Cacnac1* mutant is an L-type calcium Cav1.2 channel mutant and affects calcium signalling whereas LSD2 is an epigenetic regulator of H3K4 methylation which affects gene expression. The *Cacnac1* mutation may affect the role of the Cav1.2 channel in

depolarisation-independent calcium levels of SCN cells (Brancaccio et al. 2013) or in neuronal signalling output from the SCN (Pennartz et al. 2002). As the expression of the Cav1.2 channel is regulated by the circadian protein REV-ERBα (Schmutz et al. 2014), perhaps the regulation of LSD2 should be investigated in future to ascertain whether expression is under circadian regulation. It must also be considered that given the multiple calcium channels which exist in the mammalian brain, phase resetting at other circadian times may not be affected in the *Cacnac1* mutant due to compensation by another calcium channel (Schmutz et al. 2014). Therefore perhaps a double mutant with impaired *Kdm1a* activity should be investigated in the $Kdm1b^{T357M/T357M}$ animals to shed light on compensatory mechanisms in phase resetting. Although the consequence of disruption of LSD2 and the Cav1.2 channel may overlap, much more work is required to discern the expression of which genes are affected by the LSD2 mutant in phase resetting. Pupillary light response seemed normal in the $Kdm1b^{T357M/T357M}$ animals and therefore phase resetting is likely affected here by downstream mechanisms.

5.8.4: After effects

As the after effect screen was short, the animals were not exposed to a 12:12 T cycle. Free running data after 12:12 LD was taken from a different cohort of animals. As the free-running period of animals following 12:12 LD was much shorter than both the wild type and homozygote response to either short or long T-cycles, the T-cycle 'after effect' response was not observed and could not be statistically compared to 12:12 aftereffects. The aftereffect responses to long and short T-cycles was compared within the single cohort in order to observe any differences in mutant animals. No difference was observed ($p= 0.41$), and the response recorded cannot be assumed to be due to aftereffect reaction to T-cycles.

Circadian after effects are long term changes in free running period which last for weeks after light exposure (Pittendrigh & Daan 1976). The mechanism by which after effects are so persistent has been hypothesised to be mediated by epigenetic mechanism such as DNA methylation as epigenetic

modifications are longer lasting than protein modification (Beaule & Cheng 2011). It has previously been shown that epigenetic modification including DNA methylation contributes to circadian effects as a result of entrainment to short or long T-cycles (Azzi et al. 2014), and as such an epigenetic modifier such as LSD1 could play a role in this mechanism. C57BL/6 animals can entrain to rhythms of various lengths outside of a normal 24 hour cycle, the mechanism by which clocks have evolve d such lability may be attributed to period lengths of clocks in the absence of external light dark cycles (Roenneberg et al. 2010). Animals treated with zebularine to inhibit DNA methyltransferase activity display lack of aftereffects upon exposure to long and short T-cycles (Azzi et al. 2014). The lack of change seen in mutants in this investigation may suggest that the after effects screen was not effective. Alternatively, LSD function does not impinge on this mechanism or the mutations investigated in the current investigation do not perturb this aspect of LSD1 and LSD2 function. Other protocols used in published after-effect experiments were different to the protocol used in the current investigation. The age of animals used here was 42 days whereas 30 day-old animals were used previously (Azzi et al. 2014). Animals were allowed to entrain to 24 hour rhythms before entraining fully to the 22 hour T-cycle in the Beaule et al. paper whereas animals could not be held in circadian apparatus long enough to allow for this in the current study due to on-site regulations. Animals were also left in the T-cycle until fully entrained (Beaule & Cheng 2011, Azzi et al. 2014), which was also beyond the scope of the current experiment; clearly neither mutant nor wild type animals entrained to short T-cycles before DD (Figures 5.9a, 5.10a) which might explain why no after-effects were observed in the current experiment. Another notable difference between the current work and published works is that long T-cycles were 26 hours long (13:13) (Azzi et al. 2014) and 25 hours long (12:13) (Beaule & Cheng 2011); shorter than the 28 hour T-cycles used here. Animals entrain faster and better to T-cycles closer to their endogenous period (Bunning 1973), but in my experiment the *Kdm1a*$^{E440G/E440G}$ females entrained to 28 hour T-cycles within the 2 weeks allowed for entrainment and all animals subsequently tested appeared to entrain well. If a longer after-effect screen were able to be undertaken (animals kept in wheel-running chambers for longer)

and mutant after effects were not significantly altered, there may exist a redundancy in this mechanism. Perhaps LSDs role is fulfilled by a compensatory demethylase or a subsequent downregulation in methyltransferase expression.

5.8.5: *Ex Vivo*

Time-course RNA expression data from liver and SCN tissues extracted from *Kdm1a*^{E440G} animals was analysed to assess the impact of the mutation on circadian gene expression in the periphery and the central pacemaker. It was observed in liver samples that homozygous animals demonstrated normal levels of core clock gene expression, although the oscillation of *Cry1* expression was statistically significantly perturbed (p=0.03) (Figure 5.13). Upon closer examination, *Bmal1* expression appears advanced in mutant liver consistent with the shift in *Cry1* expression. The peak of *Dbp* expression was narrowed in mutant liver, and *Dbp* expression was significantly lower than wild type expression at ZT7 (p=0.00001)(Figure 5.13). With regards the central pacemaker, SCN samples were found to be of low quality and as such the data used in the expression profile of clock genes was too sparse to conclude any statistically robust expression changes from.

In preliminary work, the Reinke lab showed that in overexpressing NIH-3T3 cells expression of *CLOCK, Bmal1, Cry2, Per2, Dbp, Ror*α and *Rev-erb*α was dampened by the *Kdm1a*^{E440G} mutation, and *Cry2, Per2, Dbp* and *Ror*α were downregulated whilst the expression of *CLOCK* and *Bmal1* was upregulated by the *Kdm1a*^{L491H} mutation (Personal Communication Dr H. Reinke, Uni Düsseldorf, Ge). In the Reinke lab, *Kdm1a*$^{-/-}$ MEFs showed subtle shifts in the expression of negative limb genes (*Cry1, Cry2, Per1, Per2*) and *Dbp* expression but no change in *LSD2* or *Bmal1* expression in unsynchronised cells (Figure 3.3). In published work, SCN tissue from *Kdm1a*$^{SA/SA}$ mutants displayed decreased expression of *Per2, Rev-erb Cry1* and *Cry2* but no change in *Bmal1* expression (Nam et al. 2014). The authors of this paper suggested that perhaps LSD1 was involved in the regulation of the clock genes with promoters which contain E-box sequences, and that *Bmal1* expression was unaffected because its promoter instead contains a ROR element (Nam et al. 2014). Results from

these two experiments do not concur with one another, the Reinke group work does not support the hypothesis postulated in the Nam et al. paper. The current findings show that the expression of *Dbp, Bmal1, Cry1* and *Per1* in liver *in vivo* were not increased for *Kdm1a*$^{E440G/E440G}$ mutants in comparison to wild type animals. The above results may be considered unexpected as H3K4 methylation is a marker of gene activation so LSD1 disruption would be predicted to increase gene expression if demethylase activity is perturbed, which would be expected in knockout MEFs. The differences between results from these experiments can be attributed to differences in the sources of RNA and the differences between the three models of LSD1 disruption. The current investigation of the *Kdm1a*$^{E440G/E440G}$ mutant liver gene expression indicate that the mutation alters the expression of specific circadian genes but the mechanism behind the change in expression is complex and has yet to be fully elucidated.

The changes in circadian gene expression in liver may indicate a role for LSD1 in peripheral clocks, although the SCN data was of too low quality to statistically analyse. Further tests with higher sample numbers would be required to test the effect of mutations on the pacemaker as in previously published work, for example 10 SCNs were used to quantify gene expression at each timepoint in the investigation of cycling transcripts by real time PCR (Panda, Antoch, et al. 2002). Alternatively fewer samples could be used (n=3-4) but expression quantified by in situ hybridisation (DeBruyne et al. 2007a).

If addition of more SCN tissue to the analysis still did not reveal a statistically significant role for LSD1 in regulating pacemaker rhythms and its expression effects were limited to peripheral tissue such as liver, it may disrupt clock genes in a tissue specific manner or be non-essential for circadian function. For example, in fibroblasts both knockdown of CLOCK-interacting protein, Circadian (*Cipc)* and overexpression cause significant period changes and the CIPC protein has been shown to interact with CLOCK and repress CLOCK:BMAL-mediated E-box transactivation in yeast two-hybrid screens (Zhao et al. 2007). In vivo, however, knockout of *Cipc* was shown to disrupt *Per1* expression in liver

but not lung or adipose tissue (so not be essential for peripheral clock oscillation), and has no circadian phenotype *in vivo* (Qu et al. 2015). Similarly, manipulation of LSD genes in fibroblasts elicit significant changes to period (Chapter 3), LSD1 and LSD2 have been shown to interact with core clock proteins (Chapter 5) and change gene expression in multiple different ways in different tissues and systems (Figure 5.13, Personal Communication Dr H. Reinke, Uni Düsseldorf, Ge) (Nam et al. 2014). Therefore perhaps similar to CIPC, LSD1 does not play an essential role in circadian mechanisms. LSD1 expression levels are the same in $Kdm1a^{E440G/E440G}$ and $Kdm1a^{+/+}$ animals (Figure 5.13) and as such the overexpression of the mutant construct in NIH-3T3 may contribute to the decrease in circadian gene expression when compared to overexpression of wild type constructs. The differences between the *in vivo* and *in vitro* findings for $Kdm1a^{E440G}$ mutation are consistent with multiple other circadian mutants such as the *Per1-/-* mutant (where clock gene expression in the SCN is profoundly dampened but *in vivo* the animals are rhythmic (Pallier et al. 2007). Such discrepancies are discussed in more depth in later chapters (Section 8.5.4).

The lack of increase in circadian gene expression observed in the case of liver *Dbp* expression and the previous results would not be expected of a knockdown of LSD1 demethylase activity as a knockdown would be predicted to show increased methylation of H3K4 which is a marker of gene activation. This means the effect of the $Kdm1a^{E440G}$ mutation on circadian gene expression in liver (and perhaps SCN which would require analysis of more samples to truly ascertain) may be attributed to demethylase-independent mechanisms.

Ex vivo SCN slices taken from $Kdm1a^{E440G/E440G}$ animals showed no obvious difference in amplitude, phase or period of *Per2*:Luc oscillation. The *Per2*:Luc bioluminescent recording from such slices indicates whether the mutation altered SCN behaviour directly. As no change was observed, phenotypes could be attributable to a change in SCN function downstream of core clock oscillation (perhaps output pathways are affected or synchrony across the cells of the SCN for example), or

perhaps due to alterations of peripheral clock mechanisms; the SCN unaffected by *Kdm1a*^{E440G} mutation.

In the Nam et al. paper, in a similar experiment utilising slices from a *Kdm1a*$^{SA/SA}$ mutant crossed to mPer2:Luc reporter animal line, mutant slices showed a dampened amplitude of *Per2* oscillation (Nam et al. 2014). This decrease in oscillation was consistent with the decrease in *Per2* gene expression in mutant SCNs (Nam et al. 2014). The lack of change in amplitude in the current investigation is consistent with the lack of change in circadian gene expression observed in time course RNA analysis of SCN tissue (Figure 5.13). If LSD1 is playing a role in the pacemaker, the *Kdm1a*^{E440G} mutation is not disrupting this role *in vivo*, or alternatively it is compensated for. Investigation of more slices would be informative given time to generate a large cohort of animals.

As subtle circadian phenotypes were established in LSD mutants, and LSD genes are expressed in the brain, neurobehaviour was next investigated *in vivo*.

Chapter 6

LSD1 AND LSD2 BEHAVIOURAL AND HISTOLOGICAL PHENOTYPES

CHAPTER 6: LSD1 and LSD2 Behavioural and Histological Phenotypes

6.1: Introduction

Kdm1a$^{E440G/E440G}$ and *Kdm1b*$^{T357M/T357M}$ animals were examined for any behavioural abnormalities. LSDs play multiple roles in development, cell cycle and neural function which could contribute to a wide range of phenotypes. *Kdm1a* and *Kdm1b* are both expressed in tissues from all stages to adulthood which may contribute to adult phenotypes. Therefore a battery of behavioural tests was undertaken to characterise the effect of LSD mutations.

Kdm1a is expressed throughout development, ubiquitously in *Drosophila melanogaster* (Di Stefano et al. 2007) and generally through anterior tissues including neural progenitor areas in *zebrafish* (A. Li et al. 2012). LSD1 plays an essential role in gastrulation, and knockout of *Kdm1a* is lethal at e6.5 (Macfarlan et al. 2011). LSD1 also plays multiple regulatory cell-cycle and differentiation roles (Nair et al. 2012; Foster et al. 2010; Whyte et al. 2012; Amente et al. 2013) (Section 8.5.8). *Kdm1b* is expressed in the oocyte so is involved in early development but expression tapers by e7.5 (Ciccone et al. 2009). *Kdm1b* is known to play a role in imprinting (Ciccone et al. 2009).

In adults, *Kdm1a* is expressed ubiquitously and has been implicated in cell cycle regulation, being upregulated in various cancers (Nair et al. 2012). In adults, *Kdm1b* displays a more restricted expression profile. *Kdm1b* expression is high in oocytes and the intestine (Ciccone et al. 2009) and expressed at low levels in the brain (MGI website)

LSDs may play a role in neuropsychiatric behaviour of adult animals. This could be through the regulation of neural development (Fuentes et al. 2012; Han et al. 2014), or though LSD activity in the adult brain. The amine oxidase domain shared by LSD1 and LSD2 is a target inhibited by the action of monoamine oxidase inhibitors (MAOIs) such as tranylcypromine (Binda et al. 2010). MAOIs are a class of antidepressant drug which are known to inhibit MAO-A and MAO-B (both expressed in the brain). MAO inhibition in the brain decreases the breakdown of synaptic monoamines. The

disruption of monoamine systems including primarily dopamine is associated with disorders on the depression spectrum (Dunlop & Nemeroff 2007). The contribution of LSD inhibition to the therapeutic effect of MAOIs such as tranylcypromine is unknown, and therefore we felt that the effects of LSD mutations on neurobehaviour was worth investigating.

All mutant animals were also observed to be hyper-responsive to handling so any behavioural disruption which could explain this was also analysed in depth (H. Shepherd, Dr G. Banks and multiple independent handlers, personal observation).

6.2: Behavioural Phenotyping

6.2.1: Motor behaviour *Kdm1a*$^{E440G/E440G}$

To assess for gross motor or behavioural traits, animals were phenotyped by SHIRPA as described previously (Rogers et al. 2001). *Kdm1a*$^{E440G/E440G}$ showed no motor problems, only defaecating more than controls and holding a slightly higher tail position (Figure 6.1). This may be due to increased anxiety in a novel environment which may relate to the animals hyperresponse to handling.

To check for normal wellbeing and behaviour which might indicate baseline anxiety or withdrawal from the environment, digging and marble-burying behaviour was tested in a safe environment mimicking the home cage. Animals feeling unwell, anxious or depressed can display decreased propensity to dig in both tests (Deacon 2006b). Marble burying has been used as a test of neophobia and compulsive behaviour (Shinomiya et al. 2005). In marble burying and digging tasks, *Kdm1a*$^{E440G/E440G}$ animals performed as well as wild type animals (Figure 6.2).

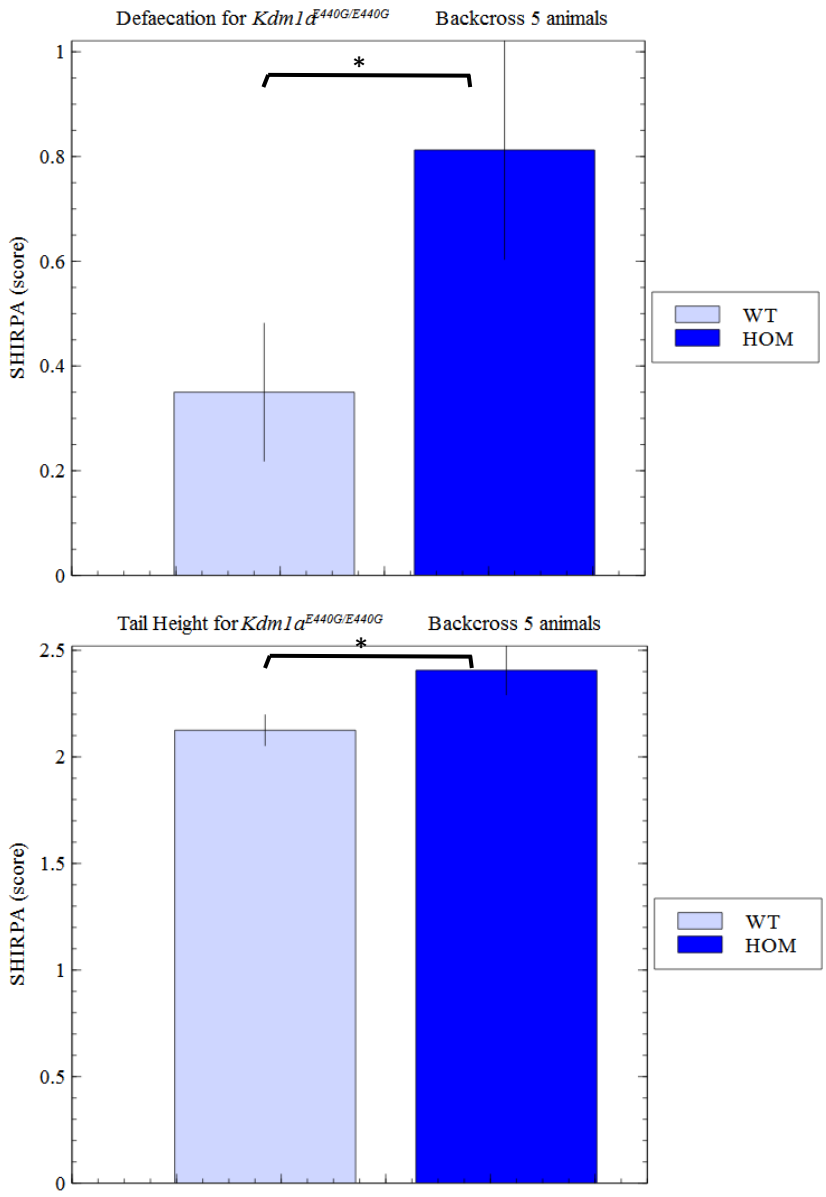

Figure 6.1: SHIRPA analysis revealed changes in defaecation and tail height in *Kdm1a*$^{E440G/E440G}$ animals

The two significant differences found in SHIRPA analysis between homozygote and wild type animals were in the amount of defaecation (homozygotes excreting twice as much (0.81 ±0.21)as wild types (0.35 ±0.13) p=0.059) and in the height of the tail when moving (2.41 ±0.11 for homozygotes, 2.13 ±0.07 for wild types p=0.037).

N=20 wild type and n=20 homozygote *Kdm1a*^{E440G} backcross 5 intercross animals. SHIRPA data was analysed by Mann Witney U test for non-parametric data. (*p<0.05, **p≤0.005, ***p≤0.001)

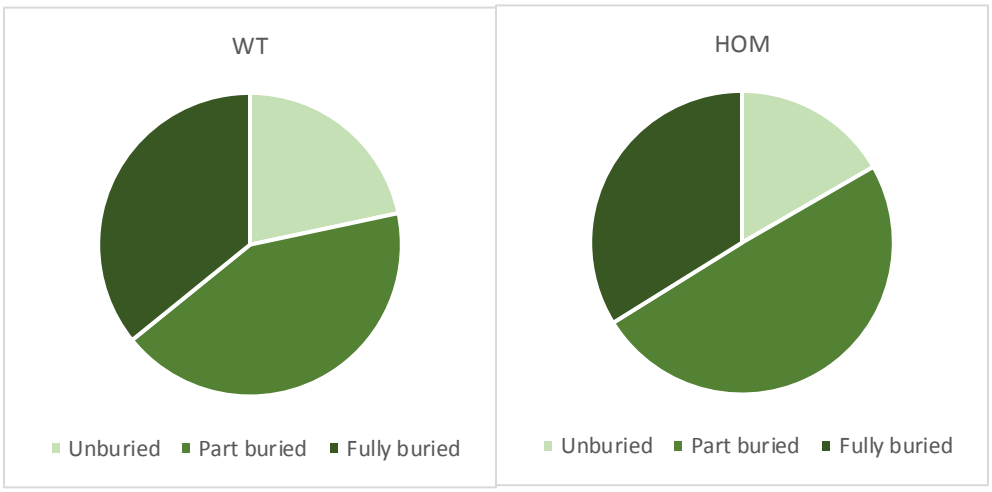

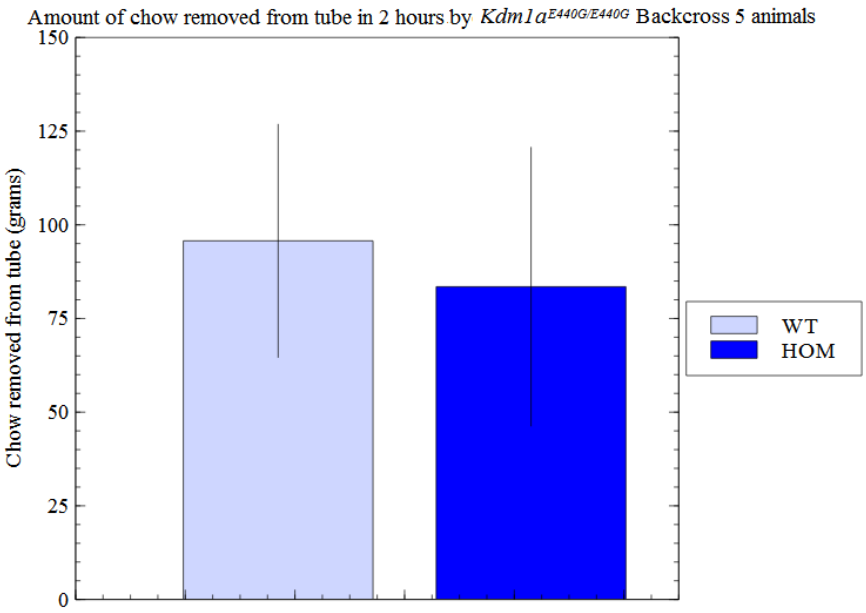

Figure 6.2: *Kdm1a*$^{E440G/E440G}$ mutant performance in marble burying and digging tests of wellbeing

Kdm1a$^{E440G/E440G}$ mutant animals performed similarly to wild types burying the same number of marbles on average (9.4 ±0.62 of 12 in the case of wild type animals, and 8 ±1.10 for homozygotes p=0.77182) and digging the same amount of chow from the tube (95.7g ±31.0 from the original 180g for wild type animals, 83.5g ±37.1 for homozygotes p=0.960).

N=20 wild type and n=20 homozygote *Kdm1a*^{E440G} backcross 5 intercross animals. Both tests were analysed with using Mann-Whitney U test for non-parametric data

6.2.2: Motor behaviour *Kdm1b*$^{T357M/T357M}$

Kdm1b$^{T357M/T357M}$ animals showed no gross motor defect during SHIRPA assessment. 50% of animals did display a deficit in ability to right themselves (Figure 6.3), perhaps due to vestibular problems which need much more in depth assessment (Section 8.6).

Kdm1b$^{T357M/T357M}$ mutant animals displayed no change in digging activity (Figure 6.4), so appear not to display a baseline level of anxiety or withdrawal from the environment.

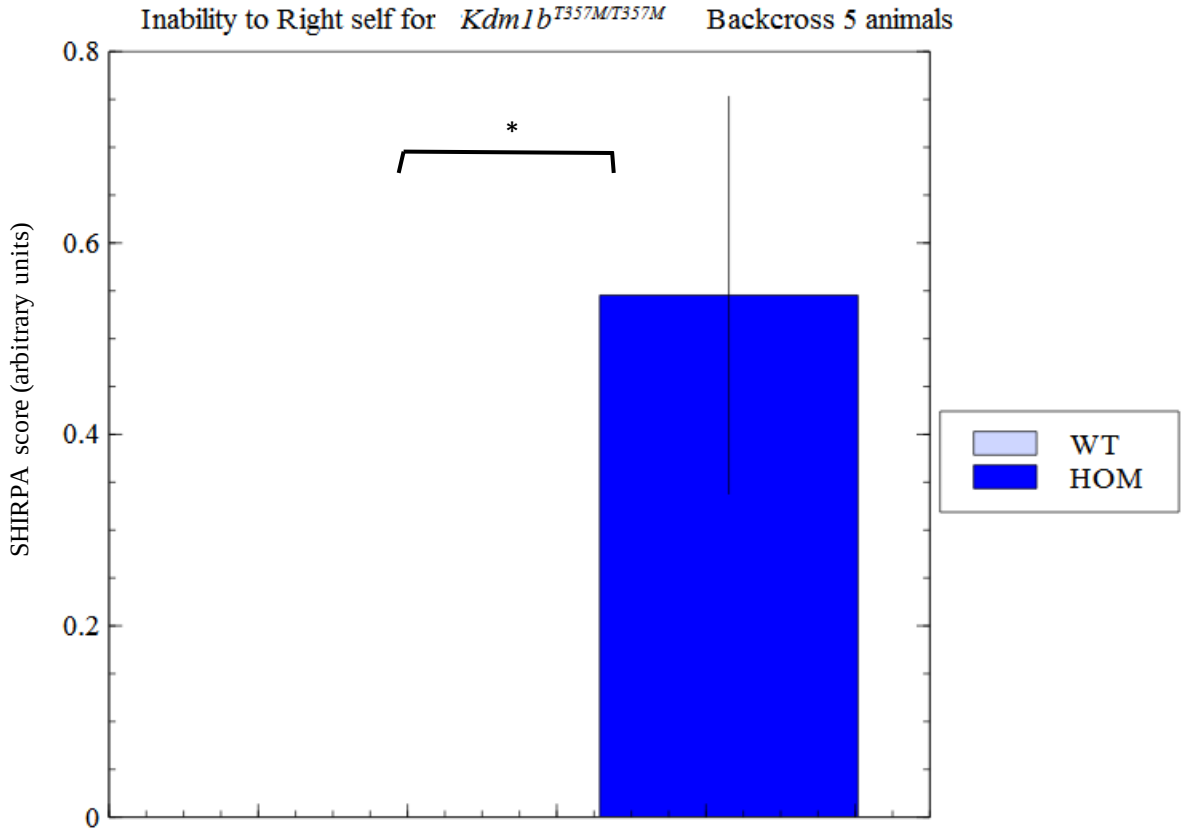

Figure 6.3: Performance of *Kdm1b*$^{T357M/T357M}$ animals in the contact righting reflex task

Kdm1b$^{T357M/T357M}$ animals were less able to right themselves in the contact righting reflex task (score 0.55 ±0.21 for homozygotes, 0.00 ±0.00 for wild type) p=0.038)

N=10 wild type and n=10 homozygote *Kdm1b*^{T357M} backcross 5 intercross animals. Contact righting data was analysed by median test for nonparametric scale data. (*p<0.05, **p≤0.005, ***p≤0.001)

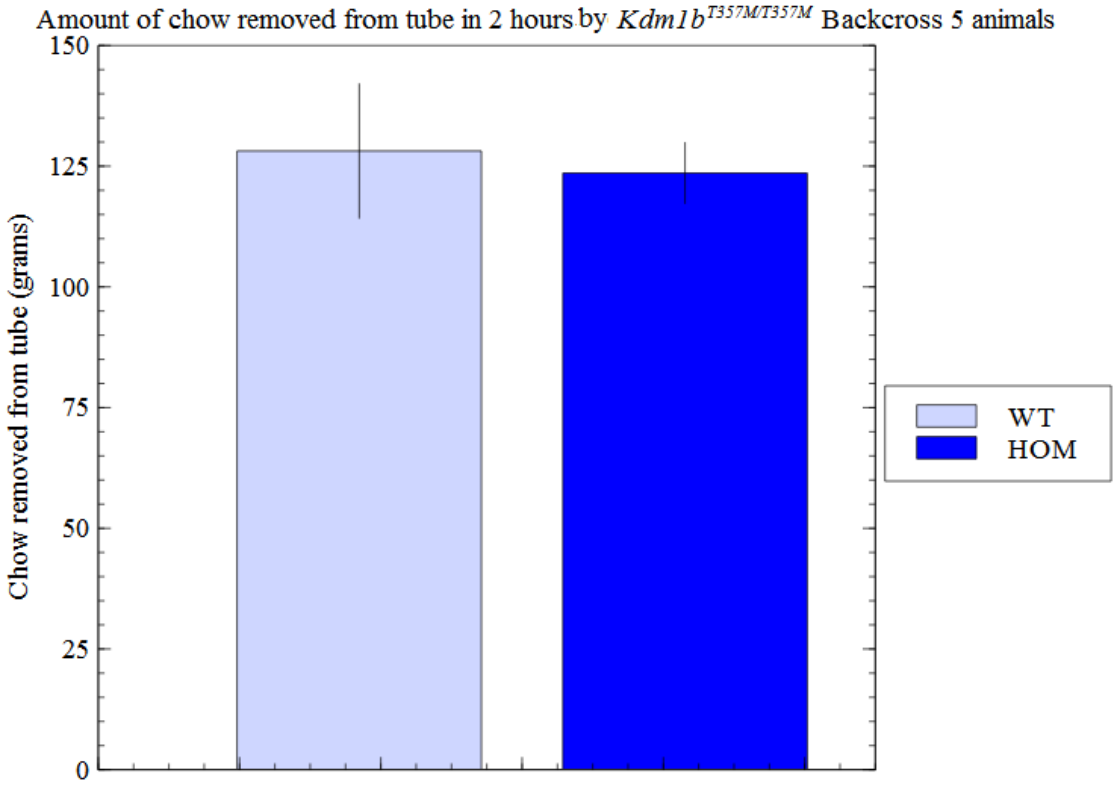

Figure 6.4: *Kdm1b*$^{T357M/T357M}$ animal performance in the digging test for wellbeing

Kdm1b$^{T357M/T357M}$ removed the same amount of chow as *Kdm1b*$^{+/+}$ s from the tube in the two hour test (123.6g ±6.2 for homozygotes, 128.2g ±13.9 for wild type p=0.748)

N=10 wild type and n=10 homozygote *Kdm1b*^{T357M} backcross 5 intercross animals. Digging data analysed by student T test.

6.2.3: Cognition and anxiety Phenotypes *Kdm1a*$^{E440G/E440G}$

Kdm1a$^{E440G/E440G}$ homozygotes displayed a trend towards less alternation than controls on the T-maze alternation test (Figure 6.5). This is suggestive of a decreased cognitive ability, although not statistically significant. The *Kdm1a*$^{E440G/E440G}$ homozygotes alternate in 52% of trials, similar to the frequency expected if the arms were chosen completely by chance. This would indicate a learning deficit with respect homozygous animals. C57BL/6 animals have previously been shown to alternate approximately 75% of the time in apparatus such as that used (with a central partition) (Deacon & Rawlins 2005), but in this investigation wild type animals only alternated 67% of the time. This is likely to be attributable to a secondary spatial cue being at play which could either affect the animals' inclination to enter one arm or other or unknowingly increase anxiety. In this instance for example, a set of noises, smells or visual clues might be present which were not able to be eliminated from the experimental set up (Bertholet & Crusio 1991). Alternatively, the level of spontaneous alternation might be affected by background effects as alternation rates vary between inbred lines (Deacon & Rawlins 2006; Bertholet & Crusio 1991).

Kdm1a$^{E440G/E440G}$ animals performed similarly to wild type in the open field arena in most parameters measured with the exception of displaying a decreased latency to enter the centre of the arena on the habituation trial (Figure 6.6). A decrease in latency to enter the middle of the arena could be due to decreased anxiety or hyperactivity or a cognitive phenotype.

Alternatively, the cognition phenotype revealed by spontaneous alternation testing (Figure 6.5) supports the hypothesis that the homozygotes fail to learn from or remember the first trial and as such latency is not increased like wild type animals. On the other hand, homozygotes do spend less time in the centre in trial 2, so perhaps the phenotype is not due to a lack of cognitive ability.

Fear conditioning tests the animals response to a mild electric shock paired with an audible tone over multiple trials. In the conditioning trial, animals are placed in an arena and exposed to the shock and tone (a conditioning trial). The next trial exposes the animals to an arena which resembles

the shock chamber but without any auditory cue or shock (a context trial) and finally animals are tested in a completely different arena, again with no shock but exposed to the auditory cue (a cue trial). In fear conditioning tests, *Kdm1a*$^{E440G/E440G}$ mutants tended to freeze less in response to the foot shock during conditioning (p=0.42), and also not to freeze as much as wild type animals in the context trial (p=0.057) whereas no difference was observed in the cue trial (Figure 6.7). This trend would suggest a decrease in ability to remember the context of the conditioning trial, or a decrease in anxiety experienced upon exposure to the context of the experiment (surroundings).

A final test encompassing anxiety to examine the agitated nature of the *Kdm1a*$^{E440G/E440G}$ animals was to expose them to confrontation with another animal in the social dominance paradigm. Social dominance tests the social behaviour of the animals, but anxious animals would be expected to react to social confrontation in a different way, for example by reversing out of the trial (which discounts the 'win' of that trial from the final analysis). Anxiety could be caused by social anxiety or anxiety in enclosed spaces. There was no significant difference between the number of wins for control animals compared to *Kdm1a*$^{E440G/E440G}$ (Figure 6.8b). However, in the case of *Kdm1a*$^{E440G/E440G}$ when results from individual animals was considered it became evident that certain mutant individuals appeared to act aggressively and win most of their trials, whereas others backed away nullifying the result in analysis (Figure 6.8a). The number of trials backed out of was nearly significantly higher than for wild type animals (Figure 6.9).

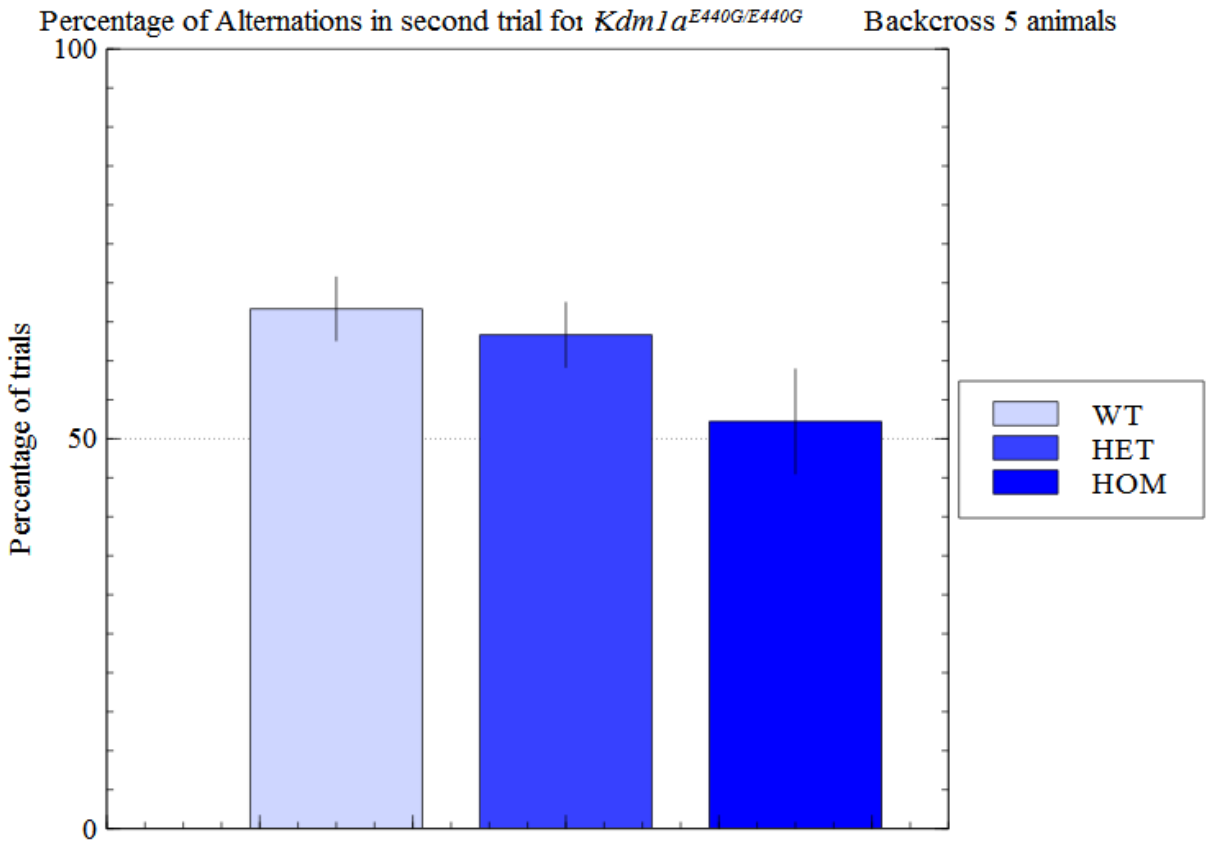

Figure 6.5: Spontaneous Alternation in *Kdm1a*$^{E440G/E440G}$ animals

Homozygous *Kdm1a*$^{E440G/E440G}$ animals display a lower alternation rate than wild types at just 52%. This is similar to the 50% rate expected of a chance choice of arm (66.6% ±4.04 alternation for wild type animals, and 52.2% ±6.68 for homozygotes, p=0.067). This indicates a near significant lack of learning or memory of the first trial.

N=20 wild type, n=20 heterozygote and n=20 homozygote *Kdm1a*^{E440G} backcross 5 intercross animals. Data was analysed by student T test.

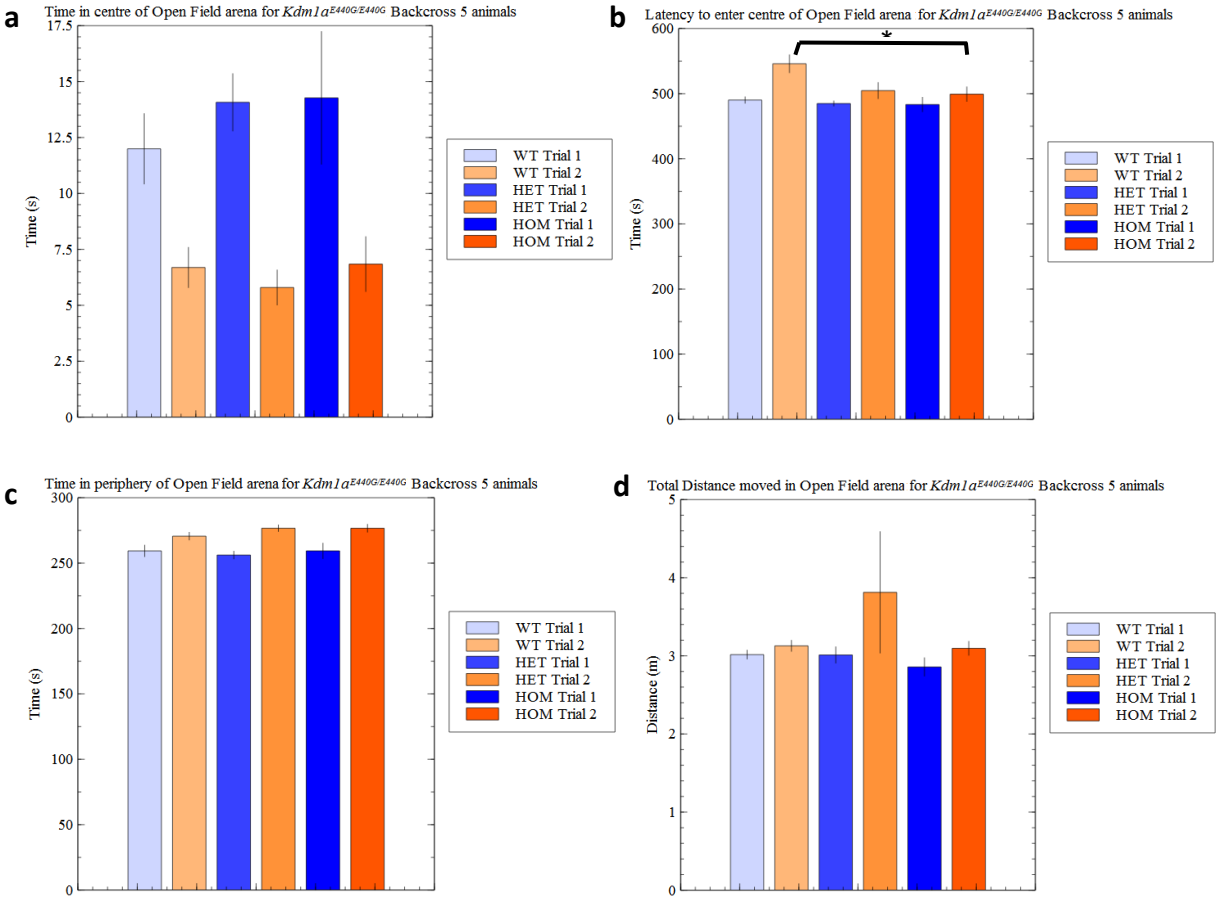
a
Time in centre of Open Field arena for Kdm1a E440G/E440G Backcross 5 animals
Time (s)
17.5
15
12.5
10
7.5
5
2.5
0
WT Trial 1
WT Trial 2
HET Trial 1
HET Trial 2
HOM Trial 1
HOM Trial 2
b
Latency to enter centre of Open Field arena for Kdm1a E440G/E440G Backcross 5 animals
Time (s)
600
500
400
300
200
100
0
*
WT Trial 1
WT Trial 2
HET Trial 1
HET Trial 2
HOM Trial 1
HOM Trial 2
c
Time in periphery of Open Field arena for Kdm1a E440G/E440G Backcross 5 animals
Time (s)
300
250
200
150
100
50
0
WT Trial 1
WT Trial 2
HET Trial 1
HET Trial 2
HOM Trial 1
HOM Trial 2
d
Total Distance moved in Open Field arena for Kdm1a E440G/E440G Backcross 5 animals
Distance (m)
5
4
3
2
1
0
WT Trial 1
WT Trial 2
HET Trial 1
HET Trial 2
HOM Trial 1
HOM Trial 2

Figure 6.6: Performance of *Kdm1a*$^{E440G/E440G}$ animals in the open field

Kdm1a$^{E440G/E440G}$ animals behave similarly to wild type animals, moving a similar total distance and spending the same amount of time in the centre and periphery. Animals do not display a change in latency to enter the centre of the arena in the second trial after habituation in the first trial, this is different to the delay in entry to the centre observed upon habituation of wild type animals.

a) Time spent in central area (11.99 s ±1.56 for wild type and 14.27 s ±2.96 for homozygotes p=0.478 for trial 1 and 6.69 s ±0.89 for wild type and 6.84 s ±1.22 for homozygotes p=0.919 for trial 2)

b) Latency to enter central area (490.24 s ±4.78 for wild type and 483.36 s ±10.94 for homozygotes for trial 1 and 545.99 s ±13.62 for wild type and 499.29 s ±11.04 for homozygotes for trial 2) (ANOVA performed on reciprocal of latency to normalise data distribution p=0.00225 indicates an interaction between trial and genotype, and p=0.5237 comparing *Kdm1a*$^{+/+}$ and *Kdm1a*$^{E440G/E440G}$ animals latency in trial 1, and p=0.0261 for trial 2. Trial 1 and trial 2 were statistically different for *Kdm1a*$^{+/+}$ animals (p=0.0008) but not for *Kdm1a*$^{E440G/+}$ animals (p=0.0586) and less so for *Kdm1a*$^{E440G/E440G}$ (p=0.3827), suggesting a lack of cognitive ability to remember previous trials)

c) Time spent in Periphery (259.35 s ±4.31 for wild type and 259.36 s ±5.82 for homozygotes p=0.999 for trial 1 and 270.62 s ±2.85 for wild type and 276.67 s ±2.92 for homozygotes p=0.1515 for trial 2)

d) Total distance moved (3.02 m ±0.06 for wild type and 2.86 m ±0.12 for homozygotes p=0.199 for trial 1 and 3.13 m ±0.07 for wild type and 3.10 m ±0.09 for homozygotes p=0.775 for trial 2)

N=20 wild type, n=20 heterozygote and n=20 homozygote *Kdm1a*^{E440G} backcross 5 intercross animals. Data was analysed by student T test with the exception of latency to enter the central area which was analysed using two way RM ANOVA. (*p<0.05, **p≤0.005, ***p≤0.001)

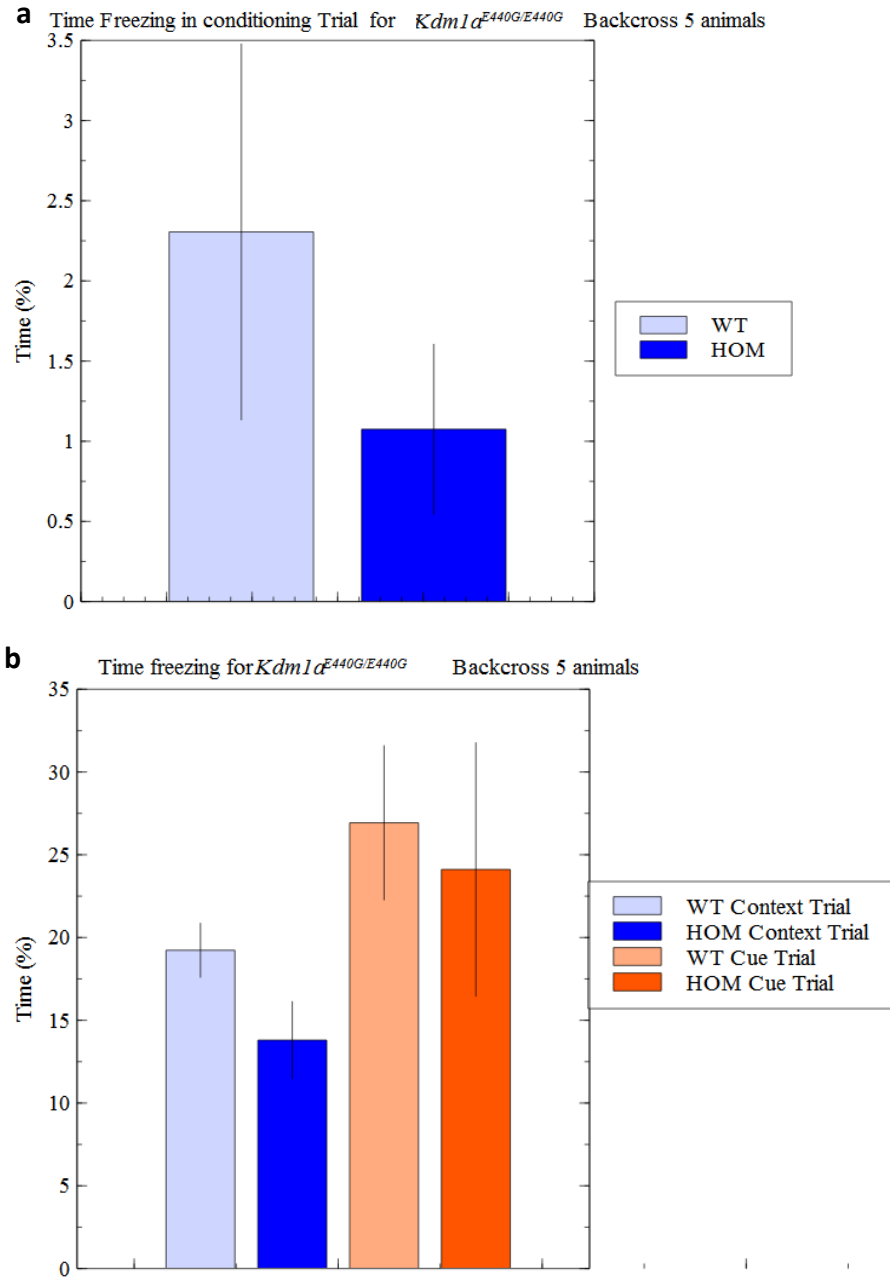

Figure 6.7: *Kdm1a*$^{E440G/E440G}$ fear conditioning

Kdm1a$^{E440G/E440G}$ animals displayed no change in baseline percentage of time freezing in response to the shock (2.31% ±1.17 for wild type and 1.07% ±0.53 for homozygotes p=0.420). Homozygotes did however freeze nearly significantly less in the context trial (in a cage similar to the test cage) (19.23% ±1.62 for wild type and 13.80% ±2.32 for homozygotes p=0.057). However, upon exposure to the cue in a novel arena, homozygous animals froze the same amount as wild types (26.93% ±4.64 for wild type and 24.11% ±7.64 for homozygotes p=0.762)

N=20 wild type and n=20 homozygote *Kdm1a*^{E440G} backcross 5 intercross animals. Data was analysed by student T test

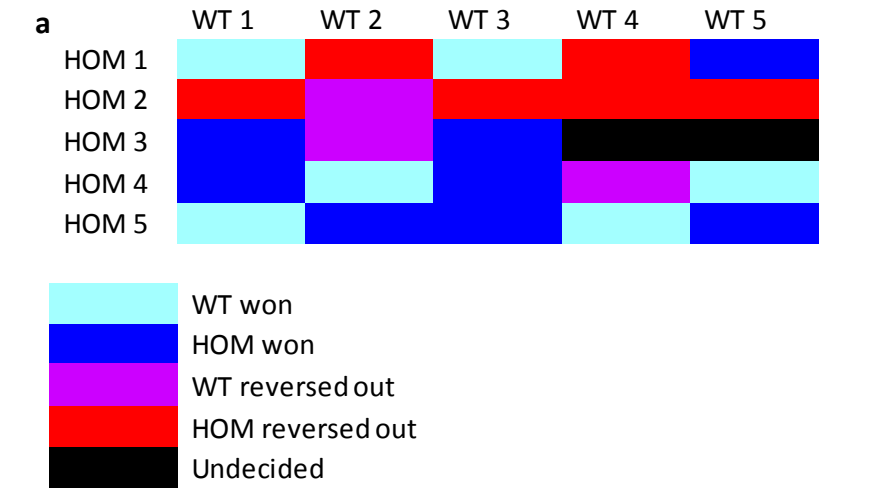

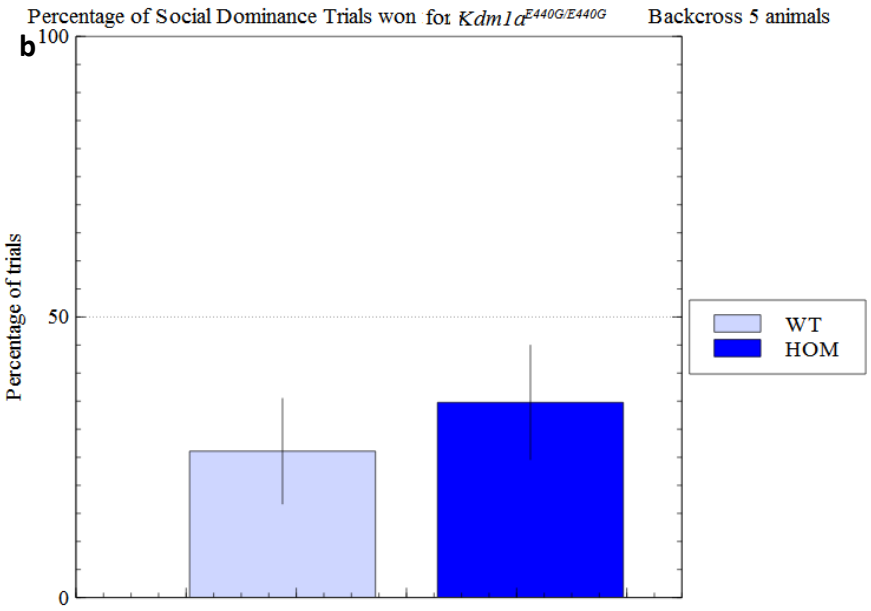

Figure 6.8: Performance of *Kdm1a*$^{E440G/E440G}$ animals in social dominance paradigm

a) Grid to show the outcome of each social dominance trial
b) Homozygous *Kdm1a*$^{E440G/E440G}$ animals won a similar amount of trials to wild type animals (p=0.16186).

N=20 wild type and n=20 homozygote *Kdm1a*^{E440G} backcross 5 intercross animals. Data analysed by student T test

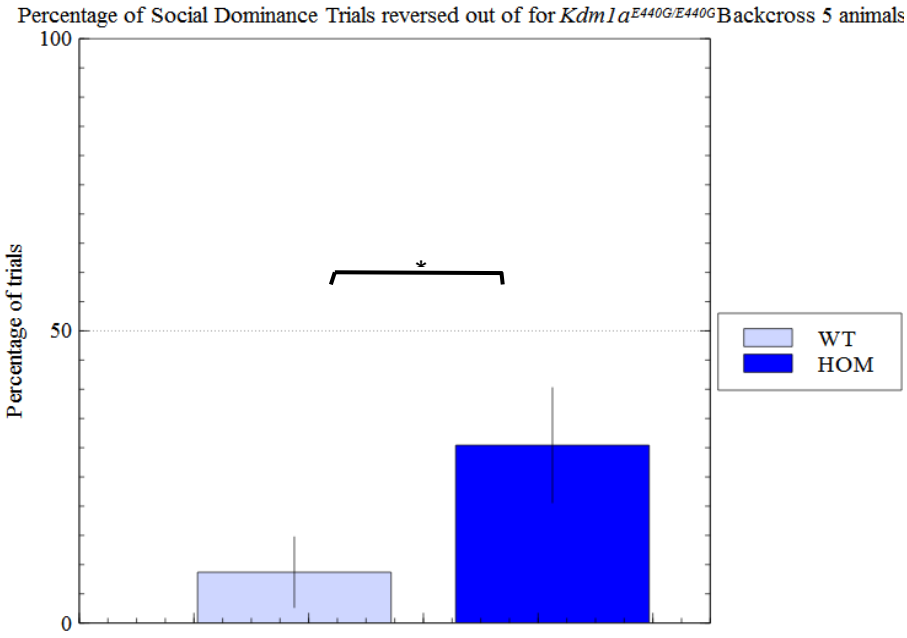

Figure 6.9: Reversal from social dominance test for *Kdm1a*$^{E440G/E440G}$ animals

Kdm1a$^{E440G/E440G}$ homozygotes were shown to reverse out of trials more frequently than wild types (30.4% ±9.81 in comparison to 8.7% ±6.01 respectively) p=0.0216.

N=5 wild type and n=5 homozygote *Kdm1a*^{E440G} backcross 5 intercross animals. Data was analysed by Chi-squared Fishers exact probability test. (*p<0.05, **p≤0.005, ***p≤0.001)

6.2.4: Cognition and anxiety Phenotypes *Kdm1b*$^{T357M/T357M}$

Kdm1b$^{T357M/T357M}$ animals did not display any change in spontaneous alternation (Figure 6.10), displaying no deficit in learning and memory. *Kdm1b*$^{T357M/T357M}$ animals performed similarly to *Kdm1b*$^{+/+}$ in the open field arena (Figure 6.11). In fear conditioning tests *Kdm1b*$^{T357M/T357M}$ animals displayed a greater response to the startle stimulus than wild type littermates (Figure 6.12). They did freeze more in the conditioning and cue trials but when considering the increase in baseline response to the shock, the animals' responses to context and cue trials did not differ from wild type (Figure 6.12). This indicates that the animals are more sensitive to the experimental protocol than control animals, but memory is intact, so do not respond differentially to the cue or context alone. There was no significant difference between *Kdm1b*$^{T357M/T357M}$ animals and controls in the social dominance test (32% of trials were won by wild type animals and 48% by *Kdm1b*$^{T357M/T357M}$ animals, p=0.402 p=0.113 by Chi-squared Fishers exact probability test).

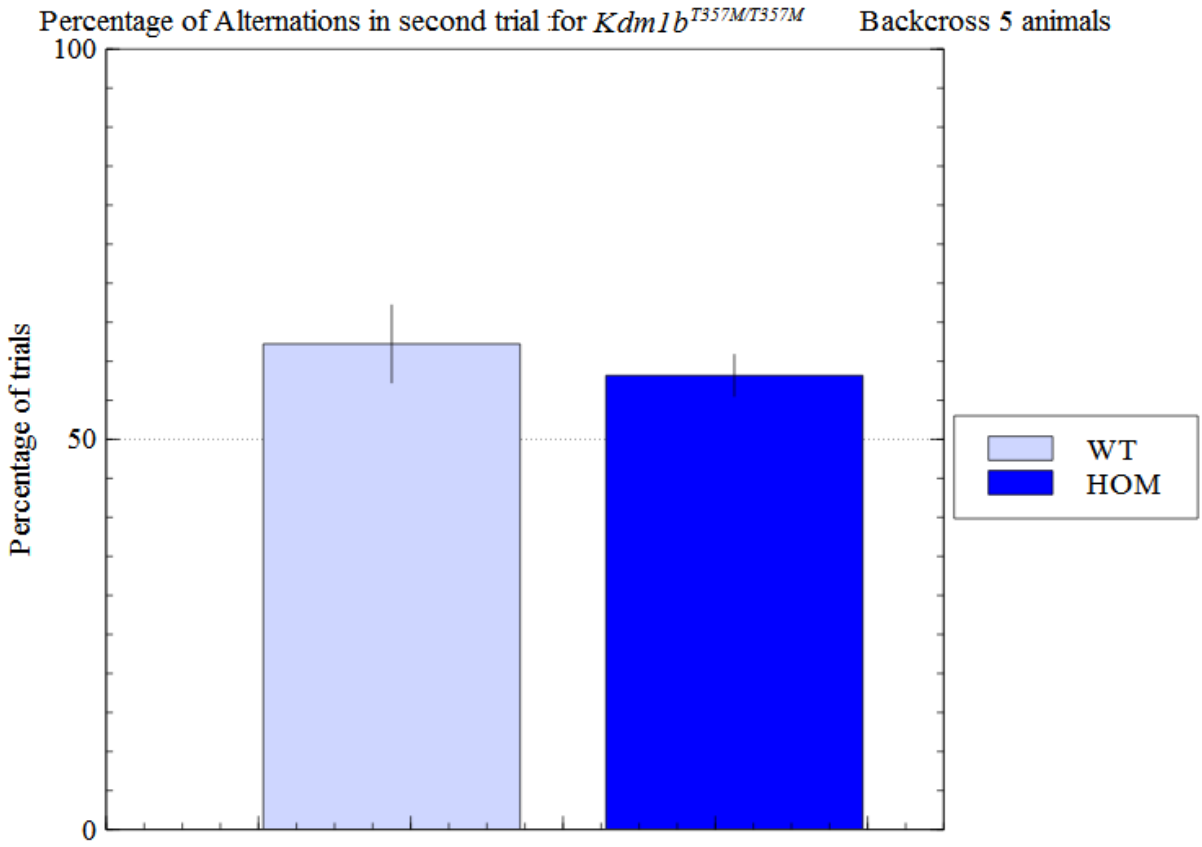

Figure 6.10: Spontaneous Alternation in *Kdm1b*$^{T357M/T357M}$ animals

Kdm1b$^{T357M/T357M}$ animals display a 58% ±2.63 similar to the 62% ±4.94 rate of spontaneous alternation observed for wild types (p=0.457).

N=10 wild type and n=10 homozygote *Kdm1b*^{T357M} backcross 5 intercross animals. Data was analysed by student T test.

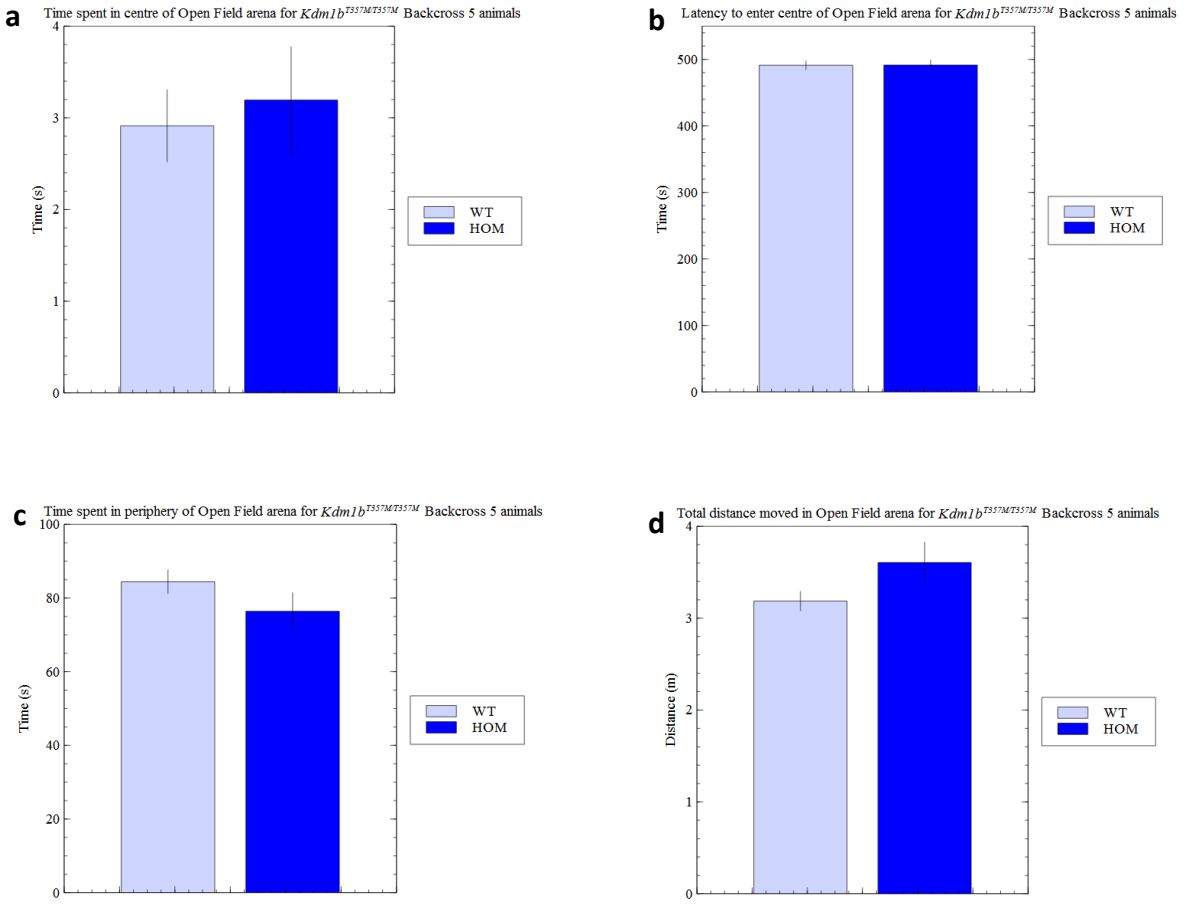

Figure 6.11: Performance of *Kdm1b*$^{T357M/T357M}$ animals in Open Field

Time spent in centre and periphery were controlled for total distance moved as it was different between groups although not significant (p=0.125)

Kdm1b$^{T357M/T357M}$ animals behave similarly to wild type animals, spending a similar proportion of time in the centre and periphery (p=0.463, p=0.903). Animals do not display a change in latency to enter the centre of the arena (p=0.710 Mann Witney U test for nonparametric data) in the second trial after habituation in the first trial, this is different to the delay in entry to the centre observed upon habituation of wild type animals.

a) Time spent in central area (29.13 s ±3.93 for wild type and 31.94 s ±5.797 for homozygotes)

b) Latency to enter central area (491.30 s ±6.23 for wild type and 491.52 s ±7.40 for homozygotes)

c) Time spent in Periphery (84.42 s ±3.18 for wild type and 76.41 s ±4.99 for homozygotes)

d) Total distance moved (3.19 m ±0.10 for wild type and 3.61 m ±0.22 for homozygotes)

N=10 wild type and n=10 homozygote *Kdm1b*^{T357M} backcross 5 intercross animals. Data was analysed by student T test with the exception of latency to enter the central area which was analysed using two way RM ANOVA.

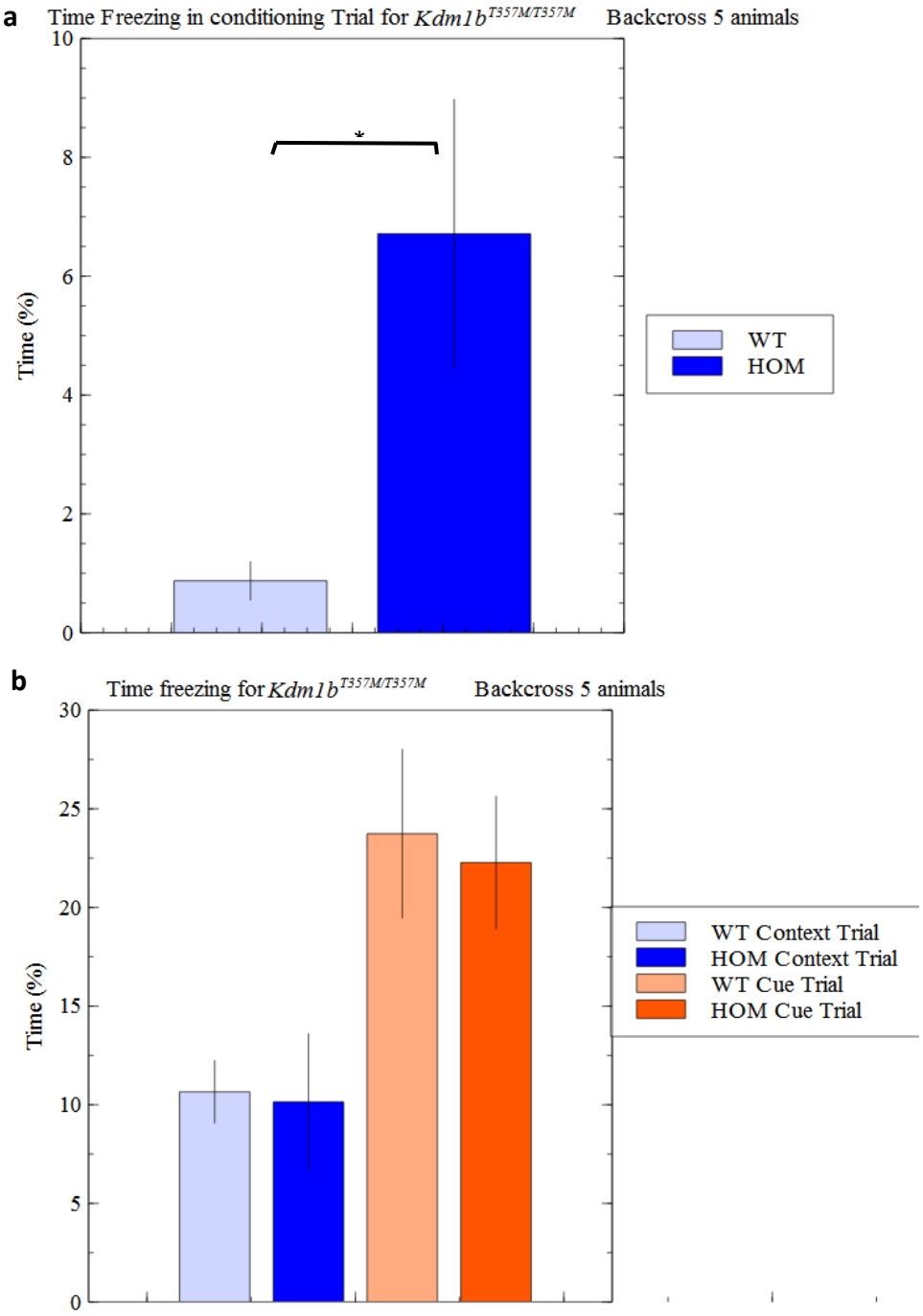

Figure 6.12: *Kdm1b*$^{T357M/T357M}$ fear conditioning

Homozygotes froze more than wild type animals in response to the foot shock (6.72% ±2.26 for homozygotes, 0.88% ±0.32 for wild types, p=0.032711). Once remaining trials were analysed correcting for this, it is apparent that fear conditioning in response to the context and the cue are intact as animals froze the same amount as wild types (in the context trial 10.14% ±3.45 for homozygotes, 10.65% ±1.57 for wild types, p=0.0969 and in the cue trial 22.28% ±3.35 for homozygotes, 23.74% ±4.26 for wild types, p=0.79272)

N=10 wild type and n=10 homozygote *Kdm1b*^{T357M} backcross 5 intercross animals. Data was analysed by student T test (*p<0.05, **p≤0.005, ***p≤0.001)

6.2.5: Acoustic Startle and Pre-Pulse Inhibition *Kdm1a*$^{E440G/E440G}$

Kdm1a$^{E440G/E440G}$ animals were tested for deficits in sensorimotor gating using the acoustic startle and Pre-Pulse inhibition (PPI) test. As the *Kdm1a*$^{E440G/E440G}$ animals are hyper-responsive when handled, it was hypothesised that they might display an increased response to the first tone (or startle response) but this was not significant (Figure 6.13a). PPI response was also comparable to controls at all volumes of pre-pulse tone (Figure 6.13b).

a

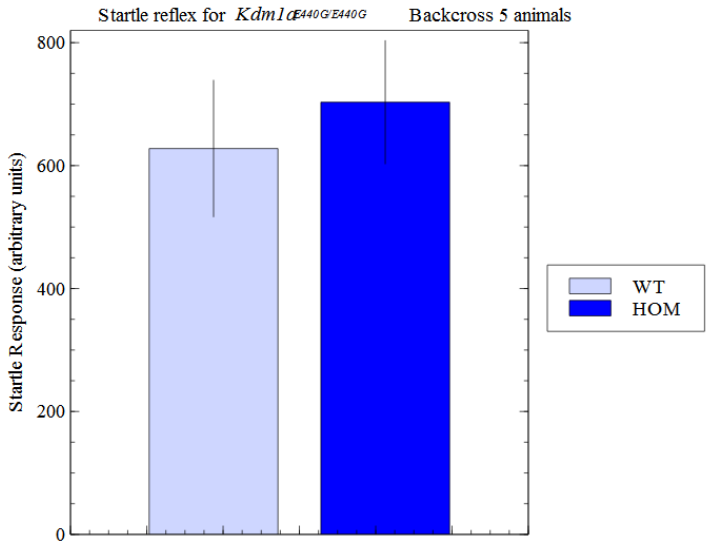

b

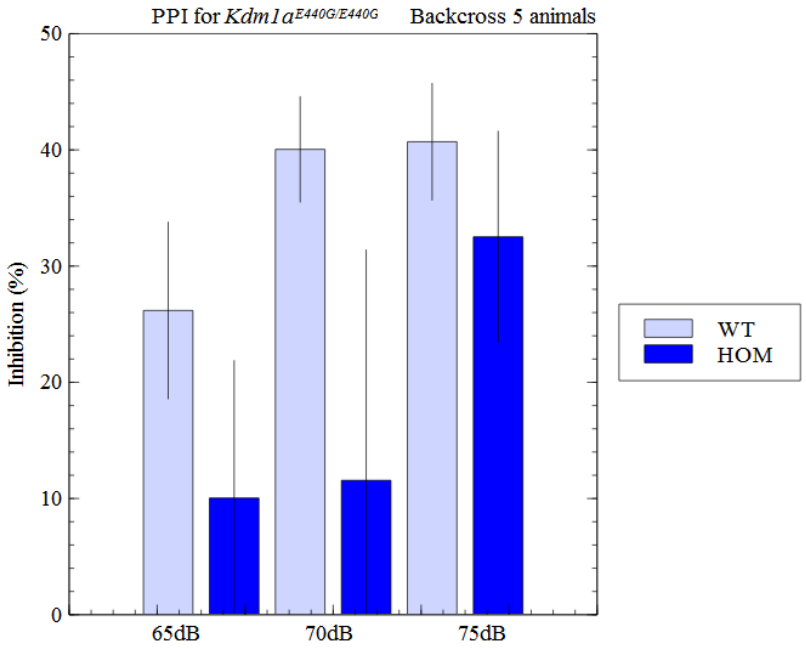

Figure 6.13: Acoustic startle and Pre-Pulse Inhibition of *Kdm1a*$^{E440G/E440G}$ animals

a) *Kdm1a*$^{E440G/E440G}$ animals display a slight increase in startle response compared to *Kdm1a*$^{+/+}$ animals (703.14 ±99.9 for homozygotes, 627.76 ±110.75 for wild types, p=0.572615).
b) *Kdm1a*$^{E440G/E440G}$ animals display a trend towards decreased PPI in each trial (for the homozygote trials 10.04 ±11.81, 11.57 ±19.81 and 32.52 ±9.07 for wild types 26.18 ±7.59, 40.04 ±4.52 and 40.70 ±5.00, p=0.257042, p=0.163747 and p=0.442009 respectively).

N=20 wild type and n=20 homozygote *Kdm1a*^{E440G} backcross 5 intercross animals. Data was analysed by student T test (*p<0.05, **p≤0.005, ***p≤0.001)

6.2.6: Acoustic Startle and Pre-Pulse Inhibition *Kdm1b*$^{T357M/T357M}$

Kdm1b$^{T357M/T357M}$ animals displayed some trends towards decreased anxiety when compared to wild type animals. A significantly decreased baseline startle response was observed (Figure 6.14a) which could be due to decreased anxiety or decreased responsiveness to the auditory stimulus (perhaps mild deafness). In the SHIRPA assessment, *Kdm1b*$^{T357M/T357M}$ animals' response to clickbox was normal so the animals are not profoundly deaf. *Kdm1b*$^{T357M/T357M}$ animals display a trend towards decreased inhibition in response to the pre-pulse although this is not a significant phenotype (Figure 6.14b). This might be due to mild hearing problems, or due to deficits in PPI gating.

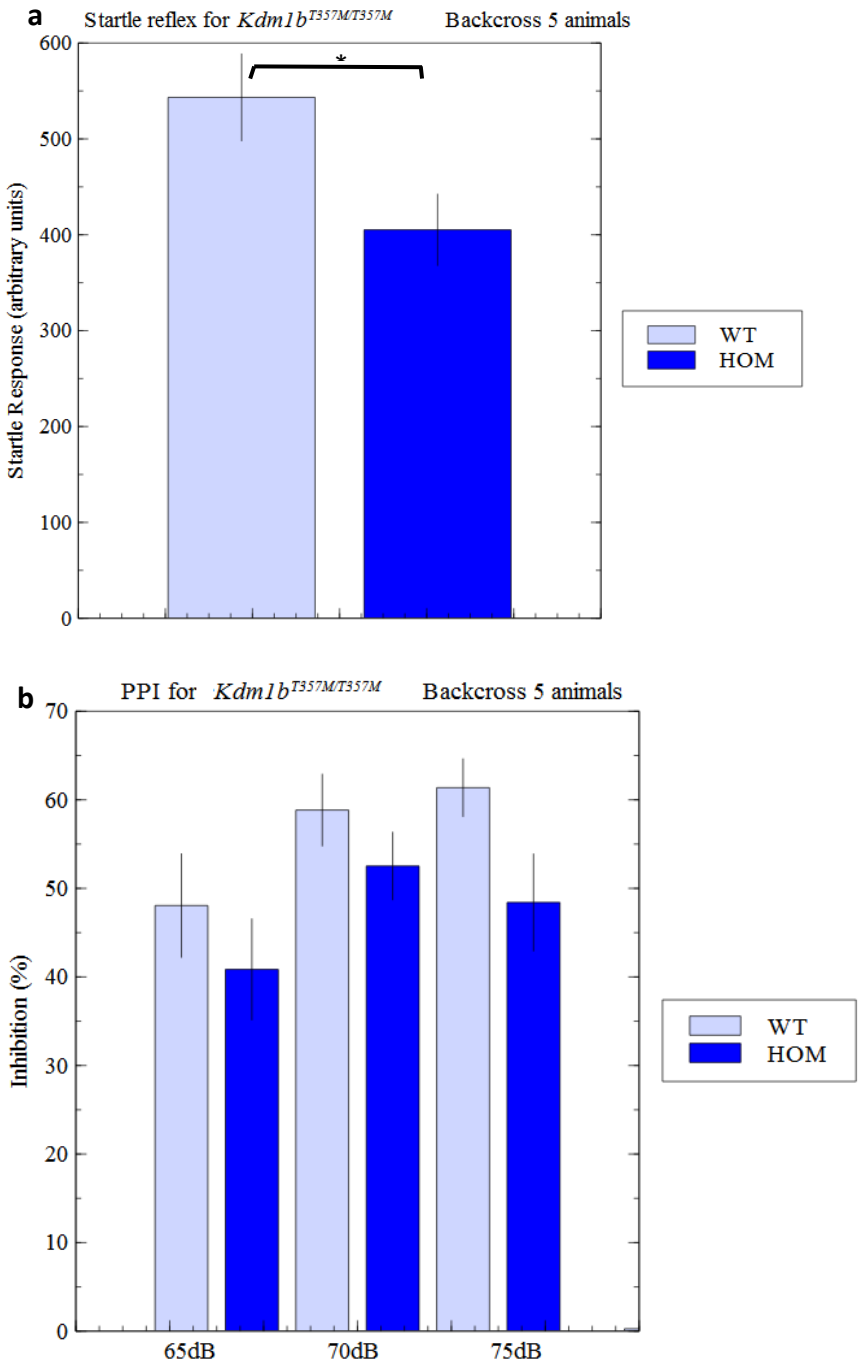

Figure 6.14: Acoustic startle and Pre-Pulse Inhibition of *Kdm1b*$^{T357M/T357M}$ animals

a) *Kdm1b*$^{T357M/T357M}$ animals display a significant decrease in startle response compared to wild type animals (405.17 ±37.04 for homozygotes and 543.32 ±45.14 for wild types, p=0.028).
b) *Kdm1b*$^{T357M/T357M}$ animals display a trend towards decreased PPI in each trial (for homozygote trials 40.85 ±5.68, 52.53 ±3.79 and 48.41 ±5.45 and for wild types 48.06 ±5.82, 58.84 ±4.03 and 61.37 ±3.23, p=0.391, P=0.271 and p=0.0695 respectively).

N=20 wild type and n=20 homozygote *Kdm1a*^{E440G} backcross 5 intercross animals. N=10 wild type and n=10 homozygote *Kdm1b*^{T357M} backcross 5 intercross animals. Data was analysed by student T test (*p<0.05, **p≤0.005, ***p≤0.001)

6.3: *Kdm1a*$^{E440G/E440G}$ Histological Assessment

To assess the whole animal for any phenotypic discrepancy as a result of any developmental impact of perturbing LSD1, animals were put through the Harwell EMPReSS histology screen for phenodeviants as previously described (EmPreSS website). *Kdm1a*$^{E440G/+}$ and *Kdm1a*$^{E440G/E440G}$ animals were similar in weight overall to wild-type (Figure 6.15).

6.3.1: Whole animal histology

The EMPReSS pathology pipeline was utilised in examination of 4 wild type and 5 homozygote *Kdm1a*$^{E440G/E440G}$ animals. No discernible differences were found between control and mutant animals across a wide range of parameters, including ventricle size and morphology of the pituitary gland. H and E staining of the hippocampus and cerebellum revealed no difference in arrangement of hippocampal, cortical or cerebellar cell layers (Figure 6.16).

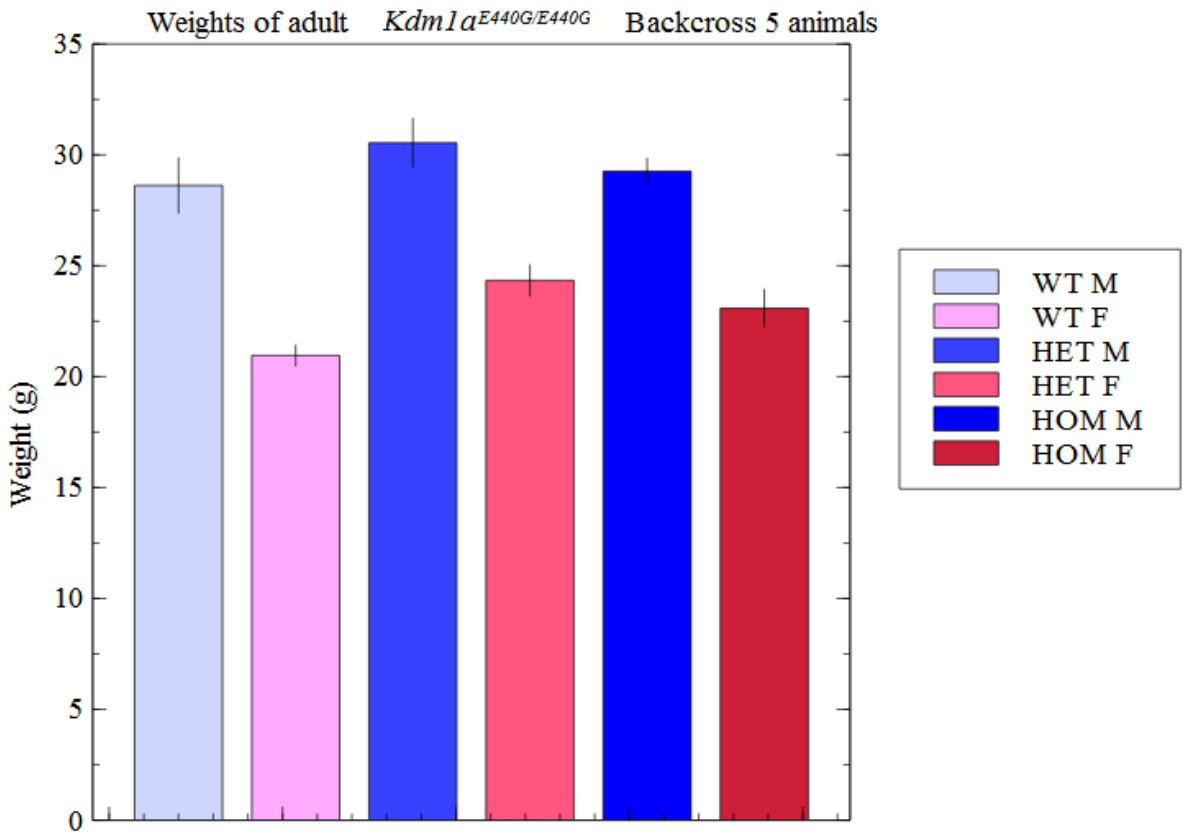

Figure 6.15: Weights of *Kdm1a*$^{E440G/E440G}$ adult animals

When analysed with ANOVA, genotype does not significantly affects weight of adult animals aged between 60 and 123 days of age (wild type males weigh 28.62g ±1.23, heterozygotes 30.5g ±1.09 and homozygotes 29.26g ±0.57, wild type females weigh 21.00g ±0.46, heterozygotes 24.34g ±0.69 and homozygotes 23.08g ±0.83 (P=0.17, F(1,30)).

N=10 wild type, n=10 heterozygote and n=10 homozygote each female and male *Kdm1a*^{E440G} backcross 5 intercross animals. Data was analysed by student T test

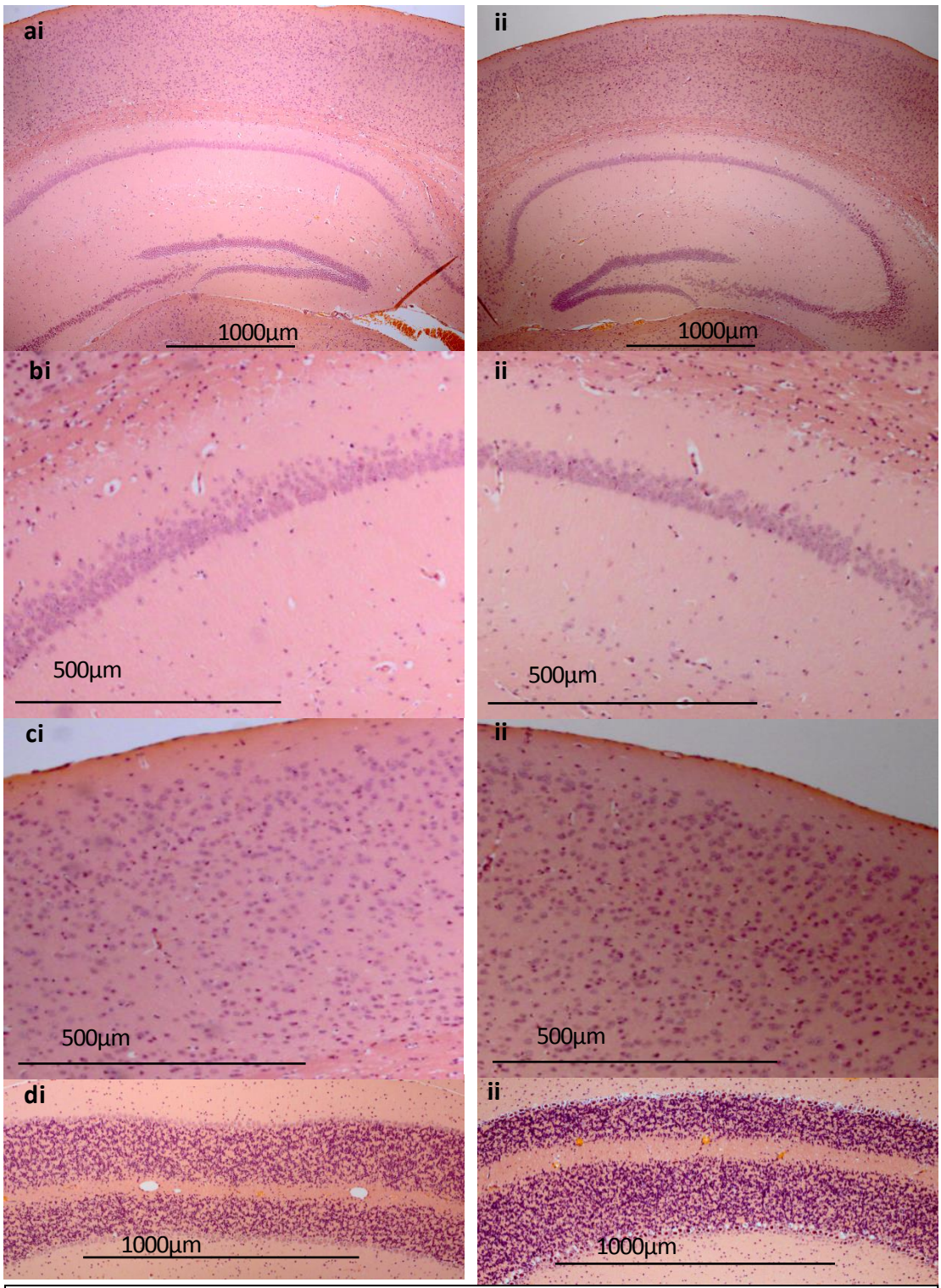

Figure 6.16: H and E staining of brain tissue from adult *Kdm1a*$^{E440G/E440G}$ animals

Cell layering looked normal in *Kdm1a*$^{E440G/E440G}$ animals. Brain slices were stained with Haemotoxylin and Eosin (H and E)

a) Hippocampus and cortex i) *Kdm1a*$^{+/+}$, ii) *Kdm1a*$^{E440G/E440G}$
b) Hippocampal layers i) *Kdm1a*$^{+/+}$, ii) *Kdm1a*$^{E440G/E440G}$
c) Cortical layers i) *Kdm1a*$^{+/+}$, ii) *Kdm1a*$^{E440G/E440G}$
d) Cerebellum i) *Kdm1a*$^{+/+}$, ii) *Kdm1a*$^{E440G/E440G}$

6.3.2: Gonad Physiology *Kdm1a*$^{E440G/E440G}$ and *Kdm1a*$^{L491H/L491H}$

Kdm1a$^{E440G/E440G}$animals had small testes, weighing 5mg on average, less than half the size of *Kdm1a*$^{+/+}$or *Kdm1a*$^{E440G/+}$ animals 12.5mg (Figure 6.17). *Kdm1a*$^{L491H/L491H}$ animals did not display this phenotype. Upon H and E staining of sections from the *Kdm1a*$^{E440G/E440G}$ gonad, seminiferous tubules were shown to be smaller than WT, displayed vacuolation and lacked elongating spermatids (Figure 6.17c). As LSD1 plays several roles and is expressed throughout development, gonads were examined at 11.5dpc for any sign of sex reversal which might propagate the development of hypogonadism in adult animals. Sex determination in male mice begins with the expression of *Sry* at 11.5 dpc followed by a cascade of events leading to testis development (*Sry* upregulating *Sox9* and the 'male differentiation pathway' which supresses female marker expression and female gonad development). If the initiation of sex determination were perturbed in the animals subsequently at E14.5 female markers such as *Stra8* or *FoxL2* might instead be expressed in male gonads as the female differentiation pathway is disinhibited. If the expression of *Sry* or any downstream male markers were disrupted, or if female markers were abnormally upregulated then female markers would be evident at 14.5dpc. *In situ* probes for female marker Stra8 showed normal distribution in female gonads only, and all gonads looked morphologically normal at this point in time. The development of the small underdeveloped testes in *Kdm1a*$^{E440G/E440G}$ mice does not involve perturbations to this early sex determination event.

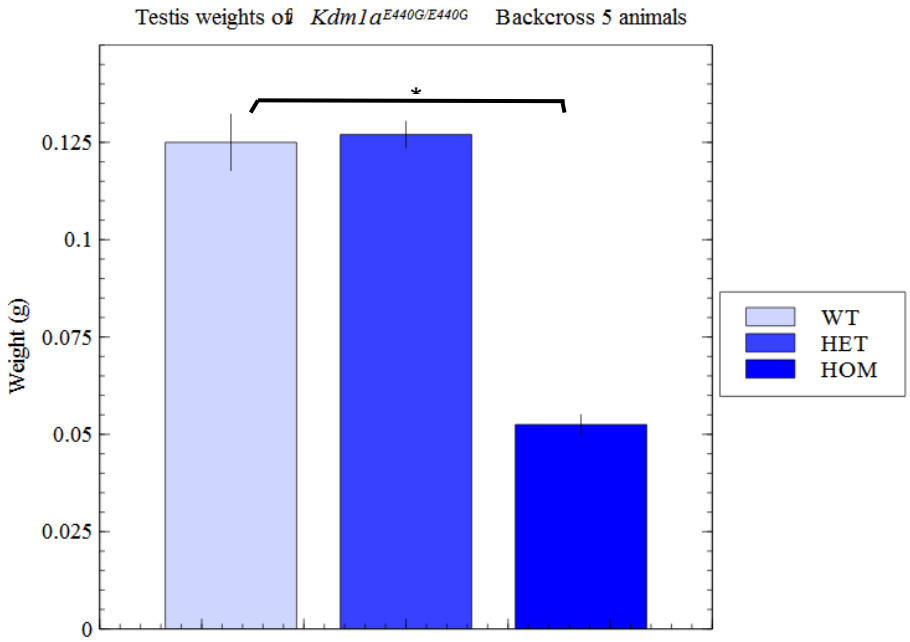
Testis weights of Kdm1a E440G/E440G Backcross 5 animals
Weight (g)
0.125
0.1
0.075
0.05
0.025
0
*
WT
HET
HOM


bi
ii
0.5 cm
0.5 cm

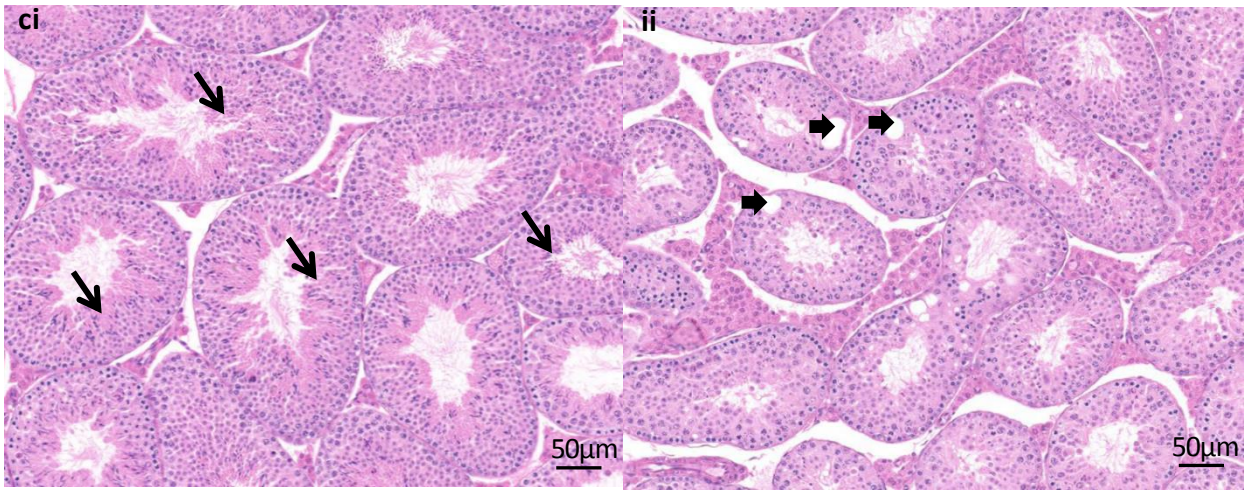
ci
ii
50µm
50µm

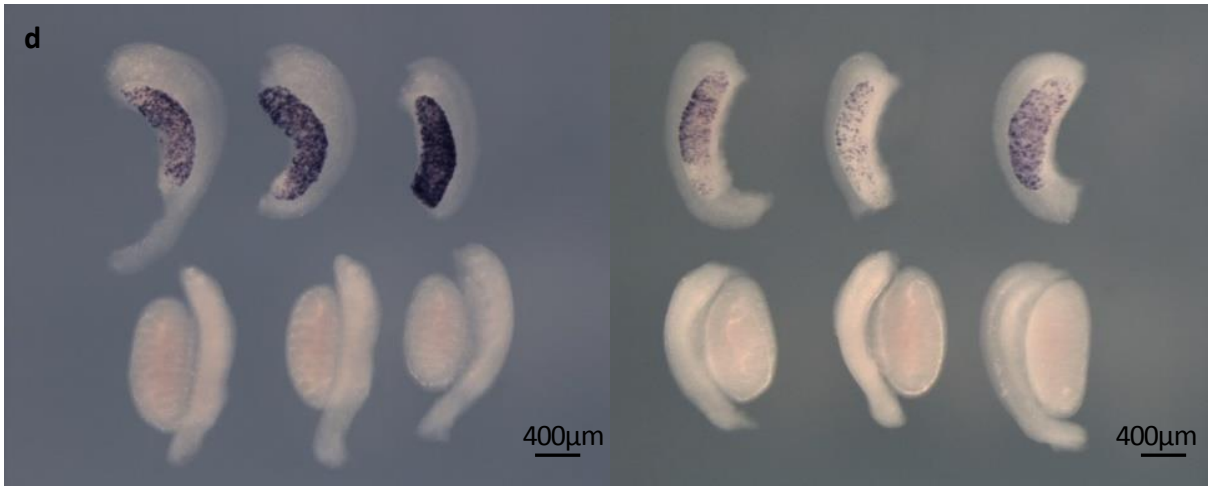

Stra8 *Kdm1a*$^{+/+}$, *Kdm1a*$^{E440G/+}$, *Kdm1a*$^{E440G/E440G}$
(XX top row, XY bottom row)

FoxL2 *Kdm1a*$^{+/+}$, *Kdm1a*$^{E440G/+}$, *Kdm1a*$^{E440G/E440G}$
(XX top row, XY bottom row)

Figure 6.17: *Kdm1a*$^{E440G/E440G}$ gonad phenotype

Kdm1a$^{E440G/E440G}$ animals displayed abnormalities in the gonads.

a) *Kdm1a*$^{E440G/E440G}$ gonads weighed 5.25mg ±0.25 on average in comparison to *Kdm1a*$^{+/+}$ 12.5mg ±0.72. (p= 0.00005)
b) Gonads were isolated for a visual comparison of the size of representative testes (i) *Kdm1a*$^{+/+}$, ii) *Kdm1a*$^{E440G/E440G}$
c) Slides were taken and stained with H and E staining to check for histological abnormalities (i) *Kdm1a*$^{+/+}$ animals had larger seminiferous tubules with elongating spermatids (arrows) ii) *Kdm1a*$^{E440G/E440G}$ animals had smaller tubules (due to reduced germinal epithelium) with no elongating spermatids, and vacuolation (arrows)
d) Gonads from 14.5dpc *Kdm1a*$^{E440G/E440G}$ animals were stained by *in situ* hybridisation for female markers *Stra8* and *FoxL2*

N=3 wild type, n=5 heterozygote and n=2 homozygote male *Kdm1a*^{E440G} backcross 5 intercross animals were used for gonad weights and imaging, a further 3 of each genotype used to cut sections and 7 embryos used for in situ experiment, including 3 homozygotes and 2 wild type animals. Gonad weight data was analysed by student T test (*p<0.05, **p≤0.005, ***p≤0.001)

6.4: Discussion

LSD1 and LSD2 play roles in multiple tissues at many stages throughout development and adulthood. Therefore an array of behavioural effects may have been precipitated by mutation of these genes.

In order to characterise LSD mutant animals, cohorts were put through a battery of behavioural tests to examine a wide array of phenotypes. Both mutants displayed altered neurobehaviour in some tests, which are summarised in table 6.1 and discussed in depth in the following section. Both *Kdm1a* and *Kdm1b* are expressed in the adult brain and therefore could be exerting direct effects on neural function in order to precipitate the observed behaviours. Both genes have also been shown to play developmental roles which could impinge on adult neurobehaviour.

LSD1 has been characterised to play a role in the development of pyramidal cortical cells using in utero shRNA manipulation of *CoREST* and *Kdm1a* (Fuentes et al. 2012). Adult phenotypes were not examined in this study but as pyramidal cells are associated with multiple adult cortical functions from neuroplasticity to cognition (Elston 2003; Salimi et al. 2008), disruption to pyramidal cell development could cause a neurobehavioural phenotype.

LSD2 is important in early development of the fertilised oocyte (Ciccone et al. 2009) and is well-documented to play a role in imprinting in particular (Ciccone et al. 2009; Zhang et al. 2013). Investigation into the role of LSD2 in development has not been characterised outside of its role in imprinting.

Mutant	♂/♀	Test	Result	Figure
Kdm1a$^{E440G/E440G}$	♂/♀	SHIRPA	Defaecation ↓	6.1
			Tail height ↑ p=0.037	
Kdm1a$^{E440G/E440G}$	♂/♀	Marble burying	ND	6.2
Kdm1a$^{E440G/E440G}$	♂/♀	Digging	ND	
Kdm1b$^{T357M/T357M}$	♀	SHIRPA	Righting reflex ↓ p=0.038	6.3
Kdm1b$^{T357M/T357M}$	♀	Digging	ND	6.4
Kdm1a$^{E440G/E440G}$	♂/♀	Spontaneous alternation	Alternation ↓	6.5
Kdm1a$^{E440G/E440G}$	♂/♀	Open field	Latency to enter centre of arena in trial 2 ↓ p=0.026	6.6
Kdm1a$^{E440G/E440G}$	♂/♀	Fear conditioning	Freezing in response to shock ND	6.7
			Freezing in response to cue ND	
			Freezing in response to context ↓	
Kdm1a$^{E440G/E440G}$	♂	Social dominance	Trials won ND	6.8
			Trials backed out of ↑ p=0.022	6.9
Kdm1b$^{T357M/T357M}$	♀	Spontaneous alternation	ND	6.10
Kdm1b$^{T357M/T357M}$	♀	Open field	ND	6.11
Kdm1b$^{T357M/T357M}$	♀	Fear conditioning	Freezing in response to shock ↑ p=0.033	6.12
			Freezing in response to cue ND	
			Freezing in response to context ND	
Kdm1a$^{E440G/E440G}$	♂/♀	PPI	Startle ND	6.13
			PPI ↓	
Kdm1b$^{T357M/T357M}$	♀	PPI	Startle ↓ p=0.028	6.14
			PPI↓	
Kdm1a$^{E440G/E440G}$	♂/♀	Weight	ND	6.15
Kdm1a$^{E440G/E440G}$	♂/♀	Brain pathology	Histology: hippocampus, cortex, cerebellum ND	6.16
Kdm1a$^{E440G/E440G}$	♂	Gonad Pathology	Testis weight ↓ p<0.001	6.17a
			Testis size appearance ↓	6.17b
			Histology: vacuolation and decreased number of elongating spermatids	6.17c
			Expression of female markers at e14.5 ND	6.17d

Table 6.1: Summary of behavioural phenotyping data

BC: Back cross; ND: No difference, NA: Not applicable (data not effective)

6.4.1: Behavioural Phenotypes *Kdm1a*$^{E440G/E440G}$

Sensorimotor gating is impaired in human patients suffering from schizophrenia and other neuropsychiatric disorders, and in mouse models of psychiatric disorders (Braff et al. 2001; Powell et al. 2009). In the *Kdm1a*$^{E440G/E440G}$ mice, PPI was not significantly affected (Figure 6.13) suggesting that sensorimotor gating across the cortico-striatal network is functional in these animals and so LSD1 does not contribute to sensory gating or modulation of the startle reflex in this model. However, although not quite significant, the animals do trend towards an increase in baseline startle response to the 110dB tone alone, concurrent with the observation that the mutants are more responsive than control animals during handling.

In the spontaneous alternation test, *Kdm1a*$^{E440G/E440G}$ animals trended towards performing worse than wild types as indicated by a lower percentage of alternations than control animals (52% and 67% trials respectively) (Figure 6.5). Spontaneous alternation mainly relies on hippocampal function or working memory (Deacon & Rawlins 2006). It must also be considered when interpreting data in alternation trials that C57BL/6 animals alternate approximately 75% of the time (Deacon & Rawlins 2005), but here wild type animals only alternated 67% of the time which could be due to secondary cues or background strain effects as discussed in Section 6.2.3.

Kdm1a$^{E440G/E440G}$ animals also demonstrate less freezing in fear conditioning context trial ($p=0.057$) than wild type animals (Figure 6.7). Freezing behaviour is a species-specific defence mechanism, indicative of a fear reaction (Bolles 1970). Upon conditioning to shocks following a tone, animals would be expected to freeze more upon exposure to the shock environment in the context trial and to the tones in the cue trial. The decrease of freezing in the context trial suggests that animals fail to remember the context of the conditioning trial as well as wild type animals. However, animals responded similarly to wild type animals in the cue trial so this is not due to a universal memory deficit. Decreased freezing in the context trial has been associated with chronic stress and post-traumatic stress in mice and humans (Milad et al. 2009; Baran et al. 2009). Alterations in dendritic

arborisation in the prefrontal cortex affect context response to conditioning (Baran et al. 2009; Miracle et al. 2006), and chronic stress has been shown to cause these morphological changes (Goldwater et al. 2009; Miracle et al. 2006). Although cortical layering in the *Kdm1a*$^{E440G/E440G}$ animals was normal (Figure 6.16), dendritic morphology could be examined in future by golgi staining. Chronic stress can be used to induce depression in mice (Keeney et al. 2006; Bartolomucci et al. 2009; Savali et al. 2014), and has been associated with changes in sleep architecture, fear conditioning, and cortical function (Cheeta et al. 1997; Keeney et al. 2006; Bartolomucci et al. 2009; Baran et al. 2009; Goldwater et al. 2009). Therefore in order to pinpoint the neural mechanisms disrupted in the *Kdm1a*$^{E440G/E440G}$ mice, which could be affecting fear conditioning in the context trial, the results from all aspects of behavioural testing must be considered together. As the animals demonstrate problems in learning in the spontaneous alternation task (Figure 6.5), perhaps the deficit in fear conditioning is due to a learning deficit.

Marginal anxiety differences between *Kdm1a*$^{E440G/E440G}$ animals and controls were established across a series of tests, including decreased latency to enter the centre of the open field on the second trial (Figure 6.6) and increased reversal from the tube in social dominance tests (Figure 6.8). Each test is anxiogenic by different means and to different extents; open field exposing the animals to a novel and unsheltered environment, and social dominance to a stressful social interaction. The increased response of the animals to an auditory startle has also been previously discussed. As the animals performed as well as controls in the digging tests (Figure 6.2) it is apparent that they do not suffer from a baseline anxiety, which might affect normal behaviour in a 'safe' environment similar to the home cage, but changes in anxiety in many behavioural tests may be of significance.

Kdm1a$^{E440G/E440G}$ animals were observably hyperresponsive to handling. LSD1 could be hypothesised as playing a role in neural networks either governing aggression or a depression-like syndrome, which has manifested as aggression in these mice. Depression has been associated with offensive and defensive behaviours in patients and rodent models of depression through unknown

mechanisms (Courtet 2010; Quiggle et al. 1992; Ferguson et al. 2005; Willner et al. 1981; Mitchell & Redfern 1992; Holmes et al. 2003). A published mouse model induced by chronic unpredictable mild stress has previously been shown to induce depression and aggression along with changes in social dominance (Yang et al. 2015). Aggression in this model was separated from the social dominance behaviour by treatment with tricyclic antidepressants (which ablated aggression and depression only), suggesting that the aggression phenotype arose due to changes in the same neural system as the depression phenotype (Yang et al. 2015). Response to tricyclic clozapine also indicates that the phenotype arises from changes in dopaminergic rather than serotonergic transmission (Yang et al. 2015). The *Kdm1a*$^{E440G/E440G}$ mutants showed no change in social dominance wins (Figure 6.8), but were aggressive on handling and observed to either behave aggressively in order to win trials in social dominance tests, or reverse away from the experiment excluding the trial from the analysis (Figure 6.9) (therefore the same number of wins were recorded as for wild types Figure 6.8).

Contrary to aggression seen in handling, backing away in the social dominance test may indicate a withdrawal from social confrontation as would be characteristic of neuropsychological disorders in man such as depression or schizophrenia (Barlow 2014). In animals exposed to social defeat paradigms in order to precipitate depression phenotypes, animals often display submissive behaviour in social dominance tests (Kudryavtseva et al. 1991; Keeney et al. 2006). The *Kdm1a*$^{E440G/E440G}$ mutants reverse in response to social contact, but also display more offensive social traits. Therefore, different animals may be manifesting a complex syndrome as different phenotypes, as occurs in patient populations and models of depression (Yang et al. 2015).

Anxiety induced by the enclosed apparatus may also contribute to reversal from the social dominance test. Observations recorded in open field however suggested a decrease in anxiety rather than an increase, so it can be concluded that any anxiety differences in the mutant animals are subtle and are elicited by specific stimuli (for example handling and enclosed spaces).

Anxiety phenotypes in mouse models of depression are known to vary, and often only certain tests evoke anxiety and animals used as models of anxiety perform as well as controls on other tests. For example, 129S6/SvEv 5HT transporter knockout animals displayed anxiety-related behaviour in a novelty-supressed feeding paradigm but performed as well as control animals on the elevated plus maze (Holmes et al. 2003). Further testing on different paradigms including a more traditional depression test like the forced swim test could shed light on the reason behind this discrepancy. As well as the highly variable nature of anxiety traits in mouse models, background can cause discrepancies in performance on anxiety tests, and the very same model of depression when bred to C57BL/6 display increased anxiety across multiple anxiety tests including the elevated plus maze (Holmes et al. 2003).

Stressful testing paradigms can lead to confound of the results of behavioural phenotyping paradigms (which is inevitable for a forced swim paradigm due to its very nature) (Barkus 2012). In the instance of forced swim testing, the stressor could be even more confounding than the anxiety tests performed in the current study. However the results of each anxiety test must be interpreted with care and attention to the type of stressor used in anxiogenesis in each case; a loud noise in the case of PPI, a shock in the case of fear conditioning, social anxiety or the enclosure in a small space for social dominance testing and even a novel open space in the case of open field testing can be considered stressful. This could explain why different tests all involving aspects of anxiety give such varied results.

6.4.2: Behavioural Phenotypes *Kdm1b*$^{T357M/T357M}$

Kdm1b$^{T357M/T357M}$ animals displayed no deficit in cognitive capability in the T maze (Figure 6.10), no change in digging behaviour in comparison to wild type animals (Figure 6.4) and no anxiety in the open field or social dominance paradigms (Figure 6.11) but a trend toward decreased pre-pulse induced inhibition and a significant decrease in startle response in the PPI test (Figure 6.14). However, regarding fear conditioning, the homozygote animals appeared to freeze more than wild

type upon administration of the aversive stimulus (Figure 6.12). As they demonstrated similar time freezing to wild types in the context and cue trials following conditioning, cognition is apparently unaffected.

Startle behaviour is influenced by multiple regulators and can be evoked by various stimuli including noise and foot shocks (Crusio et al. 2013). Increased time freezing in fear conditioning suggests that LSD2 plays a role in natural fear response through altering either emotional processing or anxiety (Bolles 1970). The *Kdm1b*$^{T357M/T357M}$ animals respond in a hypersensitive manner in response to the shock, but the PPI test data suggests a decrease in startle response in the mutant animals. This might be a complex anxiety phenotype, but the two responses may be different in testing because different mechanisms are at work, for example a hearing deficit would explain a lack of response to the auditory startle.

The decreased ability of *Kdm1b*$^{T357M/T357M}$ animals to return to upright in the SHIRPA assessment (Figure 6.3) may be due to vestibular defects which could be affected by LSD2 during development. *In situ* hybridisation or histological assessment would resolve the expression of *Kdm1b* in the developing vestibular apparatus. The assessment of the times at which expression occurred would clarify what roles *Kdm1b* plays at what developmental points. The nature of the adult phenotype could also be tested more extensively, using electron microscopy to examine the morphology of the inner ear, and behaviourally using a swim test (where animals with vestibular defects would be unable to swim) (Paffenholz et al. 2004). Auditory phenotyping including auditory brainstem response could reveal adult inner ear deficits which did not involve the vestibular apparatus.

Further supporting a potential neurophysiological role for both LSD1 or LSD2, the anti-depressant tranylcypromine acts to inhibit both LSDs *in vitro* (Binda et al. 2010), and the extent to which this accounts for the anti-depressant efficacy of the drug is unknown. Pharmacological testing of mutant animals with LSD specific inhibitors could tease this mechanism apart and inform the mechanistic interpretation of the phenotyping data presented here (discussed in section 8.6).

6.4.3: *Kdm1a*$^{E440G/E440G}$ Histology

In a pathology screen, *Kdm1a*$^{E440G/E440G}$ animals were grossly indistinguishable from littermate controls. It is possible that some developmental discrepancies were missed in the general screen in adult animals, or that the developmental phenotype is tissue specific (which correlates with previous literature (Lin et al. 2010; Di Stefano et al. 2007) discussed in Section 8.5.8) so only gonads are affected in this model.

Kdm1a$^{E440G/E440G}$ males displayed a hypogonadism with evidence of vacuolation, increased degenerate cells and a lack of elongating spermatids. This result is interesting when considering the recent identification of an SNP in LSD2 which has been associated with human disorders of sexual development (Personal Communication Dr A. Greenfield, MRC Harwell). This is the only evidence found in adult animals of where the *Kdm1a*^{E440G} mutation had an effect on the developmental process. In order to ascertain whether LSD1 plays a role in initial sex determination (occurring from 11.5dpc) *in situ* hybridisation for female markers was performed which would uncover sex reversal phenotypes if there was any ambiguity at the point of sex determination. The *in situ* data suggest that sex determination is unaffected by the *Kdm1a*^{E440G} mutation and that the development of hypogonadism in this mutant line is unrelated to events at this stage in development. LSD1 has been shown to play multiple roles which could affect gonad development, including a role in cell differentiation (Han et al. 2014; Choi et al. 2014; Wu et al. 2013) and hormone signalling (Metzger et al. 2005). Therefore this mutant line could be used in investigation of gonadal phenotypes.

Chapter 7

COMPOUND SCREENING

CHAPTER 7: Compound Screening

7.1: Introduction

In circadian research, compound screening has been successfully utilised to identify compounds active in circadian regulation and their respective targets in the circadian molecular clock. Longdaysin, Kenpaullone and Chir99021, KL001 and endosidin-1 and their respective targets CK1α and CK1ɖ (Hirota et al. 2010), GSK3β (Hirota & Kay 2009), CRYs (Hirota et al. 2012), and actin filament modifiers (Tõth et al. 2012) were identified in various compound screens. As it has been established that compound inhibitors can cause more profound circadian perturbations than knocking out a gene (including CK1ε (Lee et al. 2001; Isojima et al. 2009) and GSK3β (Hirota & Kay 2009)), compound screening can be a powerful tool in the identification of novel small molecule modulators of circadian mechanisms.

A small screen (1260 pharmacologically active compounds) looking for circadian period changes in human and mouse cell lines successfully identified two significant circadian regulators; CK1ɖ and CK1ε (Isojima et al. 2009). Inhibition of both kinases caused significant lengthening of circadian period in the screen (Isojima et al. 2009), and subsequent characterisation of the roles of the two kinases on the clock has contributed to our understanding of clock regulation (Isojima et al. 2009). Even small-scale compound screens can therefore result in important discoveries when effectively focussed, so the compounds investigated currently are carefully selected.

Compound screening has also uncovered how to investigate and manipulate known components and properties of the clock. A screen of 60000 compounds revealed a novel CRY stabiliser which lengthens circadian period, KL001 or longdaysin (Hirota et al. 2010). In order to understand how the drug was affecting the period of the clock, targets of longdaysin (CK1ɖ, CK1ε and ERK) were knocked down. The period lengthened similarly to cells treated with longdaysin (Hirota et al. 2010). Our understanding of *Cry* function was enhanced through subsequent investigation of gene expression using luciferase assays and quantitative PCR and degradation using ubiquitination assays.

Interestingly, when longdaysin was tested on U2OS cells and on mouse SCN, the lengthening of circadian period was consistent with the lengthening effects then witnessed when administered to zebrafish *in vivo* (Hirota et al. 2010). The cell-based compound screen was therefore translatable from the human cell line screen through mouse tissues and *in vivo* in zebrafish, and the results of the current compound screen could be translatable to *in vivo* scenarios.

Due to the dual role of cryptochrome in liver with regards glucose metabolism, this compound is now under development in targeting metabolic disorders which are linked with circadian dysfunction (McDonald 2012), so the compound could prove to be of experimental or clinical interest in future. Chemical engineering of highly specific small molecule inhibitors of LSD1 have already been performed with a view to suppression of LSD1 activity as a therapeutic target in cancer treatment (Gooden et al. 2008) and this approach could be used to manipulate LSD activity with regards the circadian mechanism in future.

As well as demethylase inhibition, LSD1 and LSD2 play catalysis-independent roles (Yang et al. 2010) and therefore other aspects of their function could be affected by pharmacologically active compounds and the data acquired from this compound screen could lend insight into mechanisms in this respect. And finally, previous compound screens which identified LSD1 or LSD2 inhibitors have not examined circadian parameters so the current investigation is novel in this respect.

LSD1 and LSD2 have been shown in molecular work to impact the circadian clockwork (Chapter 4). Using a complementary compound screening approach to demonstrate the role of posttranslational and epigenetic modifications in the molecular clockwork, compounds from the Enzo screen-well Phosphatase Inhibitor library (BML-2834) and Enzo screen-well Epigenetics library (BML-2836) were tested at physiologically appropriate ranges of concentration in Rat-1 Per2:Luc reporter fibroblasts. The subsequent bioluminescent rhythms were recorded and analysed with Biodare as a quantitative marker of circadian activity. Each compound was tested in triplicate in Rat-1 fibroblasts, and increase or decrease in circadian period recorded broadly in Table 7.1.

		COMPOUND						
Protein Phosphatase Inhibitors	↑							
	≡	Cantharidin	Endothall	PD-144795	OBA Ester	Cyclosporin A	BVT-948	
	↓							Levamisol
Demethylase Inhibitors	↑	**Tcyp x2**						
	≡		2,4 PD	Tcyp H				
	↓		2,4 PD					
Methyltransferase Inhibitors	↑			**5Aza2D x3**				
	≡	Zebularine	BIX-01294					
	↓							
HDAC Inhibitors	↑	MC-1293	**TSA x2**	**SAHA x2**				
	≡				Valproate	NCH-51	BML-281	Valproxam
	↓		**TSA x2**	SAHA H				
HAT Inhibitors	↑	**Garcinol x2**	CTPB		Butyrolactone 3			
	≡	Garcinol	CTPB	Anacardic Acid				
	↓							
SIRT Inhibitors	↑							
	≡		**Splitomycin x2**	EX-527	AGK2			
	↓	Sirtinol						
SIRT Activators	↑		Piceattanol low					
	≡							
	↓	Resveratrol	Piceattanol	BML-278				
mTOR Activators	↑	**Rapamycin x2**						
	≡	Rapamycin						
	↓							
Proteasome Inhibitors	↑	**Epoxomicin x2**						
	≡							
	↓	Epoxomicin						

Table 7.1: Circadian Period effects of compounds tested using lumicycle recording of bioluminescent Per2:Luc Rhythms

Phosphatase inhibitors from the Enzo screenwell libraries were tested in Rat-1 *Per2*:Luc fibroblasts. Upwards arrows in red boxes indicate period lengthening and downwards arrows in green boxes period shortening. Compounds did not perturb circadian period with the exception of levamisol.

Demethylase inhibitors were shown to shorten circadian period in most instances. 1nM tranylcypromine lengthened period from by 1.21hr on average, and 100nM 2,4-PD shortened period by 1.22hr.

Other subsets of epigenetic modifiers from the Enzo library were also tested in Rat-1 *Per2*:Luc cells to investigate which regulators were most likely to perturb circadian function, and because epigenetic modifers such as LSD1 acts in complex with multiple subsets of epigenetic modifiers including HDACs, SIRT1 and HATs (Nakamura et al. 2002; Yokoyama et al. 2014). Compounds had various effects on circadian period.

For example, SIRT1 activators had differential effects to one another. 100nM Resveratrol shortened period by 0.34 hours and 100nM Piceattanol by 1.1hr but 1nM piceattanol lengthened period by 2.4hr.

In the case of HDAC inhibitor SAHA, 10μM lengthened the period of Rat-1 cells by 0.45hr in the first trial, but when more dishes were tested, SAHA shortened the period by 0.6hr.

Such unreproducible effects across the board mean that the screen yields results which are too variable to draw statistically significant results from.

Tcyp = tranylcypromine, 2,4PD = 2, 4 Pyridinedicarboxyllic Acid, 5 Aza 2D = 5-Aza-2-deoxycytidine

N=3 dishes for each test condition in this initial compound screen, compounds of interest were tested multiple times to ascertain replicability

7.2: Compound Screening Data

In the current screen, several epigenetic modifiers altered circadian behaviour in rat-1 fibroblasts including HDAC inhibitor TSA, Histone Acetyltransferase (HAT) inhibitor Garcinol and demethylase inhibitor 2,4-Pyridine decarboxylase (2,4-PD). Interestingly a wide range of phosphatase inhibitors, some of which are known to act on highly expressed phosphatases with multiple cellular targets such as PP1A (endothall) and Calcineurin (PP3) (PD144795) appeared not to perturb circadian oscillation (Figure 7.1).

Phosphorylation events are central to the TTFL, and perturbation of phosphorylation events leads to changes in circadian period as well as other properties (Reischl & Kramer 2011). The lack of effect observed in the current screen of phosphatase inhibitors is surprising in light of the extensive literature characterising phosphorylation (including extensive manipulation of kinases such as GSK3β and CK1ɖ and Ck1ε which are known to act on clock components in multiple organisms and tissues) as central to clock function (Gallego & Virshup 2007; Partch et al. 2006; Lowrey et al.2000; Meng et al. 2008; Yoshitane et al. 2009; Reischl & Kramer 2011), including some studies utilising inhibitor small molecules (Eide et al. 2005) designed to be specific to circadian kinases (Meng et al. 2010).

Phosphorylation events also affect LSD1 function, as LSD1 has been shown to be phosphorylated by CK2 and PKCα in studies examining the subsequent functional consequences on LSD1s role in epigenetic regulation and circadian behaviour respectively (Costa et al. 2014; Nam et al. 2014). As such, phosphorylation impinges on epigenetic mechanism as well as the proteins of the molecular clock, and the characterisation of phosphorylation of LSD1 would be pertinent in understanding its circadian function in future studies.

In contrast to phosphorylase inhibitors, epigenetic modifiers had various effects on the period of the clock. No molecules were characterised to have a dose dependent effect, but this could be due to their mechanism of action being indirect to the clock (so increasing dose not increasing effect linearly as several molecular interactions or catalytic events occur between the inhibition of the

target and the clock perturbation) or due to their pharmacokinetic properties not being first-order in nature. None of the drugs tested here have any known circadian effects.

Demethylase inhibitor 2,4-PD causes a shortening in circadian period from by 1.44 hours (p=0.08), 1.07 hours (p=0.17) and 1.22 hours (p=0.05) at 1nM, 1µM and 10µM concentration when administered to rat-1 cells (Figure 7.2b). This is not a dose-dependent effect, although the drug effect is only statistically significant at a concentration of 10µM. This suggests that the action of 2,4-PD plateaus at a dose lower than 1uM in this system, so the system is saturated and increasing dose of 2,4-PD does not increase its circadian effect. 2,4-PD only demethylates jumonji domain-containing demethylases such as KDM5A (MacKeen et al. 2010) so its role in the circadian mechanism is not mediated by LSD1 or LSD2. However this result does support a role for demethylases in the clock, and as demethylases act in complex and interact with one another (Culhane & Cole 2007; Konovalov & Garcia-Bassets 2013; Suzuki & Miyata 2011), it may take effect through a mechanism involving LSD1 or LSD2 which cannot be ruled out.

The action of methyltransferase inhibitor 5-Aza-2-deoxycytidine lengthens circadian period (Figure 7.2a). This drug acts to inhibit C5-specific methyltransferases such as DNMT1 (Zhou et al. 2008) and as such regulates histone modifying supercomplexes. As LSD1 is known to function as a part of such complexes, the drug effect shown here might impinge on LSD activity.

Jmjd-specific demethylase inhibitor compound 2,4-PD showed the most robust circadian effect in this screen. The Jmjd-specificity of 2,4-PD means it is not acting through direct regulation of LSD1 or LSD2. However, it has been proposed that LSD1 and LSD2 act in synergy with the Jmjd-domain LSDs in histone regulation in cancer cell lines (Rotili et al. 2014), and therefore for a compound to impact on one or other LSD mechanism could exert a much wider impact on demethylation activity *in vivo*, and could still be affecting LSD1 or LSD2 mechanisms through indirect inhibition of Jmjd-domain LSDs.

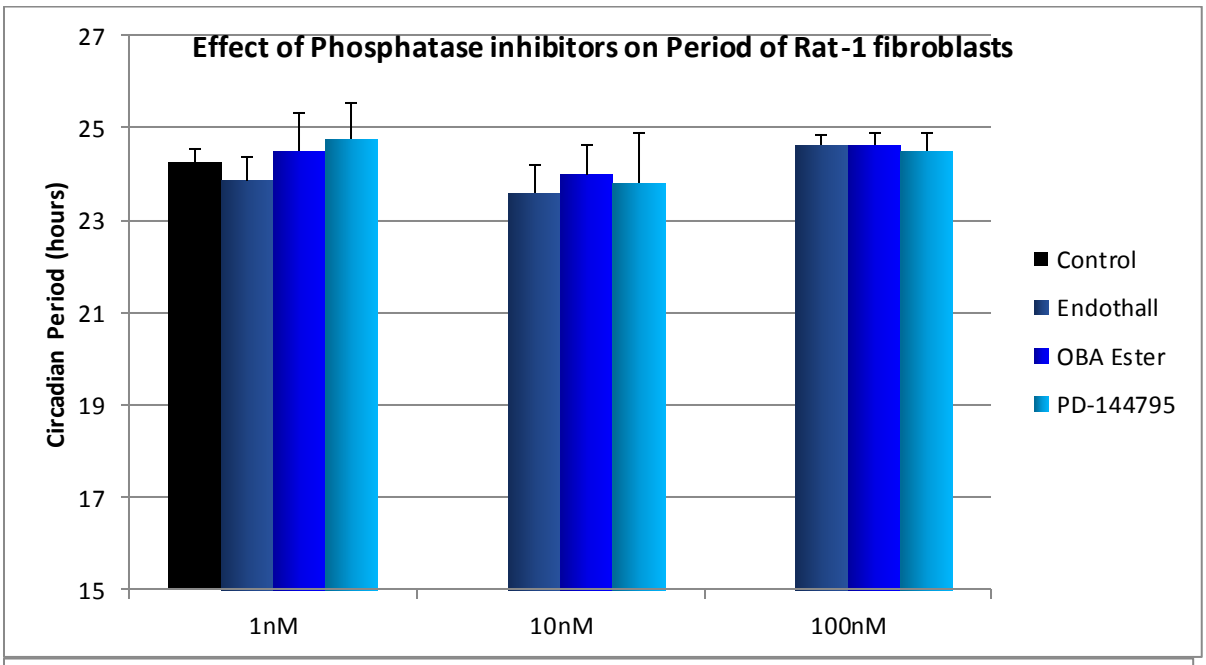

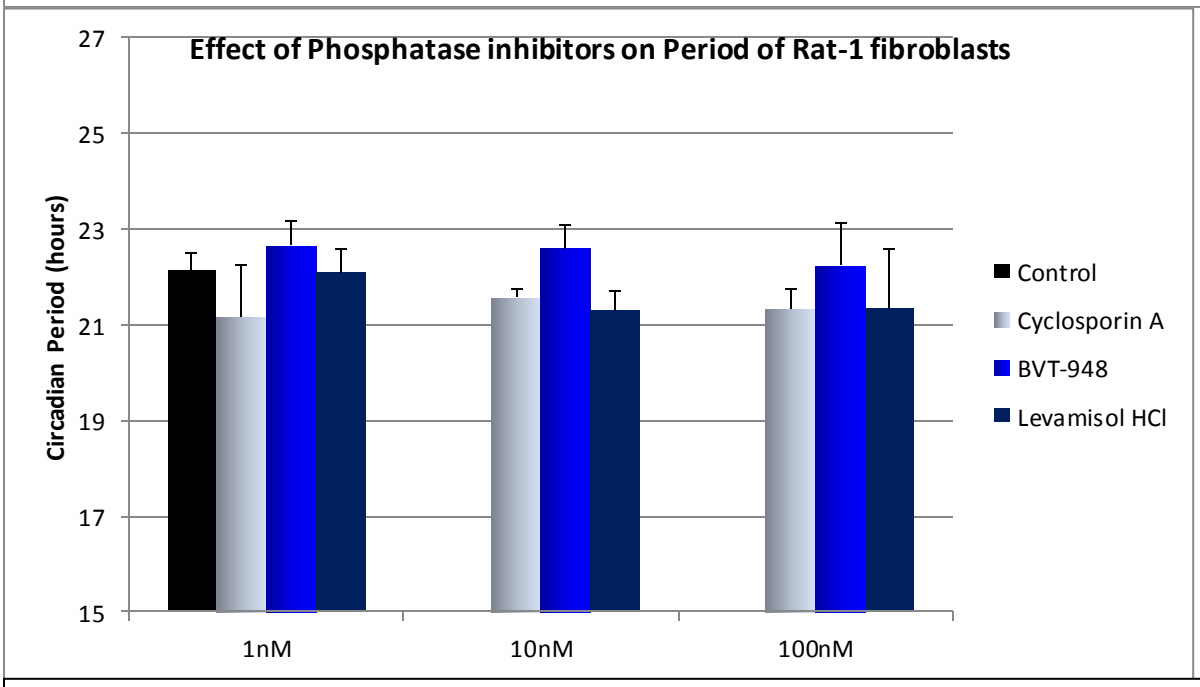

Figure 7.1: The period of Per2:Luc rhythms of Rat-1 fibroblasts treated with phosphatase inhibitor compounds

a) Endothall, OBA and PD-144795 did not change period of oscillation in Rat-1 cells (Period was 24.25 ±0.29 for vehicle dose, 23.87 ±0.52 p=0.30, 23.60 ±0.60 p=0.23 and 24.63 ±0.22 p=0.87 for endothall, 24.50 ±0.82 p=0.41, 24.00 ±0.62 p=0.42, and 24.63 ±0.27 p=0.87 for OBA and 24.77 ±0.78 p=0.97, 23.80 ±1.10 p=0.49 and 24.50 ±0.40 p=0.21 for PD-144795)

b) Cyclosporin-A, BVT-948 and levamisole HCl did not change period of oscillation in Rat-1cells (Period was 22.130± 0.35 for vehicle dose, 21.17 ±1.07 p=0.44, 21.57 ±0.18 p=0.35 and 21.33 ±0.39 p=0.20 for cyclosporin-A, 22.65 ±0.53 p=0.41, 22.6 ±0.49 p=0.40 and 22.23 ±0.88 p=0.92 for BVT-948 and 22.1 ±0.49 p=0.96, 21.3 ±0.40 p=0.20 and 21.33 ±1.26 p=0.57 for Levamisol)

N=3 dishes for each test condition in this initial compound screen.

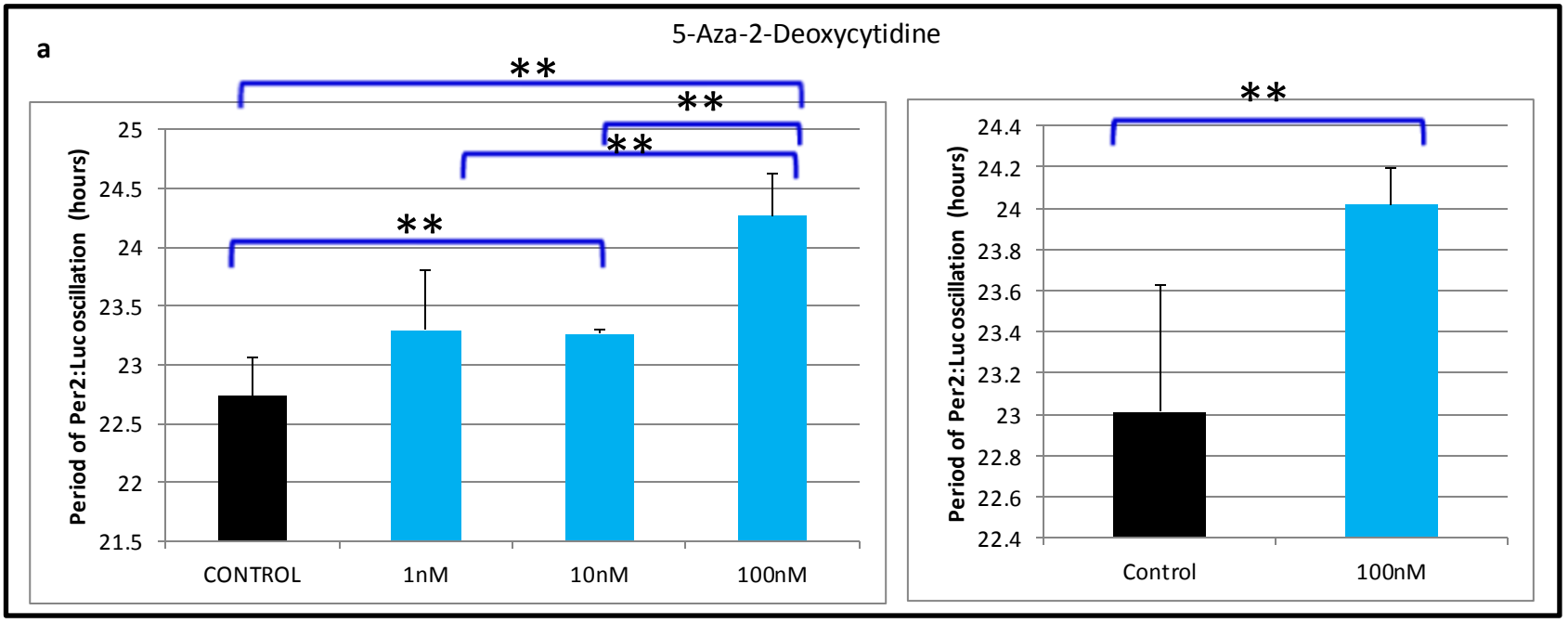
a
5-Aza-2-Deoxycytidine
**
**
**
**
Period of Per2:Lucoscillation (hours)
25
24.5
24
23.5
23
22.5
22
21.5
CONTROL
1nM
10nM
100nM
**
Period of Per2:Lucoscillation (hours)
24.4
24.2
24
23.8
23.6
23.4
23.2
23
22.8
22.6
22.4
Control
100nM

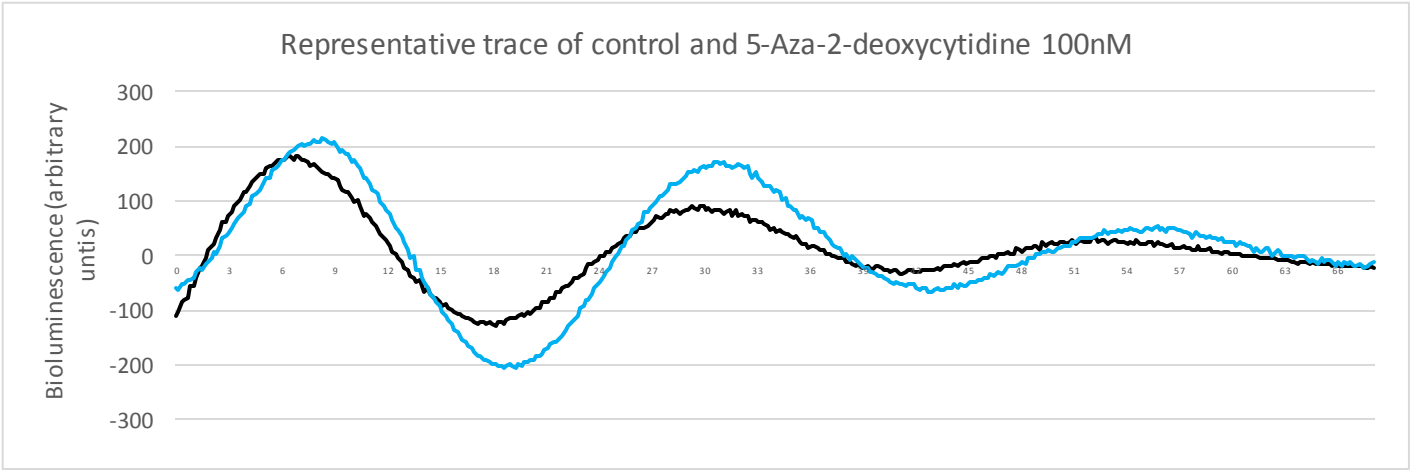
Representative trace of control and 5-Aza-2-deoxycytidine 100nM
Bioluminescence (arbitrary untis)
300
200
100
0
-100
-200
-300

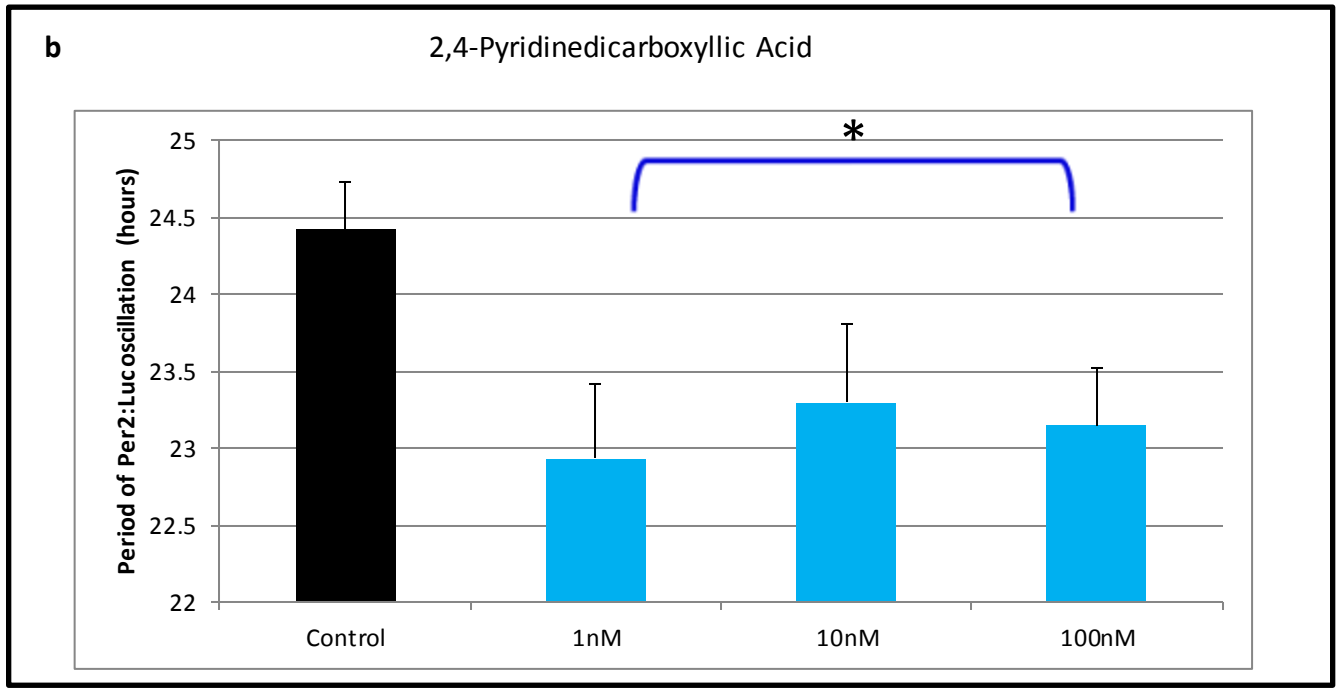
b
2,4-Pyridinedicarboxyllic Acid
Period of Per2:Lucoscillation (hours)
25
24.5
24
23.5
23
22.5
22
*
Control
1nM
10nM
100nM

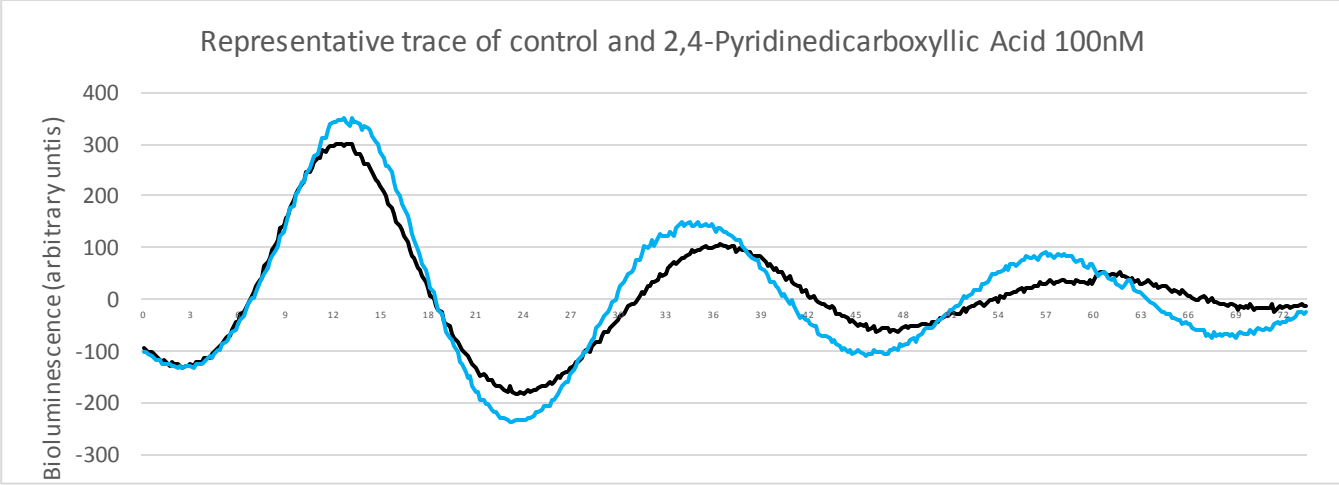
Representative trace of control and 2,4-Pyridinedicarboxyllic Acid 100nM
Bioluminescence (arbitrary untis)
400
300
200
100
0
-100
-200
-300

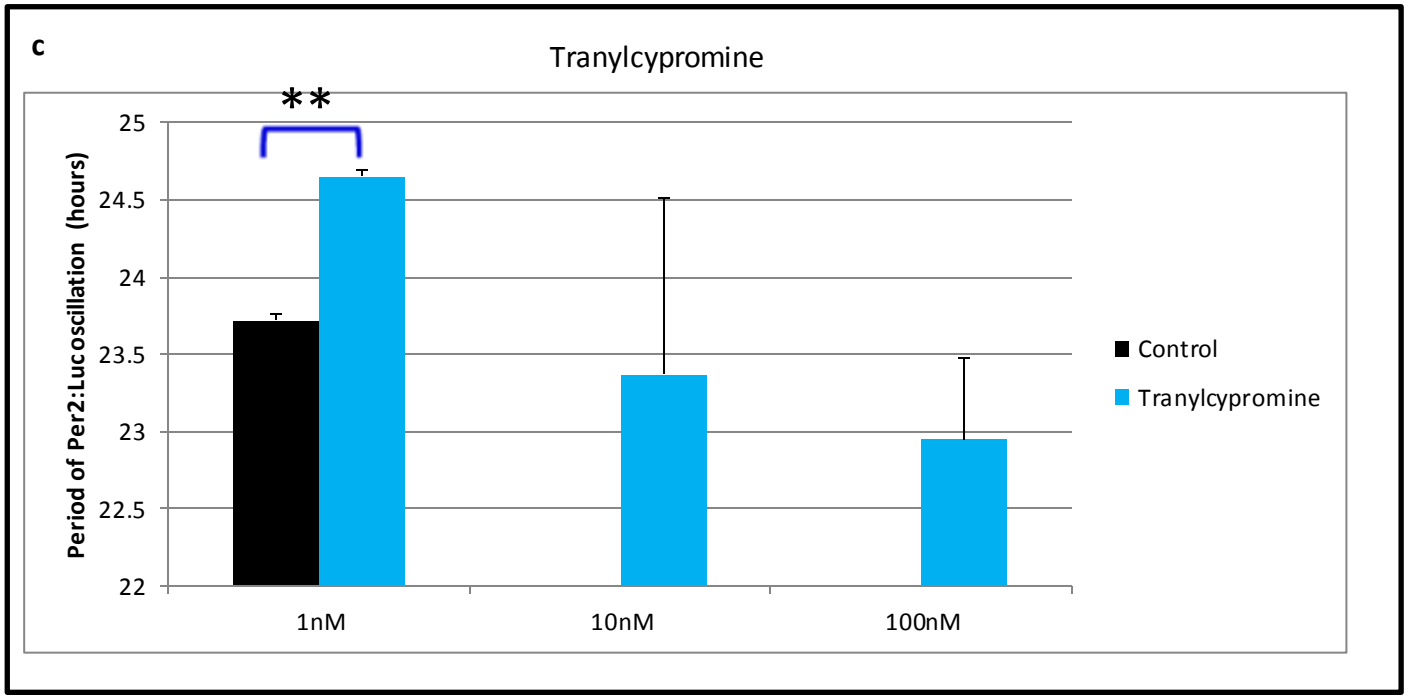
c
Tranylcypromine
**
Period of Per2:Luc oscillation (hours)
25
24.5
24
23.5
23
22.5
22
1nM
10nM
100nM
Control
Tranylcypromine

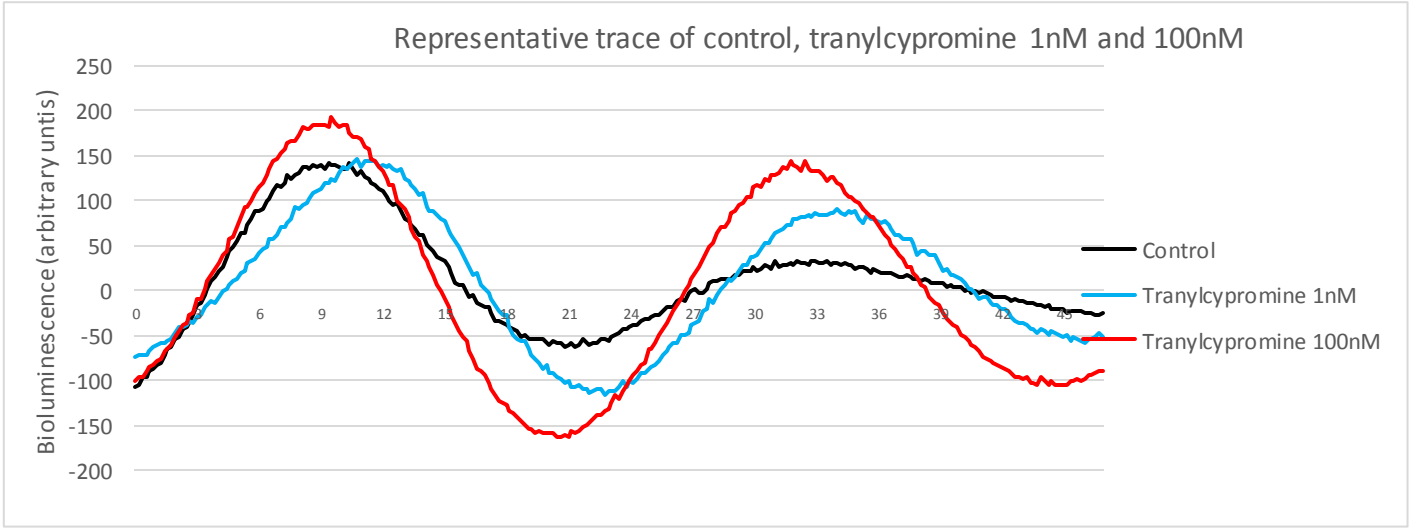
Representative trace of control, tranylcypromine 1nM and 100nM
Bioluminescence (arbitrary untis)
250
200
150
100
50
0
-50
-100
-150
-200
0
6
9
12
15
18
21
24
27
30
33
36
39
42
45
Control
Tranylcypromine 1nM
Tranylcypromine 100nM

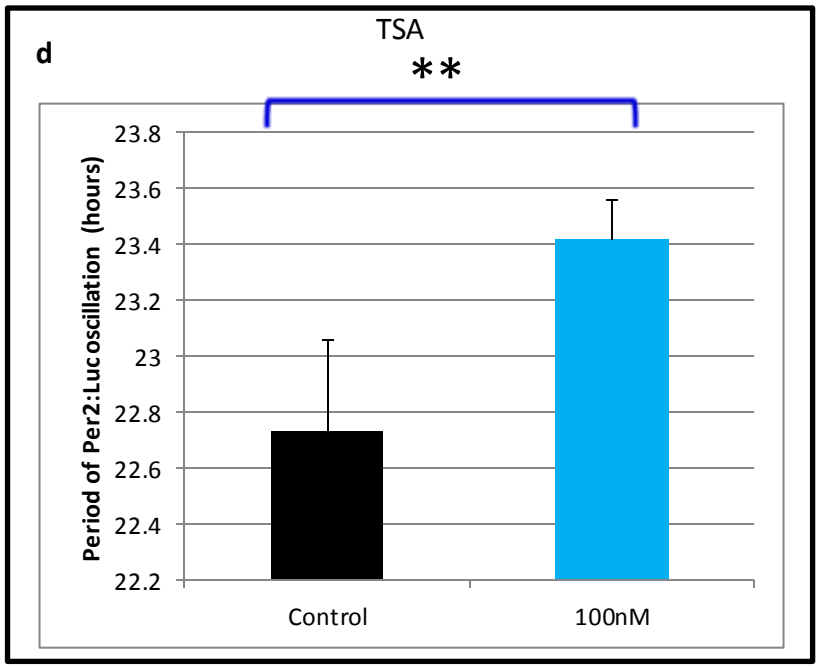
d
TSA
**
Period of Per2:Lucoscillation (hours)
23.8
23.6
23.4
23.2
23
22.8
22.6
22.4
22.2
Control
100nM

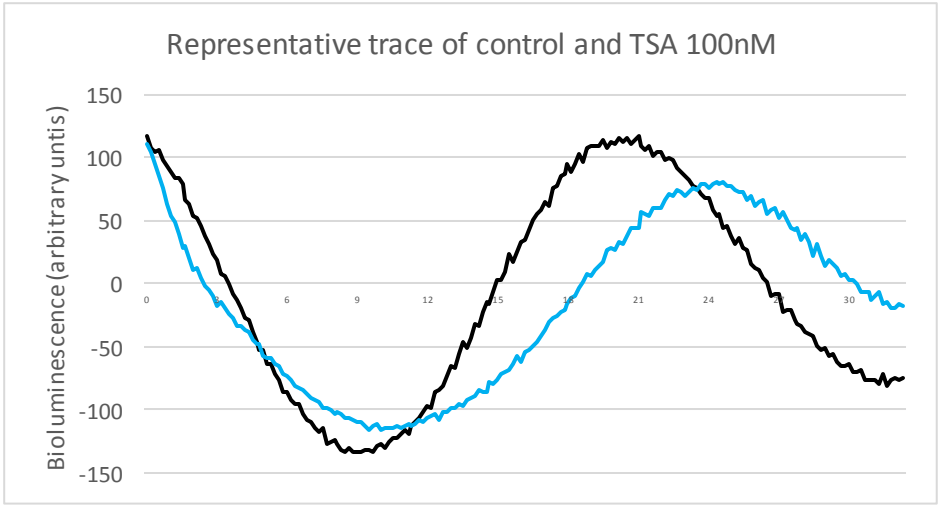
Representative trace of control and TSA 100nM
Bioluminescence (arbitrary untis)
150
100
50
0
-50
-100
-150
0
6
9
12
15
18
21
24
27
30

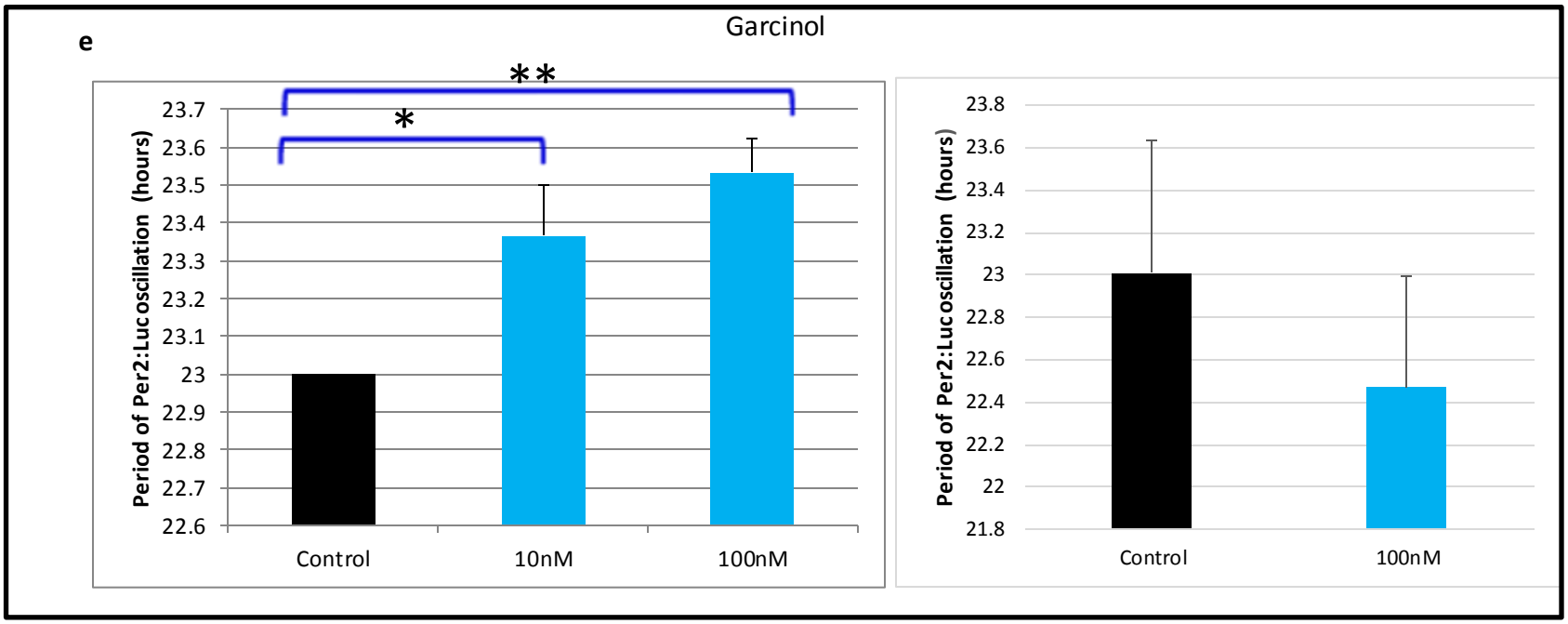
e
Garcinol
**
*
Period of Per2:Lucoscillation (hours)
23.7
23.6
23.5
23.4
23.3
23.2
23.1
23
22.9
22.8
22.7
22.6
Control
10nM
100nM
Period of Per2:Lucoscillation (hours)
23.8
23.6
23.4
23.2
23
22.8
22.6
22.4
22.2
22
21.8
Control
100nM

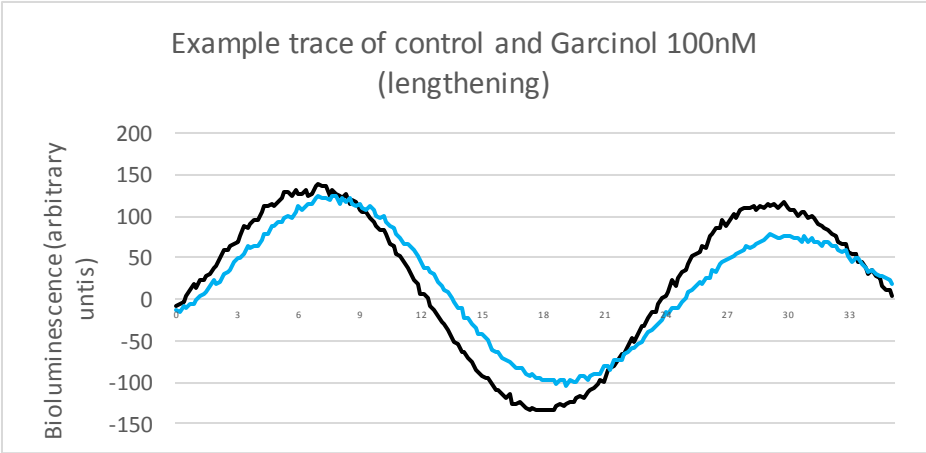
Example trace of control and Garcinol 100nM (lengthening)
Bioluminescence (arbitrary untis)
200
150
100
50
0
-50
-100
-150

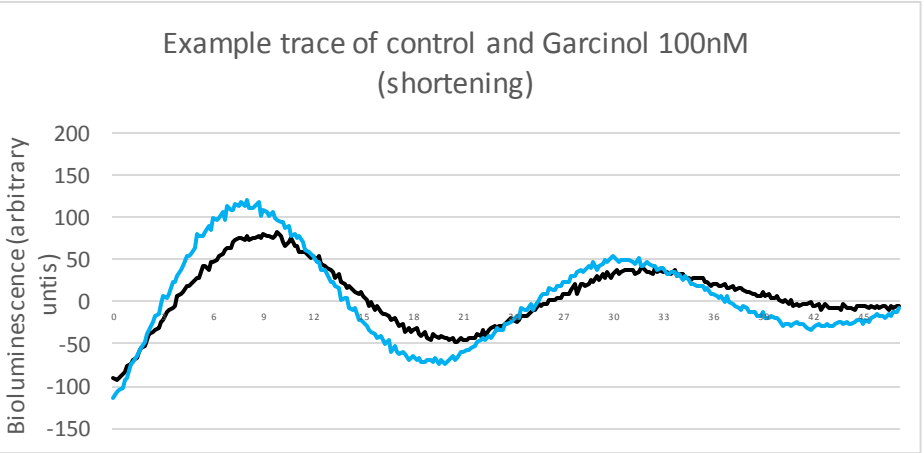
Example trace of control and Garcinol 100nM (shortening)
Bioluminescence (arbitrary untis)
200
150
100
50
0
-50
-100
-150

Figure 7.2: The period of Per2:Luc rhythms of Rat-1 fibroblasts treated with epigenetic modifier compounds

a) Methyltransferase inhibitor 5-Aza-2-deoxycytidine lengthened circadian period by 0.87hr ±0.51, 0.84hr ±0.03 and 1.84hr ±0.37 at 1nM and 10nM and 100nM ($p=0.009$, $p=0.0007$, $p=0.0001$) n=3
   Methyltransferase inhibitor 5-Aza-2-deoxycytidine lengthened circadian period by 0.97hours ±0.18 at 100nM ($p=0.01$) n=10
b) Histone demethylase inhibitor 2,4-Pyridinedicarboxyllic Acid (2,4-PD) shortened circadian period by 1.44hr ±0.49, 1.07hr ±0.51 and 1.22hr ±0.35 at 1nM, 10nM and 100nM respectively, reaching statistical significance at 100nM ($p=0.08$, $p=0.17$ and $p=0.05$) n=3
c) Histone demethylase inhibitor Tranylcypromine lengthened circadian period by 0.93hr ±0.04 ($p<0.0001$) but had no significant effect at 10nM and 100nM ($P=0.77$, $P=0.11$) n=3
d) Histone deacetylase inhibitor Trichostatin-A lengthened circadian period by 0.97hr ±0.15 at 100nM ($p=0.0006$) n=11
e) Histone acetyltransferase inhibitor Garcinol lengthened circadian period by 0.37hr ±0.14 at 10nM ($p=0.05$) and 0.53hr ±0.09 at 100nM ($p=0.004$) n=3
   Histone acetyltransferase inhibitor Garcinol trended but not significantly towards a shortening in circadian period at 100nM ($p=0.08$) n=11

All traces show a representative baseline-subtracted trace of data denoted in graphical form. Control trace is always shown in black, compound treated trace in blue unless otherwise labelled.

All experiments analysed with 2 way ANOVA and post hoc Tukey test to give pairwise comparisons. (*$p<0.05$, **$p\leq0.005$, ***$p\leq0.001$)

7.3: Compounds in SCN slices

m*Per2*:Luc animal SCNs were used to test compounds based on the results from the reporter cell screen. Robust bioluminescent recordings show that addition of 10µM 2,4P-D shortened the circadian period of the SCN oscillations *ex vivo* (Figure 7.3). This was consistent with the period-shortening effect 2,4-PD had in fibroblasts (Figure 7.2b), however rather than the 66 minute shortening observed in fibroblasts, the period only shortened by 42 minutes in the SCN slice. The effect of drugs on the SCN could be significant if a higher number of samples were tested given more time, which would make this result statistically comparable to the fibroblast screen. Period changes observed in the fibroblasts taken from mutant animals are exaggerated when compared to *in vivo* measures of period in mutant animals (Brown et al. 2005) (Section 8.4.7). The differences between peripheral and central effects of compounds is discussed later (Section 7.4.3)

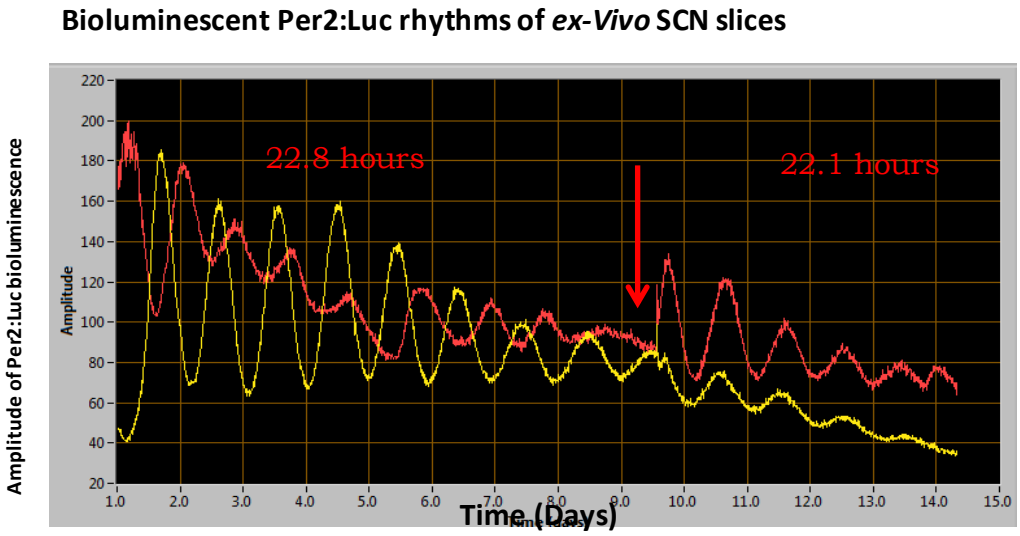

Figure 7.3: Bioluminescent Per2:Luc rhythms of *ex-Vivo* SCN slices

SCN slices oscillate with robust rhythms, and upon administration of 2,4-PD (red arrow) the circadian period of the slice shortens from 22.8 hours to 22.1 hours, consistent with the shortening of period observed in 2,4-PD treated fibroblasts earlier. Control trace from slice treated with DMSO vehicle only (in yellow) N=1 for each experimental condition shown here.

7.4: Discussion

Several epigenetic modifiers were observed to affect circadian oscillation in the *Per2*:Luc reporter cells. Conversely, phosphatase inhibitors had little impact on circadian oscillations in the fibroblast cells.

7.4.1: Phosphatase inhibitors

A large body of literature supports the importance of phosphorylation in clock mechanisms (Reischl & Kramer 2011). For example CK1ε plays a critical role in clock mechanism (Meng et al. 2008) and phosphorylation and destabilisation of Period proteins which affects circadian period. This is concordant with previous literature which has investigated compounds in a high-throughput manner using various reporter assays. Compound screening identified phosphorylating enzyme CK1α as a circadian regulator in cells and multiple model systems (Hirota et al. 2010). In the study by Hirota et al, 120000 compounds were screened using a *Bmal*:Luc expressing U2OS cell line. Perturbations in circadian rhythms of the cell line were analysed and several compounds of interest were found to result in period changes. One phosphatase inhibitor was singled out and purified due to the observed marked lengthening of the circadian period. The circadian impact of the compound (longdaysin) was tested in fibroblast, lung and SCN explants from m*Per2*:Luc mice as well as *in vivo* in *Per2*:Luc zebrafish. The compound was found to target and inhibit CK1α, and siRNA knockdown of *CK1α* abolished longdaysins period lengthening effect in cells. Finally it was confirmed that PERIOD proteins (known to be a target of CK1α) were phosphorylated more in compound treated cells (confirming the inhibition of CK1α-mediatated phosphorylation of period proteins by longdaysin) compared to untreated cells, demonstrating a mechanism by which longdaysin could be exerting its circadian effects in the cells. Conversely, in the fibroblasts used in the current investigation, phosphatase inhibitors yielded very little in the way of circadian changes which may reflect circadian differences between the Rat-1 fibroblast and U2OS cell system (Section 7.4.3). The lack of observable effect of phosphatases in the current screen might be due to a compensatory regulation

in the cells chosen for the screen. Alternatively, the compounds used in this screen target multiple phosphatases and as such the luciferase output of the cells is the culmination of multiple effects of each compound on different phosphatases. Neurospora PP1 mutants have unstable circadian rhythms and a short period of oscillation, whereas PP2A mutants display period lengthening (Yang et al. 2004).

PP1 inhibition in Drosophila lengthens period, contrary to its mutation and catalytic disruption in Neurospora (Yang et al. 2004), so again the effect of phosphatases on the clock is species dependent, most likely due to the wide range of targets affected by PP1-mediated dephosphorylation.

The most surprising observation to come from the phosphatase inhibitor screen is the lack of any circadian perturbation upon administration of PD-144795 as this compound has been shown to inhibit Casein Kinase 2 (a known circadian regulator (Lu et al. 2011; Tsuchiya et al. 2011)) as well as the phosphatase PP3 (Gualberto et al. 1998). Based on the knowledge that it inhibits CK2 with a Ki of 4uM, it would be expected that the drug would lengthen circadian period. The lack of observable effect in this case might be explained by the non-specificity of PD-144795 and roles opposing the CK2 inhibition being at play which might mask any changes effected by CK2 inhibition.

7.4.2: Epigenetic modifiers

The period shortening effect of 2,4-PD was different in magnitude when observed in fibroblasts and then in SCN slices (Figures 7.2, 7.3). One explanation could be due to the differences in expression levels of the drug targets in the two tissues. Jumonji-containing demethylases such as KDM5A and KDM4C which are targeted by 2,4-PD and indeed LSD1 have been shown to be upregulated in cancer tissue and as such are expressed in immortalised cells such as fibroblasts than in perhaps SCN (Zeng et al. 2010; Ehrbrecht et al. 2006; Lynch et al. 2012; Lv et al. 2012; Amente et al. 2013). In SCN the pacemaker nature of the tissue might also affect target expression levels with more robust oscillation patterns than in cell cultures.

Data from fibroblasts treated with inhibitors was often difficult to replicate; as shown in Figure7.2a administration of 100nM 5-Aza-2-deoxycytidine did not reliably produce a period lengthening, and in Figure 7.2e garcinol lengthened period but then shortened period non-significantly in a second test. It has previously been identified that fibroblast rhythms vary widely (Brown et al. 2005), even more so if taken from separate donors. The response of fibroblasts to compounds may also vary from the response of the SCN or other peripheral oscillators as described in the previous paragraph. Conversely, fibroblast oscillations have proven a valuable tool in circadian investigation and the oscillations do resemble SCN properties in many respects (Yagita et al. 2001). In order to verify all compound data collected in this study on fibroblasts it is necessary in future to look at systems such as SCN explants and ultimately administration of compounds *in vivo*.

To clarify which of the targets each modifier small molecule is acting through in affecting oscillations, the effect of the compounds tested here on the clock need to be further investigated using more specific molecules. For example 2,4-PD acts as a mimetic α–ketoglutarate, a cofactor of jumonji-C domain containing demethylases. This means it inhibits several demethylases, including but not limited to KDM5A and KDM5B (MacKeen et al. 2010; Kristensen et al. 2012). Other targets of 2,4-PD include *six1*, nuclear translocators and receptors, *EGL-9* (Gene-Ontology website) and 2-ketoglutarate-dependent oxygenases such as *FTO* (Derian et al. 1989; Uniprot website). So to pinpoint whether 2,4-PD sensitive demethylases are primarily responsible for circadian effects, inhibitors specific to KDM5A or KDM5B could be tested in future. No 2,4-PD targets are known to play circadian roles. More specific molecules could be identified using databases such as ZINC, or by *de novo* chemical engineering as was previously performed to design LSD1-specific inhibitors (Gooden et al. 2008). Alternatively, the targets of the drugs could be knocked down specifically using RNAi to ascertain which target is responsible for the circadian effect of each drug.

Most pertinently to the current investigation, the compound which requires further investigation is Tranylcypromine. 1nM tranylcypromine was shown to lengthen circadian period by 1.2 hours on

average but took no effect at higher concentrations. Its dose *in vivo* ranges from 0.01-5mg/kg in rodents (Gatch et al. 2006) so the doses used in this study spanned the therapeutic range. Tranylcypromine has previously been shown to inhibit both LSD1 and LSD2 (Binda et al. 2010). This is of pertinence in neurobehavioural investigations as tranylcypromine is an antidepressant. Antidepressant medications have also recently been linked to H3K4 methylation patterns (Lee et al. 2006). However, it is also known to target monoamine oxidase (MAO) A and B and dopamine receptor D2 *in vivo* (Gooden et al. 2008; Martin et al. 1995). Therefore in fibroblasts such as in the current investigation, tranylcypromine could be acting on various targets due to the non-specific nature of the drug (Neff & Yang 1974). Pharmacokinetic analysis of tranylcypromine-mediated inhibition of its MAO and LSD targets would inform what interactions are likely to affect circadian (and neurobehavioural) mechanisms, and could explain why it alters circadian period most prominently at lower doses. To shed light on the mechanism by which tranylcypromine affects cells in the current study, more specific compounds must be tested as has been previously described (Binda et al. 2010) If a compound screen were to be used as a tool to ascertain the true importance of LSD1 and LSD2 in regulation of the molecular clock, such specific compounds would be required for clarity of mechanism of action.

7.4.3 Screening systems

In order to compare the circadian properties of different experimental systems, it is necessary to consider and compare the effect of one drug on several systems. Caffeine is a stimulant known to affect circadian rhythms and used commonly to affect day-to-day activity by maintaining attention capacity in humans. Caffeine lengthens circadian period in cell cultures, but the effect of caffeine varies across experimental procedures. 5nM caffeine lengthens period of oscillation from approximately 26 hours to 28 hours in NIH-3T3 and from 26 to 31 hours in U2OS cells. This demonstrates that different cell systems respond to different extents in response to the same treatment (Oike et al. 2011). Caffeine may be acting on different targets in the two systems, or

acting in the same way on the same targets in both systems, as it has been demonstrated that the circadian properties of NIH-3T3 cells and rat-1 fibroblasts are different to each other regardless of the conserved property that both display circadian oscillation of TTFL genes (Yagita et al. 2001; Menger et al. 2007).

Caffeine also lengthens period in liver explants from Per2::Luc mice whereas in SCN caffeine phase delays oscillation (Oike et al. 2011). *In vivo* chronic caffeine phase delays activity in LD and lengthens free-running periods in DD (Oike et al. 2011). These results demonstrate that the response of a central and a peripheral pacemaker to the same dose of the same drug can be different. In the case of caffeine, previous electrophysiological experiments support this finding as caffeine has tissue dependent effects (Ding et al. 1998), postulated to be due to the effects of the diverse targets of caffeine (most of which are kinases and enzymes which affect cAMP levels, which are differentially expressed in different tissues and the cAMP concentrations could be taking differential effects in different tissues).

In light of the studies on caffeine, the properties of the central and peripheral models can be considered. The use of peripheral cells as a model of circadian oscillators remains a useful tool in circadian investigation as properties are consistent with pacemaker properties such as temporal expression of core clock genes and subsequent transcriptional cycles following the TTFL and it has been shown that *Cryptochrome* genes are essential for these oscillations (Nagoshi et al. 2005; Yagita et al. 2001). In mice, the value of period ascertained from fibroblasts also does correlate with the period of free-running activity in circadian models (Brown et al. 2005), demonstrating there is a link in genetic effects on the core clock between the peripheral and central oscillations. However, interpretation of data from peripheral models such as fibroblasts must be undertaken with caution. When fibroblasts are extracted from individual human subjects, the average period of circadian oscillation matches that observed when subjects are allowed to free-run in constant darkness, but the variability across samples is far higher than the behavioural rhythms (Brown et al. 2005). As well

as variability in expression of CCGs (Menger et al. 2007), variability in the core clock genes which might account for this discrepancy has recently been linked to DNA methylation (Wagner et al. 2014).

Chapter 8

DISCUSSION

CHAPTER 8: Discussion

8.1 Summary of Aims

The role of histone modifiers in the circadian clock has not been fully elucidated. This investigation was designed to identify, derive and select for, and characterise novel KDM1A (LSD1) and KDM1B (LSD2) mutants with a view to characterising the circadian role of the two genes. The multidisciplinary approach I use here ensures a rounded investigation of novel genes such as the LSDs, and reduces the chance of any phenotypes being overlooked. Molecular studies, circadian behavioural assays and a battery of phenotyping tests were employed to pinpoint the role of LSDs in the clock.

8.2 Summary of Results

Through screening the Harwell ENU archive, two non-synonymous mutations were found in the *Kdm1a* gene, and five in *Kdm1b* (Section 3.2). *In silico* analyses revealed that the two *Kdm1a* mutations were unlikely to affect structure (so unlikely to disrupt sensitive catalytic activity) (Section 3.3), whereas $Kdm1b^{P281L}$ and $Kdm1b^{T357M}$ mutations of *Kdm1b* are most likely to yield structural disruption (Section 3.3), and as such re-derivation of these four mutants was undertaken.

The molecular effect of mutations of LSDs was investigated. Protein interaction studies of LSD1 and LSD2 and the clock revealed that both genes interacted with multiple core clock components (Section 4.2.2.1, 4.2.2.2). Co-expression of LSD1 with its cofactor CoREST increased its interaction with REV-ERBα (Figure 4.4). This concurs with previous literature regarding LSD1 stability in the presence of CoREST (Shi et al. 2005). LSD1 mutants demonstrated a weakened interaction with CoREST (Figure 4.5), PER (figure 4.6), and CLOCK (Figure 4.7). The mutations in the tower domain of *Kdm1a* could modify this clock protein binding directly, or in a cofactor-dependent manner. To further test whether the proteins localise together and are capable of binding directly, immunofluorescent staining of overexpressing HEK293T cells revealed that several clock

components co-localised with LSD1 in the nucleus (Section 4.2.3). This supports that the interactions detected in CoIP studies could indeed be direct in nature.

The effect of mutations on chromatin modification was examined using ChIP. The *Kdm1a*^{E440G} mutation tended towards showing decreased LSD1 binding at the *Dbp* locus and decreased LSD1-mediated demethylation of H3K4 at the *Dbp* locus in MEFs (Figures 4.12 and 4.13). Compound screens supported the role of demethylation in regulation of the circadian clockwork as amongst several epigenetic effects, methyltransferase inhibition caused a lengthening in circadian period, whereas demethylase inhibition caused a shortening in circadian period (Chapter 7).

Transcription of the TTFL was also investigated in cells overexpressing mutagenized constructs, and bioluminescent Per2:Luc recordings showed that circadian period was affected by the *Kdm1a*^{E440G}, *Kdm1a*^{L491H} and *Kdm1b*^{P281L} mutations (Figure 4.1).

Overall, molecular work suggested that *in vivo* the *Kdm1a* and *Kdm1b* genes may modulate circadian rhythmicity, and as such circadian behaviour was next examined *in vivo*.

Circadian phenotyping revealed that LSD1 and LSD2 mutations caused background strain-dependent changes in circadian behaviour (Chapter 5). In the early stage phenotyping before backcrossing (to identify any circadian phenotypes which could influence further molecular work), *Kdm1a*$^{E440G/E440G}$ animals showed anticipation of lights off, decreased light-induced suppression of activity (masking), a non-significant 20min lengthening of period in DD, and 20min shortening of period in LL (Figure 5.1). *Kdm1a*$^{L491H/L491H}$ animals showed a 30min lengthening in circadian period in LL and a deficit in masking (Figure 5.1), *Kdm1b*$^{T357M/T357M}$ animals displayed circadian rhythm splitting in LL and *Kdm1b*$^{P281L/P281L}$ animals punctate running during subjective night (Figure 5.5).

At a later backcross (on a purer C57BL/6 background) animals were once again intercrossed and phenotyped. *Kdm1a*$^{E440G/E440G}$ animals demonstrated no anticipatory activity, and no change in tau or alpha (Figure 5.2). *Kdm1a*$^{E440G/E440G}$ animals were confirmed to display increased running in the light

phase when compared to littermate controls, and displayed reduced masking (Figure 5.3). *Kdm1a*$^{L491H/L491H}$ animals showed a 1.8hr decrease in alpha in LL (likely partly due to a low activity level) and a 10min shortening in circadian period in LL (Figure 5.4). *Kdm1b*$^{T357M/T357M}$ animals displayed no splitting in LL, and ran with a period and alpha similar to wild type animals (Figure 5.6).

Further analysis of the circadian behaviour of *Kdm1a*$^{E440G/E440G}$ animals was undertaken, firstly in a jet lag screen to examine the phase shift response. *Kdm1a*$^{E440G/E440G}$ mutants showed no change in phase shifting upon jet lag shifting, showed no change in the effect of phase resetting light pulses during the active phase and did not show altered circadian aftereffects after either short or long T-cycles (Figures 5.7, 5.8 and 5.10). *Kdm1b*$^{T357M/T357M}$ animals also displayed no change in phase shifting or aftereffects (Figures 5.7 and 5.10). *Kdm1b*$^{T357M/T357M}$ animals were observed to run more in the first few days after phase delay than littermate controls and onset was significantly earlier than controls on day one (Figure 5.7). *Kdm1b*$^{T357M/T357M}$ animals also showed increased phase shifting in response to the CT22 light pulse (Figure 5.8). This subtle phenotype is discussed in depth later in this chapter (Section 8.5.4).

The change in circadian period caused by *Kdm1a*^{E440G} mutation was not significant *in vivo* or in SCN slices, but fibroblasts overexpressing the mutant *Kdm1a*^{E440G} construct displayed a circadian period of 22.35hrs, 48mins shorter than cells expressing wild type constructs (Figure 4.1). The lack of significance and coherence between the data suggest that perhaps LSDs role is differential between central and peripheral clocks (Brown et al. 2005). In the instance of fibroblast rhythms, period changes and perturbations due to mutations or gene knockouts have been shown to be more exaggerated than the corresponding phenotype witnessed *in vivo* (Brown et al. 2005), mice exhibiting periods 1hr shorter than wild type animals or 0.75hrs longer yield cells with periods 4hrs shorter and 1.5hrs longer than wild type samples respectively (Brown et al. 2005).

Further investigation into the molecular impact of the *Kdm1a*^{E440G} mutation was undertaken in native tissue from mutant animals. Real time analysis of mRNA in SCN and liver tissue in mutant

animals showed that clock gene expression was intact in liver tissue with the exception of *Cry1* (Figure 5.13). Non-significant observations were made regarding the expression pattern of *Bmal1*, and at ZT7 *Dbp* expression was decreased in homozygous animal tissue (Figure 5.13). This does not concur with previous work where decrease in expression of clock genes was observed (Nam et al. 2014, Personal Communication Dr H. Reinke, Uni Düsseldorf, Ge). As methylation of H3K4 is associated with transcriptional activation (Metzger et al. 2010), it would be expected that were the *Kdm1a*^{E440G} mutation impairing the demethylase activity of LSD1 (Figure 4.13), the expression of affected genes would be increased. Therefore, RNA expression data would suggest that the circadian impact of the *Kdm1a*^{E440G} mutation may be demethylase independent. A decrease in expression of *Dbp* is witnessed in *Cry* double knockout animals but neither gene knockout individually (Anand et al. 2013). Similarrly, if LSD double mutant animals were examined, a more striking circadian phenotype might be revealed.

A battery of phenotyping tests was undertaken to examine any potential neurobehavioural abnormalities, which might affect circadian behaviour in mutant animals. *Kdm1a*$^{E440G/E440G}$ animals displayed a complex phenotype including a trend towards decreased learning and memory capability in the spontaneous alternation task (Figure 6.5) and a significant decrease in freezing in the context trial of the fear conditioning paradigm (Figure 6.7) and a possible anxiety phenotype (Section 6.2.3). The animals were observed to be less anxious in latency to enter the centre of the open field but not by other measures (Section 6.2.3). A trend towards increase in acoustic startle was observed (Figure 6.13) and animals were hyper-responsive to handling (Personal observation), but a trend towards a decrease in startle response was observed in the fear conditioning paradigm (Figure 6.7), and an increase in reversal from the social dominance task (Figure 6.9).

Kdm1b$^{T357M/T357M}$ animals did not display any overt anxiety phenotypes upon handling, and in the open field did not perform significantly differently to wild type animals in any measure (Figure 6.11). The mutant animals trended towards moving less distance overall and when other measures were

corrected for this fact, it unmasked a trend towards a decrease in time spent in the periphery of the arena in comparison to wild type animals but again this did not reach significance (Figure 6.11). In fear conditioning, the *Kdm1b*$^{T357M/T357M}$ animals were shown to have a significantly heightened startle response to the stimulus alone, and tended towards increased fear responses in the con text and cue trials, which were not significant (Figure 6.12). Conversely, the animals had a decreased startle response in the PPI experiment both with respect the stimulus alone and the pre -pulse trials, but the outcomes of trials with a pre-pulse were not significant (Figure 6.14). The animals respond differentially to the two anxiogenic stimuli, which could indicate a complex anxiety phenotype which more sensitive phenotyping tests could clarify.

Motor parameters, coordination, (Figures 6.1 and 6.2), digging behaviours (Figures 6.2 and 6.4) and pupillary light responses (Figures 5.11 and 5.12) were unaffected by either mutation with the exception of the deficit in self-righting observed in *Kdm1b*$^{T357M/T357M}$ animals (Figure 6.3).

In total these data demonstrate a difference between phenotype witnessed in early and later circadian screens due to background effects. Results suggest that the *Kdm1a*^{E440G} mutation may affect methylation affecting epigenetic regulation of the molecular clock, or may mediate demethylase independent effects through direct interaction with the molecular clock, but that on an organism level the animals display no behavioural abnormalities corresponding to the effects seen *in vitro* upon expression of mutant constructs, and as such some sort of redundancy or compensation may be at play as discussed later (Section 8.5.7). *Kdm1b*$^{T357M/T357M}$ animals display a phase resetting circadian phenotype, so LSD2 could play a role in regulation of the molecular clock.

8.3 Identification of novel LSD1 and LSD2 Mutants

8.3.1 Existing LSD models and mutations

The circadian phenotype of many existing *Kdm1a* mutants have not been characterised in whole animal behavioural experiments, and *Kdm1a*$^{-/-}$ animals are not viable so conditional knockout would

be required to ascertain any adult circadian phenotype (MGI website). Therefore the search for a novel LSD1 modification suitable to characterise its role in the circadian system (so able to be used in an adult analysis) was undertaken in this investigation. Based on prior knowledge (Section 3.1), the Harwell ENU archive was screened for mutations in the tower and FAD-binding domains of *Kdm1a*.

Regarding LSD2, no mutant models have been previously described. *Kdm1b*$^{-/-}$ animals have been looked at with a view to characterising its role in imprinting (Ciccone et al. 2009), but the animals do suffer from reproductive deficits as previously described (Ciccone et al. 2009) (Section 1.6.4) so the search for ENU mutations in *Kdm1b* was also undertaken here.

The mutants investigated in the current investigation showed different characteristics to another recently investigated novel LSD1 mutant (Nam et al. 2014). Because LSD1 has the ability to demethylate multiple protein products including histones, and is associated with SIRT1 and so the metabolic status of the cell (Nam et al. 2014), A screen for LSD1 binding partners was undertaken. PKCα was unexpectedly identified (Nam et al. 2014). PKCα had been recently shown to play a role in circadian regulation and phase resetting in knockout animals. In order to ascertain whether LSD1 phosphorylation by PKCα modified its demethylation of circadian targets, LSD1 phosphorylation site serine 112 was mutated to alanine and a knockin mouse (*Kdm1a*$^{SA/SA}$) was developed, and subsequently phenotyped (Nam et al. 2014). The circadian phenotypes of the phosphorylation site mutant include a reduced circadian amplitude in constant darkness and attenuated ability to phase reset upon exposure to nocturnal light pulses, which suggest that LSD1 may play a role in facilitation of CLOCK:BMAL1 mediated transcriptional activation and that phosphorylation of LSD1 is required for phase resetting behaviour (Nam et al. 2014). Demethylase activity of LSD1 was however not required for CLOCK:BMAL1 mediated transcriptional activation in this instance (demonstrated using a catalytic null allele). In the current investigation, tower mutant animals do not display any deficit in phase resetting although some circadian perturbation exists as circadian masking is affected in mutant animals. The lack of phase resetting phenotype in the *Kdm1a*$^{E440G/E440G}$ and *Kdm1a*$^{L491H/L481H}$

mutants may be because PKCα-mediated LSD1 phosphorylation is unaffected in these mutants. Rather the tower domain mutation was shown to affect CoREST binding *in vitro* so may play a demethylase-dependent role in clock regulation (Section 4.2.2.3). Overall it is still unclear as to whether the difference between the *Kdm1a*$^{E440G/E440G}$ and *Kdm1a*$^{L491H/L481H}$ mutants and the *Kdm1a*$^{SA/SA}$ mutant is dependent or independent of demethylase activity, and to truly test this hypothesis methylation assays will need to be performed using mutant and wild type tissues.

8.3.2 Harwell ENU archive screening

The identification of the mutants used in the current investigation was directed as previously (Quwailid et al. 2004). Based on prior knowledge of the protein domains and structure of LSD1 and LSD2 (Section 1.6.1 through 1.6.4), exons 10, 11, 12 and 19 of *Kdm1a* and 6, 7, 9 and 10 of *Kdm1b* were screened across DNA from the Harwell ENU mutant archive for mutations (Chapter 3). Two non-synonymous *Kdm1a* mutants and 5 non-synonymous *Kdm1b* mutants were identified in the tower and SWIRM domains respectively, so the efficacy of the screen was in keeping with previous work (Section 3.2, 3.4.3) (Quwailid et al. 2004). Previously the Harwell ENU mutant archive has been screened and novel mutants in genes such as *Phf11* and *DLIC1* identified (Zhang et al. 2014; Banks et al. 2011). Other ENU screening projects are also yielding novel mutant models, including the RIKEN project, where schizophrenia risk associated genes *disrupted-in-schizophrenia 1* (*DISC1*) and *Serine racemase* (*SRR*) amongst other genes have been screened and mutations successfully identified (Gondo et al. 2010). Multiple circadian phenotypes have also been identified in the forward genetics based phenotyping pipelines at MRC Harwell (Bacon et al. 2004; Mousebook website).

In this instance the four mutations chosen for IVF were strategically chosen to avoid lethality due to critical activity of LSD1 in the process of gastrulation (Section 3.4.4). The mutant animals were viable, survived to adulthood and successfully reproduced, so the choice of mutants for re-derivation was successful in this respect.

8.4 Roles of LSD1 and LSD2 in the Molecular clock

8.4.1 Demethylase activity may play a role in circadian clock regulation

The way in which LSD1 and LSD2 influence circadian oscillations could be due to demethylase-dependent or demethylase-independent mechanisms.

It would be expected that if the demethylase activity of *Kdm1a* were affected by the $Kdm1a^{E440G}$ mutation, that LSD1 demethylation at the *Dbp* locus would be decreased in the ChIP experiments, so levels of dimethyl H3K4 would be higher than in wild type MEFs (Section 4.3). This would cause an increase in *Dbp* expression (Section 4.3). ChIP results showed a non-significant increase in H3K4Me2 in MEFs (Section 4.3), but when *Dbp* expression was analysed in mutant animal liver tissue, no change in expression level was observed (although the pattern of expression was perturbed) (Section 5.7.1). The absence of an observable increase in *Dbp* expression in the mutant livers (Figure 5.13) suggests that the subtle increase in methylation of H3K4 at the *Dbp* promoter (Figure 4.13) may not be enough to affect *Dbp* expression in mutants, or alternatively that the $Kdm1a^{E440G}$ does not modulate *Dbp* expression by demethylation of H3K4.

The demethylase activity of LSD1 is not necessarily the only mechanism by which LSD1 affects the clock. Demethylase-independent LSD1 binding to CLOCK-BMAL1 was demonstrated to play a role in phase resetting in response to light, and was disrupted by the *Kdm1a* S112A phosphorylation site mutation (Nam et al. 2014). Demethylase-independent circadian affects have been described with respect other demethylases such as through inhibition of histone deacetylases by JARID1a (DiTacchio et al. 2011). As LSD1 has been shown to interact directly with many clock components (Section 4.2.2.1), the $Kdm1a^{E440G}$ and $Kdm1a^{L491H}$ mutations may affect direct interactions with the clock components. Alternatively the attenuation of the CoREST interaction (Section 4.2.2.4) in $Kdm1a^{E440G/E440G}$ and $Kdm1a^{L491H/L491H}$ mutants could be affecting clock component interaction.

8.4.2 LSD1 and LSD2 directly interact with core clock components

In vitro, LSD1 was shown to co-localise with Bmal1, Per1, Per2 and Rev-erbα, and interact directly with multiple core clock components (Sections 4.2.2.1, 4.2.3). It has been shown that LSD1 binds to CLOCK directly, both in the present study (Section 4.2.2.1) and in previous work (Nam et al. 2014), and as such the lack of CLOCK staining in the immunofluorescence experiment could be due to interference with the antibody to the FLAG epitope tag, or alternatively due to the inability of CLOCK to translocate to the nucleus in the absence of BMAL1 (Kondratov et al. 2013). LSD1 forms a part of several large demethylase complexes, acting with distinct binding partners in various tissues to elicit an array of effects through epigenetic regulation as well as independently of demethylase activity (Culhane & Cole 2007). In all, the results gathered in the present investigation demonstrate that LSD1 interacts with clock components which are known to regulate transcription (Ripperger et al. 2006, Yoshitane et al. 2009). We hypothesize that clock components form part of a large histone-modifying complex along with LSD1. The precise domains responsible for these binding events could be analysed in more depth by systematically manipulating the domains or mutating residues essential for interactions, as has been approached by the Reinke group for CLOCK and BMAL1 (Figure 4.14) (Personal Communication Dr H. Reinke, Uni Düsseldorf, Ge). Finally, other binding partners could be investigated in future by using a wider array of probes for pull-down experiments or a high throughput protein interaction screen such as yeast two-hybrid (Cagney et al. 2001). Regardless of any such detailed characterisation of interactions alone, whether LSD1 protein is binding to clock proteins and acting to demethylate or regulate clock proteins or whether conversely, the clock is regulating LSD1 function cannot be concluded. Rather it is necessary to check with functional assays for modifications upon LSD1 binding such as methylation status, similar to previous work performed to elucidate the role of LSD1 in regulation of DNMT1 (Wang et al. 2009).

8.4.3 LSD1 expression oscillates over LD cycles

It was found in preliminary experiments that LSD1 protein levels change in LD in wild type animal liver tissue (Figure 3.1), which does not concur with findings in other studies (Nam et al. 2014). Previously, *Kdm1a* gene expression and LSD1 protein levels were ascertained using real time PCR and immunoblot analyses of mouse SCN and both were demonstrably stable over 24 hours (Nam et al. 2014). In the Nam et al paper, animals were sacrificed in DD, suggesting that LSD1 levels are therefore light dependent. In the current investigation all RNA extractions for gene expression analysis were performed on tissue collected from animals in LD. Therefore LSD1 may play a prominent role in regulation of the molecular clock but disentangling the effect of the mutation from its modulation throughout LD cycles must be considered.

8.4.4 LSD1 interaction with CoREST may contribute to changes in binding to or demethylation of clock components

The decrease in CoREST binding resulting from mutations of LSD1 (Figure 4.5) could confound conclusions that can be drawn about any direct interactions of LSD1 with clock components. As shown in triple transfection co-expression immunoprecipitations, the presence of CoREST does affect the interaction of LSD1 with REV-ERBα (Figure 4.4). *In vivo* CoREST has multiple chromatin structure-modulating roles independent of LSD1 (Lunyak et al. 2002; Humphrey et al. 2001; You et al. 2001; Hakimi et al. 2002). Therefore any impact of the *Kdm1a*^{E440G} or *Kdm1a*^{L491H} mutations on LSD1:CoREST binding could have CoREST-dependent effects. For instance, CoREST binding could be perturbed in other complexes, compensatory upregulation or downregulation of complex component expression could be induced, and both of these eventualities could impact on chromatin structure independently of LSD1 demethylase function or binding. Further analysis of LSD1s role in circadian mechanisms should take into account LSD1 binding of CoREST and the role of CoREST in cellular function.

8.4.5 Impaired LSD1 and LSD2-mediated demethylation could be affecting the clock

The ChIP experiments performed here yield two main findings; firstly that demethylation patterns varied across subjects (Section 4.3). This could be due to the circadian phase of each sample (if the methylation is regulated in a circadian manner) or just due to inter-individual variation in histone methylation caused by stochastic, environmental, or genetic effects (Feil et al. 2012). Even DNA methylation marks show some variation which could be due to extraneous effects, but histone methylation marks have yet to be examined in this manner (Wagner et al. 2014). The second conclusion from the ChIP data was that overall LSD1-mediated demethylation of *Dbp* sites was impaired by *Kdm1a*$^{E440G/E440G}$ mutation to a lesser extent than observed in *Kdm1a*$^{-/-}$ cells (Figure 4.12). As illustrated in Figure 8.1, the mutation of LSD1 could have resulted in multiple outcomes for H3K4 methylation and therefore gene expression at the *Dbp* locus. The results are not significant but the direction of the observed trend supports the hypothesis that the mutant model is a knockdown of LSD1 demethylase function (represented by arrow 3 in the Figure 8.1). It also suggests that the mutation has a more subtle impact on demethylation than that observed in the knockout (Section 4.3). The role of CoREST in enhancing LSD1 demethylation of H3K4 means that the observed changes in methylation could be partly explained by the decrease in LSD1 binding to CoREST (Figure 4.5) rather than binding to H3K4 itself (Figure 4.13). Alternatively the mutation may be affecting LSD1 substrate binding or LSD1 catalytic activity in a way independent of CoREST *in vivo*, and manipulation of CoREST activity in the animal rather than *in vitro* could be explored to ascertain whether this is the case. Contrary to these findings, real-time PCR data suggests a shift but no increase in *Dbp* expression in liver (Figure 5.13) so perhaps LSD1 is taking circadian effect in a demethylase-independent manner.

In addition to the results from the current investigation into LSD1 binding and demethylase activity at the *Dbp* locus, it would be valuable to examine the role LSD1 plays at other circadian sites, especially those implicated in its mechanism of action in the *Kdm1a*^{S112A} model (*Per2, Cry1, Cry2* and

Rev-erbα) (Nam et al. 2014). As the oscillation of REV-ERBα protein expression was attenuated in *Kdm1a*$^{-/-}$ MEFs (Figure 3.4), it might be of interest to ascertain LSD1s epigenetic effects at the *Rev-erbα* locus and follow those implications right through to the level of protein expression. As LSD1 also demethylates mono-methylated H3K4 (Feil 2009), a more complete picture of its activity could be ascertained by analysis of data from ChIP of monomethyl marks at these loci as well as the dimethyl marks. Mono-, di- and tri-methylation of histone sites tend to act in one transcriptional direction (either repressing or activating expression (Kubicek & Jenuwein 2004)). H3K4 methylation is a marker of transcriptional activation (Di Stefano et al. 2007). However, a recent study showed that dimethylated H3K4 is associated with transcriptional activation whereas monomethylated H3K4 with transcriptional repression (van Dijk et al. 2005). Although it is known through the ChIP performed here that dimethyl H3K4 tends towards being increased in the mutants (Figure 4.12), which would suggest an increase in gene activation (at the *Dbp* promoter at least), the monomethylation of H3K4 has yet to be ascertained.

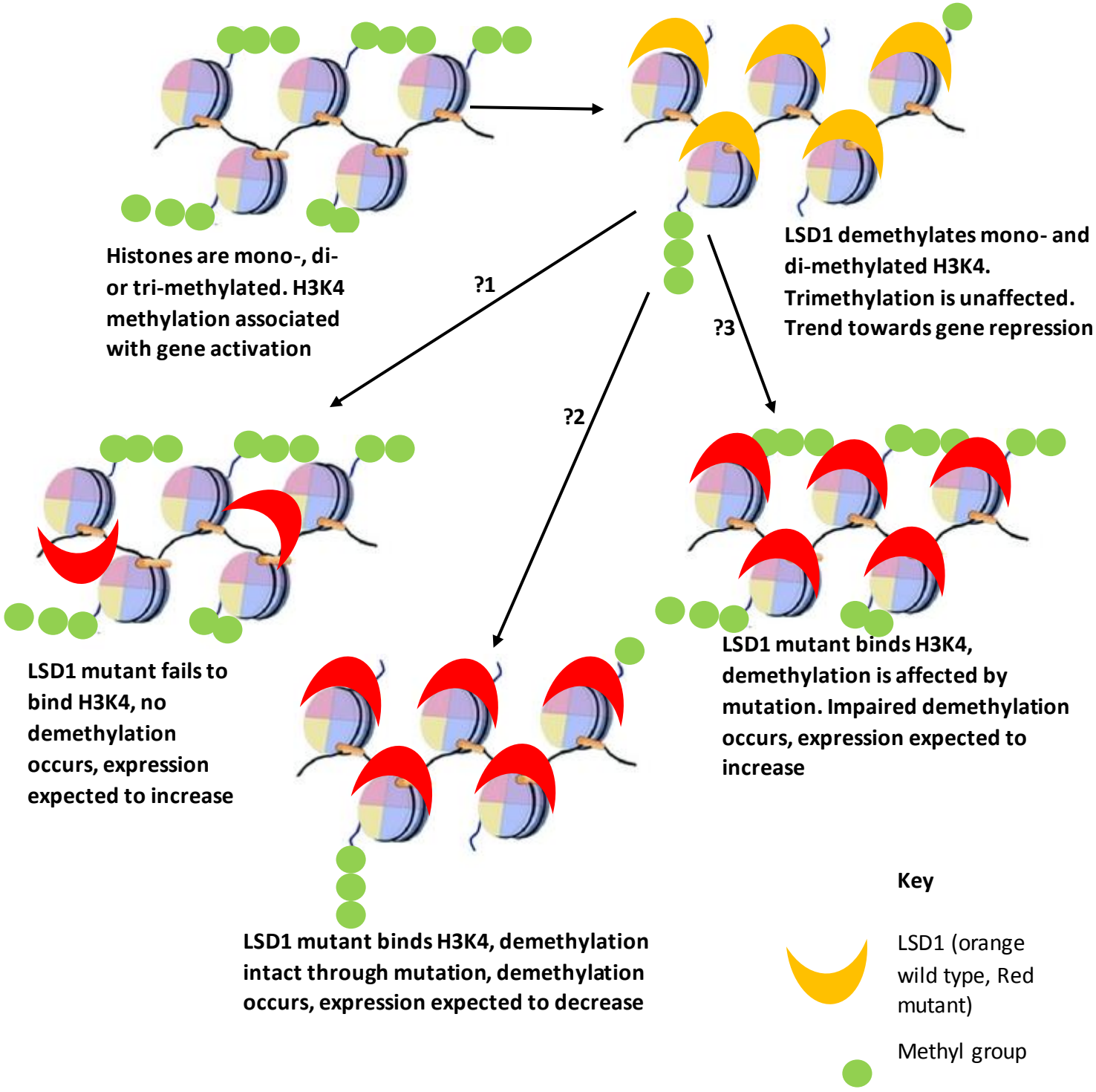

Figure 8.1: Schematic showing the effects of increased or decreased binding on methylation of H3K4

8.4.6 Compound Screen

The clock has a vast number of documented epigenetic regulators (Ripperger & Merrow 2011; Feil 2009). Previous small molecule screens have identified circadian regulators such as KL001, a cryptochrome activating molecule which upon administration to fibroblasts, lung tissue, SCN and *in vivo* in zebrafish causes period lengthening (Hirota et al. 2012). Early compound screens utilized simple western blotting techniques to detect changes in phosphorlyation states (Behshad et al. 2010). In contrast recent high throughput screens used microarrays to detect circadian related enzyme activity or real time bioluminescent reporter monitoring in explants or *in vivo* (Hirota et al. 2012). Regardless of the reporters used, such compound screens have proved successful (Hirota et al. 2012).

LSDs (along with other epigenetic mediators) are regulated by compound inhibitors in the Screenwell epigenetics library (http://www.enzolifesciences.com/BML-2836/screen-well-epigenetics-library/). From the compound screen data collected in the current investigation (Chapter 7), it can be concluded that the effect of the compounds on circadian period is highly variable. As such it would be of value to increase the number of sample systems tested, and eventually to look at *in vivo* circadian behaviour upon administration of the drugs to understand the true physiological effect of each compound (Hirota et al. 2012). Also of value would be development of more specific small molecules to pinpoint the mechanisms resulting in circadian changes in the cells, as was undertaken previously (Binda et al. 2010). Chemical engineering or screening virtual databases such as the ZINC database (Irwin 2008) for compounds with similar kinetics or binding profiles to compounds of interest could be utilised to develop more target-specific small molecules from those identified in the current investigation or already established (such as tranylcypromine (Binda et al. 2010)).

In cells overexpressing *Kdm1a*^{E440G} and *Kdm1a*^{L491H} circadian period was shortened whereas in *Kdm1b*^{P281L} expressing cells period was lengthened (Figure 4.1). Tranylcypromine is known to inhibit

both LSD1 and LSD2 (Binda et al. 2010). 1nM tranylcypromine lengthened circadian period by 1.2 hours on average, but as dose increased, the period returned to similar period to untreated cells (Figure 7.2c). This might indicate that the action of tranylcypromine lengthens period through LSD2 inhibition at low concentrations but as dose increases, the drug targets LSD1 more and affects period though inhibition of LSD1. Alternatively, tranylcypromine is acting on another target as yet unidentified in the fibroblast and U2OS cell systems. This can be determined by administering the drug to each cells treated with siRNA against LSD1, LSD2 or both. Comparing the observed circadian effect of tranylcypromine in LSD1-expressing, LSD2-expressing or both LSD1 and LSD2 expressing cells which would make clear which target it was acting on, or if it were another target altogether.

8.4.7 Conclusions of Molecular Work

From the molecular data collected in this body of work, it appears that both LSD1 and LSD2 interact with several components of the molecular clock directly, and that both the *Kdm1a*^{E440G} and *Kdm1a*^{L491H} mutation of LSD1 impair these interactions (Chapter 4). There is a possibility the *Kdm1a*^{E440G} mutant displays altered clock function as methylation in promoter regions is increased in comparison to wild type animals (Section 4.3).

There are limitations to each of the molecular techniques employed in this investigation. Firstly, the way the output of interest is detected might affect the measurements, which is why cell lines expressing reporter constructs stably were used preferentially to using cell lines which require transient reporter expression. This could perceivably affect the observed efficacy of the compounds in the current screen. Secondly, it is well known that different cell lines respond differentially to the same dose of the same compound (Oike et al. 2011), and that each cell line expresses subtle differences in endogenous clocks (Yagita et al. 2001; Menger et al. 2007) as well as potentially oscillating with different amplitudes or periods (Oike et al. 2011). It should be taken into consideration that changes in period observed upon knockdown of circadian transcripts in cells may not mirror the circadian changes seen in a whole animal, as siRNA knockdown of *Npas2*, *Rev-erbα*

and *Per2* in U2OS cells display changes in period length different to that of the corresponding knockout animal (Baggs et al. 2009). This effect is beyond explanation through efficiency of the siRNA knockdown (Baggs et al. 2009). In this investigation compound effects were analysed in rat-1 fibroblasts (Figure 7.1, 7.2) before looking into SCN slices in the final traces (Figure 7.3). Compared to using cell lines for compound investigations, brain slices are much more costly and time consuming (Sundstrom et al. 2005). One animal is required for every two slices, and in order to measure bioluminescence for the final recording the animals either need to be crossed to a reporter line or the slice needs to be transiently transfected or transduced with a reporter, which is far more complex and has a lower percentage chance of success than might be achievable in a simpler reporter cell line investigation (Al Dosari & Gao 2009, Murphy & Messer 2001). However, such slice work does confer a huge amount more physiological information which can be drawn from each trace (Hastings et al. 2005). One such example is the ability to monitor the central pacemaker itself rather than a peripheral system with only local pacemaker properties or a cell line reporter with no pacemaker ability at all (Hastings et al. 2005). If a mutation or compound were to impact rhythms in the central oscillator could potentially play an important role in the clock. Pacemaker oscillation is stringent and compensates for many external influences (Abraham et al. 2010). SCN effects could also indicate a potential for organism-wide effects (as the pacemaker confers rhythm on many targets (Aschoff 1960)), which might manifest in a stronger phenotype than perturbations in peripheral systems alone (Nakahata et al. 2008). Although this is suggestive, there is no guarantee that an observation of *ex-vivo* slice oscillation reflects the reality *in vivo*. For example, the *Clock* knockout mouse model displays a modest shortening in free running period, but the *Clock* knockout SCN oscillates with a normal period (DeBruyne et al. 2007a; DeBruyne et al. 2007b). If *Clock* is knocked down with siRNA in U2OS cells they become arrhythmic (Zhang et al. 2009), demonstrating another level of complexity when looking at a core clock component in multiple clock models. If knockdown of a core clock component such as CLOCK in such established circadian models display such variable circadian changes, then the measurements taken from those same models when

investigating epigenetic regulators of the clock could conceivably be more variable. This is due to the multiple circadian and non-circadian targets of epigenetic regulators which impinge on the clock (Ko & Takahashi 2006; DeBruyne et al. 2007b).

Many alternative systems could be employed to study oscillations in the SCN, for example primary SCN cell cultures passaged from reporter or mutant animals (Welsh et al. 2004). Another example might be to generate a stable reporter cell line by immortalising such SCN cells, as was approached previously (Allen et al. 2001; Earnest & Cassone 2005; Earnest et al. 1999; Menger et al. 2007). Upon SCN2.2 cell characterisation, characteristics were observed that indicated that the cells at hand were not SCN-like (Appendix 2). Therefore they were not used for recordings. Although both of the aforementioned options could give the opportunity to look at SCN cell function using molecular techniques, in both cases the cells would be plated and cultured either as primary neurons or as a cell line so the overall network properties of the SCN would be lost (Hastings et al. 2005, Welsh et al 2005). Therefore any compound or mutant effects affecting cell-cell coupling or network dynamics might be missed without examining the system in tact. The various merits of each system used in the current investigation are detailed in table 8.1.

Name	Stable Reporter	Synchronised by			1°	T (days	Rhythm	Contamination	Use in Project
		Forskolin	Dex	Serum					
Rat-1 Fibroblasts	Per2/Bmal1	Y	Y	Y	N	7 (can passage)	Fades over 7 days	Checked	First round of compound screening. Transient mutant construct expression
U2OS Cell Line	Per2	Y	Y	Y	N	7 (can passage)	Fades over 7 days	Checked	Transient mutant construct expression.
Mouse Embryonic Fibroblasts	Per2 (breeding)	Y	Y	Y	Y	7 (limited passages)	Fades over 7 days	N	Primary model of peripheral clock for second round of compound screening. Cross to LSD mutants for investigation.
Primary Cortical Neurones	Per2 (breeding)	Y	Y	Y	Y	14	Fades over 14 days	N	Primary model of central clock for second round of compound screening. Cross to LSD mutants for investigation.
SCN2.2 Cell Line	-	-	-	-	N	7 (can passage)	Not detected	Y	No further use.
Organotypic SCN Slice	Per2 (breeding)	N/A	N/A	N/A	Y	30+	30+	N	Pacemaker model, test of few interesting compounds only. Cross to LSD mutants for investigation, lentiviral transduction of mutant constructs for investigation.

Table 8.1: Merits and Disadvantages of Circadian Model Systems

Dex= Dexamethasone

8.5 Behavioural Phenotyping

8.5.1 Circadian Phenotypes over backcrosses

During the circadian testing of LSD1 and LSD2 mutants the phenotype observed in animals of early backcross status differed from that of the animals nearer to congenic on the C57BL/6 background (Chapter 5). Breeding programmes have been described previously (Bacon et al. 2004). Strain background influences various circadian parameters including the amount of running in LD and DD (which has been demonstrated to be higher for C57BL/6 than C3H), alpha (which is longer for C57BL/6 than C3H) and tau (which is longer for C3H animals than C57BL/6) (Banks et al. 2015). As the mutants used in the current investigation are BALB/c x C3H crossed to C57BL/6, these parameters may be affected by the proportion of G1 genetic material remaining at each backcross stage.

8.5.2 Circadian Phenotypes of LSD1 mutants

Based on *in silico* knowledge, both *Kdm1a*$^{L491H/L491H}$ and *Kdm1a*$^{E440G/E440G}$ mutations in the tower domain of *Kdm1a* would be predicted to affect CoREST binding, and as such decrease demethylase activity in similar ways (Section 1.6). Interaction studies showed that each mutation affected CoREST binding to different extents (Figure 4.5). If the two mutants were changing circadian behaviour in the same way as each other, the difference between the two mutants might be accounted for by the differential in CoREST binding between the two. However, as *Kdm1a*$^{E440G/E440G}$ animals displayed increased running through the light phase and during light pulses (Section 5.2.1.2), and *Kdm1a*$^{L491H/L491H}$ animals showed a shortened period in LL and phase resetting phenotypes but no change in the proportion of running in the light and no masking effects (Section 5.2.1.2), the difference in binding of LSD1 to CoREST cannot explain these *in vivo* differences. Rather they could be mediating different effects to one another by changing clock component binding (Section 4.2.2.4), or changing targeting of histones at circadian loci or even catalytic activity (Section 4.3).

8.5.3 Circadian Phenotypes of LSD2 mutants

At backcross 2, the *Kdm1b*$^{P281L/P281L}$ and *Kdm1b*$^{T357M/T357M}$ mutants had different circadian behaviour phenotypes (Section 5.2.2.1). Both mutant lines showed a lack of masking, but in LD *Kdm1b*$^{P281L/P281L}$ animals displayed activity in the dark phase, whereas *Kdm1b*$^{T357M/T357M}$ animals displayed splitting in LL (Section 5.2.2.1). This discrepancy could indicate that the two mutations which both lie in the SWIRM domain (which could affect LSD2 binding to its correct target sites (http://www.ebi.ac.uk/interpro/entry/IPR007526)) have separate circadian effects. *Kdm1b*$^{P281L/P281L}$ animals were not tested at backcross 5 due to time constraints. However, the absence of many circadian phenotypes in backcross 5 *Kdm1b*$^{T357M/T357M}$ animals (Section 5.2.2.2) suggests that either the circadian effects of LSD2 mutants, like LSD1 mutants, are background dependent (Banks et al. 2015), or that LSD2 plays at most a minor role in regulation of the clock, which is not evident on a purer C57BL/6 background (Banks et al. 2015).

8.5.4 Conclusions of Circadian Phenotyping

There were substantial differences between the circadian effect of each of the mutations identified in the current point mutation screen on outputs *in vivo* and *in vitro* (Chapter 4 and Chapter 5). *In vitro* circadian findings contrasted to those *in vivo*. Whereas demethylase inhibition with compounds shortened circadian period in U2OS cells, and overexpression of the mutant constructs in fibroblasts caused shortened circadian period in *Kdm1a*^{E440G} and *Kdm1a*^{L491H}mutants, *in vivo* there was no significant change in circadian period for *Kdm1a*$^{E440G/E440G}$ and *Kdm1a*$^{L491H/L491H}$ mutants, so the mutations do not mimic LSD inhibition in cell lines. As the two LSD1 mutations affect LSD1 function differentially and are therefore clearly not simply knockdowns of LSD1 activity, the outcome of LSD1 inhibition might be predicted to be different to that of either mutation.

Another explanation for the discrepancy in period change between cells and animals is that the cell system is fundamentally different to the situation *in vivo*. For example in *Clock*$^{-/-}$ animals, behavioural rhythms are shortened but SCN tissue oscillations are normal and peripheral tissues

including lung and liver are arrhythmic (DeBruyne et al. 2007a; DeBruyne et al. 2007b; Baggs et al. 2009). Therefore LSD1 inhibition by compounds could be predicted to be discrepant to mutant mice even in cases where the compound is specific to a known target. Mutant overexpression in cells also caused changes in circadian period, unlike mutant animals *in vivo*. Again, differences between the two models can explain this, and it must be considered that gene overexpression is not a physiologically accurate representation of how the mutations affect the cell system. Compensation and redundancy in a whole animal are much more complex and wide ranging than *in vitro* as so many factors influence circadian behaviour network-wide and can be at play through development of the circadian system (Reppert & Weaver 2002).

The difference between the circadian properties of tissues (even the pacemaker itself) *in vitro* in comparison to whole animal behaviour *in vivo* can also be discrepant. Examples include the *Transgenic R6/2* Huntingdon's disease mouse (Pallier et al. 2007) and the *Per1*$^{-/-}$ mutant mouse (Pendergast et al. 2009). In the R6/2 mouse, the SCN oscillates with a robust rhythm but the animal is arrhythmic in wheel-running assays (Pallier et al. 2007; Morton et al. 2005). Conversely in the Per1-/- animals, the SCN displays weak or absent circadian *Per2*:Luc oscillations in *ex vivo* explants but the animals continue to run in a circadian manner (Pendergast et al. 2009). When the SCN of these animals was monitored, the molecular rhythm of clock gene expression is dampened but the electrical activity of the SCN is intact in freely-behaving mice (Takasu et al. 2013). The mechanism by which this occurs is still unknown. The above findings suggest that the molecular rhythms observed in a mutant model may not reflect the properties of the SCN and as such the electrical coupling and neural output of the LSD mutant SCN would be of interest in understanding its true role in the clock (Hastings et al. 2005). Also, in order to compare properties of the mutant SCN tissue to that of the whole animal, *Kdm1a*$^{E440G/E440G}$ and *Kdm1a*$^{L491H/L491H}$ mutation behaviours observed *in vivo* such as masking must be tested in the *in vitro* SCN system. This might yield more comparative results than examining the period of gene expression or neural output, as the period of circadian behaviour is unaffected in the mutant animals *in vivo*.

Many important clock component mutant animals also display a very mild phenotype when compared to the circadian disruption witnessed *in vitro*, such as *Per1-/-* animals (Pendergast et al. 2009). $Cry1^{-/-}$ and $Cry2^{-/-}$ animals also demonstrated an unexpectedly subtle change in circadian behaviour, in this instance due to redundancy in the negative feedback loop (compensation of Cry1 loss in the Cry1-/- animals by Cry2 and vice versa). Further investigation of such redundancy in the Cry knockout animals showed the importance of the cryptochromes through the arrhythmia precipitated in the double knockout animal (van der Horst et al. 1999). Therefore further investigation might clarify the role of LSDs further if redundancy is at play. For instance, if $Kdm1a^{E440G/E440G}$ and $Kdm1b^{T357M/T357M}$ animals were crossed together, any redundancy between the two genes may be unmasked; if LSD1 were to compensate for the $Kdm1b^{T357M}$ mutation in $Kdm1b^{T357M/T357M}$ animals, it would be predicted that circadian disruption resulting from $Kdm1b^{T357M}$ mutation would be unmasked and the $Kdm1a^{E440G}$ mutant phenotype were worsened or modified accordingly.

To tease apart the roles of LSD1 from LSD2 using mutant animals, LSD1 and LSD2 wheel-running phenotypes could be examined *in vivo* whilst using inhibitor compounds. Pharmacological manipulation of circadian enzymes CK1ɖ and CK1ε has been previously used to examine the respective roles of the two isoforms *in vivo* (Meng et al. 2010). Firstly, *in vitro* CK1ɖ-selective and CK1ε-selective inhibitors PF-670462 and PF-4800567 were analysed in a dose response experiment in cells, and then in *ex-vivo* SCN slices from wild type and CK1 *Tau* mutant animals to ascertain to what extent each isoform affected circadian oscillation (Meng et al. 2010). The roles of the CK1 enzymes were subsequently verified by analysis of circadian wheel-running phenotypes in compound-treated wild type and mutant animals (Meng et al. 2010). LSD1-selective and LSD2-selective compounds could be tested on LSD mutant animals *in vivo* to ascertain if inhibition of the two demethylases rescued or worsened the phenotype observed in the untreated mutants, and dose response experiments *in vivo* and *in vitro* could indicate to what extent other demethylases played a role independent of LSD1 and LSD2. In order to use these mutant animals for examination

of the roles of demethylase inhibitors, circadian masking or phase resetting responses should be monitored as these parameters are affected by LSD mutations (Chapter 5).

8.5.5 Neurobehavioural Phenotypes

Kdm1a$^{E440G/E440G}$ and *Kdm1b*$^{T357M/T357M}$ animals appeared to display complex behavioural phenotypes. These included subtle anxiety phenotypes (Section 6.2.3, 6.2.4), which were not immediately reminiscent of any models of major circadian or neuropsychiatric disorders.

8.5.6 *Kdm1a*$^{E440G/E440G}$ Phenotypes

Kdm1a$^{E440G/E440G}$ animals appear to be of normal weight, there is no evidence for changes in aversive learning as demonstrated in the fear conditioning test and both anxiety and circadian measurements are disrupted in subtle ways (Chapter 6). Overall results do not clearly suggest the animals are a model for depression, but several of the parameters tested in *Kdm1a*$^{E440G/E440G}$ animals which were impaired (such as cognition and social interactions) could be affected by depression (Cryan & Holmes 2005), so a depression phenotype should not be entirely ruled out. As LSD1 is inhibited by the antidepressant tranylcypromine (Binda et al. 2010), the use of inhibitor compounds in the *Kdm1a*^{E440G} model could inform the behavioural analysis further and also have implications on the treatment of depression or lead to refinement of existing LSD1 inhibitors such as tranylcypromine (Binda et al. 2010). The characterisation of a depression phenotype would ideally involve a depression test such as the forced swim paradigm or tail suspension test followed up with measurements considering anxiety, sleep or EEG alterations, cognitive deficits, anhedonia, weight discrepancies and alterations in the HPA axis (Cryan & Holmes 2005). As well as FST or TST, metabolite testing could be performed to investigate HPA axis function to test for depression directly as the stress axis is implicated in a subset of human patients suffering from the disorder (Pariante & Lightman 2008). Depression testing has yet to be approached using LSD1 conditional knockout animals or using existing models such as the S112A animal which displays circadian deficits (Nam et al. 2014), so such investigations would also be of merit in ascertaining the role of LSD1 in

the brain on mood regulation. If depression phenotypes were not observed in LSD models, this may be due to the complexity of the (usually polygenic) disorder in humans may not be adequately emulated by models generated by mutation of a single residue or perturbation of just one locus (Redei et al. 2001), and as such the role of LSD1 in depression could still not be ruled out.

8.5.7 Interpretation of behavioural data

Behaviour in animals is complex and multiple neural pathways are involved in processing environmental scenarios and producing a phenotypic response (Reppert & Weaver 2002). In order to isolate such responses, a series of phenotyping paradigms were employed in the current investigation to give a complete data set (Chapter 6). However, data from each test must be considered in the context of others, and conclusions drawn with great care (Kalueff et al. 2007).

Anxiety is a complex behavioural phenomenon (Neumann et al. 2011). Although anxiety phenotypes were observed in some tests on *Kdm1a*$^{E440G/E440G}$ and *Kdm1b*$^{T357M/T357M}$ mutant animals (Section 6.2.3, 6.2.4), the measures recorded could be affected by non-anxiety related phenotypes such as motor deficits (which could affect freezing time or startle reflexes recorded by PPI equipment) or cognition (and inability to process information like a pre-shock tone which must be remembered from trial to trial for fear conditioning to occur, for example) (Kalueff et al. 2007). As *Kdm1a*$^{E440G/E440G}$ animals displayed deficits in cognition (Section 6.2.3), this could confound results observed in anxiety testing as the animals are less able to process information than wild type counterparts.

In any behavioural test, there is inherently inter-individual variability (Lewejohann et al. 2011). In this study, 10 mice of each genotype were used in as many tests as cohort size allowed for, which increased the power of the study and reduced the observable variability. However, as was evident in the social dominance paradigm, individual variation could still account for the lack of observed phenotype when data from many mice was collated (Figure 6.8). In the case of *Kdm1a*$^{E440G/E440G}$, it was evident that the animals behaved in one of two distinct ways upon commencing a social dominance trial; by acting aggressively and forcing the opposite mouse back (which would score a

'win') or completely conversely, avoiding social interaction altogether by backing away from the other animal (scoring a 'lose'). In the case of the wild type animals, these two extremes were rarely witnessed and rather the mouse would explore the other animal and then through trying to escape the tube one mouse or other would be pushed from the tube. This leads to both groups of animals averaging similar numbers of wins but through two very discrepant responses. Therefore phenotyping data must be considered with care and attention to detail in order to ascertain true phenotypes, as was recorded in social dominance tests where the number of trials backed out of was found to be significantly higher for homozygous animals in comparison to wild type controls even though total number of wins was not significantly different between the two groups (Figure 6.9).

Care must also be taken when looking across anxiety data from different paradigms (Carola et al. 2002; Llc 2001). Anxiety phenotypes were evident in both the *Kdm1a*$^{E440G/E440G}$ and *Kdm1b*$^{T357M/T357M}$ animals although different tests demonstrated different changes in behaviour (Section 6.2.3, 6.2.4). *Kdm1a*$^{E440G/E440G}$ animals display a decrease in latency to enter the centre of the open field arena suggestive of decreased anxiety (Section 6.2.3). In many other anxiety tests performed here including time spent in the centre of the arena, activity levels and the latency in the first trial, homozygotes were not statistically different to control animals (Section 6.2.3). This does not indicate an overt hyperanxiety or hypoanxiety as is evident across the results of multiple measures but many animal models display a complex combination of anxiety phenotypes which are not universal across multiple behavioural tests (Carola et al. 2002; Llc 2001). The lack of difference in the first trial may be due to behavioural effects precipitated by exposure to a novel environment (such as hyperactivity in a novel environment, which is a phenotype observed in the serotonin receptor knockout anxiety model (Ramboz et al. 1998)).

Upon handling, the *Kdm1a*$^{E440G/E440G}$ animals were observably easily agitated but in a trial like the open field where animals are not interfered with, this might not explain the latency observation

(Section 6.2.3). The agitation observed on handling was not apparent in many anxiety tests. This could be due to discrepancies in the stimulus used or the measures taken as anxiety output in the tests (Neumann et al. 2011). It would therefore be of value in this instance to design a behavioural test where handling is the anxiogen, even if this is practically challenging.

Hyperactivity could result in reducing the difference between mutants and controls in the first trial instance but as activity levels were consistent across groups, hyperactivity can also be ruled out in this instance. Therefore the latency difference observed during the open-field test could be due to either anxiety or a memory deficit.

8.5.8 Developmental phenotypes of Kdm1a$^{E440G/E440G}$ mutants

Neurobehaviour assessed in adult animals could be affected by developmental processes (Hoerder-Suabedissen et al. 2013). LSD1 plays important roles throughout development and is essential for gastrulation, which is why LSD1 knockout is embryonic lethal (Macfarlan et al. 2011). LSD1 has been implicated in key developmental gene expression (Foster et al. 2010), cell cycle regulation (Nair et al. 2012) and is essential for progenitor stem cell differentiation (Sun et al. 2011; Macfarlan et al. 2011; Whyte et al. 2012). The mechanism by which LSD1 allows differentiation of various stem cells is under investigation, and miR-137 has been shown to regulate LSD1 activity in neural differentiation (Sun et al. 2011). LSD1 is essential for DNMT1-associated cell reprogramming in the epithelial to mesenchymal transition (EMT) (Lin et al. 2010; McDonald et al. 2011). EMT mechanisms are key to embryogenesis and in carcinogenesis (Lin et al. 2010), and have been associated with BRCA1 induced breast cancer mechanism (Wu et al. 2012). The role of LSD1 in regulation of cell cycle and differentiation genes links its role in development to its role in cancer and dysregulation of LSD1 can contribute to either cancer propagation or to a failure of stem cells to differentiate in development (Joska et al. 2014; Zhang et al. 2012). LSD1 is essential for and therefore expressed in early mammalian development. Its expression patterns have been fully assessed in zebrafish and in *Drosophila melanogaster*, and early in development is ubiquitous in both instances (Di Stefano et al.

2007; Lin et al. 2010). In the case of zebrafish, this expression becomes more anterior through the developmental process localising in particular in neural progenitor areas, and siRNA and chemical inhibition induces a failure of neural development (Lin et al. 2010). In *Drosophila melanogaster*, expression remains ubiquitous throughout development but LSD1 activity is tissue specific in viable individuals, and neural development remains intact whereas ovarian development is perturbed and all viable individuals are sterile (Di Stefano et al. 2007). A mammalian LSD1 flox allele mutant containing E413G and M448V mutations in the tower domain display a perinatal-lethal heart defect phenotype, again demonstrating a tissue specific developmental effect of LSD1 (Nicholson et al. 2013). Together the literature on the fundamental developmental roles of LSD1 allow for the possibility that LSD1 mutation could lead to sex-specific or tissue-specific phenotypes. In the *Kdm1a*$^{E440G/E440G}$ mutants, we observed a male-specific gonadal phenotype in our histological assessment. Other organ systems appear to be normal in the mutants, but more subtle phenotypes could still exist in adult animals due to developmental deficits which were undetected in this general screen. The behavioural perturbations observed in *Kdm1a*$^{E440G/E440G}$ and *Kdm1a*$^{L491H/L491H}$ mutant animals may also have been founded in developmental abnormalities, especially given the associations of LSD1 with neural progenitor differentiation (Fuentes et al. 2012; Han et al. 2014). Neuropsychiatric disorders like schizophrenia and autism in humans have been associated with developmental perturbations (Hoerder-Suabedissen et al. 2013), and established schizophrenia risk genes such as Disrupted in Schizophrenia-1 (DISC1) have been demonstrated to play roles in development, and neural development particularly (Singh et al. 2011). Interestingly, mir-137 has been recently identified as a player in schizophrenia and therefore may link LSD1 mechanisms in development to neuropsychiatric behaviours in adults (Yin et al. 2014). As *Kdm1a*$^{E440G/E440G}$ and *Kdm1a*$^{L491H/L491H}$ mutants survive to adulthood the essential role of LSD1 in gastrulation is not perturbed by the mutations, and the heart appears normal in adult animals. As the mutants do display some phenotypes (Chapters 5 and 6), LSD1 function is in some way being affected, which is predicted to be due to the change in CoREST binding (Figure 4.5) and therefore efficiency in

demethylating histone and other substrates (Section 4.3), perhaps including DNMT1 which is essential for EMT and maintaining DNA methylation (Lin et al. 2010; Wang et al. 2009). However any change in the developmental process could be caused by the mutations interfering with LSD1 binding or demethylation of multiple complex elements involved in development. This could include the CoREST-HDAC complex, the NuRD complex or other development-specific transcriptional complexes or alternatively molecular clock components (as the clock is known to influence developmental processes such as stem cell differentiation (Brown 2014))

8.6 Future Work

8.6.1 Alternative LSD1 and LSD2 models for circadian investigation

There are further experiments required in the circadian characterisation of LSD1 and LSD2 which were not investigated here due to time constraints. Only four exons of each gene were screened in the current investigation and as the mutation of these domains was deemed most likely to yield a non-lethal model of circadian disruption. However, as the mutants displayed such a subtle phenotype, in future investigations, exons encoding domains necessary for catalysis could be disrupted postnatally by conditional disruption using tamoxifen-inducible ubiquitin-Cre recombinase technology. Alternatively, conditional knockout of LSD1 in SCN would bypass disruption of the role of *Kdm1a* in development.

Alternatively newer techniques allowing the targeting of any gene of interest such as the CRISPR-Cas9 system has the potential to surpass the use of ENU screening in genetic investigations (Wang et al. 2013). CRISPR-Cas9 utilises the ability of the Cas9 protein to recognise specific DNA sequences dictated by the presence of guide RNA (gRNA) templates which can be designed to match any sequence in the genome (Ran et al. 2013). Cas9 can introduce breakages which induce repair pathways which can be hijacked to introduce specific mutations (Ran et al. 2013). More recently, mutations rendering the Cas9 DNA nuclease inactive have allowed for various modifications of the

target DNA sequence by almost any domain fused to the Cas9 component (including activation through Cas9 fusion with enhancer domains, repression with repressor domains or visualisation through attaching a reporter such as GFP) (Ran et al. 2013). Other advantages of the CRISPR-Cas9 system are numerous. Firstly, modification by CRISPR can be made permanent (unlike transient RNAi-mediated gene disruption), and can be used in high-throughput investigations (unlike nuclease strand break and repair manipulation using Zinc-Finger Nucleases and Transcription-Activator Like Effector Nucleases, ZFNs and TALENs). This will allow investigators to introduce human SNPs identified in patient populations into target genes to generate rodent models (Wang et al. 2013). Another advantage is that multiple manipulations may be introduced into one system, and finally the modifications can be controlled temporally by introducing the Cas9 phage at any developmental stage (for example before or after *Sry*-mediated sex determination at 11.5dpc which might be of interest in LSD1 function), allowing for the generation of multiple complex models of clinical relevance (Wang et al. 2013). And finally, CRISPR technology has already been demonstrated to rescue disease phenotypes (Yin et al. 2014) and as such shows promise in future treatment of familial circadian disorders such as in single-mutation causative gene FASPS or DSPS cases, as well as more complex polygenetic disorders. An example of where CRISPR could be used to e rescue a monogenic phenotype is the CRISPR knockout kit of the human *AANAT* gene (associated with a subset of DSPS families), which is already available for use in cloning (for example http://www.scbt.com/sirna/table-annat.html).

If CRISPR technology were used to investigate LSD1, it would be interesting to specifically disrupt residues essential for CLOCK or BMAL1 binding in order to disrupt its direct interaction with clock components. This would lend insight into whether it affects clock oscillations in a core clock component-binding dependent manner.

There are still clear advantages with regards discoveries of importance through serendipity, which is only preserved in unbiased methods such as ENU mutant screening. Serendipitously, during the

undertaking of the current study, the association of SNPs in *Kdm1b* with the development of human disorders of sexual development was found (Personal Communication, Dr A. Greenfield, MRC Harwell). This is encouraging for future work into the clarification of the role of LSDs in gonad development.

8.6.2 CoREST disruption

It would also be pertinent to examine CoREST mutants in respect of LSD1 mutant behaviour. If the interaction of LSD1 with clock proteins is truly disrupted as molecular results might suggest (Figure 4.5), a double LSD1-CoREST mutant would be expected to behave similarly to the LSD1 mutant alone if the knockout of CoREST was additive to that of LSD1 (whereas if epistatic effects dependent on background were observed the phenotype would be difficult to predict (Shimomura et al. 2001)). Confounds resulting from the multiple roles of CoREST in other chromatin modifying complexes (Lunyak et al. 2002; Humphrey et al. 2001; You et al. 2001; Hakimi et al. 2002) may also contribute to any phenotype observed.

8.6.3 Thorough Molecular Characterisations

It might be useful to investigate the effect of LSD mediated demethylation at circadian loci such as Rev-erbα or its regulators CLOCK and BMAL1 using ChIP as the LSD1 knockout caused a disruption in REV-ERBα protein level oscillation (Figure 3.4). If demethylation of H3K4 at this locus were impaired, it would indicate that the change in protein level was due to an LSD1 histone demethylase-dependent mechanism rather than a direct interaction with REV-ERBα or rather due to modification, and so lend insight into LSD1s role in the clock.

CoIPs and ChIPs have previously been performed at timepoints over a 24 hour timespan in circadian investigations to ascertain when interaction and histone methylation was taking place (Alenghat et al. 2008; Johnstone et al. 2012). This would show whether LSD1 was binding to clock proteins or modifying histones in a circadian manner or constitutively. Using native tissue (SCN as well as

peripheral tissue) for protein and chromatin analyses, rather than overexpressing cell lines, would give a more physiologically accurate representation of the interactions and histone modifications at play *in vivo* (Turner 2001). By comparing patterns of direct interaction and demethylation patterns, the role of LSDsin clock regulation over the 24 hour day could be clarified.

It has already been shown that circadian modulators can be identified through compound screens such as the current one (Gale & Yan 2015; Hirota et al. 2012). As discussed earlier, the activity of LSDs in histone modification is difficult to isolate with small-molecule inhibitors *in situ*, as demethylases are known to act in concert with each other and form large chromatin modifying complexes (Culhane & Cole 2007). Studies into cancer mechanisms have led to the development of compounds of much greater specificity to LSDs (Suzuki & Miyata 2011; Ma et al. 2015) and if novel compounds such as these were screened for circadian effects, it would result in a clearer picture of the circadian impact of LSD disruption.

If compounds were screened in mutant SCN slices as well as wild-type tissue, mutant oscillations could be examined in situ, and further to this whether those effects were demethylase dependent (reversible with demethylase inhibitors), and whether other mechanisms were partially responsible (whether drug treatments were sufficient to rescue the mutant phenotype) (Meng et al. 2010). This experiment is theoretically plausible, but would require the breeding of many more animals which was not possible within the limits of the current project.

8.6.4 Further behavioural work, and developmental phenotyping

Although behavioural investigation of ENU mutants coupled with SCN studies can give some insight into the true role of the gene in question in the pacemaker, in reality the circadian system is far too complex to verify the true role of one gene in the system using wheel running assays alone (Banks & Nolan 2011). Wheel running output is dependent on many subtle genetic influences, individual variability is high and confounds such as feeding schedules are difficult to tease apart (Banks & Nolan 2011). Sleep measurements such as EEG or video tracking and analysis with ANYmaze software

(Stoelting, Wood Dale, IL, USA) (Fisher et al. 2012) can provide some confirmatory data with regards the biological rhythm but again, the same confounds outside of circadian drive from the pacemaker itself exist in such assays. Behavioural phenotyping including tests performed in the current investigation can shed light on the existence of confounds such as anxiety or motor problems (Kas & Van Ree 2004), but again separating the role of the SCN itself is of great difficulty in such a complex network of neural afferents involving so many behavioural outputs (Banks & Nolan 2011).

Circadian data in the current investigation is firstly confounded by the impact of single-housing of normally group-housed animals, and as such developing a system able to track circadian outputs of multiple animals in a cage would be valuable in abolishing this confound (Personal Communication, Dr L. Brown, NDCN University of Oxford).

Secondly and pertinently, LSD1 and LSD2 inhibition by monoamine inhibitors including the antidepressant tranylcypromine lends credence to the possibility that LSDs might play a role in monoaminergic signalling which is central to mood regulation and is disrupted in depressed patients (Heninger et al. 1996). The mood of mutants should be assessed with FST or TST paradigms as depression may contribute to the masking of circadian or other behavioural phenotypes (Kas & Van Ree 2004).

Finally, one of the most striking phenotypes of the *Kdm1a*$^{E440G/E440G}$ mutants was that found in the morphology of the adult gonad. To find out exactly what this can be attributed to, the development of the mutant animal gonads must be more extensively characterised. It appears that gonads look normal at the point of sex determination and there was no evidence of sex reversal in *Kdm1a*$^{E440G/E440G}$ animals (Figure 6.17). Looking at morphology over time would help to pinpoint the mechanism of development affected by *Kdm1a*^{E440G} mutation and subsequently relevant signalling pathways which could be perturbed in development could be ascertained and investigated as a result (Small et al. 2005). Developmental issues could impact on the behaviours observed in adult

animals similar to many previous neurodevelopmental models (Lassi et al. 2012; Keays, Tian, et al. 2007; Hoerder-Suabedissen et al. 2013).

8.7 Final conclusions

The importance of the role of epigenetics in regulation of the clock is becoming evident (Azzi et al. 2014; Sahar & Sassone-Corsi 2012; Ripperger & Merrow 2011). The role of demethylases has only recently been recognised as a dynamic process which can contribute to circadian mechanisms (Ripperger & Schibler 2006), and individual demethylases appear to play multiple demethylase activity-dependent and -independent roles in regulation of the clock (Section 1.6).

In this investigation, reverse genetics was employed to identify novel mutations of LSD1 and LSD2 and the circadian impact of the mutations was subsequently characterised (Chapter 3). LSD1 and LSD2 interact with clock proteins (Figure 4.2, 4.3) and *Kdm1a* mutation affects circadian mechanisms both *in vitro* (Figure 4.5, 4.6, 4.7), and to a lesser extent *in vivo* (Chapter 5). It was shown that the mutations of *Kdm1a* affected interaction with LSD1 cofactor CoREST (Figure 4.5) and iwith multiple clock components (Figure 4.6, 4.7). The $Kdm1a^{E440G}$ mutation was shown to attenuate LSD1 binding to and demethylation of circadian loci and could suggest the mutation to be a knockdown of function when compared to knockout MEFs (Section 4.3), more samples need testing to confirm this. Overexpression of LSD1 and LSD2 mutants caused changes in circadian period in cell lines (Figure 4.1).

$Kdm1a^{E440G/E440G}$ animals displayed decreased light-induced masking and altered running in the light phase (Figure 5.2 and 5.3). $Kdm1b^{T357M/T357M}$ animals displayed a deficit in phase resetting in response to the CT22 light pulse and were observed to show abnormal re-entrainment to a 6hr phase delay (Figure 5.8). These findings suggest that LSD1 and LSD2 contribute to the regulation of circadian mechanisms, perhaps playing a role in the circadian response to light downstream of ipRGC function in the retina.

Differences between animals at different backcrosses (Chapter 5) demonstrate that strain background effects are of great importance in characterising circadian behaviour in ENU models. Discrepancy between the *in vivo* wheel running activities of mutations (Figures 5.2 and 5.4) demonstrate that each mutation may impinge on LSD activity in different ways despite both affecting the same protein domain. Differences between the circadian impact of each mutation *in vitro* and *in vivo* (Chapters 4 and 5) demonstrate that LSD1 and LSD2 effects on circadian mechanism *in vitro* could be compensated for or redundant *in vivo*, and highlight the limitations of models used in circadian investigation in consideration of the true physiological state *in vivo*.

Kdm1a$^{E440G/E440G}$ animals display a complex behavioural phenotype including a learning and memory deficit (Section 6.2.3). *Kdm1b*$^{T357M/T357M}$ animals display changes in startle responses (Figure 6.14). Tests which differentiate between aspects of depression-like behaviour could help to clarify the roles of LSDs in the regulation of neurobehaviour. *Kdm1a*$^{E440G/E440G}$ mutation also causes a gonadal phenotype (Figure 6.17), and *Kdm1b*$^{T357M/T357M}$ a deficit in self-righting (Figure 6.3) which both require further investigation.

Although the roles of LSD1 and LSD2 in circadian mechanism have been investigated and some circadian effects are observed upon mutation of both genes, many aspects of their function remain to be clarified. The roles of epigenetic modifiers require characterisation of changes at the level of epigenetic regulation, demethylase-independent regulation, resulting transcript expression in multiple tissues and resulting protein expression in multiple tissues to truly understand the nature of their input into clock mechanisms. The *Kdm1a*$^{E440G/E440G}$ mutant demonstrates promise as a tool for the investigation of LSD1 function in the clock and its function appears to be multifaceted in nature.

APPENDIX 1: OPPF Cloning

In order to analyse the interaction of LSDs with clock components, GST tagged constructs were generated in the OPPF. Methods are detailed in (OPPF website). High throughput InFusion cloning was undertaken and resulting constructs amplified using Phusion polymerase before sequencing to confirm correct insertion (Figure A1.1).

Primers used are detailed in Table A1.1, and vectors as listed in the methods Chapter. Figure A1.2 is the PCR confirmation of amplification of constructs.

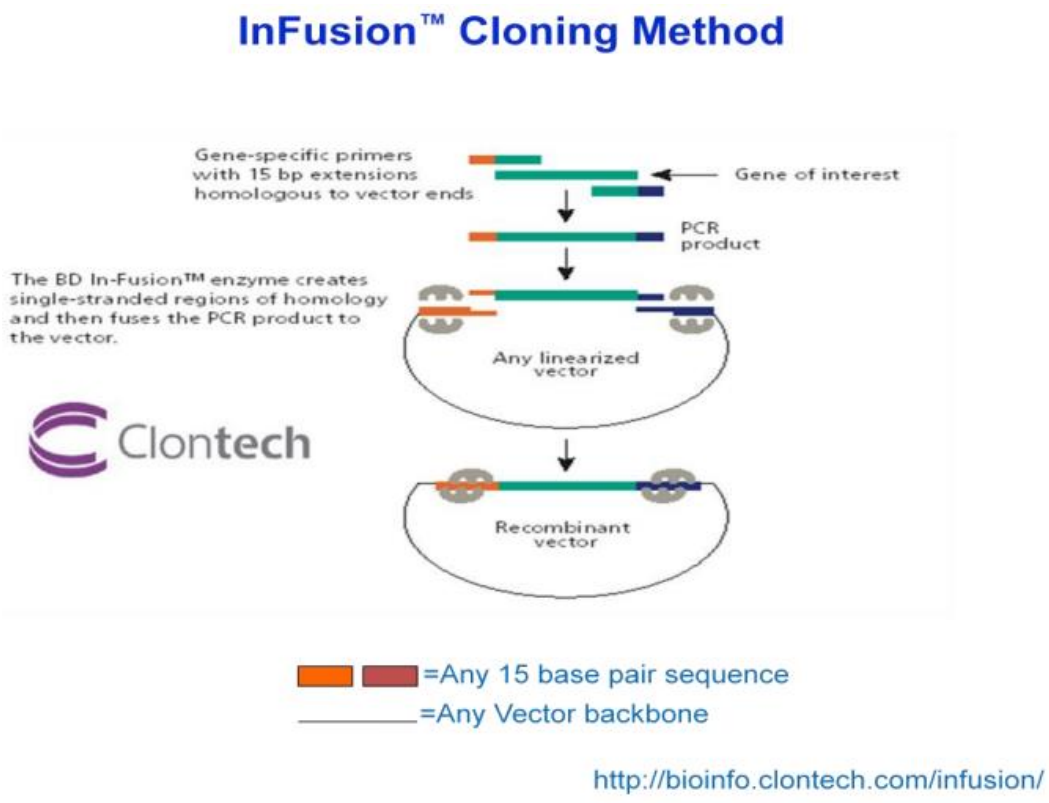

Figure A1.1: Schematic of OPPF cloning procedure

insert	Forward Primer	Reverse Primer
LSD1	ATGTTGTCTGGGAAGAAGGCGGC	GGGTTCATACTGATCACCCGGGCCA
LSD2	ATGGCCGCATCTCGAGGGAG	CGTCGGAAACCCGGGCCA
CRY1	ATGGGGGTGAACGCCGTGC	GTTTCAGGTCGCCGTCTCGTCATTG
CRY2	ATGGCGGCGGCTGCTGTG	CGGTCGTTCGTTCCTGAGGAGATCT
BMAL1	ATGGCGGACCAGAGAATGGAC	CACTGAACGGTACCGGCGAC
PER1	ATGAGTGGTCCCCTAGAAGGGGCC	GGACGTCTTCTTTTGTCGTGGTCG
PER2	ATCAATGGATACGTGGACTTCTCCCC	GGGGTCCTATCTCCGGGTATGC
CLOCK	ATGTTGTTTACCGTAAGCTGTAGTAA AATGAGCTCG	GCTGGGAAGGTTCCAAGTTGGTGTC

Table A1.1: OPPF cloning primers

a

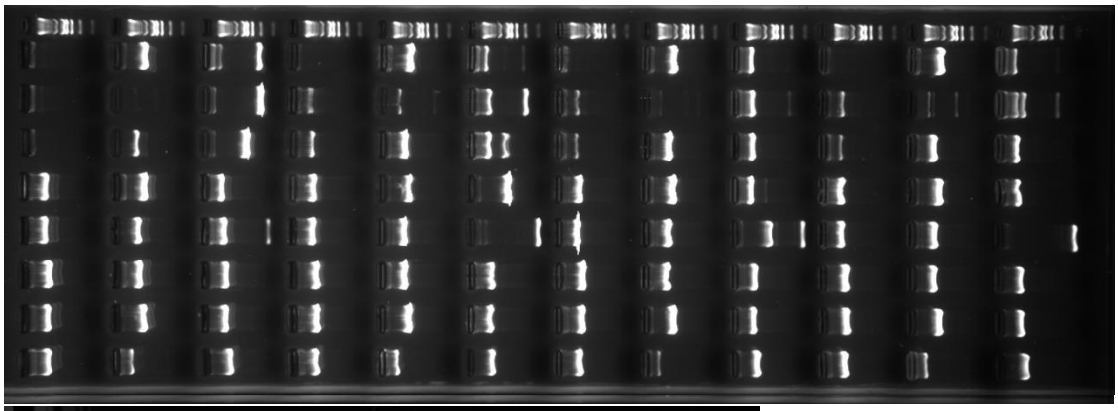

b

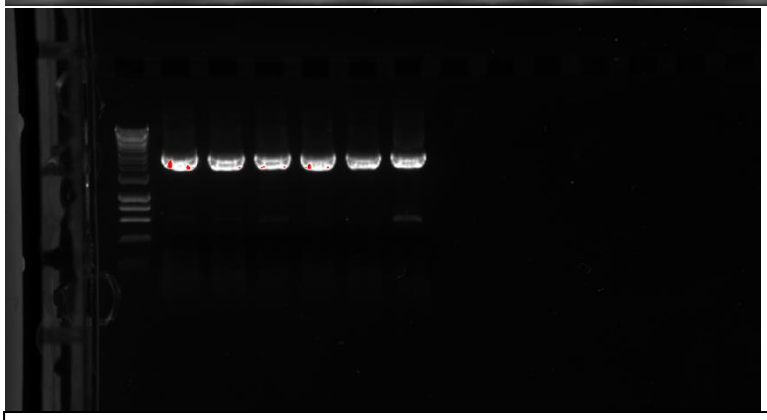

Figure A1.2: OPPF cloning PCRs

a) Whole plate Phusion amplification
b) LSD1-POPINJ KOD amplification

APPENDIX 2: SCN2.2 cells

In order to assess the effects of compounds on SCN tissue in screening, several slice cultures would be required. As such it would be beneficial to use less animals and beneficial to reduce variability across samples by replacing the slice cultures with immortalised SCN cells. SCN2.2 cells were previously characterised to display pacemaker properties (Earnest et al. 1999).

Coverslips coated in SCN2.2 cells were stained immunofluorescently using anti-VIP antibodies and anti-Somatostatin antibodies, which are known to stain SCN cells. SCN2.2 cells were also stained with DyeI, which stains neuronal cell membranes (Section 2.6.2). No staining was observed using VIP and somatostatin antibodies, suggesting the cells are not SCN-like. Very few cells were identified using DyeI (Figure A2.1) suggesting a low percentage of the culture to be neuronal.

SCN2.2 cells were also synchronised and tested for circadian gene oscillation over 24 hours. No circadian genes were shown to oscillate in the cultures (Figure A2.2)

SCN2.2 cells were subsequently not used in the current investigation.

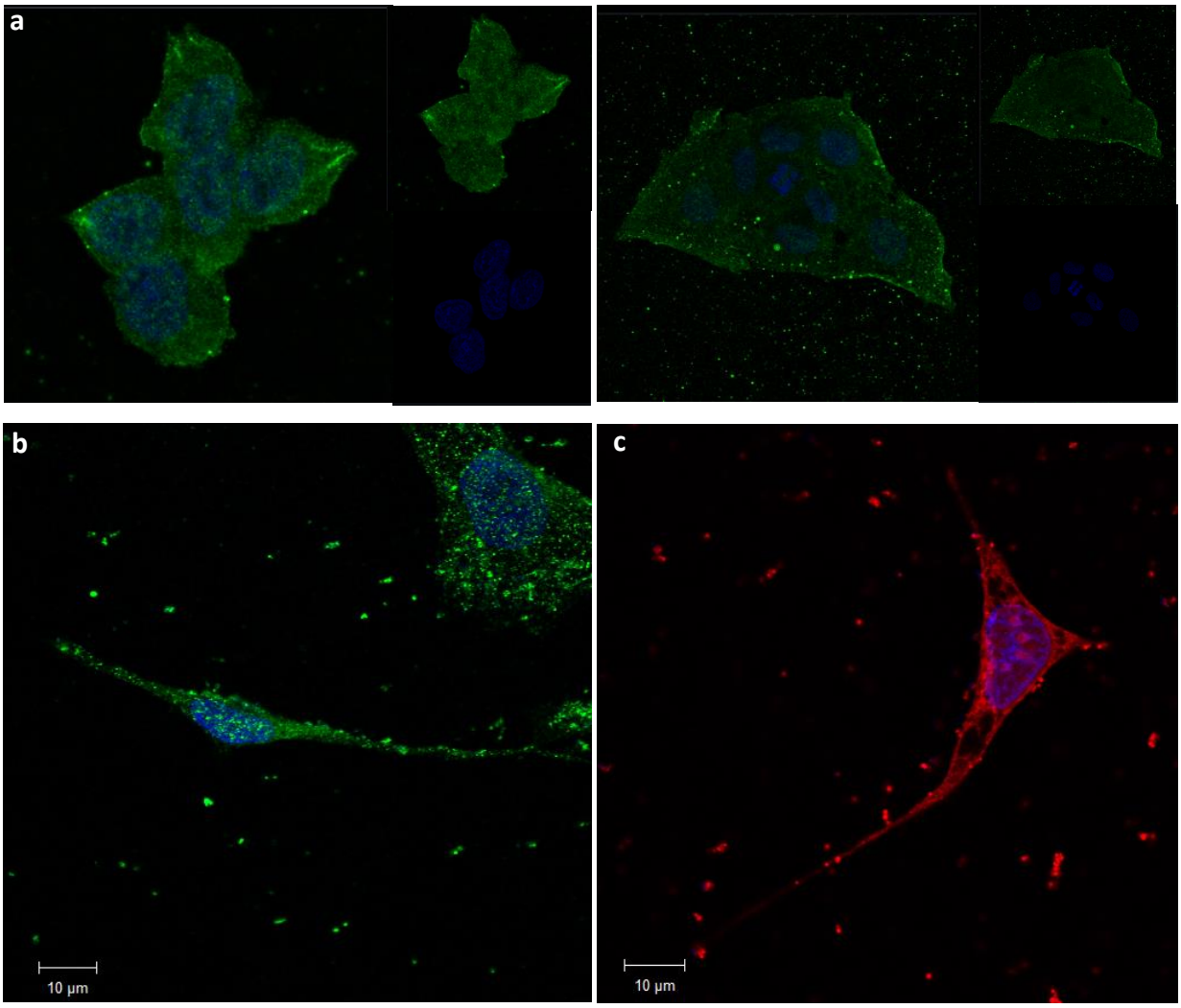

Figure A2.1: Staining and characterisation of SCN2.2 cultures (from confluent coverslips)

a) Anti-VIP
b) Anti-Somatostatin
c) DiI

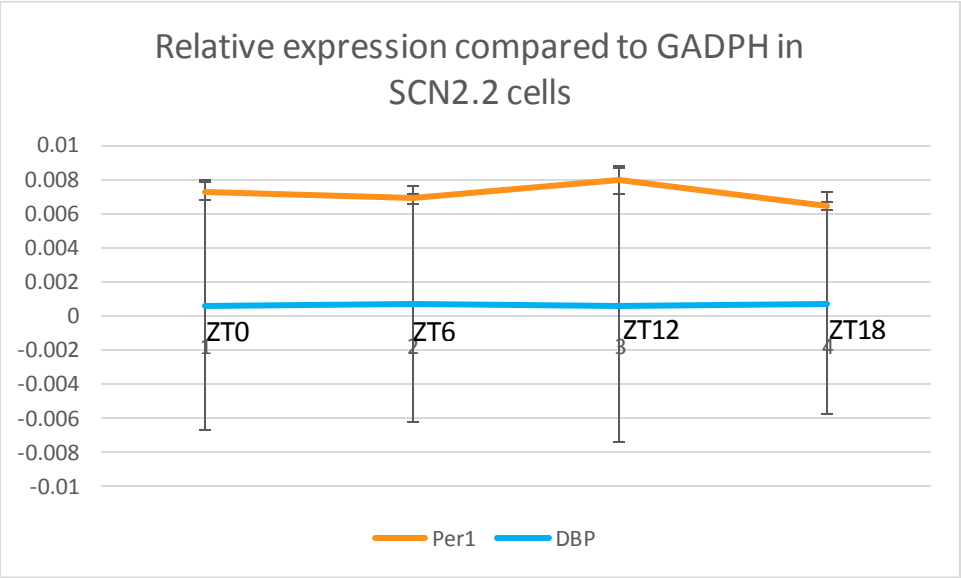

Figure A2.2: qPCR amplification of clock genes showed no oscillation in SCN2.2 cultures

N=3 and 3 technical replicates per timepoint

BIBLIOGRAPHY

Acevedo-Arozena, A. et al., 2008. ENU mutagenesis, a way forward to understand gene function. *Annual review of genomics and human genetics*, 9, pp.49–69.

Ahnaou, A. & Drinkenburg, W.H.I.M., 2011. Disruption of glycogen synthase kinase-3-beta activity leads to abnormalities in physiological measures in mice. *Behavioural Brain Research*, 221(1), pp.246–252.

Al Dosari, M. & Gao, X., 2009. Nonviral gene delivery: principle, limitations, and recent progress. *The AAPS journal*, 11(4), pp.671-681

Albrecht, U. et al., 1997. A differential response of two putative mammalian circadian regulators, mper1 and mper2, to light. *Cell*, 91(7), pp.1055–1064.

Alenghat, T. et al., 2008. Nuclear receptor corepressor and histone deacetylase 3 govern circadian metabolic physiology. *Nature*, 456(December), pp.997–1000.

Allen, G. et al., 2001. Oscillating on borrowed time: diffusible signals from immortalized suprachiasmatic nucleus cells regulate circadian rhythmicity in cultured fibroblasts. *The Journal of neuroscience : the official journal of the Society for Neuroscience*, 21(20), pp.7937–7943.

Alvarez, J.D. et al., 2003. Non-cyclic and developmental stage-specific expression of circadian clock proteins during murine spermatogenesis. *Biology of reproduction*, 69(1), pp.81–91.

Amente, S., Lania, L. & Majello, B., 2013. The histone LSD1 demethylase in stemness and cancer transcription programs. *Biochimica et Biophysica Acta - Gene Regulatory Mechanisms*, 1829(10), pp.981–986.

Anand, S.N. et al., 2013. Distinct and separable roles for endogenous CRY1 and CRY2 within the circadian molecular clockwork of the suprachiasmatic nucleus, as revealed by the Fbxl3(Afh) mutation. *The Journal of Neuroscience*, 33(17), pp.7145–53.

Angoa-Pérez, M. et al., 2013. Marble burying and nestlet shredding as tests of repetitive, compulsive-like behaviors in mice. *Journal of visualized experiments : JoVE*, (82), p.50978.

Antoch, M.P. et al., 1997. Functional identification of the mouse circadian Clock gene by transgenic BAC rescue. *Cell*, 89(4), pp.655–667.

Aschoff, J., 1960. Exogenous and endogenous components in circadian rhythms. *Cold Spring Harbor symposia on quantitative biology*, 25, pp.11–28.

Aschoff, J., 1999. Masking and parametric effects of high-frequency light-dark cycles. *The Japanese journal of physiology*, 49(1), pp.11–18.

Asher, G. et al., 2008. SIRT1 Regulates Circadian Clock Gene Expression through PER2 Deacetylation. *Cell*, 134(2), pp.317–328.

Aton, S.J. et al., 2005. Vasoactive intestinal polypeptide mediates circadian rhythmicity and synchrony in mammalian clock neurons. *Nature neuroscience*, 8(4), pp.476–483.

Azzi, A. et al., 2014. Circadian behavior is light-reprogrammed by plastic DNA methylation. *Nature neuroscience*, 17(3), pp.377–82.

Bacon, Y. et al., 2004. Screening for novel ENU-induced rhythm, entrainment and activity mutants. *Genes, Brain and Behavior*, 3, pp.196–205.

Baggs, J.E. et al., 2009. Network features of the mammalian circadian clock. *PLoS Biology*, 7(3), pp.0563–0575.

Balsalobre, A., Marcacci, L. & Schibler, U., 2000. Multiple signaling pathways elicit circadian gene expression in cultured Rat-1 fibroblasts. *Current Biology*, 10(20), pp.1291–1294.

Banks, G. et al., 2015. Genetic background influences age-related decline in visual and nonvisual retinal responses, circadian rhythms, and sleep. *Neurobiology of Aging*, 36(1), pp.380–393.

Banks, G.T. et al., 2011. Behavioral and other phenotypes in a cytoplasmic Dynein light intermediate chain 1 mutant mouse. *The Journal of neuroscience : the official journal of the Society for Neuroscience*, 31(175), pp.5483–5494.

Banks, G.T. & Nolan, P.M., 2011. Assessment of Circadian and Light-Entrainable Parameters in Mice Using Wheel-Running Activity. *Current Protocols in Mouse Biology*, 1, pp.369–381.

Baran, S.E. et al., 2009. Chronic stress and sex differences on the recall of fear conditioning and extinction. *Neurobiology of Learning and Memory*, 91(3), pp.323–332.

Barbaric, I. et al., 2007. Spectrum of ENU-induced mutations in phenotype-driven and gene-driven screens in the mouse. *Environmental and Molecular Mutagenesis*, 48(2), pp.124–142.

Barkus, C., 2012. Genetic Mouse Models of Depression. *Curr Top Behav Neurosci*.

Barlow, D., 2014. *Clinical Handbook of Psychological Disorders, Fifth Edition : A Step-by-Step Treatment*,

Baron, R. et al., 2011. Molecular mimicry and ligand recognition in binding and catalysis by the histone demethylase LSD1-CoREST complex. *Structure*, 19(2), pp.212–220.

Baron, R. & Vellore, N.A., 2012. LSD1/CoREST is an allosteric nanoscale clamp regulated by H3-histone-tail molecular recognition. *Proceedings of the National Academy of Sciences*, 109(31), pp.12509–12514.

Bartness, T.J., Song, C.K. & Demas, G.E., 2001. SCN efferents to peripheral tissues: implications for biological rhythms. *Journal of biological rhythms*, 16(3), pp.196–204.

Bartolomucci, A. et al., 2009. Acute and chronic social defeat: Stress protocols and behavioral testing. *Neuromethods*, 42, pp.261–275.

Bass, J. & Takahashi, J.S., 2010. Circadian integration of metabolism and energetics. *Science (New York, N.Y.)*, 330(6009), pp.1349–1354.

Baudet, M.-L. et al., 2011. miR-124 acts through CoREST to control onset of Sema3A sensitivity in navigating retinal growth cones. *Nature Neuroscience*, 15(1), pp.29–38.

Beaule, C. & Cheng, H.-Y.M., 2011. The Acetyltransferase CLOCK Is Dispensable for Circadian Aftereffects in Mice. *Journal of Biological Rhythms*, 26(6), pp.561–564.

Bechtold, D.A., Gibbs, J.E. & Loudon, A.S.I., 2010. Circadian dysfunction in disease. *Trends in Pharmacological Sciences*, 31(5), pp.191–198.

Behshad, E., et al., 2010 Phosphorylation State-Dependent High Throughput Screening of the c-Met Kinase. *Curr Chem Genomics*, 4, pp.27-33.

Bell-Pedersen, D. et al., 2005. Circadian rhythms from multiple oscillators: lessons from diverse organisms. *Nature reviews. Genetics*, 6(7), pp.544–556.

Benca, R., 2000. Psychiatric sleep-wake disorders. in New Oxford Textbook of Psychiatry, vol 1 pp. 1021-1026, Oxford. Oxford University Press

Bertholet, J.Y. & Crusio, W.E., 1991. Spatial and non-spatial spontaneous alternation and hippocampal mossy fibre distribution in nine inbred mouse strains. *Behavioural brain research*, 43(2), pp.197–202.

Bienz, M., 2006. The PHD finger, a nuclear protein-interaction domain. *Trends in Biochemical Sciences*, 31(1), pp.35–40.

Binda, C. et al., 2010. Biochemical, structural, and biological evaluation of tranylcypromine derivatives as inhibitors of histone demethylases LSD1 and LSD2. *Journal of the American Chemical Society*, 132(3), pp.6827–6833.

Binda, C., Mattevi, A. & Edmondson, D.E., 2002. Structure-function relationships in flavoenzyme-dependent amine oxidations: A comparison of polyamine oxidase and monoamine oxidase. *Journal of Biological Chemistry*, 277(27), pp.23973–23976.

Bliss, T.V.P. & Errington, M.L., 1977. "Reeler" mutant mice fail to show spontaneous alternation. *Brain Research*, 124(1), pp.168–170.

Bolles, R.C., 1970. Species-specific defence reactions and avoidance learning. *Psychological Review*, vol. 77(no. 1), pp.pp. 32–48.

Borb, A.A. & Achermann, P., 1999. Sleep homeostasis and Models of Sleep Regulation. *J Biol Rhythms*, vol.14 (no. 6), pp, 559-570

Borbély, A.A., 1982. Sleep regulation: Circadian Rhythm and Homeostasis. *Sleep*, pp, 83-103

Bradley, C. et al., 2007. Carcinogen-induced histone alteration in normal human mammary epithelial cells. *Carcinogenesis*, 28(10), pp.2184–2192.

Braff, D.L., Geyer, M.A. & Swerdlow, N.R., 2001. Human studies of prepulse inhibition of startle: Normal subjects, patient groups, and pharmacological studies. *Psychopharmacology*, 156(2-3), pp.234–258.

Brancaccio, M. et al., 2013. A Gq-Ca2+ Axis controls circuit-level encoding of circadian time in the suprachiasmatic nucleus. *Neuron*, 78(4), pp.714–728.

Brown, S. a., 2014. Circadian clock-mediated control of stem cell division and differentiation: beyond night and day. *Development (Cambridge, England)*, 141(16), pp.3105–3111.

Brown, S.A. et al., 2005. PERIOD1-associated proteins modulate the negative limb of the mammalian circadian oscillator. *Science (New York, N.Y.)*, 308(5722), pp.693–696.

Brown, S.A. et al., 2002. Rhythms of mammalian body temperature can sustain peripheral circadian clocks. *Current Biology*, 12(18), pp.1574–1583.

Brown, S.E. et al., 2007. Variations in DNA methylation patterns during the cell cycle of HeLa cells. *Epigenetics : official journal of the DNA Methylation Society*, 2(1), pp.54–65.

Brunello, N. et al., 2000. Depression and sleep disorders: clinical relevance, economic burden and pharmacological treatment. In *Neuropsychobiology*. pp. 107–119.

Buhr, E.D., Yoo, S.-H. & Takahashi, J.S., 2010. Temperature as a universal resetting cue for mammalian circadian oscillators. *Science (New York, N.Y.)*, 330(6002), pp.379–385.

Buijs, R. et al., 2013a. Peripheral circadian oscillators: Time and food. *Progress in Molecular Biology and Translational Science*, 119, pp.83–103.

Buijs, R.M., Escobar, C. & Swaab, D.F., 2013b. The circadian system and the balance of the autonomic nervous system. *Handbook of Clinical Neurology*, 117, pp.173–191.

Buijs, R.M. & Kalsbeek, A., 2001. Hypothalamic integration of central and peripheral clocks. *Nature reviews. Neuroscience*, 2(7), pp.521–526.

Bunning, E., 1973. *The physiological clock. Circadian rhythms and biological chronometry*, New York: Springer.

Cagney, G. & Uetz, P., 2001. High-throughput screening for protein-protein interactions using yeast two-hybrid arrays. C*urrent protocols in protein science / editorial board, John E. Coligan ... [et al.],* Ch. 19, Unit 19.6

Camacho, F. et al., 2001. Human casein kinase Idelta phosphorylation of human circadian clock proteins period 1 and 2. *FEBS letters*, 489(2-3), pp.159–165.

Carola, V. et al., 2002. Evaluation of the elevated plus-maze and open-field tests for the assessment of anxiety-related behaviour in inbred mice. *Behavioural Brain Research*, 134(1-2), pp.49–57.

Cervoni, N. & Szyf, M., 2001. Demethylase Activity Is Directed by Histone Acetylation. *Journal of Biological Chemistry*, 276(44), pp.40778–40787.

Cheeta, S. et al., 1997. Changes in sleep architecture following chronic mild stress. *Biological psychiatry*, 41(96), pp.419–427.

Chen, Y. et al., 2006. Crystal structure of human histone lysine-specific demethylase 1 (LSD1). *Proceedings of the National Academy of Sciences of the United States of America*, 103(38), pp.13956–13961.

Choi, J. et al., 2014. Modulation of lysine methylation in myocyte enhancer factor 2 during skeletal muscle cell differentiation. *Nucleic Acids Research*, 42(1), pp.224–234.

Ciccone, D.N. et al., 2009. KDM1B is a histone H3K4 demethylase required to establish maternal genomic imprints. *Nature*, 461(September), pp.415–418.

Clinical-Trial, http://clinicaltrials.gov/ct2/show/NCT02034123?term=lysine+specific+demethylase&rank=2.

Cohrs, S., 2008. Sleep disturbances in patients with schizophrenia: Impact and effect of antipsychotics. *CNS Drugs*, 22(11), pp.939–962.

Collas, P. & Dahl, J.A., 2008. Chop it, ChIP it, check it: the current status of chromatin immunoprecipitation. *Frontiers in bioscience : a journal and virtual library*, 13, pp.929–943.

Costa, R. et al., 2014. The lysine-specific demethylase 1 is a novel substrate of protein kinase CK2. *Biochimica et biophysica acta*, 1844(4), pp.722–9.

Courtet, P., 2010. [Suicidal risk in recurrent depression]. *Encephale*, 36 Suppl 5(0013-7006 (Print)), pp.S127–S131.

Crusio, W.E. et al., 2013. *Behavioral Genetics of the Mouse: Volume 1, Genetics of Behavioral Phenotypes*,

Cryan, J.F. & Holmes, A., 2005. The ascent of mouse: advances in modelling human depression and anxiety. *Nature reviews. Drug discovery*, 4(9), pp.775–790.

Culhane, J.C. & Cole, P.A., 2007. LSD1 and the chemistry of histone demethylation. *Current Opinion in Chemical Biology*, 11(5), pp.561–568.

Day, J.J. & Sweatt, J.D., 2011. Epigenetic Mechanisms in Cognition. *Neuron*, 70(5), pp.813–829.

Deacon, R.M.J., 2006a. Burrowing in rodents: a sensitive method for detecting behavioral dysfunction. *Nature protocols*, 1(1), pp.118–121.

Deacon, R.M.J., 2006b. Digging and marble burying in mice: simple methods for in vivo identification of biological impacts. *Nature protocols*, 1(1), pp.122–124.

Deacon, R.M.J. & Rawlins, J.N.P., 2005. Hippocampal lesions, species-typical behaviours and anxiety in mice. *Behavioural Brain Research*, 156(2), pp.241–249.

Deacon, R.M.J. & Rawlins, J.N.P., 2006. T-maze alternation in the rodent. *Nature protocols*, 1(1), pp.7–12.

Deboer, T., Détári, L. & Meijer, J.H., 2007. Long term effects of sleep deprivation on the mammalian circadian pacemaker. *Sleep*, 30(3), pp.257–262.

DeBruyne, J.P. et al., 2006. A Clock Shock: Mouse CLOCK Is Not Required for Circadian Oscillator Function. *Neuron*, 50(3), pp.465–477.

DeBruyne, J.P., Weaver, D.R. & Reppert, S.M., 2007a. CLOCK and NPAS2 have overlapping roles in the suprachiasmatic circadian clock. *Nature neuroscience*, 10(5), pp.543–545.

DeBruyne, J.P., Weaver, D.R. & Reppert, S.M., 2007b. Peripheral circadian oscillators require CLOCK. *Current Biology*, 17(14).

Derian, C.K. et al., 1989. Inhibitors of 2-ketoglutarate-dependent dioxygenases block aspartyl ??-hydroxylation of recombinant human factor IX in several mammalian expression systems. *Journal of Biological Chemistry*, 264(12), pp.6615–6618.

Van Dijk, K. et al., 2005. Monomethyl histone H3 lysine 4 as an epigenetic mark for silenced euchromatin in Chlamydomonas. *The Plant cell*, 17(9), pp.2439–2453.

Ding, J.M. et al., 1998. A neuronal ryanodine receptor mediates light-induced phase delays of the circadian clock. *Nature*, 394(6691), pp.381–384.

DiTacchio, L. et al., 2011. Histone Lysine Demethylase JARID1a Activates CLOCK-BMAL1 and Influences the Circadian Clock. *Science*, 333(6051), pp.1881–1885.

Doi, M., Hirayama, J. & Sassone-Corsi, P., 2006. Circadian Regulator CLOCK Is a Histone Acetyltransferase. *Cell*, 125(3), pp.497–508.

Duncan, W.C., 1996. Circadian rhythms and the pharmacology of affective illness. *Pharmacology and Therapeutics*, 71(3), pp.253–312.

Dunlap, J.C. et al., 1997. Light-Induced Resetting of a Mammalian Circadian Clock Is Associated with Rapid Induction of the. *Cell*, 91, pp.1043–1053.

Dunlap, J.C., 1999. Molecular bases for circadian clocks. *Cell*, 96(2), pp.271–290.

Dunlop, B.W. & Nemeroff, C.B., 2007. The role of dopamine in the pathophysiology of depression. *Archives of general psychiatry*, 64(3), pp.327–337.

Duong, H.A. et al., 2011. A molecular mechanism for circadian clock negative feedback. *Science (New York, N.Y.)*, 332(6036), pp.1436–1439.

Earnest, D.J. et al., 1999. Immortal time: circadian clock properties of rat suprachiasmatic cell lines. *Science (New York, N.Y.)*, 283(5402), pp.693–695.

Earnest, D.J. & Cassone, V.M., 2005. Cell culture models for oscillator and pacemaker function: Recipes for dishes with circadian clocks? *Methods in Enzymology*, 393, pp.558–578.

Easton, A., Arbuzova, J. & Turek, F.W., 2003. The circadian Clock mutation increases exploratory activity and escape-seeking behavior. *Genes, brain, and behavior*, 2(1), pp.11–19.

Ebihara, S. et al., 1986. Genetic control of melatonin synthesis in the pineal gland of the mouse. *Science (New York, N.Y.)*, 231(4737), pp.491–493.

Ebihara, S., Tsuji, K. & Kondo, K., 1978. Strain differences of the mouse's free-running cricadian rhythm in continuous darkness. *Physiology and Behavior*, 20(6), pp.795–799.

Echizenya, M. et al., 2013. Total sleep deprivation followed by sleep phase advance and bright light therapy in drug-resistant mood disorders. *Journal of Affective Disorders*, 144(1-2), pp.28–33.

Edgar, D.M., Dement, W.C. & Fuller, C.A., 1993. Effect of SCN lesions on sleep in squirrel monkeys: evidence for opponent processes in sleep-wake regulation. *The Journal of neuroscience : the official journal of the Society for Neuroscience*, 13(3), pp.1065–1079.

Edwards, J., 2012. *Investigating the Roles of Zinc Finger Homeobox Gene 3 in Circadian Rhythms*. University of Oxford.

Ehrbrecht, A. et al., 2006. Comprehensive genomic analysis of desmoplastic medulloblastomas: Identification of novel amplified genes and separate evaluation of the different histological components. *Journal of Pathology*, 208(4), pp.554–563.

Eide, E.J. et al., 2005. Control of Mammalian Circadian Rhythm by CKIε-Regulated Proteasome-Mediated PER2 Degradation. *Molecular and cellular biology*, 25(7), pp.2795–2807.

Elston, G.N., 2003. Cortex, Cognition and the Cell: New Insights into the Pyramidal Neuron and Prefrontal Function. *Cerebral Cortex*, 13(11), pp.1124–1138.

Emens, J. et al., 2009. Circadian misalignment in major depressive disorder. *Psychiatry Research*, 168(3), pp.259–261.

EmPreSS, http://empress.har.mrc.ac.uk/.

Ensembl, http://www.ensembl.org/index.html.

Ersland, K.M. et al., 2012. Gene-based analysis of regionally enriched cortical genes in GWAS data sets of cognitive traits and psychiatric disorders. *PLoS ONE*, 7(2).

Escobar, C. et al., 2011. Circadian Disruption Leads to Loss of Homeostasis and Disease. *Sleep Disorders*, 2011, pp.1–8.

Etchegaray, J.P. et al., 2006. The polycomb group protein EZH2 is required for mammalian circadian clock function. *Journal of Biological Chemistry*, 281(30), pp.21209–21215.

Etchegaray, J.-P. et al., 2003. Rhythmic histone acetylation underlies transcription in the mammalian circadian clock. *Nature*, 421(6919), pp.177–182.

Fang, R. et al., 2010. Human LSD2/KDM1b/AOF1 regulates gene transcription by modulating intragenic H3K4me2 Methylation. *Molecular Cell*, 39(2), pp.222–233.

Feil, R., 2009. Epigenetics: Ready for the marks. *Nature*, 461(7262), pp.359–360.

Feil, R. & Fraga, M., 2012. Epigenetics and the environment: emerging patterns and implications. Nat Rev Genetics, 13, pp.97-109

Feng, D. et al., 2011. A circadian rhythm orchestrated by histone deacetylase 3 controls hepatic lipid metabolism. *Science (New York, N.Y.)*, 331(6022), pp.1315–1319.

Ferguson, C.J. et al., 2005. Social isolation, impulsivity and depression as predictors of aggression in a psychiatric inpatient population. *Psychiatric Quarterly*, 76(2), pp.123–137.

Fisher, S.P. et al., 2012. Rapid Assessment of Sleep-Wake Behavior in Mice. *Journal of Biological Rhythms*, 27(1), pp.48–58.

Fogg, P. et al., 2014. Class IIa histone deacetylases are conserved regulators of circadian function. *J Biol Chem*, 289(49), pp.34341–34348.

Forneris, F. et al., 2007. Structural basis of LSD1-CoREST selectivity in histone H3 recognition. *Journal of Biological Chemistry*, 282(28), pp.20070–20074.

Foster, C.T. et al., 2010. Lysine-specific demethylase 1 regulates the embryonic transcriptome and CoREST stability. *Molecular and cellular biology*, 30(20), pp.4851–4863.

Fray, M.D., 2009a. Biological methods for archiving and maintaining mutant laboratory mice. Part I: Conserving mutant strains. *Methods in Molecular Biology*, 561, pp.301–319.

Fray, M.D., 2009b. Biological methods for archiving and maintaining mutant laboratory mice. Part II: Recovery and distribution of conserved mutant strains. *Methods in Molecular Biology*, 561, pp.321–332.

Fuentes, P. et al., 2012. CoREST/LSD1 control the development of pyramidal cortical neurons. *Cerebral Cortex*, 22(6), pp.1431–1441.

Fustin, J.M. et al., 2013. XRNA-methylation-dependent RNA processing controls the speed of the circadian clock. *Cell*, 155(4).

Gale, M. & Yan, Q., 2015. High-throughput screening to identify inhibitors of lysine demethylases. *Epigenomics*, 7(1), pp.57–65.

Gallego, M. & Virshup, D.M., 2007. Post-translational modifications regulate the ticking of the circadian clock. *Nature reviews. Molecular cell biology*, 8(2), pp.139–148.

Gamsby, J.J. et al., 2013. The circadian Per1 and Per2 genes influence alcohol intake, reinforcement, and blood alcohol levels. *Behavioural Brain Research*, 249, pp.15–21.

Gatch, M.B. et al., 2006. Effects of monoamine oxidase inhibitors on cocaine discrimination in rats. *Behavioural pharmacology*, 17(2), pp.151–159.

Gene-Ontology, http://pubchem.ncbi.nlm.nih.gov/compound/10365#section=Gene-Ontology--Biological-Process.

Godinho, S.I.H. et al., 2007. The after-hours mutant reveals a role for Fbxl3 in determining mammalian circadian period. *Science (New York, N.Y.)*, 316(5826), pp.897–900.

Godinho, S.I.H. & Nolan, P.M., 2006. The role of mutagenesis in defining genes in behaviour. *European journal of human genetics : EJHG*, 14(6), pp.651–659.

Goldwater, D.S. et al., 2009. Structural and functional alterations to rat medial prefrontal cortex following chronic restraint stress and recovery. *Neuroscience*, 164(2), pp.798–808.

Gondo, Y. et al., 2010. ENU-based gene-driven mutagenesis in the mouse: a next-generation gene-targeting system. *Experimental animals / Japanese Association for Laboratory Animal Science*, 59(5), pp.537–548.

Gooden, D.M. et al., 2008. Facile synthesis of substituted trans-2-arylcyclopropylamine inhibitors of the human histone demethylase LSD1 and monoamine oxidases A and B. *Bioorganic and Medicinal Chemistry Letters*, 18(10), pp.3047–3051.

Gualberto, A. et al., 1998. p53 transactivation of the HIV-1 long terminal repeat is blocked by PD 144795, a calcineurin-inhibitor with anti-HIV properties. *Journal of Biological Chemistry*, 273(12), pp.7088–7093.

Hakimi, M.-A. et al., 2002. A core-BRAF35 complex containing histone deacetylase mediates repression of neuronal-specific genes. *Proceedings of the National Academy of Sciences of the United States of America*, 99(11), pp.7420–7425.

Han, X. et al., 2014. Destabilizing LSD1 by Jade-2 promotes neurogenesis: An antibraking system in neural development. *Molecular Cell*, 55(3), pp.482–494.

Harmar, A.J. et al., 2002. The VPAC2 receptor is essential for circadian function in the mouse suprachiasmatic nuclei. *Cell*, 109(4), pp.497–508.

Hasler, G., 2010. Pathophysiology of depression: do we have any solid evidence of interest to clinicians? *World psychiatry : official journal of the World Psychiatric Association (WPA)*, 9(3), pp.155–161.

Hastings, M., O'Neill, J.S. & Maywood, E.S., 2007. Circadian clocks: Regulators of endocrine and metabolic rhythms. *Journal of Endocrinology*, 195(2), pp.187–198.

Hastings, M.H. et al., 2005. Analysis of circadian mechanisms in the suprachiasmatic nucleus by transgenesis and biolistic transfection. *Methods in Enzymology*, 393, pp.579–592.

Hastings, M.H., Brancaccio, M. & Maywood, E.S., 2014. Circadian pacemaking in cells and circuits of the suprachiasmatic nucleus. *Journal of Neuroendocrinology*, 26(1), pp.2–10.

Hastings, M.H. & Herzog, E.D., 2004. Clock genes, oscillators, and cellular networks in the suprachiasmatic nuclei. *Journal of biological rhythms*, 19(5), pp.400–413.

Hatori, M. et al., 2014. Lhx1 maintains synchrony among circadian oscillator neurons of the SCN. *eLife*, p.in press.

Hattar, S. et al., 2003. Melanopsin and rod-cone photoreceptive systems account for all major accessory visual functions in mice. *Nature*, 424(6944), pp.76–81.

Haydon, M.J. et al., 2013. Photosynthetic entrainment of the Arabidopsis thaliana circadian clock. *Nature*, 502(7473), pp.689–92.

He, F. et al., 2010. Structural insight into the zinc finger CW domain as a histone modification reader. *Structure*, 18(9), pp.1127–1139.

Heninger, G.R., Delgado, P.L. & Charney, D.S., 1996. The revised monoamine theory of depression: a modulatory role for monoamines, based on new findings from monoamine depletion experiments in humans. *Pharmacopsychiatry*, 29(1), pp.2–11.

Herzog, E.D., 2007. Neurons and networks in daily rhythms. *Nature reviews. Neuroscience*, 8(10), pp.790–802.

Hirano, A. et al., 2013. FBXL21 regulates oscillation of the circadian clock through ubiquitination and stabilization of cryptochromes. *Cell*, 152(5), pp.1106–1118.

Hirayama, J. et al., 2007. CLOCK-mediated acetylation of BMAL1 controls circadian function. *Nature*, 450(7172), pp.1086–1090.

Hirota, T. et al., 2010. High-throughput chemical screen identifies a novel potent modulator of cellular circadian rhythms and reveals CKIα as a clock regulatory kinase. *PLoS Biology*, 8(12).

Hirota, T. et al., 2012. Identification of Small Molecule Activators of Cryptochrome. *Science*, 337(6098), pp.1094–1097.

Hirota, T. & Kay, S.A., 2009. High-throughput screening and chemical biology: new approaches for understanding circadian clock mechanisms. *Chemistry & biology*, 16(9), pp.921–927.

Hoerder-Suabedissen, A. et al., 2013. Expression profiling of mouse subplate reveals a dynamic gene network and disease association with autism and schizophrenia. *Proceedings of the National Academy of Sciences of the United States of America*, 110(9), pp.3555–60.

Holmes, A. et al., 2003. Mice lacking the serotonin transporter exhibit 5-HT(1A) receptor-mediated abnormalities in tests for anxiety-like behavior. *Neuropsychopharmacology : official publication of the American College of Neuropsychopharmacology*, 28(12), pp.2077–2088.

Van der Horst, G.T. et al., 1999. Mammalian Cry1 and Cry2 are essential for maintenance of circadian rhythms. *Nature*, 398(6728), pp.627–630.

Huang, J. et al., 2007. p53 is regulated by the lysine demethylase LSD1. *Nature*, 449(7158), pp.105–108.

Hughes, R.N., 2004. The value of spontaneous alternation behavior (SAB) as a test of retention in pharmacological investigations of memory. *Neuroscience and Biobehavioral Reviews*, 28(5), pp.497–505.

Humphrey, G.W. et al., 2001. Stable Histone Deacetylase Complexes Distinguished by the Presence of SANT Domain Proteins CoREST/kiaa0071 and Mta-L1. *Journal of Biological Chemistry*, 276(9), pp.6817–6824.

Irwin, J., 2008. Using ZINC to acquires a virtual screening library. *Curr Prot Bioinf*, suppl.22

Isobe, Y., Fujioi, J. & Nishino, H., 2001. Circadian rhythm of melatonin release in pineal gland culture: Arg-vasopressin inhibits melatonin release. *Brain Research*, 918(1-2), pp.67–73.

Isojima, Y. et al., 2009. CKIepsilon/delta-dependent phosphorylation is a temperature-insensitive, period-determining process in the mammalian circadian clock. *Proceedings*

of the National Academy of Sciences of the United States of America, 106(37), pp.15744–15749.

Jackson, http://research.jax.org/grs/type/gemm/.

Jagannath, A. et al., 2013. The CRTC1-SIK1 pathway regulates entrainment of the circadian clock. *Cell*, 154(5), pp.1100–1111.

Jarriault, S. & Greenwald, I., 2002. Suppressors of the egg-laying defective phenotype of sel-12 presenilin mutants implicate the CoREST corepressor complex in LIN-12/Notch signaling in C. elegans. *Genes and Development*, 16(20), pp.2713–2728.

Jeans, A.F. et al., 2007. A dominant mutation in Snap25 causes impaired vesicle trafficking, sensorimotor gating, and ataxia in the blind-drunk mouse. *Proceedings of the National Academy of Sciences of the United States of America*, 104(7), pp.2431–2436.

Johnson, C.H., Egli, M. & Stewart, P.L., 2008. Structural Insights into a Circadian Oscillator. *Science*, 322(5902), pp.697–701.

Johnson, C.H., Kondo, T. & Golden, S., 1999. Circadian clocks enhance fitness in cyanobacteria. *Photochemistry and Photobiology*, 69, p.6S–6S.

Johnson, R.F., Moore, R.Y. & Morin, L.P., 1988. Loss of entrainment and anatomical plasticity after lesions of the hamster retinohypothalamic tract. *Brain research*, 460(2), pp.297–313.

Johnstone, S.R. et al., 2012. MAPK phosphorylation of connexin 43 promotes binding of cyclin e and smooth muscle cell proliferation. *Circulation Research*, 111(2), pp.201–211.

Joska, T., Zaman, R. & Belden, W., 2014. Regulated DNA Methylation and the Circadian Clock: Implications in Cancer. *Biology*, 3(3), pp.560–577.

Justice, M.J. et al., 2000. Effects of ENU dosage on mouse strains. *Mammalian Genome*, 11(7), pp.484–488.

Justice, M.J. et al., 1999. Mouse ENU mutagenesis. *Human Molecular Genetics*, 8(10), pp.1955–1963.

Kalueff, A. et al., 2007. What's wrong with my mouse model?. Advances and strategies in animal modeling of anxiety and depression. *Behav Brain Res*, 179(1), pp.1-18

Karytinos, A. et al., 2009. A novel mammalian flavin-dependent histone demethylase. *Journal of Biological Chemistry*, 284(26), pp.17775–17782.

Kas, M.J.H. & Van Ree, J.M., 2004. Dissecting complex behaviours in the post-genomic era. *Trends in Neurosciences*, 27(7), pp.366–369.

Katada, S. & Sassone-Corsi, P., 2010. The histone methyltransferase MLL1 permits the oscillation of circadian gene expression. *Nature structural & molecular biology*, 17(12), pp.1414–1421.

Keays, D.A., Clark, T.G., et al., 2007. Estimating the number of coding mutations in genotypic and phenotypic driven N-ethyl-N-nitrosourea (ENU) screens: Revisited. *Mammalian Genome*, 18(2), pp.123–124.

Keays, D.A., Tian, G., et al., 2007. Mutations in α-Tubulin Cause Abnormal Neuronal Migration in Mice and Lissencephaly in Humans. *Cell*, 128(1), pp.45–57.

Keeney, A. et al., 2006. Differential effects of acute and chronic social defeat stress on hypothalamic-pituitary-adrenal axis function and hippocampal serotonin release in mice. *Journal of Neuroendocrinology*, 18(5), pp.330–338.

Keers, R. et al., 2012. Reduced anxiety and depression-like behaviours in the circadian period mutant mouse afterhours. *PLoS ONE*, 7(6).

Kelley, L.A. & Sternberg, M.J.E., 2009. Protein structure prediction on the Web: a case study using the Phyre server. *Nature protocols*, 4(3), pp.363–371.

Kennaway, D.J., 2010. Clock genes at the heart of depression. *Journal of psychopharmacology (Oxford, England)*, 24(2 Suppl), pp.5–14.

Kim DH et al., 2014. Crucial roles of MLL3 and MLL4 as epigenetic switches of the hepatic circadian clock controlling bile acid homeostasis. *Hepatology*.

King, D.P. et al., 1997. Positional cloning of the mouse circadian clock gene. *Cell*, 89(4), pp.641–653.

Ko, C.H. & Takahashi, J.S., 2006. Molecular components of the mammalian circadian clock. *Human Molecular Genetics*, 15(SUPPL. 2).

Kondratov, R. V. et al., 2003. BMAL1-dependent circadian oscillation of nuclear CLOCK: Posttranslational events induced by dimerization of transcriptional activators of the mammalian clock system. *Genes and Development*, 17(15), pp.1921–1932.

Konovalov, S. & Garcia-Bassets, I., 2013. Analysis of the levels of lysine-specific demethylase 1 (LSD1) mRNA in human ovarian tumors and the effects of chemical LSD1 inhibitors in ovarian cancer cell lines. *Journal of ovarian research*, 6(1), p.75.

Kristensen, L.H. et al., 2012. Studies of H3K4me3 demethylation by KDM5B/Jarid1B/PLU1 reveals strong substrate recognition in vitro and identifies 2,4-pyridine-dicarboxylic acid as an in vitro and in cell inhibitor. *FEBS Journal*, 279(11), pp.1905–1914.

Kubicek , S. & Jenuwein, T., 2004. A Crack in Histone Lysine Methylation. *Cell*, 119, pp.903-906

Kudryavtseva, N.N., Bakshtanovskaya, I. V & Koryakina, L.A., 1991. Social model of depression in mice of C57BL/6J strain. *Pharmacology, biochemistry, and behavior*, 38(2), pp.315–320.

Kuhlman, S.J. et al., 2003. Phase resetting light pulses induce Per1 and persistent spike activity in a subpopulation of biological clock neurons. *The Journal of neuroscience : the official journal of the Society for Neuroscience*, 23(4), pp.1441–1450.

Kumar, N. et al., 2010. Regulation of adipogenesis by natural and synthetic REV-ERB ligands. *Endocrinology*, 151(7), pp.3015–3025.

Ladurner, A.G., 2003. Tick-tock goes the acetylation clock. *Nature structural biology*, 10(2), p.83.

Lamia, K.A. et al., 2009. AMPK regulates the circadian clock by cryptochrome phosphorylation and degradation. *Science (New York, N.Y.)*, 326(5951), pp.437–440.

Lander, E.S. et al., 2001. Initial sequencing and analysis of the human genome. *Nature*, 409(6822), pp.860–921.

Landgraf, D., Shostak, A. & Oster, H., 2012. Clock genes and sleep. *Pflugers Archiv European Journal of Physiology*, 463(1), pp.3–14.

Lassi, G. et al., 2012. Loss of Gnas imprinting differentially affects REM/NREM sleep and cognition in mice. *PLoS Genetics*, 8(5).

Lee, C. et al., 2001. Posttranslational mechanisms regulate the mammalian circadian clock. *Cell*, 107(7), pp.855–867.

Lee, H.-W. et al., 2013. Real-time single-molecule co-immunoprecipitation analyses reveal cancer-specific Ras signalling dynamics. *Nature communications*, 4, p.1505.

Lee, J. et al., 2011. Loss of Bmal1 leads to uncoupling and impaired glucose-stimulated insulin secretion in β-cells. *Islets*, 3(6), pp.381–388.

Lee, M.G. et al., 2005. An essential role for CoREST in nucleosomal histone 3 lysine 4 demethylation. *Nature*, 437(September), pp.432–435.

Lee, M.G. et al., 2006. Histone H3 Lysine 4 Demethylation Is a Target of Nonselective Antidepressive Medications. *Chemistry and Biology*, 13(6), pp.563–567.

Lefta, M., Wolff, G. & Esser, K. a., 2011. Circadian rhythms, the molecular clock, and skeletal muscle. *Current Topics in Developmental Biology*, 96, pp.231–271.

Leloup, J.C. & Goldbeter, A., 2008. Modeling the circadian clock: From molecular mechanism to physiological disorders. *BioEssays*, 30(6), pp.590–600.

Levine, J.D. et al., 1994. Altered circadian pacemaker functions and cyclic AMP rhythms in the Drosophila learning mutant dunce. *Neuron*, 13(4), pp.967–974.

Lewejohann, L., Zipser, B. & Sachser, N., 2011. "Personality" in laboratory mice used for biomedical research: A way of understanding variability? *Developmental Psychobiology*, 53(6), pp.624–630.

Li, A. et al., 2012. Lysine-specific demethylase 1 expression in zebrafish during the early stages of neuronal development. *Neural Regeneration …*, 7(34), pp.2719–2726.

Li, J. et al., 2012. Lithium impacts on the amplitude and period of the molecular circadian clockwork. *PLoS ONE*, 7(3).

Li, Z. 2013. Circadian rhythms and mood: Opportunities for multi-level analysis in genomics and neuroscience. *Bioessays,* 36, pp. 305-315

Lin, T. et al., 2010. Requirement of the histone demethylase LSD1 in Snai1-mediated transcriptional repression during epithelial-mesenchymal transition. *Oncogene*, 29(35), pp.4896–4904.

Llc, C.R.C.P., 2001. *Methods of BEHAVIOR ANALYSIS in NEUROSCIENCE*,

Lowrey, P.L. et al, 2000. Functional Characterization of the Mammalian Circadian Mutation tau. *Science*.

Lu, S.X. et al., 2011. A Role for Protein Kinase Casein Kinase2 -Subunits in the Arabidopsis Circadian Clock. *PLANT PHYSIOLOGY*, 157(3), pp.1537–1545.

Lu, S.X. & Tobin, E.M., 2011. Chromatin remodeling and the circadian clock: Jumonji C-domain containing proteins. *Plant Signaling & Behavior*, 6(6), pp.810–814.

Lucas, R.J. et al., 2003. Diminished pupillary light reflex at high irradiances in melanopsin-knockout mice. *Science (New York, N.Y.)*, 299(5604), pp.245–247.

Lunyak, V. V et al., 2002. Corepressor-dependent silencing of chromosomal regions encoding neuronal genes. *Science (New York, N.Y.)*, 298(5599), pp.1747–1752.

Lupi, D. et al., 2006. Light-evoked FOS induction within the suprachiasmatic nuclei (SCN) of melanopsin knockout (Opn4-/-) mice: a developmental study. *Chronobiology international*, 23(1-2), pp.167–179.

Lv, T. et al., 2012. Over-expression of LSD1 promotes proliferation, migration and invasion in non-small cell lung cancer. *PLoS ONE*, 7(4).

Lynch, J.T., Harris, W.J. & Somervaille, T.C.P., 2012. LSD1 inhibition: a therapeutic strategy in cancer? *Expert Opinion on Therapeutic Targets*, pp.1–11.

Ma, L. et al., 2015. Design, Synthesis, and Structure–Activity Relationship of Novel LSD1 Inhibitors Based on Pyrimidine–Thiourea Hybrids As Potent, Orally Active Antitumor Agents. *J Med Chem*, 58(4), pp.1705–1716.

Macfarlan, T.S. et al., 2011. Endogenous retroviruses and neighboring genes are coordinately repressed by LSD1/KDM1A. *Genes and Development*, 25(6), pp.594–607.

MacKeen, M.M. et al., 2010. Small-molecule-based inhibition of histone demethylation in cells assessed by quantitative mass spectrometry. *Journal of Proteome Research*, 9(8), pp.4082–4092.

Maltby, V.E. et al., 2012. Histone H3K4 demethylation is negatively regulated by histone H3 acetylation in Saccharomyces cerevisiae. PNAS, 108(45), pp. 18505-18510.

Manolio, T.A. et al., 2009. Finding the missing heritability of complex diseases. *Nature*, 461(7265), pp.747–753.

Martin, K.F. et al., 1995. Dopamine D2 receptors: a potential pharmacological target for nomifensine and tranylcypromine but not other antidepressant treatments. *Pharmacology, biochemistry, and behavior*, 51(4), pp.565–569.

Masri, S. & Sassone-Corsi, P., 2010. Plasticity and specificity of the circadian epigenome. *Nature neuroscience*, 13(11), pp.1324–1329.

Maywood, E.S. et al., 2011. A diversity of paracrine signals sustains molecular circadian cycling in suprachiasmatic nucleus circuits. *Proceedings of the National Academy of Sciences of the United States of America*, 108(34), pp.14306–14311.

McCarthy, M.J. & Welsh, D.K., 2012. Cellular Circadian Clocks in Mood Disorders. *Journal of Biological Rhythms*, 27(5), pp.339–352.

McCurry, S.M. & Ancoli-Israel, S., 2003. Sleep dysfunction in Alzheimer's disease and other dementias. *Current Treatment Options in Neurology*, 5(3), pp.261–272.

McDonald, K., 2012. Discovery of chemical that affects biological clock offers new way to treat diabetes.

McDonald, O.G. et al., 2011. Genome-scale epigenetic reprogramming during epithelial-to-mesenchymal transition. *Nature structural & molecular biology*, 18(8), pp.867–874.

Meng, Q.J. et al., 2008. Setting Clock Speed in Mammals: The CK1ε tau Mutation in Mice Accelerates Circadian Pacemakers by Selectively Destabilizing PERIOD Proteins. *Neuron*, 58(1), pp.78–88.

Meng, Q.-J. et al., 2010. Entrainment of disrupted circadian behavior through inhibition of casein kinase 1 (CK1) enzymes. *Proceedings of the National Academy of Sciences of the United States of America*, 107(34), pp.15240–15245.

Menger, G.J. et al., 2007. Circadian profiling of the transcriptome in NIH/3T3 fibroblasts: comparison with rhythmic gene expression in SCN2.2 cells and the rat SCN. *Physiological genomics*, 29(3), pp.280–289.

Menke, A., Klengel, T. & B. Binder, E., 2012. Epigenetics, Depression and Antidepressant Treatment. *Current Pharmaceutical Design*, 18(36), pp.5879–5889.

Messeri, P., Eleftheriou, B.E. & Oliverio, A., 1975. Dominance behavior: a phylogenetic analysis in the mouse. *Physiology and Behavior*, 14(1), pp.53–58.

Metzger, E. et al., 2005. LSD1 demethylates repressive histone marks to promote androgen-receptor-dependent transcription. *Nature*, 437(7057), pp.436–439.

Metzger, E. et al., 2010. Phosphorylation of histone H3T6 by PKCbeta(I) controls demethylation at histone H3K4. *Nature*, 464(7289), pp.792–796.

MGI, http://www.informatics.jax.org/allele/MGI:4359289.

Milad, M.R. et al., 2009. Neurobiological Basis of Failure to Recall Extinction Memory in Posttraumatic Stress Disorder. *Biological Psychiatry*, 66(12), pp.1075–1082.

Millar, A.J. et al., 1992. A novel circadian phenotype based on firefly luciferase expression in transgenic plants. *The Plant cell*, 4(9), pp.1075–1087.

Miracle, A.D. et al., 2006. Chronic stress impairs recall of extinction of conditioned fear. *Neurobiology of Learning and Memory*, 85(3), pp.213–218.

Mistlberger, R.E. et al., 1983. Recovery sleep following sleep deprivation in intact and suprachiasmatic nuclei-lesioned rats. *Sleep*, 6(3), pp.217–233.

Mistlberger, R.E., 2005. Circadian regulation of sleep in mammals: Role of the suprachiasmatic nucleus. *Brain Res Rev*, 49, pp.429-454

Mitchell, P.J. & Redfern, P.H., 1992. Acute and chronic antidepressant drug treatments induce opposite effects in the social behaviour of rats. *Journal of Psychopharmacology*, 6(2), pp.241–257.

Montanaro, N., Casoli, R. & Babbini, M., 1965. Influence of the inhibition of monoamine oxidase on daily oscillation of the serotonin content of the brain. *Archivio italiano di scienze farmacologiche*, 15(1), pp.84–86.

Morton, A.J. et al., 2005. Disintegration of the sleep-wake cycle and circadian timing in Huntington's disease. *The Journal of neuroscience : the official journal of the Society for Neuroscience*, 25(1), pp.157–163.

Mousebook, http://www.mousebook.org/phenotype-view/behavior-neurological%20phenotype?field_line_value=&field_procedure_name_value=2&field_parameter_name_value=&field_mp_term_value=&field_analysis_methods_value=1.

Mulligan, P. et al., 2011. A SIRT1-LSD1 Corepressor Complex Regulates Notch Target Gene Expression and Development. *Molecular Cell*, 42(5), pp.689–699.

Murphy, K.M. et al., 2002. Evaluation of Temperature Gradient Capillary Electrophoresis for Detection of the Factor V Leiden Mutation: Coincident Identification of a Novel Polymorphism in Factor V. *Molecular Diagnosis*, 7(1), pp.35–40.

Murphy, R. & Messer, A., 2001. Gene transfer methods for CNS organotypic cultures: a comparison of three nonviral methods. Mol Ther: the journal of the American Society of Gene Therapy, 3(1), pp.113-121.

Murray, G. et al., 2009. Nature's clocks and human mood: the circadian system modulates reward motivation. *Emotion (Washington, D.C.)*, 9(5), pp.705–716.

Nagoshi, E. et al., 2005. Circadian gene expression in cultured cells. *Methods in enzymology*, 393(2000), pp.543–57.

Nair, V.D. et al., 2012. Involvement of histone demethylase LSD1 in short-time-scale gene expression changes during cell cycle progression in embryonic stem cells. *Molecular and cellular biology*, 32(23), pp.4861–76.

Nakahata, Y. et al., 2008. The NAD+-Dependent Deacetylase SIRT1 Modulates CLOCK-Mediated Chromatin Remodeling and Circadian Control. *Cell*, 134(2), pp.329-340

Nakajima, M. et al., 2005. Reconstitution of circadian oscillation of cyanobacterial KaiC phosphorylation in vitro. *Science (New York, N.Y.)*, 308(5720), pp.414–415.

Nakamura, T. et al., 2002. ALL-1 is a histone methyltransferase that assembles a supercomplex of proteins involved in transcriptional regulation. *Molecular Cell*, 10(5), pp.1119–1128.

Nam, H. et al., 2014. Phosphorylation of LSD1 by PKCα Is Crucial for Circadian Rhythmicity and Phase Resetting. *Molecular Cell*, 53(5), pp.791–805.

Neelamegam, R. et al., 2012. Brain-penetrant LSD1 inhibitors can block memory consolidation. *ACS Chemical Neuroscience*, 3, pp.120–128.

Neff, N.H. & Yang, H.Y., 1974. Another look at the monoamine oxidases and the monoamine oxidase inhibitor drugs. *Life sciences*, 14(11), pp.2061–2074.

Neumann, I.D. et al., 2011. Animal models of depression and anxiety: What do they tell us about human condition? *Progress in neuro-psychopharmacology & biological psychiatry*, 35(6), pp.1357–1375.

NFold3, http://www.reading.ac.uk/bioinf/nFOLD/.

Ng, L. et al., 2007. Neuroinformatics for genome-wide 3D gene expression mapping in the mouse brain. *IEEE/ACM Transactions on Computational Biology and Bioinformatics*, 4(3), pp.382–392.

Nicholson, T.B. et al., 2013. A Hypomorphic Lsd1 Allele Results in Heart Development Defects in Mice. *PLoS ONE*, 8(4).

Nicholson, T.B. & Chen, T., 2009. LSD1 demethylates histone and non-histone proteins. *Epigenetics*, 4(3), pp.129–132.

Nievergelt, C.M. et al., 2006. Suggestive evidence for association of the circadian genes PERIOD3 and ARNTL with bipolar disorder. *American Journal of Medical Genetics - Neuropsychiatric Genetics*, 141 B(3), pp.234–241.

Nightingale, K.P. et al., 2007. Cross-talk between Histone Modifications in Response to Histone Deacetylase Inhibitors MLL4 LINKS HISTONE H3 ACETYLATION AND HISTONE H3K4 METHYLATION. J Biol Chem, 282, pp. 4408-4416.

Nolan, P.M. et al., 2000. A systematic, genome-wide, phenotype-driven mutagenesis programme for gene function studies in the mouse. *Nature genetics*, 25(4), pp.440–443.

Nottke, A., Colaiácovo, M.P. & Shi, Y., 2009. Developmental roles of the histone lysine demethylases. *Development (Cambridge, England)*, 136(6), pp.879–889.

Noveroske, J.K., Weber, J.S. & Justice, M.J., 2000. The mutagenic action of N-ethyl-N-nitrosourea in the mouse. *Mammalian Genome*, 11(7), pp.478–483.

O'Neill, J.S. et al., 2011. Circadian rhythms persist without transcription in a eukaryote. *Nature*, 469(7331), pp.554–558.

O'Neill, J.S. & Reddy, A.B., 2011. Circadian clocks in human red blood cells. *Nature*, 469(7331), pp.498–503.

Oike, H. et al., 2011. Caffeine lengthens circadian rhythms in mice. *Biochemical and Biophysical Research Communications*, 410(3), pp.654–658.

Oliver, P.L. et al., 2012. Disrupted circadian rhythms in a mouse model of schizophrenia. *Current biology : CB*, 22(4), pp.314–9.

Oliver, P.L. & Davies, K.E., 2012. New insights into behaviour using mouse enu mutagenesis. *Human Molecular Genetics*, 21(R1).

Van Ooijen, G. et al., 2011. Proteasome function is required for biological timing throughout the twenty-four hour cycle. *Current Biology*, 21(10), pp.869–875.

OPPF, http://www.oppf.rc-harwell.ac.uk/OPPF/protocols/cloning.jsp.

Oster, H. et al., 2006. The circadian rhythm of glucocorticoids is regulated by a gating mechanism residing in the adrenal cortical clock. *Cell Metabolism*, 4(2), pp.163–173.

Oxenkrug, G.F. et al., 1988. Melatonin plasma response to MAO inhibitor: influence on human pineal activity? *Acta psychiatrica Scandinavica*, 77(2), pp.160–162.

Paffenholz, R. et al., 2004. Vestibular defects in head-tilt mice result from mutations in Nox3, encoding an NADPH oxidase. *Genes and Development*, 18(5), pp.486–491.

Pallier, P.N. et al., 2007. Pharmacological imposition of sleep slows cognitive decline and reverses dysregulation of circadian gene expression in a transgenic mouse model of Huntington's disease. *The Journal of neuroscience : the official journal of the Society for Neuroscience*, 27(29), pp.7869–7878.

Panda, S., Antoch, M.P., et al., 2002. Coordinated transcription of key pathways in the mouse by the circadian clock. *Cell*, 109(3), pp.307–320.

Panda, S., Sato, T.K., et al., 2002. Melanopsin (Opn4) requirement for normal light-induced circadian phase shifting. *Science (New York, N.Y.)*, 298(5601), pp.2213–2216.

Pariante, C.M. & Lightman, S.L., 2008. The HPA axis in major depression: classical theories and new developments. *Trends in Neurosciences*, 31(9), pp.464–468.

Parmentier, R. et al., 2002. Anatomical, physiological, and pharmacological characteristics of histidine decarboxylase knock-out mice: evidence for the role of brain histamine in behavioral and sleep-wake control. *The Journal of neuroscience : the official journal of the Society for Neuroscience*, 22(17), pp.7695–7711.

Partch, C.L. et al., 2006. Posttranslational regulation of the mammalian circadian clock by cryptochrome and protein phosphatase 5. *Proceedings of the National Academy of Sciences of the United States of America*, 103(27), pp.10467–10472.

Pendergast, J.S., Friday, R.C. & Yamazaki, S., 2010. Distinct functions of period2 and period3 in the mouse circadian system revealed by in vitro analysis. *PLoS ONE*, 5(1).

Pendergast, J.S., Friday, R.C. & Yamazaki, S., 2009. Endogenous rhythms in Period1 mutant suprachiasmatic nuclei in vitro do not represent circadian behavior. *The Journal of neuroscience : the official journal of the Society for Neuroscience*, 29(46), pp.14681–14686.

Pennartz, C.M.A. et al., 2002. Diurnal modulation of pacemaker potentials and calcium current in the mammalian circadian clock. *Nature*, 416(6878), pp.286–290.

Peschke, E. & Peschke, D., 1998. Evidence for a circadian rhythm of insulin release from perifused rat pancreatic islets. *Diabetologia*, 41(9), pp.1085–1092.

Phyre2, http://www.sbg.bio.ic.ac.uk/~phyre2/html/page.cgi?id=index.

Picciotto, M.R. & Wickman, K., 1998. Using knockout and transgenic mice to study neurophysiology and behavior. *Physiological reviews*, 78(4), pp.1131–1163.

Pittendrigh, C.S. & Daan, S., 1976. A functional analysis of circadian pacemakers in noctural rodents: I. The stability and lability of circadian frequency. *Journal of Comparative Physiology A*, 106, pp.223–252.

Polyphen, http://genetics.bwh.harvard.edu/pph2/.

Powell, S.B., Zhou, X. & Geyer, M.A., 2009. Prepulse inhibition and genetic mouse models of schizophrenia. *Behavioural Brain Research*, 204(2), pp.282–294.

Prickaerts, J. et al., 2006. Transgenic mice overexpressing glycogen synthase kinase 3beta: a putative model of hyperactivity and mania. *The Journal of neuroscience : the official journal of the Society for Neuroscience*, 26(35), pp.9022–9029.

Prut, L. & Belzung, C., 2003. The open field as a paradigm to measure the effects of drugs on anxiety-like behaviors: A review. *European Journal of Pharmacology*, 463(1-3), pp.3–33.

Pymol, http://pymol.sourceforge.net.

Qu, Z. et al., 2015. Inactivation of Cipc alters the expression of Per1 but not circadian rhythms in mice. *Science China Life Sciences*, 58(4), pp.368–372.

Quiggle, N.L. et al., 1992. Social information processing in aggressive and depressed children. *Child development*, 63(6), pp.1305–1320.

Quwailid, M.M. et al., 2004. A gene-driven ENU-based approach to generating an allelic series in any gene. *Mammalian Genome*, 15(8), pp.585–591.

Ralph, M.R. & Menaker, M., 1988. A mutation of the circadian system in golden hamsters. Science, 241(4870), pp.1225-1227

Ramanathan, C. et al., 2012. Monitoring Cell-autonomous Circadian Clock Rhythms of Gene Expression Using Luciferase Bioluminescence Reporters. *Journal of Visualized Experiments*, (67).

Ramboz, S. et al., 1998. Serotonin receptor 1A knockout: an animal model of anxiety-related disorder. *Proceedings of the National Academy of Sciences of the United States of America*, 95(24), pp.14476–14481.

Ran, F.A. et al., 2013. Genome engineering using the CRISPR-Cas9 system. *Nature protocols*, 8(11), pp.2281–308.

Rea, M.A., Glass, J.D. & Colwell, C.S., 1994. Serotonin modulates photic responses in the hamster suprachiasmatic nuclei. *The Journal of neuroscience : the official journal of the Society for Neuroscience*, 14(6), pp.3635–3642.

Redei, E. et al., 2001. Novel animal models of affective disorders. *Sem Clin Neuropsychiatry*, 6(1), pp.43-67

Rees, D.A. & Alcolado, J.C., 2005. Animal models of diabetes mellitus. *Diabetic medicine : a journal of the British Diabetic Association*, 22(4), pp.359–370.

Reischl, S. & Kramer, A., 2011. Kinases and phosphatases in the mammalian circadian clock. *FEBS Letters*, 585(10), pp.1393–1399.

Reppert, S.M. & Weaver, D.R., 2002. Coordination of circadian timing in mammals. *Nature*, 418(6901), pp.935–941.

Ripperger, J. a & Schibler, U., 2006. Rhythmic CLOCK-BMAL1 binding to multiple E-box motifs drives circadian Dbp transcription and chromatin transitions. *Nature genetics*, 38(3), pp.369–374.

Ripperger, J.A. & Merrow, M., 2011. Perfect timing: Epigenetic regulation of the circadian clock. *FEBS Letters*, 585(10), pp.1406–1411.

Roecklein, K.A. et al., 2009. A missense variant (P10L) of the melanopsin (OPN4) gene in seasonal affective disorder. *Journal of Affective Disorders*, 114(1-3), pp.279–285.

Roenneberg, T. et al., 2012. Social jetlag and obesity. *Current Biology*, 22(10), pp.939–943.

Roenneberg, T., Rémi, J. & Merrow, M., 2010. Modeling a circadian surface. *Journal of biological rhythms*, 25, pp.340–349.

Rogers, a. S. et al., 2004. A mutation in Drosophila simulans that lengthens the circadian period of locomotor activity. *Genetica*, 120(1-3), pp.223–232.

Rogers, D.C. et al., 2001. SHIRPA, a protocol for behavioral assessment: Validation for longitudinal study of neurological dysfunction in mice. *Neuroscience Letters*, 306(1-2), pp.89–92.

Rosenfeld, P. et al., 1988. Ontogeny of the type 2 glucocorticoid receptor in discrete rat brain regions: an immunocytochemical study. *Brain research*, 470(1), pp.119–127.

Rotili, D. et al., 2014. Pan-histone demethylase inhibitors simultaneously targeting Jumonji C and lysine-specific demethylases display high anticancer activities. *Journal of Medicinal Chemistry*, 57(1), pp.42–55.

Roybal, K. et al., 2007. Mania-like behavior induced by disruption of CLOCK. *Proceedings of the National Academy of Sciences of the United States of America*, 104(15), pp.6406–6411.

Ruby, N.F. et al., 2002. Role of melanopsin in circadian responses to light. *Science (New York, N.Y.)*, 298(5601), pp.2211–2213.

Sahar, S. & Sassone-Corsi, P., 2012. Circadian rhythms and memory formation: regulation by chromatin remodeling. *Frontiers in Molecular Neuroscience*, 5.

Sahlem, G. & Kalivas, B., 2014. Adjunctive triple chronotherapy (combined total sleep deprivation, sleep phase advance, and bright light therapy) rapidly improves mood and suicidality in suicidal depressed inpatients: an open label pilot study. *J Psychiatric Res*, 59, pp.101–107.

Saini, C. et al., 2013. Real-time recording of circadian liver gene expression in freely moving mice reveals the phase-setting behavior of hepatocyte clocks. *Genes and Development*, 27(13), pp.1526–1536.

Salimi, I., Friel, K.M. & Martin, J.H., 2008. Pyramidal tract stimulation restores normal corticospinal tract connections and visuomotor skill after early postnatal motor cortex activity blockade. *The Journal of neuroscience : the official journal of the Society for Neuroscience*, 28(29), pp.7426–7434.

Savali, G. et al., 2014. Diurnal oscillation of amygdala clock gene expression and loss of synchrony in a mouse model of depression. *Int J Neurosychpharmacology*, 18(5).

Scanbur, http://www.scanbur.com/.

Schmidt, T.M. et al., 2011. Melanopsin-positive intrinsically photosensitive retinal ganglion cells: from form to function. *The Journal of neuroscience : the official journal of the Society for Neuroscience*, 31(45), pp.16094–101.

Schmutz, I. et al., 2014. A Specific Role for the REV-ERBα–Controlled L-Type Voltage-Gated Calcium Channel CaV1.2 in Resetting the Circadian Clock in the Late Night. *J Biol Rhythms*, 29(4), pp.288–298.

Schmutz, J. et al., 2004. Quality assessment of the human genome sequence. *Nature*, 429(6990), pp.365–368.

Schofield, P.N., Hoehndorf, R. & Gkoutos, G. V., 2012. Mouse genetic and phenotypic resources for human genetics. *Human Mutation*, 33(5), pp.826–836.

Schwartz, J.R.L. & Roth, T., 2008. Neurophysiology of Sleep and Wakefulness: Basic Science and Clinical Implications. *Current Neuropharmacology*, 6(4), pp.367–378.

Schwartz, W.J. & Zimmerman, P., 1990. Circadian timekeeping in BALB/c and C57BL/6 inbred mouse strains. *The Journal of neuroscience : the official journal of the Society for Neuroscience*, 10(11), pp.3685–3694.

Scoumanne, A. & Chen, X., 2007. The lysine-specific demethylase 1 is required for cell proliferation in both p53-dependent and -independent manners. *Journal of Biological Chemistry*, 282(21), pp.15471–15475.

Shi, Y. et al., 2004. Histone demethylation mediated by the nuclear amine oxidase homolog LSD1. *Cell*, 119(7), pp.941–953.

Shi, Y.J. et al., 2005. Regulation of LSD1 histone demethylase activity by its associated factors. *Molecular Cell*, 19(6), pp.857–864.

Shimomura, K. et al., 2001. Genome-wide epistatic interaction analysis reveals complex genetic determinants of circadian behavior in mice. *Genome research*, 11(6), pp.959–980.

Shinomiya, K. et al., 2005. Effect of paroxetine on marble-burying behavior in mice. *Methods and findings in experimental and clinical pharmacology*, 27(10), pp.685–687.

Shuboni, D. & Yan, L., 2010. Nighttime dim light exposure alters the responses of the circadian system. *Neuroscience*, 170(4), pp.1172–1178.

Siepka, S.M. et al., 2007. Genetics and neurobiology of circadian clocks in mammals. In *Cold Spring Harbor Symposia on Quantitative Biology*. pp. 251–259.

SIFT, http://sift.jcvi.org/.

Silver, R. et al., 1996. A diffusible coupling signal from the transplanted suprachiasmatic nucleus controlling circadian locomotor rhythms. *Nature*, 382(6594), pp.810–813.

Singh, K.K. et al., 2011. Common DISC1 polymorphisms disrupt Wnt/GSK3?? signaling and brain development. *Neuron*, 72(4), pp.545–558.

Smale, L., Lee, T. & Nunez, A. a, 2003. Mammalian diurnality: some facts and gaps. *Journal of biological rhythms*, 18, pp.356–366.

Small, C.L. et al., 2005. Profiling gene expression during the differentiation and development of the murine embryonic gonad. *Biology of reproduction*, 72(2), pp.492–501.

Snyder, S.H. & Axelrod, J., 1965. Circadian rhythm in pineal serotonin: effect of monoamine oxidase inhibition and reserpine. Science (New York, N.Y.), 149, pp.542–544.

Söding, J., 2005. Protein homology detection by HMM-HMM comparison. *Bioinformatics*, 21(7), pp.951–960.

Spencer, S. et al., 2013. Circadian genes Period 1 and Period 2 in the nucleus accumbens regulate anxiety-related behavior. *European Journal of Neuroscience*, 37(2), pp.242–250.

Spoelstra, K., Oklejewicz, M. & Daan, S., 2002. Restoration of self-sustained circadian rhythmicity by the mutant clock allele in mice in constant illumination. *Journal of biological rhythms*, 17(6), pp.520–525.

Stavropoulos, P., Blobel, G. & Hoelz, A., 2006. Crystal structure and mechanism of human lysine-specific demethylase-1. *Nature structural & molecular biology*, 13(7), pp.626–632.

Di Stefano, L. et al., 2007. Mutation of Drosophila Lsd1 Disrupts H3-K4 Methylation, Resulting in Tissue-Specific Defects during Development. *Current Biology*, 17(9), pp.808–812.

Stokkan, K.A. et al., 2001. Entrainment of the circadian clock in the liver by feeding. *Science (New York, N.Y.)*, 291(5503), pp.490–493.

Sun, G. et al., 2011. miR-137 forms a regulatory loop with nuclear receptor TLX and LSD1 in neural stem cells. *Nature Communications*, 2, p.529.

Sun, Y. et al., 2008. Neurological deficits and glycosphingolipid accumulation in saposin B deficient mice. *Human Molecular Genetics*, 17(15), pp.2345–2356.

Sundstrom, L. et al. 2005. Organotypic cultures as tools for functional screening in the CNS. *Drug Disc Today*, 10(14), pp.993-1000

Suzuki, T. & Miyata, N., 2011. Lysine demethylases inhibitors. *Journal of Medicinal Chemistry*, 54, pp.8236–8250.

Takahashi, J.S. et al., 2010. Emergence of noise-induced oscillations in the central circadian pacemaker. *PLoS Biology*, 8(10).

Takahashi, J.S., Pinto, L.H. & Vitaterna, M.H., 1994. Forward and reverse genetic approaches to behavior in the mouse. *Science (New York, N.Y.)*, 264(5166), pp.1724–1733.

Takasu, N.N. et al., 2013. In Vivo Monitoring of Multi-Unit Neural Activity in the Suprachiasmatic Nucleus Reveals Robust Circadian Rhythms in Period1-/- Mice. *PLoS ONE*, 8(5).

Tochio, N. et al., 2006. Solution structure of the SWIRM domain of human histone demethylase LSD1. *Structure*, 14(3), pp.457–468.

Toh, K.L. et al., 2001. An hPer2 phosphorylation site mutation in familial advanced sleep phase syndrome. *Science (New York, N.Y.)*, 291(5506), pp.1040–1043.

Tokonami, N. et al., 2014. Local Renal Circadian Clocks Control Fluid-Electrolyte Homeostasis and BP. *Journal of the American Society of Nephrology : JASN*, 25(7), pp.1430–9.

Tominaga, K. et al., 1992. Effects of 5-HT1A receptor agonists on the circadian rhythm of wheel-running activity in hamsters. *European journal of pharmacology*, 214(1), pp.79–84.

Tõth, R. et al., 2012. Prieurianin/endosidin 1 is an actin-stabilizing small molecule identified from a chemical genetic screen for circadian clock effectors in Arabidopsis thaliana. *Plant Journal*, 71(2), pp.338–352.

Tsuchiya, Y. et al., 2011. Involvement of the Protein Kinase CK2 in the Regulation of Mammalian Circadian Rhythms. *Science Signaling*, 2(73), pp.1–11.

Turner, B., 2001. ChIP with Native Chromatin: Advantages and Problems Relative to Methods Using Cross-Linked Material. *Mapping Protein/DNA Interactions by Cross-Linking*.

Ueda, H.R. et al., 2005. System-level identification of transcriptional circuits underlying mammalian circadian clocks. *Nature genetics*, 37(2), pp.187–192.

Uniprot, http://www.uniprot.org/uniprot/Q9C0B1.

Vanselow, K. et al., 2006. Differential effects of PER2 phosphorylation: Molecular basis for the human familial advanced sleep phase syndrome (FASPS). *Genes and Development*, 20(19), pp.2660–2672.

Venter, J.C. et al., 2001. The sequence of the human genome. *Science (New York, N.Y.)*, 291(5507), pp.1304–1351.

Vijg, J. & Campisi, J., 2008. Puzzles, promises and a cure for ageing. *Nature*, 454(7208), pp.1065–1071.

Virshup, D.M. et al., 2007. Reversible protein phosphorylation regulates circadian rhythms. In *Cold Spring Harbor Symposia on Quantitative Biology*. pp. 413–420.

Visel, A., Thaller, C. & Eichele, G., 2004. GenePaint.org: an atlas of gene expression patterns in the mouse embryo. *Nucleic acids research*, 32(Database issue), pp.D552–D556.

Vogel, C. & Marcotte, E.M., 2012. Insights into the regulation of protein abundance from proteomic and transcriptomic analyses. *Nature Reviews Genetics*.

Wagner, S. et al., 1997. GABA in the mammalian suprachiasmatic nucleus and its role in diurnal rhythmicity. *Nature*, 387(6633), pp.598-603

Wagner, J.R. et al., 2014. The relationship between DNA methylation, genetic and expression inter-individual variation in untransformed human fibroblasts. *Genome biology*, 15(2), p.R37.

Wang, H. et al., 2013. One-step generation of mice carrying mutations in multiple genes by CRISPR/cas-mediated genome engineering. *Cell*, 153(4), pp.910–918.

Wang, J. et al., 2011. Novel histone demethylase LSD1 inhibitors selectively target cancer cells with pluripotent stem cell properties. *Cancer Research*, 71(23), pp.7238–7249.

Wang, J. et al., 2009. The lysine demethylase LSD1 (KDM1) is required for maintenance of global DNA methylation. *Nature genetics*, 41(1), pp.125–129.

Wang, X. et al., 2012. MLL1, a H3K4 methyltransferase, regulates the TNF -stimulated activation of genes downstream of NF- B. *Journal of Cell Science*, 125(17), pp.4058–4066.

Wartha, K., Herting, F. & Hasmann, M., 2014. Fit-for purpose use of mouse models to improve predictivity of cancer therapeutics evaluation. *Pharmacology and Therapeutics*.

Weber, M. et al., 2009. Running wheel activity is sensitive to acute treatment with selective inhibitors for either serotonin or norepinephrine reuptake. *Psychopharmacology*, 203(4), pp.753–762.

Welsh, D.K. et al., 2004. Bioluminescence imaging of individual fibroblasts reveals persistent, independently phased circadian rhythms of clock gene expression. *Current Biology*, 14(24), pp. 2289-2295.

Welsh, D.K., Imaizumi, T. & Kay, S.A., 2005. Real-time reporting of circadian-regulated gene expression by luciferase imaging in plants and mammalian cells. *Methods in Enzymology*, 393, pp.269–288.

Welsh, D.K., Takahashi, J.S. & Kay, S.A., 2010. Suprachiasmatic nucleus: cell autonomy and network properties. *Annual review of physiology*, 72, pp.551–577.

Whyte, W. et al., 2012. Enhancer decommissioning by LSD1 during embryonic stem cell differentiation.

Willner, P., Theodorou, A. & Montgomery, A., 1981. Subchronic treatment with the tricyclic antidepressant DMI increases isolation-induced fighting in rats. *Pharmacology, biochemistry, and behavior*, 14(4), pp.475–479.

Wu, Y. et al., 2013. The Deubiquitinase USP28 Stabilizes LSD1 and Confers Stem-Cell-like Traits to Breast Cancer Cells. *Cell Reports*, 5(1), pp.224–236.

Wu, Z.-Q. et al., 2012. Canonical Wnt signaling regulates Slug activity and links epithelial-mesenchymal transition with epigenetic Breast Cancer 1, Early Onset (BRCA1) repression. *Proceedings of the National Academy of Sciences*, 109(41), pp.16654–16659.

Xu, Y. et al., 2005. Functional consequences of a CKIδ mutation causing familial advanced sleep phase syndrome. *Nature*, 434(7033), pp.640–644.

Xydous, M. et al., 2012. Nicotinamide treatment reduces the levels of histone H3K4 trimethylation in the promoter of the mper1 circadian clock gene and blocks the ability

of dexamethasone to induce the acute response. *Biochimica et Biophysica Acta - Gene Regulatory Mechanisms*, 1819(8), pp.877–884.

Yagita, K. et al., 2001. Molecular mechanisms of the biological clock in cultured fibroblasts. *Science (New York, N.Y.)*, 292(5515), pp.278–281.

Yamaguchi, Y. et al., 2013. Mice genetically deficient in vasopressin V1a and V1b receptors are resistant to jet lag. *Science (New York, N.Y.)*, 342(6154), pp.85–90.

Yamazaki, S. & Takahashi, J.S., 2005. Real-time luminescence reporting of circadian gene expression in mammals. *Methods in Enzymology*, 393, pp.288–301.

Yang, C. et al., 2015. Enhanced Aggressive Behaviour in a Mouse Model of Depression. *Neurotox Research*, 27, pp.129–142.

Yang, M. et al., 2006. Structural Basis for CoREST-Dependent Demethylation of Nucleosomes by the Human LSD1 Histone Demethylase. *Molecular Cell*, 23, pp.377–387.

Yang, Y. et al., 2004. Distinct roles for PP1 and PP2A in the Neurospora circadian clock. *Genes and Development*, 18(3), pp.255–260.

Yang, Z. et al., 2010. AOF1 is a histone H3K4 demethylase possessing demethylase activity-independent repression function. *Cell research*, 20(3), pp.276–287.

Yin, J. et al., 2014. MiR-137: A new player in schizophrenia. *International Journal of Molecular Sciences*, 15(2), pp.3262–3271.

Yokoyama, A. et al., 2014. Identification of myelin transcription factor 1 (MyT1) as a subunit of the neural cell type-specific lysine-specific demethylase 1 (LSD1) complex. *Journal of Biological Chemistry*, 289, pp.18152–18162.

Yoo, S.H. et al., 2013. Competing E3 ubiquitin ligases govern circadian periodicity by degradation of CRY in nucleus and cytoplasm. *Cell*, 152(5), pp.1091–1105.

Yoo, S.-H. et al., 2004. PERIOD2::LUCIFERASE real-time reporting of circadian dynamics reveals persistent circadian oscillations in mouse peripheral tissues. *Proceedings of the National Academy of Sciences of the United States of America*, 101(15), pp.5339–5346.

Yoshitane, H. et al., 2009. Roles of CLOCK phosphorylation in suppression of E-box-dependent transcription. *Molecular and cellular biology*, 29(13), pp.3675–3686.

You, A. et al., 2001. CoREST is an integral component of the CoREST- human histone deacetylase complex. *Proceedings of the National Academy of Sciences of the United States of America*, 98(4), pp.1454–1458.

Yu, X. et al., 2014. Circadian Factor BMAL1 in Histaminergic Neurons Regulates Sleep Architecture. *Curr Biol*, 24(23), pp.2838–2844.

Zeng, J. et al., 2010. The Histone Demethylase RBP2 Is Overexpressed in Gastric Cancer and Its Inhibition Triggers Senescence of Cancer Cells. *Gastroenterology*, 138(3), pp.981–992.

Zhang, E. et al., 2009. A Genome-wide RNAi Screen for Modifiers of the Circadian Clock in Human Cells. *Cell*, 139(1), pp.199-210.

Zhang, L. et al., 2012. Promoter methylation of seven clock genes in total leukocytes from different-aged healthy subjects. *Biological Rhythm Research*, 43(6), pp.631–637.

Zhang, Q. et al., 2013. Structure-function analysis reveals a novel mechanism for regulation of histone demethylase LSD2/AOF1/KDM1b. *Cell research*, 23(2), pp.225–41.

Zhang, Y. et al., 2014. Functional analysis of a novel ENU-induced PHD finger 11 (Phf11) mouse mutant. *Mammalian Genome*, 25(11-12), pp.573–582.

Zhang, Y.Z. et al., 2010. Distribution of lysine-specific demethylase 1 in the brain of rat and its response in transient global cerebral ischemia. *Neuroscience Research*, 68(1), pp.66–72.

Zhao, W.-N. et al., 2007. CIPC is a mammalian circadian clock protein without invertebrate homologues. *Nature cell biology*, 9(3), pp.268–275.

Zhou, Q. et al., 2008. Inhibition of histone deacetylases promotes ubiquitin-dependent proteasomal degradation of DNA methyltransferase 1 in human breast cancer cells. *Molecular cancer research : MCR*, 6(5), pp.873–883.

Zhou, X. et al., 2011. Sleep, wake and phase dependent changes in neurobehavioral function under forced desynchrony. *Sleep*, 34, pp.931–941.